

Satellite Image Atlas  
of Glaciers of the World

G R E E N L A N D



United States Geological Survey  
Professional Paper 1386-C

**Cover:** Landsat 1 MSS digitally enhanced false-color composite image of the south slope of the Inland Ice northwest of Julianehåb (Qaqortoq), South Greenland. The image shows the well-defined edge of the Inland Ice, which spreads over the lowlands of South Greenland toward the outer coast. In some areas, the snowline is clearly visible. The marginal areas of the ice sheet in this area have undergone strong thinning during this century. (Landsat image 22061-13461, 13 September 1980; Path 3, Row 17 from Canada Centre for Remote Sensing, Ottawa, Ontario.)

# GREENLAND

By ANKER WEIDICK

*With a section on*

LANDSAT IMAGES OF GREENLAND

By RICHARD S. WILLIAMS, Jr., *and* JANE G. FERRIGNO

## SATELLITE IMAGE ATLAS OF GLACIERS OF THE WORLD

*Edited by* RICHARD S. WILLIAMS, Jr., *and* JANE G. FERRIGNO

---

U.S. GEOLOGICAL SURVEY PROFESSIONAL PAPER 1386-C

*Landsat images are the basis for a  
discussion of the glaciology, geography,  
and climatology of Greenland, the second  
largest areal and volumetric concentration  
of present-day glacier ice*



# U.S. DEPARTMENT OF THE INTERIOR

**BRUCE BABBITT, *Secretary***

## U.S. GEOLOGICAL SURVEY

**Gordon P. Eaton, *Director***

Any use of trade, product, or firm names in this publication is for  
descriptive purposes only and does not imply endorsement by the  
U.S. Government

Technical editing by John M. Watson  
Design and illustrations by Lynn Hulett  
Graphics Team: Arlene Compher, Maura Hogan, Dave Murphy, and  
Jane Russell  
Typesetting by Carolyn McQuaig

---

### Library of Congress Cataloging in Publication Data

(Revised for vol. C)

Satellite image atlas of glaciers of the world.

(U.S. Geological Survey professional paper ; 1386)

Includes bibliography.

Contents:—ChB. Antarctica / by Charles Swinbank ; with sections on The “dry valleys” of Victoria Land, by Trevor J. Chinn,  
[and] Landsat images of Antarctica, by Richard S. Williams, Jr., and Jane G. Ferrigno—C Greenland / Weidick.

Supt. of Docs. no.: I 19.16:138&C

1. Glaciers—Remote sensing. I. Williams, Richard S. 11. Ferrigno, Jane G. 111. Series.

GB2401.72.R42S28 1988 551.3'12 874500497

---

For sale by the U.S. Geological Survey, Information Services  
Box 25286, Federal Center, Denver, CO 80225



## Foreword

On 23 July 1972, the first Earth Resources Technology Satellite (ERTS 1 or Landsat 1) was successfully placed in orbit. The success of Landsat inaugurated a new era in satisfying mankind's desire to better understand the dynamic world upon which we live. Space-based observations have now become an essential means for monitoring global change.

The short- and long-term cumulative effects of processes that cause significant changes on the Earth's surface can be documented and studied by repetitive Landsat images. Such images provide a permanent historical record of the surface of our planet; they also make possible comparative two-dimensional measurements of change over time. This Professional Paper demonstrates the importance of the application of Landsat images to global studies by using them to determine the current distribution of glaciers on our planet. As images become available from future satellites, the new data will be used to document global changes in glacier extent by reference to the image record of the 1970's.

Although many geological processes take centuries or even millenia to produce obvious changes on the Earth's surface, other geological phenomena, such as glaciers and volcanoes, cause noticeable changes over shorter periods. Some of these phenomena can have a worldwide impact and often are interrelated. Explosive volcanic eruptions can produce dramatic effects on the global climate. Natural or culturally induced processes can cause global climatic cooling or warming. Glaciers respond to such warming or cooling periods by decreasing or increasing in size, thereby causing sea level to rise or fall.

As our understanding of the interrelationship of global processes improves and our ability to assess changes caused by these processes develops further, we will learn how to use indicators of global change, such as glacier variation, to more wisely manage the use of our finite land and water resources. This Professional Paper is an excellent example of the way in which we can use technology to provide needed earth-science information about our planet. The international collaboration represented by this report is also an excellent model for the kind of cooperation that scientists will increasingly find necessary in the future in order to solve important earth-science problems on a global basis.



Gordon P. Eaton  
Director,  
U.S. Geological Survey

## Preface

This chapter is the fifth to be released in U.S. Geological Survey Professional Paper 1386, *Satellite Image Atlas of Glaciers of the World*, a series of 11 chapters. In each chapter, remotely sensed images, primarily from the Landsat 1, 2, and 3 series of spacecraft, are used to study the glacierized regions of our planet and monitor glacier changes. Landsat images, acquired primarily during the middle to late 1970's, were used by an international team of glaciologists and other scientists to study various geographic regions or discuss glaciological topics. In each geographic region, the present areal distribution of glaciers is compared, wherever possible, with historical information about their past extent. The atlas provides an accurate regional inventory of the areal extent of glacier ice on our planet during the 1970's as part of a growing international scientific effort to measure global environmental change on the Earth's surface.

The second largest glacier on the Earth, the Inland Ice, also known as the Greenland ice sheet, covers about 80 percent of Greenland. (See Chapter B, Antarctica, for a discussion of the Earth's largest present-day ice sheet.) The Inland Ice is the Northern Hemisphere's largest remnant of the Ice Age, that period when extensive ice sheets covered North America and Eurasia. From the viewpoint of environmental change, the Greenland ice sheet is significant globally for three reasons: (1) climatologically, it is a large regional center of cooling; (2) hydrologically, it represents a significant component of the hydrologic cycle because of its long-term storage of freshwater (equivalent to about 6.5 m of global sea-level rise if completely melted); and (3) from a glaciologic-hazard perspective, it annually discharges a large number of icebergs into fjords and the surrounding oceans.

The great areal extent of the Inland Ice, estimated at  $1,736,095 \pm 100$  km<sup>2</sup>, makes it difficult to observe and study the ice sheet in its entirety. Greenland also has approximately  $48,599 \pm 100$  km<sup>2</sup> of local ice caps and other types of glaciers in its coastal and island areas beyond the margin of the ice sheet. Accurate knowledge of the thickness of the ice is limited to only a few areas (for example, about 3,200 m thick at the Greenland Ice Sheet Project Two (GISP 2) site on the interior ice divide at 72° 35' N. latitude, 38°28' W. longitude, at an elevation of about 3,100 m); total ice volume is estimated at 2,600,000 km<sup>3</sup> for the Inland Ice and 20,000 km<sup>3</sup> for other glaciers. Glaciologists estimate that from 35 to 50 percent of the annual discharge of ice from the Greenland ice sheet is in the form of icebergs and calf ice. The total mass balance of the Inland Ice is considered to be in near equilibrium.

Chapter C uses Landsat images, grouped according to the coastal regions of West, North, and East Greenland, as the basis for a discussion of the glaciological features of the Inland Ice, outlet glaciers, local ice caps, and valley glaciers of Greenland. The review of each geographic region examines the general geology, climatology, and glaciology (including mass balance, glacier variation, and glaciological hazards) and a specific discussion of the particular glaciological aspects of each region. Therefore, the chapter provides a comprehensive overview of the Greenland ice sheet that is highlighted with discussions of key glaciological features and problems.

Richard S. Williams, Jr.

Jane G. Ferrigno

Editors

## About this Volume

U.S. Geological Survey Professional Paper 1386, *Satellite Image Atlas of Glaciers of the World*, contains 11 chapters designated by the letters A through K. Chapter A is a general chapter containing introductory material and a discussion of the physical characteristics, classification, and global distribution of glaciers. The next nine chapters, B through J, are arranged geographically and present glaciological information from Landsat and other sources of data on each of the geographic areas. Chapter B covers Antarctica; Chapter C, Greenland; Chapter D, Iceland; Chapter E, Continental Europe (except for the European part of the former Soviet Union), including the Alps, the Pyrenees, Norway, Sweden, Svalbard (Norway), and Jan Mayen (Norway); Chapter F, Asia, including the European part of the former Soviet Union, China (P.R.C.), India, Nepal, Afghanistan, and Pakistan; Chapter G, Turkey, Iran, and Africa; Chapter H, Irian Jaya (Indonesia) and New Zealand; Chapter I, South America; and Chapter J, North America. The final chapter, K, is a topically oriented chapter that presents related glaciological topics.

The realization that one element of the Earth's cryosphere, its glaciers, was amenable to global inventorying and monitoring with Landsat images led to the decision, in late 1979, to prepare this Professional Paper, in which Landsat 1, 2, and 3 multispectral scanner (MSS) and Landsat 2 and 3 return beam vidicon (RBV) images would be used to inventory the areal occurrence of glacier ice on our planet within the boundaries of the spacecraft's coverage (between about 81° north and south latitudes). Through identification and analysis of optimum Landsat images of the glacierized areas of the Earth during the first decade of the Landsat era, a global benchmark could be established for determining the areal extent of glaciers during a relatively narrow time interval (1972 to 1982). This global "snapshot" of glacier extent could then be used for comparative analysis with previously published maps and aerial photographs and with new maps, satellite images, and aerial photographs to determine the areal fluctuation of glaciers in response to natural or culturally induced changes in the Earth's climate.

To accomplish this objective, the editors selected optimum Landsat images of each of the glacierized regions of our planet from the Landsat image data base at the EROS Data Center in Sioux Falls, S. Dak., although some images were also obtained from the Landsat image archives maintained by the Canada Centre for Remote Sensing, Ottawa, Ontario, Canada, and by the European Space Agency in Kiruna, Sweden, and Fucino, Italy. Between 1979 and 1981, these optimum images were distributed to an international team of more than 50 scientists who agreed to author a section of the Professional Paper concerning either a geographic area or a glaciological topic. In addition to analyzing images of a specific geographic area, each author was also asked to summarize up-to-date information about the glaciers within the area and to compare their present areal distribution with historical information (for example, from published maps, reports, and photographs) about their past extent. Completion of this atlas will provide an accurate regional inventory of the areal extent of glaciers on our planet during the 1970's.

Richard S. Williams, Jr.  
Jane G. Ferrigno  
Editors

# CONTENTS

	Page
Abstract -----	<b>C1</b>
Introduction -----	<b>1</b>
Areas -----	<b>2</b>
Place-names and geographic and hydrologic divisions of Greenland -----	<b>3</b>
Geographic place-names in Greenland -----	<b>7</b>
Greenlandic place-names -----	<b>7</b>
European place-names -----	<b>9</b>
General glaciological conditions -----	<b>10</b>
Field measurements -----	<b>14</b>
Glacier variation -----	<b>16</b>
 FIGURES 1-5. Sketch maps of:	
1. Greenland divided into hydrological regions superimposed on the geographical and political administrative divisions ----	<b>5</b>
2. The flowlines of the Inland Ice -----	<b>6</b>
3. Greenland delineating topography of the Inland Ice -----	<b>8</b>
4. The estimated altitude of the present glaciation limit in Greenland -----	<b>10</b>
5. The distribution of precipitation in Greenland -----	<b>11</b>
6. Graph showing computed annual ablation in West Greenland in millimeters per year from work by Braithwaite -----	<b>12</b>
7. Sketch map showing Reeh's 1985 estimated calf-ice discharge from the Greenland ice sheet in cubic kilometers per year water equivalent based on the assumption of an equilibrium state -----	<b>12</b>
8. Sketch map showing location of energy and mass-balance measurements in Greenland -----	<b>15</b>
 TABLE 1. List of Greenlandic town names -----	<b>9</b>
2. Estimated mass balance of the Inland Ice (Greenland ice sheet) in cubic kilometers per year (water equivalent) -----	<b>12</b>
3. Estimates on the calf-ice production from tidal outlet glaciers of the Inland Ice -----	<b>13</b>
 Analyses of selected Landsat images -----	<b>16</b>
FIGURE 9. Index map to the nominal scene centers of Landsat 1, 2, and 3 multispectral scanner and return beam vidicon images of Greenland and environs -----	<b>17</b>
10. Index map showing the areal coverage of Landsat images used as illustrations in the text -----	<b>18</b>
 West Greenland -----	<b>19</b>
Climatic conditions -----	<b>19</b>
Glaciological conditions -----	<b>19</b>
Mass-balance investigations -----	<b>20</b>
Glacier variations and glacier hazards -----	<b>22</b>
Images of South Greenland -----	<b>24</b>
Images of southern West Greenland -----	<b>27</b>
Images of central West Greenland -----	<b>33</b>
Images of northern West Greenland -----	<b>39</b>
 FIGURE 11. Mass-balance curves in relation to elevation, measured at localities in South and West Greenland -----	<b>21</b>
12. <b>A</b> , Part of a Landsat 3 MSS image showing the head of Søndre Sermilik, South Greenland; <b>B</b> , Sketch map showing variation in the position of the terminus of Sermeq in Søndre Sermilik between 1881 and 1979 -----	<b>25</b>
13. Annotated Landsat 1 MSS image of the southern margin of the Inland Ice -----	<b>26</b>

	Page
14. Annotated parts of two Landsat MSS images of the Inland Ice margin of South-West Greenland including Frederiksbåb Isblink, the largest piedmont glacier in West Greenland -----	<b>C28</b>
15. Annotated parts of two Landsat 1 MSS images of the outer coast and Inland Ice margin in the vicinity of Godthåbsfjord, southern West Greenland -----	<b>29</b>
16. Oblique aerial photograph of the Inland Ice margin in the head of Kangersuneq taken 20 August 1948, looking east -----	<b>30</b>
17. Annotated Landsat 3 MSS image of four local ice caps and the Inland Ice margin in the vicinity of Sukkertoppen Iskappe, southern West Greenland -----	<b>31</b>
18. Oblique aerial photograph of local ice caps in the area south of Søndre Strømfjord taken 20 August 1948, looking east -----	<b>32</b>
19. Inland Ice margin east of the Søndre Strømfjord Air Base. <b>A</b> , Annotated part of a Landsat 3 MSS image; <b>B</b> , Sketch of field classification of the Inland Ice margin at “Mint Julep” station based on investigations during 1953; <b>C</b> , Generalized cross section of glacier facies according to Benson and Motyka-----	<b>34</b>
20. <b>A</b> , Annotated Landsat 2 MSS image of Jakobshavn Isbræ and Jakobshavn Isfjord, central West Greenland; <b>B</b> , Sketch map of the ice streams in the Inland Ice that feed into the Jakobshavn Isbræ outlet glacier; <b>C</b> , Sketch map of ice margin changes around Jakobshavn Isbræ -----	<b>36</b>
21. Annotated Landsat 2 MSS image mosaic of Disko and Nûgssuaq, central West Greenland -----	<b>38</b>
22. <b>A</b> , Annotated Landsat 1 MSS image mosaic of Umanak Fjord complex, central West Greenland; <b>B</b> , Sketch map of the interior of northern Disko Bugt and Umanak Fjord complex-----	<b>40</b>
23. Oblique aerial photograph of the front of Store Gletscher taken 15 July 1948, looking southeast -----	<b>42</b>
24. <b>A</b> , Landsat 2 MSS image of the Inland Ice margin in the southern part of Melville Bugt, northern West Greenland; <b>B</b> , Sketch map of the Inland Ice margin showing named outlet glaciers -----	<b>43</b>
25. Oblique aerial photograph of the southernmost branch (Kakivfait sermiat) of Giesecke Bræer taken 23 July 1949, looking east-----	<b>44</b>
26. Enlargement of part of a Landsat 2 MSS image of the Inland Ice margin in Melville Bugt between Cornell Gletscher and Giesecke Bræer, northern West Greenland -----	<b>45</b>
<b>TABLE 4.</b> Average temperatures for the months of January and July, annual average temperatures, and annual precipitation at selected stations in West Greenland -----	<b>19</b>
5. Selected calf-ice-producing outlet glaciers from the Inland Ice in West Greenland known or observed to have had historic termini fluctuations of $\geq 5$ km -----	<b>23</b>
6. Selected land-based glaciers, West Greenland, exhibiting first-order variations -----	<b>24</b>
North Greenland -----	<b>46</b>
Climatic conditions -----	<b>46</b>
Glaciological conditions-----	<b>46</b>
Mass-balance investigations -----	<b>49</b>
Glacier variations and glacier hazards -----	<b>50</b>
Images of North-West Greenland -----	<b>51</b>
Images of North Greenland -----	<b>56</b>
Images of North-East Greenland -----	<b>64</b>

	Page
FIGURE 27. A, Oblique aerial photograph of Harald Moltke Bræ and Store Landgletscher taken 21 August 1948, looking southeast; B, Photograph of the ice cliffs of Store Landgletscher near "Camp Tuto" -----	C47
28. Sketch of the formation, balance, and waning of an ice cliff based on the investigations at "Red Rock," Nunatarssuaq, Thule-----	48
29. Graph of the mass balance of the west slope of the Inland Ice at the "Nunatarssuaq Ice Ramp," Thule-----	50
30. A, A part of an annotated Landsat 1 MSS image of the Inland Ice margin and local ice caps around Wolstenholme Fjord and Inglefield Bredning, North-West Greenland; B, Sketch map showing recession and readvance of Harald Moltke Bræ between 1916 and 1976 -----	52
31. Annotated Landsat 2 MSS false-color composite image of Inglefield Land, North-West Greenland-----	53
32. Oblique aerial photograph of the local ice cap over the southern part of Inglefield Land taken 19 July 1950, looking northeast -----	54
33. Oblique aerial photograph of the Inland Ice margin between Hiawatha Gletscher and Humboldt Gletscher in Inglefield Land taken 22 July 1953, looking north -----	55
34. Annotated Landsat 2 RBV image of Washington Land showing Humboldt Gletscher and Petermann Gletscher, North Greenland -----	57
35. A, A part of a Landsat 2 RBV image of the Inland Ice margin between Nyeboe Land and Wulff Land, North Greenland; B, Sketch map of the area of A showing names of main geographic features -----	58
36-38. Oblique aerial photographs of:	
36. Expanded foot of an outlet piedmont glacier from a local ice cap in the central part of Nares Land, North Greenland -----	59
37. The Inland Ice margin at an unnamed outlet glacier between Steensby Gletscher and Ryder Gletscher, Warming Land North Greenland-----	59
38. C.H. Ostenfeld Gletscher and Victoria Fjord taken 5 July 1953, looking southeast -----	60
39. Sketch map of the Peary Land area showing location of figures 38, 40, and 42 -----	60
40. Oblique aerial photograph of northernmost Peary Land seen from the west -----	61
41. A, Part of an annotated Landsat 2 RBV image of the head of Independence Fjord showing Marie Sophie Gletscher and Academy Gletscher, North Greenland; B, Updated sketch map of the changing positions of the termini of Marie Sophie Gletscher and Academy Gletscher -----	62
42. Oblique aerial photograph of the head of Independence Fjord taken 10 August 1951, looking north -----	63
43. Annotated Landsat 2 MSS image of the terminus of the glacier lobes of Nioghalvfjærdsbræ and Zachariæ Isstrøm, North-East Greenland -----	65
44. Oblique aerial photograph of Zachariæ Isstrøm taken 15 August 1950, looking west -----	66
45. Annotated Landsat 1 MSS image of Storstrømmen and L. Bistrup Bræ at Borgfjorden, North-East Greenland -----	67
46. A, Landsat 1 MSS false-color composite image mosaic of the coastal area between Germania Land and Kejser Franz Joseph Fjord, North-East Greenland; B, Sketch map of the area covered by the Landsat image mosaic showing the names of the main geographic features ----	68
TABLE 7. Average temperatures for the months of January and July, annual average temperatures, and annual precipitation at selected stations in North Greenland-----	46
8. Calf-ice-producing outlet glaciers from the Inland Ice in North Greenland exhibiting first-order variations -----	51

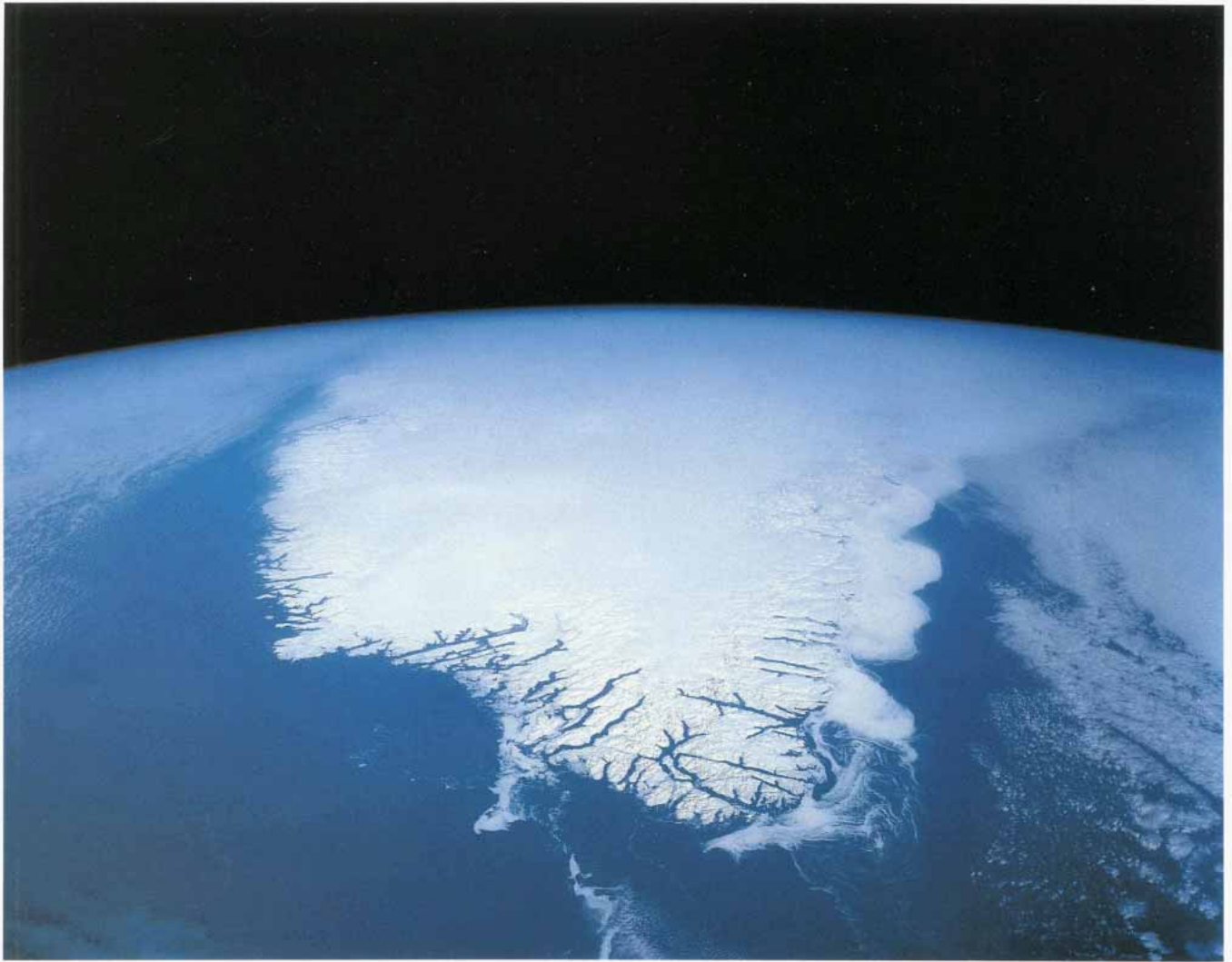
East Greenland -----	Page <b>C69</b>
Climatic conditions -----	<b>69</b>
Glaciological conditions -----	<b>71</b>
Mass-balance investigations -----	<b>72</b>
Glacier variations and glacier hazards -----	<b>73</b>
Images of northern East Greenland -----	<b>75</b>
Images of central East Greenland -----	<b>80</b>
Images of southern East Greenland -----	<b>82</b>
Images of South-East Greenland -----	<b>85</b>

FIGURE 47. **A**, Graph of observed 10-year running-mean temperatures at Angmagssalik and Upernavik compared with 10-year running-mean  $0^{18}/0^{16}$  values at six Greenland ice sheet stations; **B**, Map showing location of meteorological stations and ice-core drilling sites used for graphs in **A**-----

48. Oblique aerial photograph of the upper parts of Waltershausen Gletscher taken 17 August 1950, looking northwest -----	<b>70</b>
49. Annotated Landsat 3 MSS image of the Inland Ice margin between Hisinger Gletscher at the head of Kejser Franz Joseph Fjord and Daugaard-Jensen Gletscher in Nordvestfjord, inner Scoresby Sund fjord complex, East Greenland -----	<b>73</b>
50. Ground gravimetric and airborne radio-echosounding profiles in East Greenland -----	<b>76</b>
51. Oblique aerial photograph of Daugaard-Jensen Gletscher taken 17 August 1950, looking south -----	<b>77</b>
52. Annotated Landsat 1 MSS image of Scoresby Land between Kong Oscar Fjord and Nordvestfjord, East Greenland -----	<b>77</b>
53. Graph showing changes in the positions of the termini of four glaciers in Greenland -----	<b>78</b>
54. Oblique aerial photograph of the Stauning Alper taken 8 August 1951, looking northeast -----	<b>79</b>
55. Annotated Landsat 1 MSS false-color composite image of the central part of the Scoresby Sund fjord complex, East Greenland -----	<b>79</b>
56. Oblique aerial photograph of Renland in the central part of Scoresby Sund taken 17 August 1950, looking southwest -----	<b>80</b>
57. <b>A</b> , Annotated Landsat 2 MSS image of the outer part of Kong Christian IX Land between Scoresby Sund and Blossville Kyst, East Greenland, showing complex moraine patterns; <b>B</b> , Annotated Landsat 1 MSS image of same area as <b>A</b> -----	<b>81</b>
58. Oblique aerial photograph of the moraines between Bartholin Brae and Dendritgletscher taken 8 August 1951, looking east -----	<b>83</b>
59. Annotated Landsat 2 MSS image of the coastal area between Kangerdlugssuaq and Agga Ø, East Greenland -----	<b>84</b>
60. Annotated Landsat 1 MSS image of the area north of Angmagssalik, South-East Greenland -----	<b>86</b>
61. Map of the head of Sermilik and Sermiligâq fjords at Angmagssalik, South-East Greenland, showing changes in the position of glacier termini by comparing Landsat images with previously published maps -----	<b>87</b>
62. Oblique aerial photograph of the front of Helheimgletscher in the eastern head of Sermilik Fjord near Angmagssalik, 12 August 1984, looking west -----	<b>87</b>
63. <b>A</b> , Landsat 1 MSS image mosaic of the coast from Johan Petersen Fjord to Kap Cort Adelaer, South-East Greenland; <b>B</b> , Sketch map of the area covered in <b>A</b> showing geographic place-names and location and determination of the subglacial topography at the "Dye-3" station and environs -----	<b>88</b>



	Page
64. Oblique aerial photograph of the Inland Ice margin seen from a point 65°31' N. lat, 38°45' W. long, 12 August 1984, looking north -----	C89
65. Annotated Landsat 2 MSS image of the area around Kap Farvel, the southern tip of Greenland -----	90
TABLE 9. Average temperatures for the months of January and July, annual average temperatures, and annual precipitation at selected stations in East Greenland -----	69
10. Maximum summit elevations of selected mountain peaks along the eastern border of the Inland Ice according to the International Civil Aviation Organization map sheets (1:1,000,000 scale) -----	72
11. Outlet glaciers that have exhibited first-order variations in East Greenland -----	74
Concluding Remarks -----	91
FIGURE 66. NOAA-H advanced very high resolution radiometer image of most of Greenland acquired on 25 June 1990 showing the Inland Ice, outlet glaciers, and separate ice caps -----	93
Acknowledgments -----	92
Landsat images of Greenland, by Richard S. Williams, Jr., and Jane G. Ferrigno -----	94
Introduction -----	94
Index map to optimum Landsat 1, 2, and 3 images of Greenland -----	98
Table of optimum Landsat 1, 2, and 3 images of Greenland -----	99
FIGURE 67. Map of the optimum Landsat 1, 2, and 3 multispectral scanner and return beam vidicon images of Greenland -----	96
References Cited -----	102
TABLE 12. Geographic place-names of the cited natural features and towns in Greenland -----	108
13. Stations on the Greenland ice sheet (Inland Ice) -----	115
14. Optimum Landsat 1, 2, and 3 images of Greenland -----	116
PLATE 1. Map of Greenland showing the Greenland ice sheet (Inland Ice), outlet glaciers, local ice caps, and principal towns -----	in pocket



Space Shuttle photograph of the southern part of Greenland taken 29 March 1992. The north-looking view shows part of the Greenland ice sheet (the Inland Ice), rocky coastal areas covered by snow, and numerous fjords. The Inland Ice is the largest remnant of the Ice Age in the Northern Hemisphere and has an extent greater than 1.7 million square kilometers. In some places it is more than 3,000 meters thick. Photograph number S45-152-105 courtesy of NASA.

## GREENLAND

By ANKER WEIDICK<sup>1</sup>

### Abstract

Greenland has the second largest glacier on Earth, the Inland Ice, also known as the Greenland ice sheet. The Inland Ice is the largest relic of the Ice Age in the Northern Hemisphere. Currently, Greenland is significant climatologically as a center of cooling, hydrologically as a large storage area in the hydrologic cycle, and, from a hazard perspective, because it produces large quantities of icebergs.

Because of the extent of the Inland Ice, estimated to be 1,736,095,210 square kilometers, it is difficult to observe and study the ice sheet. In addition to the ice sheet, Greenland has approximately 48,599,210 square kilometers of local ice caps and glaciers in the rocky coastal and island areas. Detailed knowledge of the ice thickness is available only in a few areas, but estimates of total ice volume are 2,600,000 cubic kilometers for the Inland Ice and 20,000 cubic kilometers for the local coastal glaciers. Generalized sketch maps show glaciation limits, flowlines in the ice, surface contours, and distribution of precipitation. It is estimated that 35 to 50 percent of the accumulation is released as calf ice and icebergs. The total mass balance of the Inland Ice is considered to be in a state of near equilibrium. Most accumulation studies have been made on a regional scale, but long-term mass-balance studies have been made in a few areas of West Greenland that have a potential for hydroelectric power development. Glacier variation has been studied locally. Recently, remote sensing techniques, including the analysis of Landsat images, have been used to provide more accurate and detailed glaciological information on a regional scale.

Chapter C uses Landsat imagery as a basis for a discussion of the glaciological features of the Inland Ice, outlet glaciers, local ice caps, and valley glaciers of Greenland. Landsat scenes have been selected from the coastal regions of West, North, and East Greenland. Descriptions start with the southern tip of the island and continue in a clockwise direction. The review of each area includes (1) background information on the geology, climatology, and glaciology, including studies on mass balance, glacier variation, and glaciological hazards and (2) a specific discussion, based on selected Landsat images, that addresses the particular characteristics of each region. The chapter provides a comprehensive view of the glaciology of Greenland and is highlighted with discussions of specific glaciological features and problems.

## Introduction

The subcontinent of Greenland contains the second largest glacier on the Earth—the Inland Ice (Greenland ice sheet, second in size to the Antarctic ice sheet). Greenland also has numerous local glaciers, but the large inland ice sheet and its margin attract the greatest attention (plate 1). The Inland Ice is by far the largest relic of the ice age in the Northern Hemisphere. Presently, it serves as a center of cooling and as a buffer in the hydrologic cycle by storing vast amounts of water in the form of ice. The Inland Ice also creates a hazard by the production of vast quantities of icebergs. This production is estimated to be between 150 and 310 km<sup>3</sup> a<sup>-1</sup> (cubic kilometers per year) of water equivalent, which is more than one-third of the total annual accumulation of 425 to 630 km<sup>3</sup> a<sup>-1</sup> (see table 2).

The large areal extent of the Inland Ice makes it difficult for anyone to observe the ice sheet comprehensively and discuss its glaciological features. This chapter uses Landsat imagery as a basis for the discussion of the Inland Ice, outlet glaciers, local ice caps, and valley glaciers of Greenland.

A total description of Greenland's glaciers according to the European standard (for example, glacier atlases of Switzerland or Norway and Sweden) is scarcely realistic not only because of the overwhelming number of glaciers but because of the widely differing information base. Until recently, the age range of aerial photographs of any particular area extended from the 1940's to the most recent decade. Uniform aerial photographic coverage of the entire coastal region was first achieved in 1987 at 1:150,000 scale (West Greenland in 1985, North Greenland in 1978, and East Greenland in 1981 and 1987) by Mark Hurd Corp., Minneapolis, Minn., for the National Survey and Cadastre (NSC), Denmark.<sup>2</sup>

This new aerial photographic coverage will provide the means of establishing a uniform description of the status of glaciers in Greenland. Landsat images will be especially helpful for this purpose by giving a better regional determination of the variations of the snowline and related glaciological conditions and by furnishing a tool for determining and monitoring contemporaneous glacier fluctuation for the whole of Greenland.

Since the launch of the first Landsat satellite on 23 July 1972, the subsequent series of satellites has furnished a great variety of information on Greenland's glaciers; a selection of sequential scenes can therefore be made to illustrate glaciological phenomena. In this chapter, the selection has been made geographically. Landsat scenes have been selected from the coastal regions of all of the geographic areas of Greenland and are discussed in a clockwise direction from a starting point at the southern tip of the island. The review of each area includes general background information of the geology, climatology, and glaciology. Particular features and problems of each region are addressed specifically. As a result, the chapter gives a comprehensive view of the glaciology of Greenland.

## Areas

Data pertaining to the area of Greenland and its ice cover vary essentially because of the following two factors.

1. The map base improves continually. As an example, the geographic positions of the northern parts of the island only recently have been established accurately, the basis being the geodetic satellite positioning technique (Lillestrand and Johnson, 1971; Madsen, 1979; Forsberg and Madsen, 1981), and the compilation of maps using this new information for topographic (National Survey and Cadastre, Denmark) and geologic (Grønlands Geologiske Undersøgelse — The Geological Survey of Greenland) purposes is still progressing.
2. Previous estimates of the immense area of the Inland Ice are based on compilation from numerous large-scale maps that do not show the correct delineation between the Greenland ice sheet (the Inland Ice) and contiguous local ice caps and ice fields.

The estimates given here for the areal distribution of the glacierized and nonglacierized parts of Greenland are from W.L. Weng (written commun. 1995), NSC, who used a new 1:2,500,000-scale map of

---

<sup>2</sup> Formerly named the Geodetic Institute, Copenhagen.

Greenland for his calculations. Weng calculated the total area of Greenland, including the coastal islands, to be  $2,166,086 \pm 100 \text{ km}^2$ , of which the Inland Ice constitutes  $1,736,095 \pm 100 \text{ km}^2$ , or 80 percent. Weng further analyzed the ice-covered and ice-free areas of Greenland. The total ice-covered area is  $1,755,637 \pm 100 \text{ km}^2$ , which is composed of the Inland Ice ( $1,707,038 \pm 100 \text{ km}^2$ , not including nunataks within the ice sheet), 265 local glaciers on the main island ( $44,838 \text{ km}^2$ ), and 36 glaciers on the coastal islands ( $3,761 \text{ km}^2$ ). The ice-free area totals  $410,449 \pm 100 \text{ km}^2$ , which is composed of the main coastal area ( $334,391 \text{ km}^2$ ), 953 nunataks within the main ice sheet ( $29,057 \text{ km}^2$ ), 45 nunataks in the coastal areas ( $951 \text{ km}^2$ ), and ice-free areas on the coastal islands ( $46,050 \text{ km}^2$ ).

Based on earlier estimates, the ice-free coastal areas seem to be evenly divided between West, North, and East Greenland. Local glaciers seem to cover about 15 percent of West Greenland (Weidick, 1985), 50 percent of North Greenland, and 35 percent of East Greenland, but revision of these figures is possible.

The estimated volume of the Inland Ice given by Holtzschler and Bauer (1954) is approximately  $2,600,000 \text{ km}^3$  of ice, on the basis of soundings of the ice thickness at that time. This figure will be corrected continually as detailed knowledge of the ice thickness increases.

Little is known about the thickness of local glaciers in Greenland, but if the glaciers are divided into groups by size and compared with the average thickness of similar groups located elsewhere, an estimate of the total volume of local glaciers is about  $20,000 \text{ km}^3$  of ice.

The following discussion illustrates that satellite images furnish a sound basis for delineating the Inland Ice from the local ice caps and ice fields and for providing a more homogeneous basis for division and calculation of the glacierized area of Greenland. In this context, it is important to discuss the resolution limitations of Landsat data. Landsat multispectral scanner (MSS) and Landsat 1 and 2 return beam vidicon (RBV) images have a picture element (pixel) resolution of 79 m. [Editor's note: An object on the Earth's surface that has a diameter of 79 m would be contained within a single MSS pixel and therefore be unresolvable other than as a difference in tone, if any, from adjacent pixels. In other words, a snowpatch can be detected, although not measured, when it is wholly contained within a single pixel. Assuming sufficient contrast between the object (for example, "white" snowpatch) and the surrounding area, photogrammetrists calculate that an object must include about 3.3 pixels to actually be resolved spatially. Therefore, a snowpatch or a small glacier would have to encompass a minimum dimension of 260 m to be delineated. From a practical viewpoint, however, 1 km is the rule of thumb used as the minimum glacier size detectable on a Landsat MSS image under optimum conditions. At a scale of 1:1,000,000, 1 km represents 1mm. Meier (1974) noted that glaciologists involved in glacier inventories recommended that  $0.1 \text{ km}^2$  be used as the minimum area for mapping perennial snowpatches and small glaciers.] The Landsat 4 and 5 thematic mapper (TM) and the Landsat 3 RBV have a pixel resolution of 30 m, so theoretically, TM images could be used to map perennial snowpatches and small glaciers.

## **Place-Names and Geographic and Hydrologic Divisions of Greenland**

Greenland can be divided into smaller regions for administrative purposes and scientific discussions. The primary glaciological division consists of three main units: West, North, and East Greenland. Each division has a distinct glaciological character and an ice-free coastal strip of somewhat more than  $100,000 \text{ km}^2$ . The small area of South Greenland

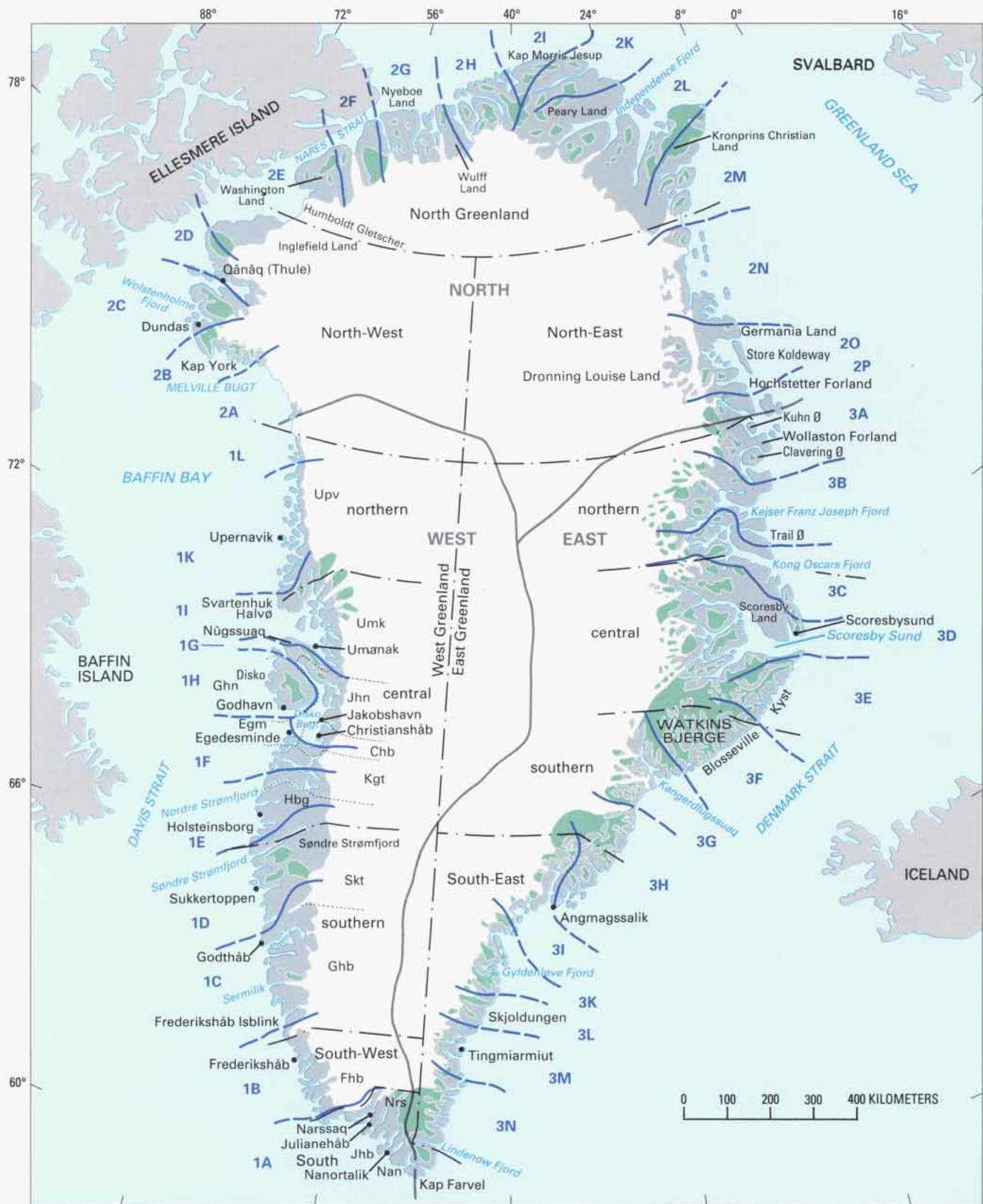
falls into the West Greenland subdivision and is discussed there. Subdivisions of the main areas then can be made into districts of northern West Greenland, North-West Greenland, and so on (fig. 1). These arbitrary districts are used throughout this chapter, although for glaciological purposes North-West and North-East Greenland are consolidated with and grouped under the heading of "North Greenland."

However, the division is unsatisfactory for the proper cataloging of detailed information, especially the localization of the individual glaciers and sectors of the Inland Ice and their connections to coastal hydrological basins, such as fjords and watersheds. For this purpose, a first-order division of Greenland into hydrological regions was made by The Geological Survey of Greenland, and these regions also are shown on figure 1. In addition, for those areas of primary interest in the planning of future use of hydropower in Greenland (mainly West Greenland), this subdivision scheme has been applied to the individual outlet glaciers and lobes emanating from the Inland Ice. The coding of the individual glaciers is made according to recommendations made by the Temporary Technical Secretariat for the World Glacier Inventory (Muller and others, 1977; Muller, 1978; Weidick and others, 1992). Each glacier is characterized by an 8-digit code, of which the two first digits are shown in figure 1. The third digit denotes the fjord complex in the district, the fourth and the fifth digits the basin in the fjord, and the last three digits are the number of the glacier in the basin. For example, Jakobshavn Isbrae in central West Greenland (see fig. 20) is denoted 1GC06002, indicating that it is glacier number 2 in basin number 6 in fjord C, district G, in West Greenland (1). Although only completed in West Greenland from the south to as far north as lat 71° N., this coding has already proved valuable, particularly in avoiding the confusion caused by glaciers that have the same Greenlandic name. Also, those unnamed glaciers (the majority) have been given an address (specific identification) for the filing of information.

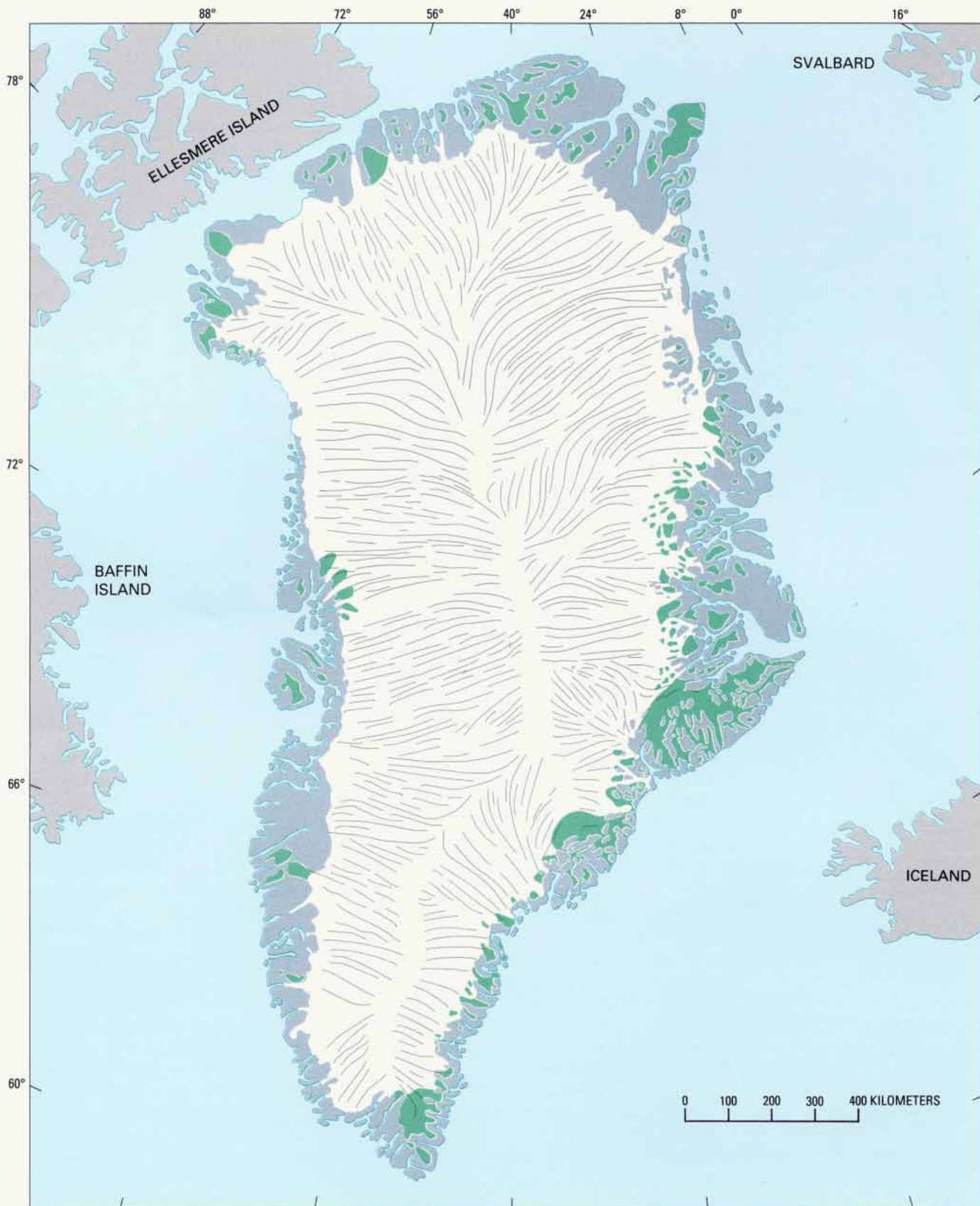
A still unsolved problem is how to divide the Inland Ice into exact sectors so that each sector is connected to a specific hydrological basin or a fjord along the coast. Such a division is required, because direct mass-balance measurements on the Greenland ice sheet can be made only in a few selected sectors (for logistical reasons) and because the accuracy of the mass-balance determinations here is to a great degree dependent on the correct delineation of the glacier area involved. Another important determination in Greenland is the separation between the Inland Ice and local ice caps, and this differentiation is also illustrated in figure 1 but in a very generalized fashion.

Several attempts have been made to determine the flowlines so they could be used for sector division (Reeh, 1979; Weidick and Olesen, 1980; Radok and others, 1982). An example delineating flowlines for the entire Greenland ice sheet is shown in figure 2. These flowlines have been used as the basis for the primary division into the West, North, and East Greenland parts of the Inland Ice shown in figure 1. However, for detailed sector division sufficient measurements of bottom and surface topography of the ice sheet still are lacking, in spite of the extensive measurements made by airborne radio-echosounding surveys (Gudmandsen, 1976, 1980). The extremely wet ice of the western slope of the ice sheet in South-West and West Greenland has caused transmission problems for large-scale airborne radio-echosounding investigations; however, these problems have been solved for detailed small-scale mapping of marginal areas from helicopter (Thorning and others, 1986). Landsat images having a low solar elevation angle can express details of the subglacial topography on the ice sheet surface even at ice thicknesses of 1,000m or more. Several images that show this phenomenon are shown

**Figure 1.—Hydrological regions of Greenland superimposed on a map of the geographical and political administrative divisions. Heavy gray lines distinguish the main division of the Inland Ice into west, North, and East Greenland, based on the flowlines given by Radok and others (1982) (see fig. 2). Solid and dashed blue lines are boundaries between hydrological regions (dashed where projected off the coastline). The numbers 1, 2, and 3 refer to west, North, and East, respectively; the letters run consecutively, clockwise in each of the three main divisions. Dash-dot lines indicate the geographical divisions used in this work. The straight dotted lines indicate the political administrative divisions (communes) of South and West Greenland. Local ice caps and ice domes are shown in green. Ice-free areas are shown in dark gray.**







**Figure 2.**—The flowlines of the Inland Ice (redrawn from Radok and others, 1982, based on work by B. McInnes, University of Colorado). Local ice caps and ice domes are shown in green. Ice-free areas are shown in dark gray.

later in the chapter (see figs. 20, 49, 57, 59). Although these surface expressions of the subglacial topography are liable to be distorted because of the flow of ice, the general image provides an important information supplement to the soundings made by airborne radio-echosounding surveys (or from seismic or gravimetric surveys). Radar altimetry from satellites (Brooks, 1979; Zwally and others, 1981; Bind-schadler, 1984; Bind-schadler and others, 1989) is also an important method for determining surface topography, because it is possible with this method to determine the elevation of the surface of the Inland Ice to within a few meters and geographic location to better than a hundred meters. A sketch map showing surface topography based on satellite radar altimetry and data from the Electromagnetics Institute, Technical University of Denmark, has been prepared (fig. 3).

## **Geographic Place-Names in Greenland**

Although the text closely follows place-names used on map sheets published by the National Survey and Cadastre, Denmark, and those authorized by the Greenland Place-Name Committee, reference to expedition reports sometimes has necessitated the use of unauthorized names. The latter place-names are shown by quotation marks.

Place-names in Greenland originate either from Greenlandic (Inuit) or European (mainly Danish) roots. Greenlandic place-names dominate East Greenland south of Scoresby Sund and all of West and North-West Greenland. Other foreign place-names are concentrated in regions outside these areas. For some well-known localities in West Greenland (for example, most towns and a few fjords and glaciers), Greenlandic and European names are both in use.

A few place-names mentioned in the text have undergone a change in geographic location during recent decades. For example, the original location of the place-name Thule was at Dundas; it was later moved north to the locality of Qânâq in the 1950's, whereas the original Thule place-name continued in use at its original location by being incorporated into the name of a U.S. military base at Dundas, Thule Air Base.<sup>3</sup> The place-name for Thule Air Base now applied by Greenlandic authorities is Pitugfik (the new Greenlandic spelling is Pituffik). Also, the area named Knud Rasmussen Land (formerly covering a region in East Greenland) has been relocated; it now covers the Inland Ice margin of North Greenland. Another source of confusion is the fact that in some instances the same glaciers have been described under different names by different expeditions. An example is the glacier originally called Frøya Glacier. The authorized name is Frejagletscher, but the original name also has been used in this text.

## **Greenlandic Place-Names**

Because of the descriptive character of Greenlandic place-names (for example, "Sermeq": "the glacier"; "Kangerdlugssuaq": "the great fjord"), the same place-name can be repeated at several different locations. Thus, "Kangerdlugssuaq" could be used in this text for Søndre Strømfjord in West Greenland, Inglefield Bredning in North Greenland, or Scoresby Sund or the fjord of Kangerdlugssuaq in East Greenland. "Sermeq" could

---

<sup>3</sup> Within the United States of America, military airfields are called "Air Force Bases," such as Andrews Air Force Base outside Washington, D.C. Foreign airfields operated by the U.S. military are called "Air Bases," such as Thule Air Base and the former Søndre Strømfjord Air Base in Greenland.



Figure 3.—Delineation of topography of the Inland Ice. The contours on the Inland Ice that define two major domes are based on various sources (especially data of the Electromagnetics Institute, Technical University of Denmark; Brooks, 1979;

Bindshadler, 1984). The contour interval is 100 m. Local ice caps and ice domes are shown in green. Ice-free areas are shown in dark gray.

refer to Sermeq in South Greenland or Upernavik Isstrøm in North-West Greenland. Also, in the references, the same problem appears for the variations Sermeq avangnardleq (“northern glacier”) or Sermeq kujatdleq (“southern glacier”). To provide a more precise location and avoid confusion, the code for the hydrological provinces indicated in figure 1 can be used with the glacier place-names.

Another problem is in the spelling of Greenlandic place-names. The original spelling (formalized in 1851) was altered after a spelling reform decreed by Greenland authorities in 1973, but it will take a long time before the modern spelling of Greenlandic place-names will appear on map sheets of Greenland. In this text, therefore, the older spelling is applied according to the National Survey and Cadastre’s map sheets, but the list given in table 1 gives an idea of the principles of the new spelling compared to the old.

TABLE 1.—*List of Greenlandic town names*

Danish usage	Conventional Greenlandic	New Greenlandic
Nanortalik	Nanortalik	Nanortalik
Julianehåb	Qaqortoq	Qaqortoq
Frederikshåb	Påmiut	Paamiut
Godthåb	Nûk	Nuuk
Sukkertoppen	Manîtsaq	Maniitsaq
Holsteinsborg	Sisimiut	Sisimiut
Egedesminde	Ausiait	Aasiaat
Christianshåb	Qasigiánguit	Qasigiannguit
Godhavn	Qeqertarsuaq	Qeqertarsuaq
Jakobshavn	Ilulíssat	Ilulissat
Umanak	Umánaq	Ummannaq
Upernavik	Upernavik	Upernavik
Thule	Qânâq	Qaanaaq
Scoresbysund	Igdlorqortôrmiut	Illoqqortoormiut
Angmagssalik	Tasîlaq	Tasiilaq

**European Place-Names**

Although Danish predominates the European-derived geographic place-names, a great variety of other nationalities have provided names to features in Greenland. When the place-names of the map sheets are used in the descriptions, a pleonastic style can result, such as “the island of Hovgaard Ø” (“the island of Hovgaard island”). In order to avoid this, it should be mentioned here that “Ø(er)” means island(s) “top(pe)”, “bjerg(e)”, or “fjeld(e)” means mountain(s); “Kap” means Cape; “Sund(e)” or “fjord(e)” means sound(s), inlet(s), or fjord(s); “klint(er)” means cliff(s); and “sø(er)” means lake(s). In glacier place-names, the Danish words for glacier (“bræ,” “jökul,” and “gletscher”) are borrowed from Norwegian (“jökul,” “bre”), Icelandic (“jökull”), or German (“gletscher”). The latter word dominates in more recent place-names. “Isstrøm” (Danish) was first used by H. Rink in the 1850’s for ice streams proper, but it has subsequently been used in a wider sense as names for outlet glaciers that exhibit significant calf-ice production. It should also be noted that “Scoresby Sund” designates the fjord complex, whereas “Scoresbysund” is the town at the fjord. The same rule applied to “Prins Christian Sund” and “Prins Christianssund,” the meteorological station at the sound. Table 12 is a list of geographic place-names of towns and natural features in Greenland cross-referenced to figures and tables included in the text. Alternative names are provided also, where more than one name is currently used or has been used historically. Table 13 is a list of the names and locations of scientific and other stations on the Greenland ice sheet.





**Figure 4.** —The estimated altitude of the present glaciation limit in Greenland. Contours (dashed where inferred) are given in meters (modified from Weidick, 1976). Contour interval is 250 m. Ice-free areas are shown in dark gray,

## General Glaciological Conditions

The estimated height of the glaciation limit, the lowest altitude at which glaciers can develop, is shown in figure 4. The topographic contours are based on the best available maps; therefore, the contour lines are very generalized, especially because the size of the smallest glaciers plotted varies from map sheet to map sheet.

Generally, in the ice-free coastal areas outside the margin of the Greenland ice sheet, the height of the glaciation limit roughly coincides with heights for the firn line of local ice caps and other glaciers, and this coincidence seems also in general to be the case with the Inland Ice.

Much emphasis is placed on the mass-balance conditions of the Inland Ice. In general, its marginal extent has changed very little during the last few centuries, although some outlet glaciers apparently have responded with great sensitivity to climatic change. For observed changes in termini positions of 5 km or more, the term “first-order variation” will be used in the following analyses of Landsat images. Even when the present errors in estimation are allowed for, the mass balance of the Inland Ice can be considered to be in a state of near equilibrium (Reeh, 1985). Using the new calculation of  $1,736,095 \pm 100 \text{ km}^2$  (Weng, written commun., 1995) as the area of the Greenland ice sheet, Reeh’s (1985) figures of  $1,440,000 \text{ km}^2$  (83 percent) as the area of accumulation and  $290,000 \text{ km}^2$  (17 percent) as the area of ablation of the ice sheet have not changed substantially.

**Figure 5.**—Distribution of precipitation in Greenland (in grams per square centimeter per year) from Reeh's 1984 compilation (Reeh, 1985). Contours dashed where inferred. Ice-free areas are shown in dark gray.



Figure 5 shows the distribution of precipitation over all of Greenland in grams per square centimeter per year (Reeh, 1985). The net balance over the accumulation area of the Inland Ice is estimated to be around  $+0.3$  to  $0.4 \text{ m a}^{-1}$  (water equivalent). The mean net balance in the ablation area is considered to be about  $-1.0$  to  $-1.3 \text{ m a}^{-1}$ , but these values are based on only a very few measurements, predominantly around Disko Bugt in West Greenland. Figure 6 shows the computed annual ablation in West Greenland in millimeters per year for the period 1965–74 (after Braithwaite, 1980b).

Table 2 shows five estimates of the total mass balance, the first four of which were discussed by Fristrup (1966). The estimates show that between 35 and 50 percent of the accumulation is released as calf ice and icebergs. Ice production from calving is concentrated in the Disko Bugt area and Umanak district of West Greenland. From these areas a long series of measurements on the rate of flow and on calf-ice production from the individual outlet glaciers was carried out by Bauer and others (1968) and Carbone and Bauer (1968). Table 3 lists the measured mean rate of movement in kilometers per year and the estimated calf-ice production in cubic kilometers per year of ice equivalent. The calf-ice-producing outlet glaciers attain maximum velocities of as much as 6 to 7  $\text{km a}^{-1}$  at their termini (table 3). Figure 7 gives the estimated calf-ice discharge from the Greenland ice sheet in cubic kilometers per year (water equivalent) (Reeh, 1985). The horizontal component of the rate of movement of the

TABLE 2.—Estimated mass balance of the Inland Ice (Greenland ice sheet) in cubic kilometers per year (water equivalent)  
[—, not calculated]

	Source				
	Loewe, 1936	Bauer, 1954	Benson, 1960, 1962	Bader, 1961	Reeh, 1985
Accumulation---	425	446	500	630	—
Ablation-----	295	315	272	120-270	—
Calving-----	150	215	215	240	310
Net -----	-20	-84	+13	+270 to +120	—

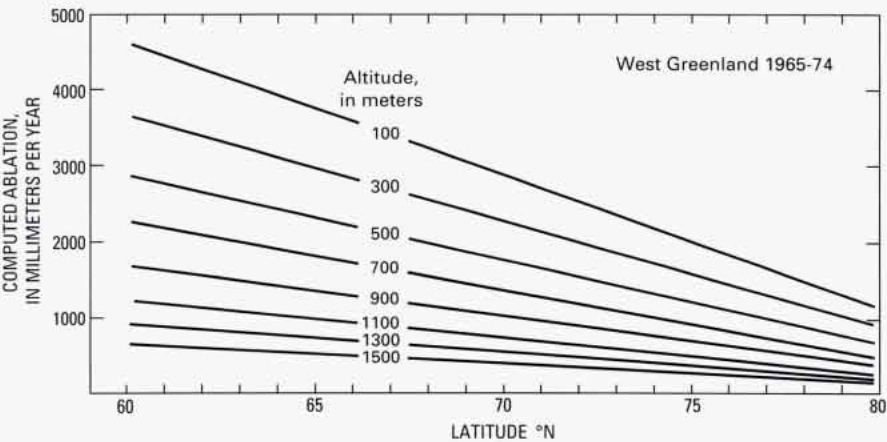


Figure 6.—Computed annual ablation in West Greenland in millimeters per year from work by Braithwaite (1980b).

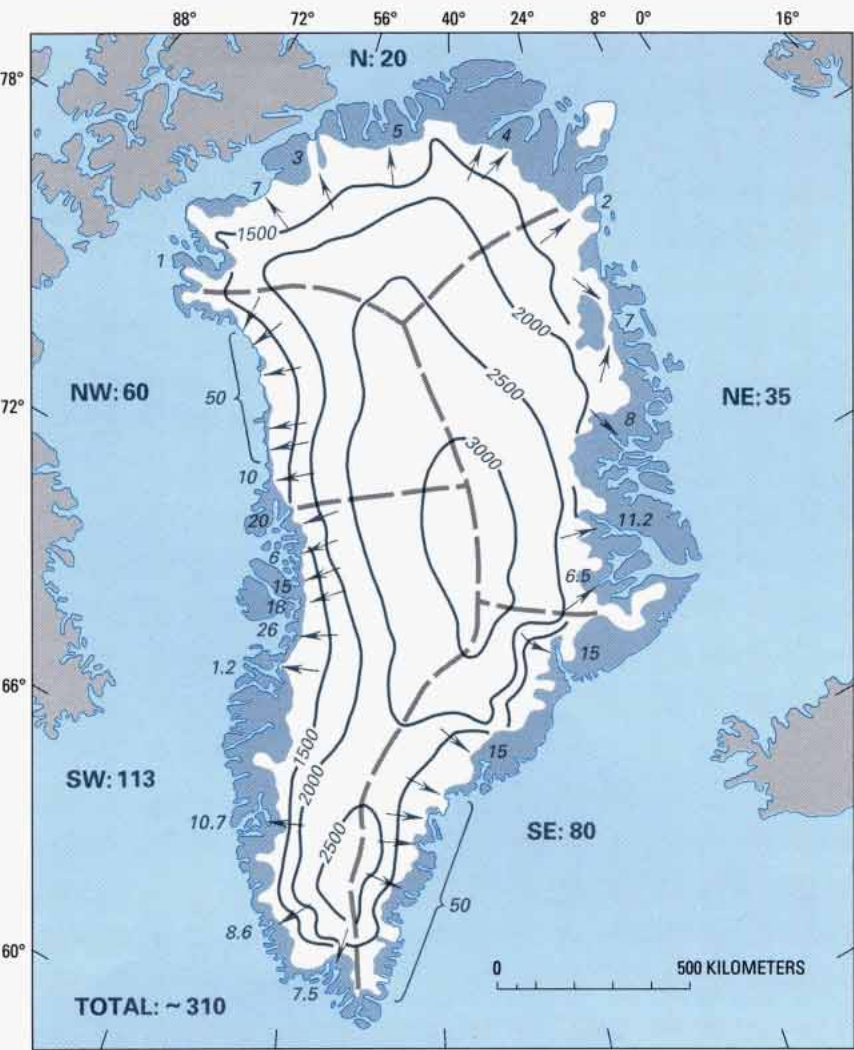


Figure 7.—Reeh's 1985 estimated calving ice discharge from the Greenland ice sheet in cubic kilometers per year water equivalent based on the assumption of an equilibrium state (Reeh, 1985). More recent estimates for the North Greenland calving ice production show the same total as given here (20 cubic kilometers per year), but with strong discrepancies in the figures for individual glaciers. The contours indicate elevation in meters.



TABLE 3. – *Estimates on the calf-ice production from tidal outlet glaciers of the Inland Ice*  
[V<sub>m</sub>, Range of mean rate of movement at front in kilometers per year; P, calf-ice production in cubic kilometers of ice per year; Do., ditto]

Glacier code	Name of glacier	V <sub>m</sub>	P	Reference or data source
South and South-West Greenland				
1AH08022 .....	Eqalorutsit kangigdlît sermiat	3.7	4.4	Knudsen (1983), Weidick (1988a). Weidick and Olesen (1980). Do. Do.
1AH06002 .....	Eqalorutsit kitdlît sermiat	3.7	2.5	
1IAI5001 .....	Sermilik Bræ	1.1	.2	
1BB05004.....	Arsuk Brae	.9	.1	
Central West Greenland				
1FC19002. ....	Nordenskiöld Gletscher	1.1–1.1	1.0–1.0	Bauer and others (1968); Carbournell and Bauer (1968).
1GB07001. ....	Sarqardliup sermia	.3–.3	2 - 2	Do.
1GB06001.....	Alángordliupsernia	.3–.3	.1–.1	Do.
1GC06002.....	Jakobshavn Isbræ	5–7	26–44	Do.
1GC04001.....	Sermeq avangnardleq	.4–.5	.2–2	Do.
1GF06001.....	Eqip sermia	.8–1.1	.7–1.0	Do.
1GF04001.....	Kangilerngata sermia	.8–1.2	8–15	Do.
1GH18001.....	Sermeq kujatdleq	2.6–3.5	8.4–9.9	Do.
1GH17001.....	Sermeq avangnardleq	1.9–2.3	4.8–8.1	Do.
1IB12001 .....	Store Gletscher	4.24.9	13.2–17.5	Do.
1IB11001 .....	Lille Gletscher	.4–.4	.1–2	Do.
1IB03001 .....	Sermilik	1.3–1.9	1.0–2.5	Do.
1IC09002 .....	Kangigdleq	1.5–2.2	1.0–1.5	Do.
1IC07001 .....	Sermeq silardleq	3.2–3.2	5.2–6.0	Do.
1ID20001 .....	Perdlerfiup sermia	.6–1.2	.4–.9	Do.
1IE24004 .....	Kangerdluarssûp sermia	.3–.4	.2–3	Do.
1IF.....	Kangerdlugssûp sermerssua	1.3–1.9	1.6–2.8	Do.
1IG.....	Rink Isbræ	3.7–4.5	10.5–16.7	Do.
1IH.....	Umiámáko Isbrae	1.4–1.9	1.2–2.0	Do.
1IL.....	Ingia Isbrae	1.2–1.2	1.1–1.1	Do.
Northern West Greenland				
1KG .....	Upernavik Isstrøm		6.4	R.C. Kollmeyer (written commun., 1984). Do.
1LC .....	Hayes Gletscher		7.7	
North-West Greenland				
2AB .....	Steenstrup Gletscher		7.9	R.C. Kollmeyer (written commun., 1984).
2AC .....	Dietrichson Gletscher		4.5	Do.
2AD .....	Nansen Gletscher		8.2	Do.
2AF .....	Kong Oscar Gletscher		7.7	Do.
2AG .....	Peary Gletscher		7.9	Do.
2AH .....	Rink Gletscher		3.0	Do.
2AH.....	Døcker Smith Gletscher		2.6	Do.
2BA .....	Gade Gletscher		9.8	Do.
2BA .....	unnamed glacier		6.6	Do.
2CE .....	Harald Moltke Brae	.03–1.0	.1–2	Mock (1966).
2D .....	Heilprin Gletscher		3.9	R.C. Kollmeyer (written commun., 1984).
2D. ....	Tracy Gletscher		4.0	Do.
North Greenland				
2E .....	Humboldt Gletscher		7.7	Do.
2F .....	Petermann Gletscher	.9	.6*	Higgins (1990).
2G .....	Steensby Gletscher	.4	.3*	
2G .....	Ryder Gletscher	.5	.7*	Do.
2H. ....	C.H. Ostenfeldt Gletscher	.8	.5*	Do.
2H. ....	Jungersen Gletscher	.4	.1	Do.
2H. ....	Henson Gletscher	.2	.04	Do.
2L .....	Mane Sophie Gletscher	.2–3	.1	Do.
2L .....	Academy Gletscher	.1–.3	.1	Do.
2L .....	Hagen Brae	.5	.5	Do.
2M. ....	Nioghalvfjærdsbræ—North	.2	.9	Higgins (1988).
2M.....	Nioghalvfjærdsbræ—East	.3	1.9	Do.

TABLE 3. – *Estimates on the calf-ice production from tidal outlet glaciers of the Inland Ice – Continued*

Glacier code	Name of glacier	$V_m$	P	Reference or data source
<b>North-East Greenland</b>				
2N.....	Zachariae Isstrøm-North	.3	2.4	Do.
2N.....	Zachariae Isstrøm-South	.5	5.0	Do.
2O.....	Storstrømmen	.2–1.8	–	Koch and Wegener (1930); Reeh and others (1993).
<b>East Greenland</b>				
3D.....	F. Graae Gletscher	1.4	1.0	Olesen and Reeh (1969).
3D.....	Charcot Gletscher	.5	.2	Do.
3D.....	Daugaard-Jensen Gletscher	3.0	10.0	Do.
3D.....	Vestfjord Gletscher	1.9	2.5	Olesen and Reeh (1973).

\* Occasional disintegration of floating front (ice-island formation).

calf-ice-producing outlet glaciers is extremely high at the front. For other parts of the ice margin, the rate of horizontal movement is usually greatest near the firn line (25 to 200 m a<sup>-1</sup>) and decreases upglacier and downglacier from the firn line (Nobles, 1960; Bauer and others, 1968).

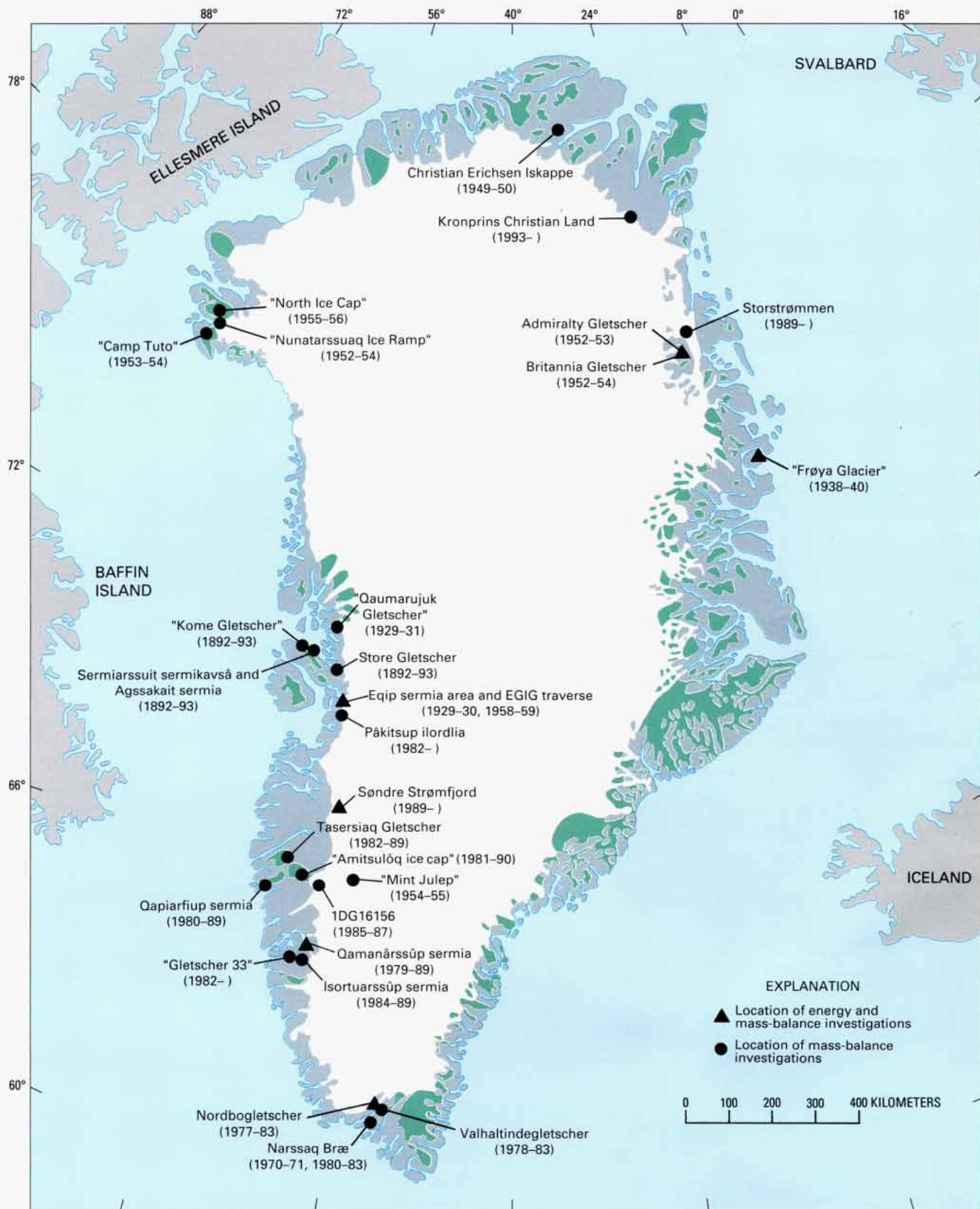
The information on the calf-ice production, as well as that of the frontal positions of these glacier lobes up to now, has been the result of time-restricted and isolated observations. It is therefore questionable whether the information is representative of termini positions in general. In addition, the heights of glacier termini are poorly known. Also, seasonal fluctuations of the termini of outlet glaciers might be large enough to make sporadic observations misleading. The use of Landsat images to monitor fluctuations will be valuable for future corrections and better overall estimates of calf-ice production.

## Field Measurements

Results from conventional mass- and energy-balance measurements are still scarce in Greenland, and, up to about 1980, measurements were confined to a few stakes and a maximum of 1 to 2 budget years at each locality. A review of most of this early work is given by Braithwaite (1980a). Because of the growing interest in hydroelectric power development, which will utilize discharge from outlet glaciers and from the margin of the Inland Ice, long-term mass-balance studies were initiated in West Greenland by The Geological Survey of Greenland in the late 1970's. The localities for long-term investigations are plotted on figure 8. The stations in West Greenland will supplement and add a good deal of information to the earlier measurements, carried out in the northern and northeastern parts of Greenland. A review of the results obtained in West Greenland has been given by Thomsen (1986), and a history of the glaciological work for the hydropower planning on the Inland Ice margin at Pâkitsoq near Jakobshavn was given by Thomsen and others (1988).

It should be emphasized that the main glaciological work on the Inland Ice in Greenland has been focused on the determination of accumulation on a regional (areal) scale (Benson, 1962), on studies of ice cores obtained from intermediate-depth and deep-drilling projects, and on airborne radio-echosoundings surveys (Gudmandsen, 1976, 1980). Ice-core analyses provide climatic as well as geologic information that covers the last 100,000 years (Dansgaard and others, 1969). Four deep-drilling projects penetrated to or near the bottom of the Greenland ice sheet. Drilling operations at ("Camp Century" in 1966 reached a depth of 1,371 m, and at "Dye-3" in 1981, they reached a depth of 2,037 m (Langway and others, 1985). Reeh (1989) evaluated the information provided by the deep ice cores and gave a review of the dynamic and climatic history of the Greenland ice sheet. The two most recent ice cores have been obtained

**Figure 8. – Location of energy and mass-balance measurements in Greenland.** Most measurements in West Greenland after 1980 have been made by The Geological Survey of Greenland (GGU). The dates in parentheses show the time span of measurements at each locality. The older measurements of West Greenland refer to investigations by the expeditions of Drygalski, 1891–93 (Drygalski, 1897), Wegener, 1929–31 (Loewe and Wegener, 1933), Schuster (1954), LaChapelle (1955), and Expédition Glaciologique Internationale au Groenland (EGIG) 1958–59 (Ambach, 1972). Those in North Greenland refer to the Snow, Ice, and Permafrost Research Establishment/[U.S. Army Corps of Engineers] Cold Regions Research and Engineering Laboratory (SIPRE/CRREL) investigations of 1952–56 (Schytt, 1955; Nobles, 1960; Goldthwait, 1971) and the Danish Peary Land Expeditions of 1949–50 (Høy, 1970). In East Greenland, data are from the Swedish Expeditions of 1938–40 (Ahlmann, 1942; Eriksson, 1942) and the British North Greenland Expedition of 1952–54 (Lister, 1958). Since 1989, new mass- and energy-balance measurements were initiated in connection with the EPOC (European Programme on Climatology and Natural Hazards) of the European Economic Community. These are located at Søndre Strømfjord (Univ. Utrecht, Netherlands), Pâkitsoq ilordlia (Univ. Zürich, Switzerland, and GGU, Denmark), and Storstrømmen and Kronprins Christian Land (Alfred-Wegener-Institut, Bremerhaven, Germany). Local ice caps and ice domes are shown in green. Ice-free areas are shown in dark gray.



from the “Summit” area. In 1992, the European Greenland Ice Core Project (GRIP) drilled nearly through the ice sheet and produced a 3,028.8- m-long ice core. In 1993, the second Greenland Ice Sheet Project (GISP2) sponsored by the United States drilled completely through the ice sheet, recovering 1.55 m of bedrock core and a 3,053.44-m-long ice core (Putscher, written commun., 1994) (see table 13 and plate 1 for the location of these four drill sites).

Remote sensing, especially radio-echosounding techniques, has already furnished promising contributions (Gudmandsen 1976, 1980) to the regional-scale mapping of the seasonal variations of the physical character of snow and ice and also the internal conditions of the ice sheet (for example, the extent of ice horizons). To achieve a better understanding and interpretation of the results of aerial and satellite remote sensing, it is also important to follow up Benson’s original mapping of glacier facies (Benson, 1962) with detailed mapping of the properties of the fresh snow on the surface of the Greenland ice sheet (Fushimi and others, 1979).

## **Glacier Variation**

Changes in climate alter mass balance, which alters the volume and areal extent of a glacier. Such volumetric and areal variations can be monitored on a local glacier by conventional methods of surveying; however, this work seems nearly impossible on the Inland Ice because of its enormous area and volume and the varying climatic conditions between its margins and interior and between its northern, central, and southern parts. Also, because the Greenland ice sheet is so extensive, different parts can have a different mass-balance at the same time. In fact, such work has been carried out only along a traverse from Disko Bugt to the “Station Centrale” by the Expedition Glaciologique Internationale au Groenland (EGIG) between 1960 and 1968 (Hofmann, 1964, 1974; Seckel, 1977).

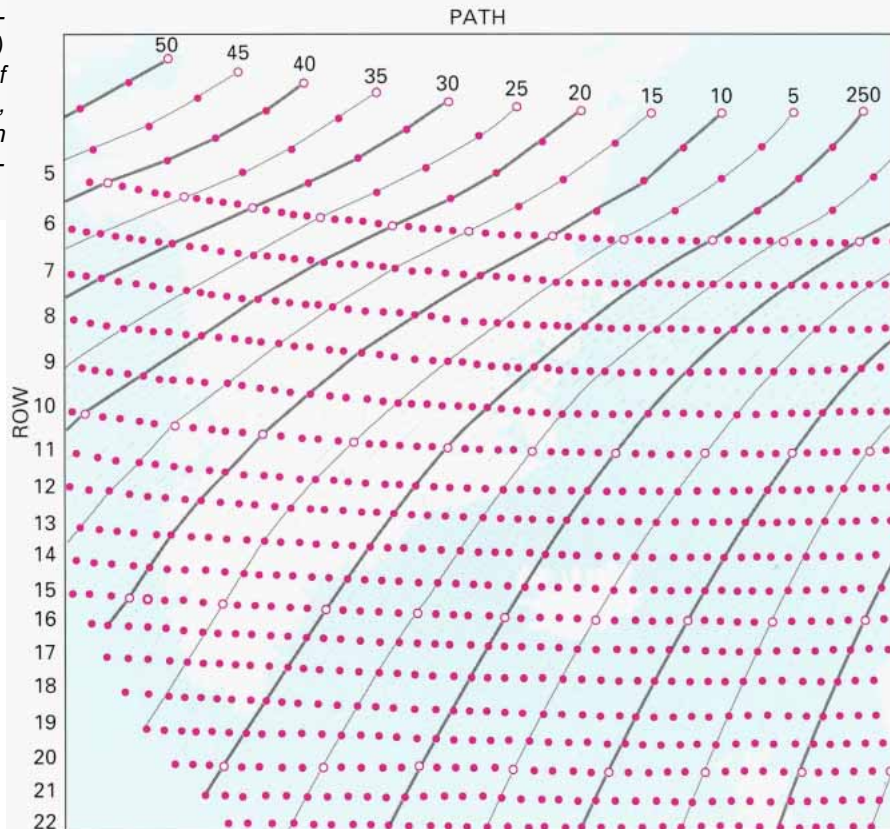
Much-improved geodetic ground surveys are now possible with the Global Positioning System (GPS) of satellites; radar and laser altimetry from satellites can provide data about elevations of the surface of the ice sheet (Brooks, 1979; Zwally and others, 1981; Bindshadler, 1984; Bindshadler and others, 1989; Zwally, 1989; Douglas and others, 1990) (fig. 3). Because new satellite-based technology has so radically changed surveying methods in remote areas, repeated detailed surveys of the surface of the Inland Ice are now feasible. Airborne laser altimetry surveys, combined with GPS, can provide geodetically accurate profiles of the ice sheet (Krabill and others, 1993; Thomas and others, 1993, in press a,b).

The final result of a change in climate and mass balance is a change in position of the glacier terminus. Although the response time for the same climatic fluctuation varies widely for individual glaciers, it would be valuable to determine to what extent fluctuations in margins of local ice caps, other glaciers, and outlet glaciers from the Inland Ice are in phase. An investigation of the variations in position of all outlet glaciers and the entire margin of the Greenland ice sheet is not realistic, but it would be possible to select glaciers for such an analysis by confining measurements to only those termini that have exhibited first-order variation ( $\geq 5$  km). In the following analyses of Landsat images, the results of a preliminary assessment are presented.

## **Analyses of Selected Landsat Images**

The Landsat satellite is able to acquire data of about 95 percent of Greenland, or all of the area south of about lat 81°30’N. Coverage is

**Figure 9.**—Nominal scene centers of Landsat 1, 2, and 3 multispectral scanner (MSS) and return beam vidicon (RBV) images of Greenland and environs. North of Row 5, only nominal scene centers for every fifth path are shown because of orbit convergence at higher latitudes.



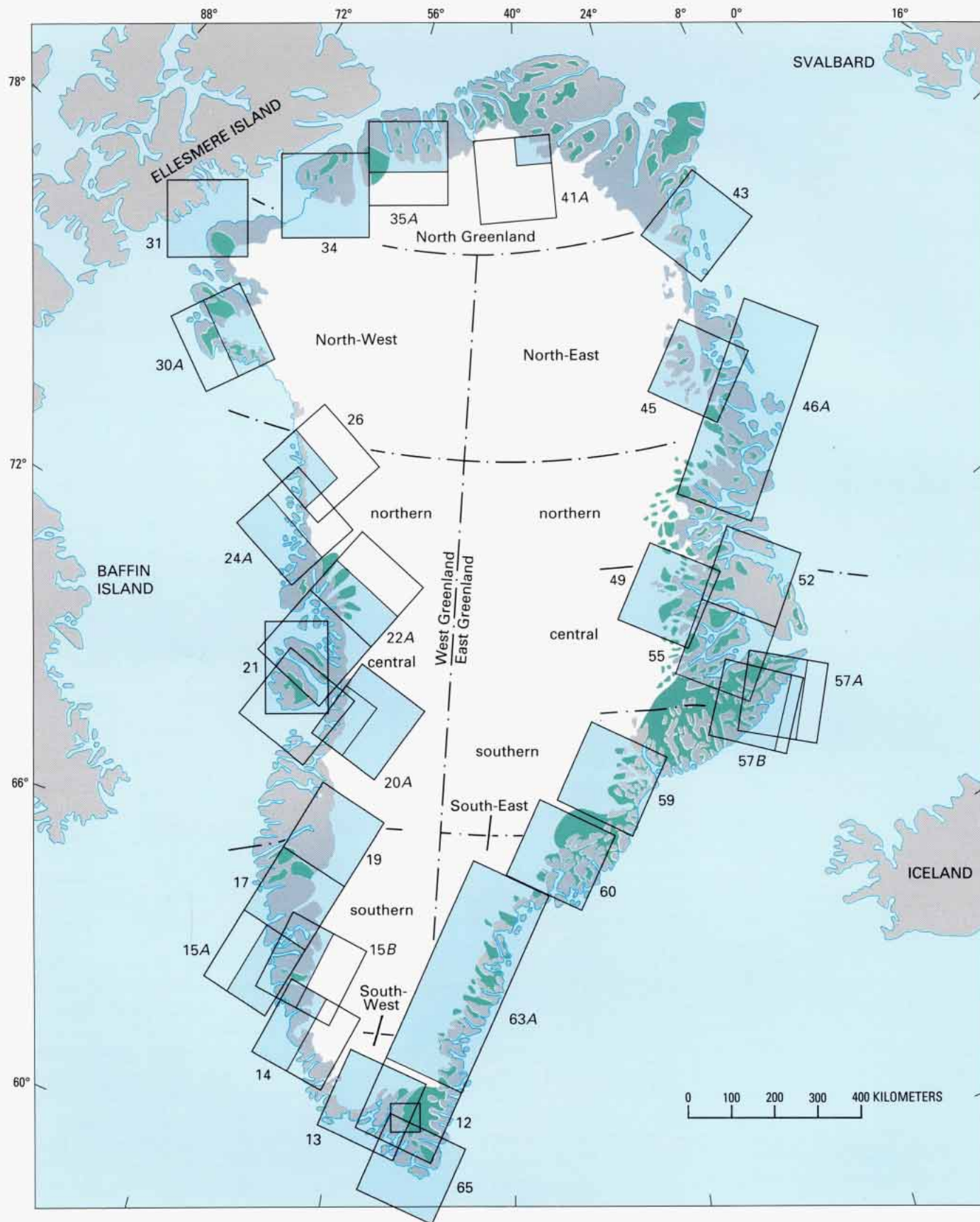
therefore available of most of the Inland Ice as well as some parts of the ice-free area on the northern margin of the ice sheet.

The Landsat orbital path traverses Greenland from northeast to southwest (Path 243 to Path 53, fig. 9). Data are acquired from Row 1 in the north to Row 18 at the southern tip of Greenland, a total of more than 450 Path/Row intersections. Although each of these Path/Row intersections, or nominal scene centers, determines the location of a scene covering Greenland, there is substantial overlap. If the overlaps were eliminated, about 100 scenes would be required to give complete Landsat coverage of Greenland.

Landsat imagery of Greenland has been acquired since 1972 and has been archived by the United States at the EROS Data Center, Sioux Falls, S. Dak.; by the European Space Agency, Kiruna, Sweden, and Frascati, Italy; and by the Canada Centre for Remote Sensing, Ottawa, Canada. More than 2,000 multispectral scanner (MSS) and return beam vidicon (RBV) images were acquired between 1972 and 1982 by Landsats 1, 2, and 3; most of these images were examined and evaluated to determine the optimum imagery for glaciological purposes for Greenland. The optimum images for each nominal scene center are listed in table 14 and coded on figure 67. Optimum images of the margins of the Inland Ice are usually acquired in late summer, at the end of the ablation season, after maximum snowmelt has occurred. Optimum images for the interior parts of the Greenland ice sheet are usually acquired during October or February, when subtle surface morphology is emphasized by the low solar elevation angle. See section "Landsat Images of Greenland" for a more complete evaluation and discussion of the subject.

In the following discussion, only a selection of scenes that represent the best of the available images showing glaciological features characteristic of Greenland has been used. The location of the selected Landsat images is shown in figure 10.





**Figure 10.**—Areal coverage of Landsat images used as illustrations in the text. The outline indicates coverage of a total Landsat scene or sequence of scenes along an orbital path. The darker blue area indicates the part of the scene used in the numbered figures.

# West Greenland

## Climatic Conditions

The patterns of annual precipitation, as shown on figure 5 and in table 4, indicate a decrease in precipitation from south to north along the west coast of Greenland. Relatively continental conditions are associated with the inland parts of the ice-free coastal strip, where annual precipitation at the margin of the Inland Ice at lat 67° N. measures only 145 mm (at the Sandre Strømfjord Air Base).

Continentality is also evident in table 4, which provides data on temperature and precipitation at Sandre Stramfjord and Narssarssuaq. These are both inland meteorological stations, whereas all the others are close to the coast.

The instrumentally recorded climatic fluctuations since the last century are discussed in detail by Lysgaard (1949). He states that the January mean temperature at Jakobshavn rose 4.4 °C from the 1882–1911 mean to the 1911–40 mean; the July mean temperature rose 0.4 °C from the 1875–1904 mean to the 1907–36 mean, while the annual mean temperature rose 1.9 °C from the 1882–1911 mean to the 1911–40 mean. The primary warming period took place during the 1920's. Since the 1950's, firn coring on the Inland Ice (Dansgaard and others, 1973) indicates a subsequent cooling trend that has been seen also in the updating of climatic records shown on figure 47. Temperature conditions are now similar to those of the 1920's.

Fluctuations in precipitation have been studied by Vibe (1967) and Weidick (1968). No clear trends are evident, nor do the data allow tracing of any zonal shift of precipitation maxima or minima.

## Glaciological Conditions

Local ice caps and local glaciers are concentrated in regions around southernmost Greenland, especially in the following areas: Godthåb, Sukkertoppen, Disko-Nûgssuaq, and Svartenhuk Halve. Connections of local ice caps to the Greenland ice sheet occur at the ice caps in the Sukkertoppen region and in South Greenland. The line of demarcation between the two glacier types is not obvious in South Greenland but can be more or less placed at the depression in the ice cover east of Narssarssuaq (see fig. 13).

The greatest apparent response to climatic fluctuations is shown by some of the calf-ice-producing tidal outlet glaciers of the Inland Ice, often by those that have the highest calf-ice production. On the Landsat images these tidal outlet glaciers are associated with easily delineable ice

TABLE 4.—Average temperatures for the months of January and July, annual average temperatures, and annual precipitation at selected stations in West Greenland  
[Data refer to 1961–70 averages from the Danish Meteorological Institute, Copenhagen]

Station	Location		Average temperatures (°C)			Average annual precipitation (millimeters per year)
	°N lat	°W long	January	July	Annual	
Julianeabåb . . . . .	61	46	−3.3	+7.2	+1.4	860
Narssarssuaq . . . . .	61	45	−4.2	+10.2	+1.7	606
Godthåb . . . . .	64	52	−5.8	+6.6	−.8	839
Søndre Strømfjord . . . . .	67	51	−20.9	+10.5	−6.3	145 <sup>1</sup>
Holsteinsborg . . . . .	67	54	−10.7	+6.2	−3.1	350
Jakobshavn . . . . .	69	51	−11.8	+8.0	−3.6	244
Upernavik . . . . .	73	56	−16.6	+4.9	−6.9	267

<sup>1</sup> Measurements 1981–90.

streams that extend deeply into the Greenland ice sheet (see figs. 20 and 22). The production of calf ice in West Greenland in general is related to the continuous release of small or large parts of the floating terminus and only rarely by disintegration of parts of the floating lobes.

Although the main production of calf ice from Greenland glaciers is concentrated in outlet glaciers from the Inland Ice in central West Greenland around Disko Bugt and Nûgssuaq peninsula (see fig. 7), only the inner parts of the ice-filled fjords generally are inaccessible for boats. Farther out, the scatter of the icebergs can be seen clearly on the Landsat images. Frequent calving, calf-ice storage, and dispersal of icebergs depend on currents and variations of the sea-ice cover, which also can be monitored on the Landsat images (Stove and others, 1984?).

## Mass-Balance Investigations

Mass-balance investigations have been made at the stations shown on the map in figure 8. However, only in a few cases do the older observations cover a total budget year. Even then, comparisons between different localities are difficult because of different nomenclature and techniques of measurement (Braithwaite, 1980a).

Present-day mass-balance investigations have been concentrated in West Greenland in connection with the mapping of hydropower potential in this region. The investigations were initiated in 1977 and in 1988 covered four outlet glaciers from the Inland Ice and four local glaciers distributed over the localities shown in figure 8. More recently, measurements have been made in connection with climatology and natural hazard studies.

The investigations of hydropower potential originally included glaciers in South Greenland at lat  $61^{\circ}$  N., but the investigations there ended in 1983. The South Greenland investigations covered 2 local glaciers (Narssaq Brae and Valhaldindegletscher) and one outlet glacier from the Inland Ice (Nordbogletscher). The results from the budget years 1982–83 are shown in figure 11 and illustrate the decrease of the height of the equilibrium line altitude (ELA) from the interior of the coastal region (1,300–1,400 m at Nordbogletscher and Valhaldindegletscher) to 70 km closer to the outer coast (1,000–1,100 m at Narssaq Brae), according to Clement (1984a). The trend in height is concordant with that of the glaciation limit, as shown in figure 4.

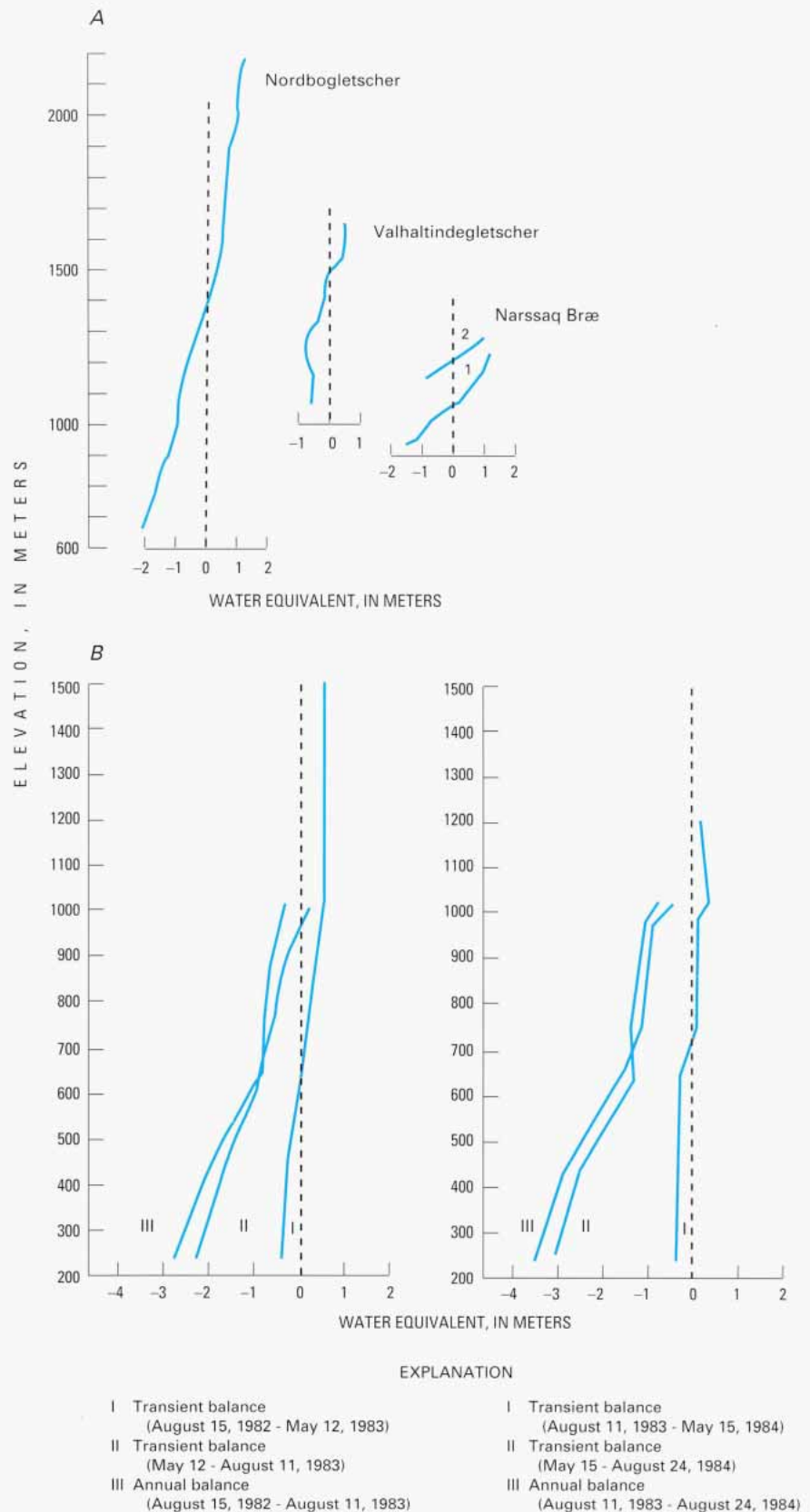
The same trend of the decrease of the height of the ELA from the interior of West Greenland to the outer coast can be demonstrated for the other localities of West Greenland shown in figure 8. An example is “Amitsulôq ice cap” (an ELA of about 1,050 m) in the inland region for the budget year of 1981–82 compared to Qapiarfiup sermia at the coast (an ELA of about 800 m), 110 km southwest of “Amitsulôq ice cap,” in the same budget year (Olesen and Andreasen, 1983). Both sites are located at about  $66^{\circ}$  N.

The mass-balance series from West Greenland localities also allows for a determination of the variation in trends of the annual mass-balance curves at the single locality and, therefore, also in variations of the height of the ELA from year to year. An example of these variations is shown in figure 11 from Pâkitsuip ilordlia near Jakobshavn, Disko Bugt, at  $69^{\circ}$  N. (Thomsen and others, 1988). The height of the ELA at the Inland Ice margin at this locality was 1,030 m in the budget year 1982–83 and between 1,200 and 1,300 m in 1983–84. Calculated variations of the ELA on the basis of the climatic record from Jakobshavn and the mass-balance measurements were made by Braithwaite and Thomsen (1984a); they indicated a mean height of the ELA of 1,300 m for the period of 1961–83.



Ice ablation on the southwestern slope of the Inland Ice shows a close correlation to temperature and poor correlation to global radiation, according to the investigations of Braithwaite and Olesen (1984).

Determination of the total annual mass balance in terms of total annual gain or loss of water volume can be undertaken in Greenland in the



**Figure 11.** Mass-balance curves in relation to elevation, measured at localities in South and West Greenland. **A**, Net-balance curves for two local glaciers (Valhaltindegletscher and Narssaq Bræ, the latter consisting of two nearly separate units, indicated 1 and 2 in the figure) and for Nordbogletscher, a part of the Inland Ice margin. All localities are situated in South Greenland and all results are from the budget year of 1982-83. Narssaq Bræ is situated close to the outer coast, whereas Nordbogletscher and Valhaltindegletscher are situated inland (from Clement, 1984a). **B**, Mass-balance curves from the Inland Ice margin at Pâkitsup ilordlia near Jakobshavn (from Thomsen and others, 1988). The curves of the two consecutive budget years of 1982-83 and 1983-84 illustrate the annual variation of ablation conditions.

conventional way for the local glaciers (cirque glaciers, valley glaciers, and ice caps). This is possible because total glacier area and areal distribution can be determined on the basis of the surface mapping of the glacier, and the mass-balance results can be controlled by adherent discharge measurements of meltwater at the glacier margin. For outlet glaciers of the Inland Ice, the delineation of the specific glacier area that is connected to the specific outlet or marginal sector of the Inland Ice is difficult to define. Determination of the size of the accumulation or ablation area here requires a detailed knowledge of both the surface and subsurface topography, and monitoring of water loss requires knowledge of variations in englacial and subglacial drainage of meltwater during the ablation season. A total study to determine the feasibility of hydropower exploitation at a given site of the Inland Ice margin therefore requires application of remote sensing, radio-echosounding, and ice drilling operations to an extent that usually is not required for local glaciers. The total procedure of such an investigation of a sector of the Inland Ice margin is described for Pâkitsup ilordlia by Thomsen and others (1988). In addition to delineation of the individual sectors of the ice sheet, other problems such as meltwater retention in snow and the land heating effect between the ice-free coastal areas and the margin of the Inland Ice exemplify the serious difficulties encountered in the theoretical determination of the meltwater discharge from local Greenland ice caps as well as from the Inland Ice.

Although the western slope of the Inland Ice has attracted the greatest interest for mass-balance measurements, the extent of the slush zone (Muller, 1962) or slush facies (Williams and others, 1991), the undefined lower part of the wet-snow facies of Benson (1967) and Benson and Motyka (1979), is extremely difficult to measure, owing to its wide extent (30–50 km wide). The only detailed investigations in such an area were made by the U.S. Army at Camp “Mint Julep” (lat 66°17' N., long 47°46' W.), located on the western slope of the Inland Ice at 1,800 m. The net ablation was given as  $0.6 \text{ m a}^{-1}$  water equivalent (LaChapelle, 1955). Figures 17 and 19 demonstrate the extent and appearance of this zone on Landsat images and also the problems of determining its meltwater conditions. Williams (1987), in his analysis of Landsat MSS images of the Vatnajökull ice cap in southeastern Iceland, and Williams and others (1991), in their analysis of Landsat thematic mapper (TM) images of Brúarjökull outlet glacier, Iceland, have endeavored to correlate spectral reflectance, as measured by the MSS or TM sensors, with the concept of glacier facies as initially developed by Benson (1959) and Muller (1962) and later modified by Benson (1961, 1962, 1967) and Benson and Motyka (1979). Thomsen and Thomsen (1986), Thomsen and Braithwaite (1987), and Thomsen and others (1988) have used remote-sensing data in modeling runoff from the ice sheet margin for hydropower planning.

## Glacier Variations and Glacier Hazards

Relatively good records are available on glacier variations throughout the last 100 to 150 years for some of the outlet glacier lobes in West Greenland. Weidick (1968) pointed out that some glacier fronts began to recede in the early part of the 19th century in the southern part of West Greenland, but the general tendency for recession did not become evident until around 1890. The main recession took place between 1920 and the 1950's, but, since then, a growing tendency to readvance has been noticed for many local glaciers and also for sectors of the Inland Ice.

First-order variations ( $\geq 5$  km) are shown by some calf-ice-producing outlet glaciers from the Inland Ice and by deglaciation of valleys that were covered by piedmont glaciers earlier in this century. These glaciers are tabulated in tables 5 and 6 with reference to the figures on which they appear. As will be seen from the descriptions of the figures, readvances are still not common at these localities, although they might be more frequent in the future, if they follow the general trend exhibited in neighboring localities.

The occurrence of surging local glaciers has been reported from the Disko and Nûgssuaq areas, where a number of glaciers have had a period of pronounced surge activity during the Little Ice Age. More tentative documentation of surgelike behavior of outlet glaciers has been reported by Weidick (1988a,b) for Sermeq, an outlet glacier from the ice cap in the southernmost part of Greenland (see fig. 12), and Eqalorutsit kitdlît sermiat, an outlet glacier from the south slope of the Inland Ice (see fig. 13).

Glacier hazards encompass phenomena such as glacier outburst floods (jökulhlaups) from ice-dammed lakes and ice avalanches, and a review of records of these events from West Greenland has been given by Weidick and Olesen (1980). As long as the main human activity is confined to settlements close to the outer coast, there will be little actual interest for research in these subjects. However, with the spread of mining and tourism into the inland regions, the hazards will attract increasing interest.

Jökulhlaups from ice-dammed lakes have been reported frequently, the largest ones releasing volumes of several cubic kilometers of water. Refilling of lakes between jökulhlaups usually takes several years, and satellite monitoring can give an approximate prediction of the anticipated occurrence of jökulhlaups. For example, Rist (1974) used a combination of successive Landsat images and field observations in Iceland to measure the volume of water discharged after a jökulhlaup from Grænalón, an ice-dammed lake on the southwestern margin of Vatnajökull.

TABLE 5.—Selected calf-ice-producing outlet glaciers from the Inland Ice in West Greenland known or observed to have had historic termini fluctuations of  $\geq 5$  km (first-order variations)

Glacier code	Name	Reference
1AC07020	Sermeq	Fig. 12
1AH06002	Eqalorutsit kitdlît sermiat	Fig. 13
1CH23003	Kangiata nunâta sermia	Fig. 15, 16
1CH06002	Jakobshavn Isbræ	Fig. 20
1IH	Umiámáko Isbræ	Fig. 22
1KG	Upernavik Isstrøm	Fig. 24
1KK	Giesecke Bræer (collective name for Qeqertarsûp sermia and Kakivfait sermiat)	Fig. 24, 25
1KL	Ussing Bræer	Fig. 26
1LC	Hayes Gletscher	Kollmeyer (1980)

In West Greenland, records of the largest ice-dammed lakes have been published by Weidick and Olesen (1980). The largest one described in West Greenland is Iluliagdlop tasia, which is situated between two large ice caps in the Sukkertoppen region at lat 65°45' N. (see figs. 17 and I8), and the most well known is Hullet at the south slope of the Inland Ice near Narssarssuaq (see fig. 13). Hullet is described further in the next section.

Recent investigations of a great ice-dammed lake (Tiningnilik) at the Inland Ice margin near Christianshåb at lat 69° N. (see fig. 20) were made by Braithwaite and Thomsen (1984b). They determined an upland

TABLE 6. — *Selected land-based glaciers, West Greenland, exhibiting first-order variations*

Glacier code	Name	Figure in text
1DF20002	Evighedsfjord (head)	17
1HB15029	Kuánerssui	21

ablation area on the Inland Ice margin by means of digital processing of Landsat scenes and based the filling of the lake on the ablation computed from information on mass-balance measurements and the climatic record at Jakobshavn. The variations of the lake level were determined for the period 1942-83, and the time for filling Tinínílik was determined to be 9 to 10 years, after which a release of nearly 2 km<sup>3</sup> of water took place. The determined interval of 9 to 10 years agreed with the record of aerial photographs and Landsat images and also with the older records on the time of filling of the lake reported by Koch and Wegener (1930) from a visit at the locality in 1913. Ice avalanches have been described only rarely in Greenland, but damage to buildings has been reported from South Greenland and southern West Greenland (Weidick and Olesen, 1980).

## Images of South Greenland

This area is covered by the Landsat scenes presented in figures 12 and 13. Figure 12A shows the Sermeq glacier at the head of Søndre Sermilik fjord, where a well-documented total recession of 11 km during this century for the terminus of the glacier is indicated on the sketch map (fig. 12B). Information since 1972 is derived from sequential Landsat images, which confirm a rapid recession since the last aerial photographs of the area were acquired in 1953. The final disappearance of the tidal outlet glacier in the 1960's is believed to be the result of the general thinning during the preceding years (Weidick, 1988a). The terminus of the outlet glacier is now partly on land. A future readvance of the Sermeq glacier may be expected if, as hypothesized by Post (1975), it exhibits the cyclical retreat-advance behavior of about 50 tidal outlet glaciers in Alaska. The possible resulting advance could be monitored easily by successive satellite images.

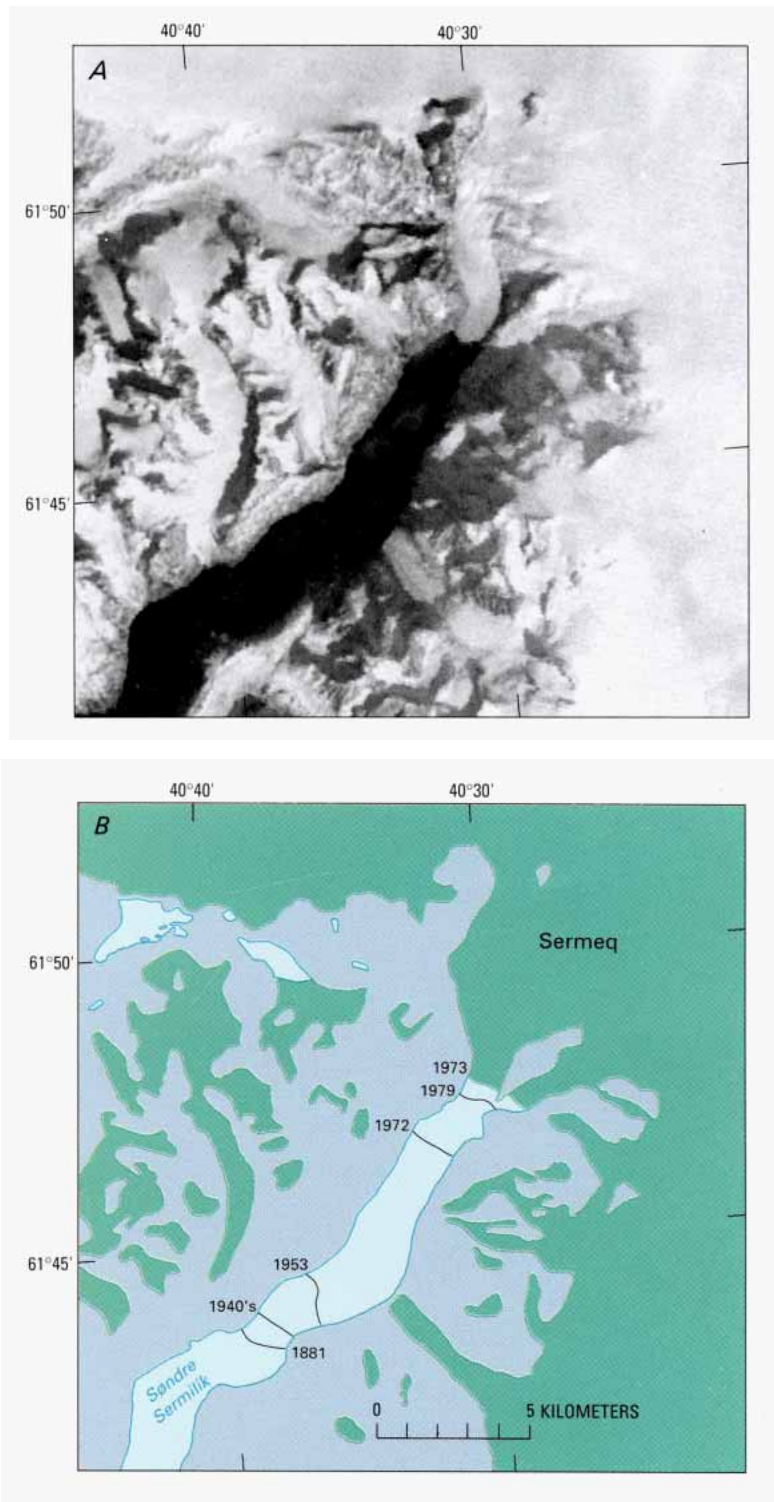
In figure 13, the entire area around Tunugdliarfik fjord is shown, and the Landsat image covers the towns of Narssaq and Julianehåb (Qaqortoq), as well as Narssarssuaq, the center of tourism in Greenland. The coastal landscape forms a deep reentrant in the southern margin of the Inland Ice proper, and a subglacial continuation of the main patterns of this feature can be traced to the interior nunataks (around peak 2,820 m) and even farther to the east coast.

The southern border of the Inland Ice can be placed approximately at peak 2,163 m. Because of the low solar elevation angle, the subglacial ridges between the protruding nunataks can be traced, so a more detailed picture of the subglacial landscape can be delineated than by contours on a topographic map.

The calf-ice-producing outlet glaciers of the Inland Ice are Qôrqup sermia, Eqalorutsit kangigdlît sermiat, and Eqalorutsit kitdlît sermiat, which have a combined estimated calf-ice production of a few cubic kilometers per year (Weidick and Olesen, 1980). Flow patterns on the surface of these outlet glacier lobes indicate the main flow direction of these ice streams in the Inland Ice.

The lack of snow cover on the outlet glaciers described above and on the surrounding terrain up to an elevation of 500 m is pronounced, in spite

**Figure 12.**—A, Part of a Landsat 3 MSS image showing the head of Søndre Sermilik, South Greenland. The Landsat image (30750-13300, band 5; 24 March 1980; Path 1, Row 17) is from the European Space Agency, Kiruna, Sweden. B, Variation in the position of the terminus of Sermeq in Søndre Sermilik between 1881 and 1979.



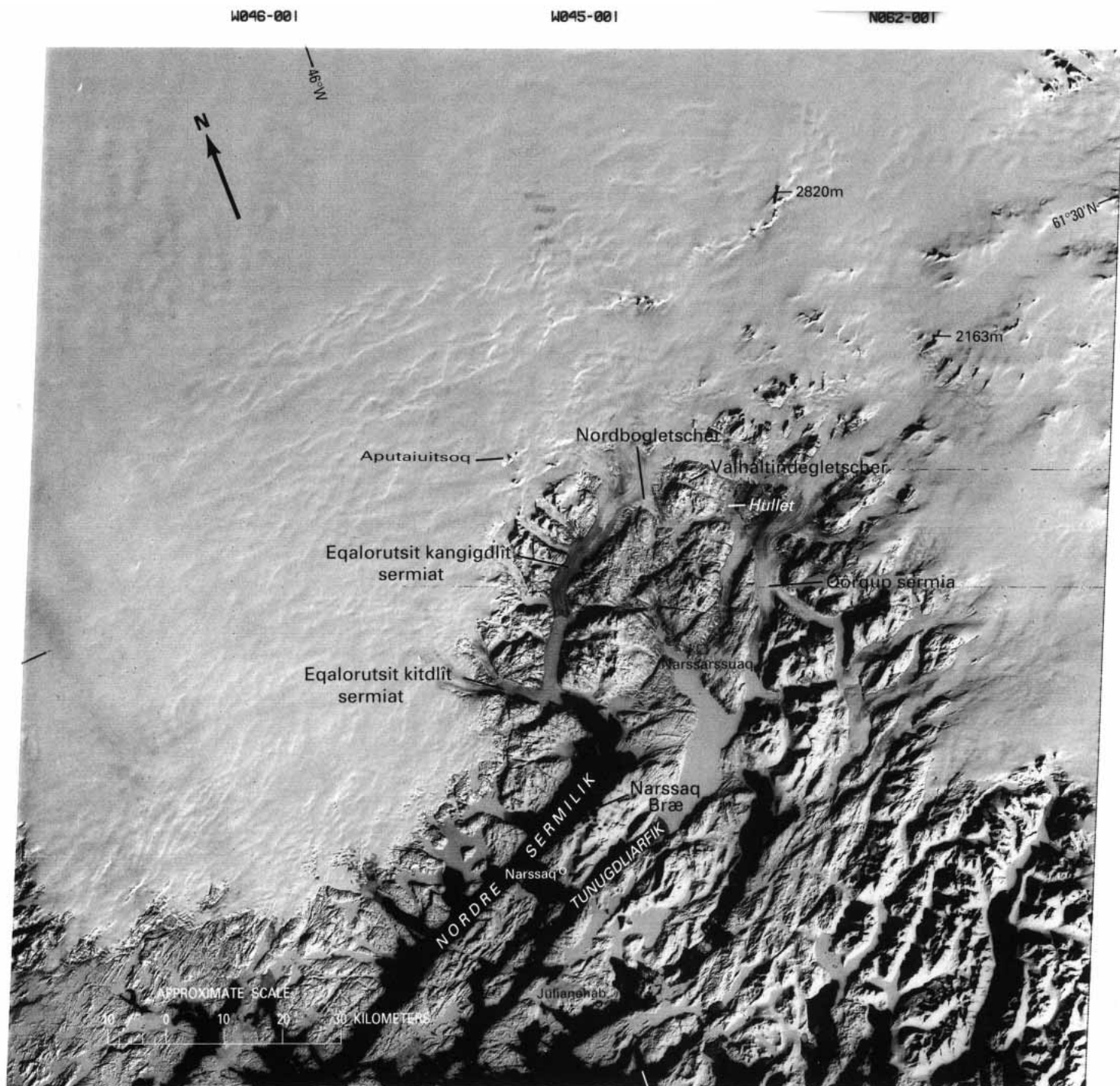
of the season (late winter). The lack of snow is ascribed to the frequent occurrence of foehn winds from the Inland Ice, which occur mainly during the winter months.

Ice-dammed lake Hullet is indicated on figure 13; Hullet is known for its periodic glacier outburst floods (jökulhlaups). The jökulhlaups occur under a glacier lobe, flow down valley to Narssarssuaq, and take place at intervals of 1 to 2 years, each time releasing about 0.5 km<sup>3</sup> of water (Dawson, 1983; Clement, 1984b). The lake level shown on the image is close to its maximum height.



A remarkable pattern in the behavior of the Inland Ice margin shown on figure 13 has been taking place. Strong thinning and retreat of the Inland Ice margin from the middle of the 19th century are documented for that part of the ice margin north of Nordre Sermilik to Eqalorutsit kitdlit sermiat. This last lobe was already known to be undergoing recession in 1894. Throughout the 20th century, it has continued to retreat approximately 4 km, although indications are that this recession has been interrupted by surgelike readvances. The sector around Eqalorutsit kangigdlit sermiat (including Nordbogletscher) has had a continuous expansion of its margin during the present century. The advance has buried old soil, so this expansion must be considered to be

**Figure 13.**—Annotated Landsat 1 MSS image of the southern margin of the Inland Ice. Landsat image (1228-13531, band 7; 8 March 1973; Path 2, Row 17) from the EROS Data Center, Sioux Falls, S. Dak.



00MAR73 C N61-24/W045-43 N N61-22/W045-36 MSS 7 R SUN EL22 AZ158 198-3177-N-1-N-D-IL NASA ERTS E-1228-13531-7 01

the largest one during postglacial time. On the other hand, farther south, in the region around Narssarssuaq, the general recession is like that north of Sermilik fjord and is well documented. The long-term advance of a local sector of the Inland Ice might be explained by a local shift of direction of flow of the glacier caused by the general thinning of the margin of the Inland Ice during this century or by a shift in the distribution of the accumulation over the south slope of the Inland Ice.

## Images of Southern West Greenland

The region is covered by four Landsat scenes; the two southernmost (figs. 14 and 15) illustrate the general character of the landscape in the southern part of the area. In this part of Greenland, the ice-free coastal strip is relatively narrow and has numerous alpine peaks. The two northern images show the inner and wider northern part of the strip of land as having plateaus, local ice caps, and the Inland Ice margin (see figs. 17 and 19).

Figure 14 shows the Inland Ice margin from Frederikshåb Isblink to Sermilik fjord, an area situated between the towns of Frederikshåb (Pâmiut) and Godthåb (Nûk). On the black and white image (fig. 14A), it is evident that Frederikshåb Isblink has undergone strong thinning, because a clear trimline zone surrounds its terminus. Although noticeable thinning had already been described in 1878, most of the thinning has occurred during this century. Because of the thinning, the southern parts of the glacier's terminus are covered with an extensive ablation moraine. The concentric zonation of the ablation moraine indicates its origin as a shear moraine, which has formed by the thinning of the ice margin. The curvilinear orientation of medial moraines at the upper parts of the southern margin of Frederikshåb Isblink, and at Sermilik (the glacier in the head of Sermilik fjord), provides evidence for changes in flow of different parts of the margin of the Inland Ice.

Ice-dammed lakes are found along the entire ice margin, and a reduction in level of the large lake at the northern flank of Frederikshåb Isblink is indicated by a marked trimline. Recurrent draining is not recorded for these ice-dammed lakes. The great amount of silt in the meltwater from the Inland Ice is evident because the connected lakes are gray (clear water appears black).

The right-hand Landsat image (fig. 14B) is a false-color infrared composite version of the same image shown in figure 14A. The pink represents shrub vegetation, which grows primarily on south-facing slopes. The approximate extent of the ablation area is shown by the blue of the ice margin at Frederikshåb Isblink as well as at Sermilik, and flow patterns indicate the main trunk of the outlet glacier.

The transient snowline (boundary between bare glacier ice or superimposed ice and firn or newly fallen snow) is between 700 and 900 m to the south and over the outer coast and 1,000 to 1,300 m to the north and over the Inland Ice. The local ice caps are clearly discernible because of their zonation of white firn and blue ablation areas. The light blue of the lakes and fjords indicates glacial rock flour (finely disseminated sediment in suspension) being carried into these water bodies by runoff from outlet glaciers along the margin of the Inland Ice.

Figure 15 also consists of two images, which cover the area of Godthåbsfjord in its total extent. On the left-hand false-color infrared composite image (fig. 15A), the transient snowline increases from 400 m



at the outer coast to about 1,000m in the inland areas. Therefore, only on the largest and most active outlet glaciers of the local ice caps, which cover the alpine landscape between Alángordlia and Buksefjorden, are blue ablation areas visible. The relatively dense arctic vegetation (mainly heather and willow shrub) in the interior parts of the fjords is recorded in pink, whereas the location of the town of Godthåb appears gray-white. In Buksefjorden the first hydroelectric powerplant in Greenland was opened on 1 October 1993, supplying the capital, Godthåb (Nûk), with energy.

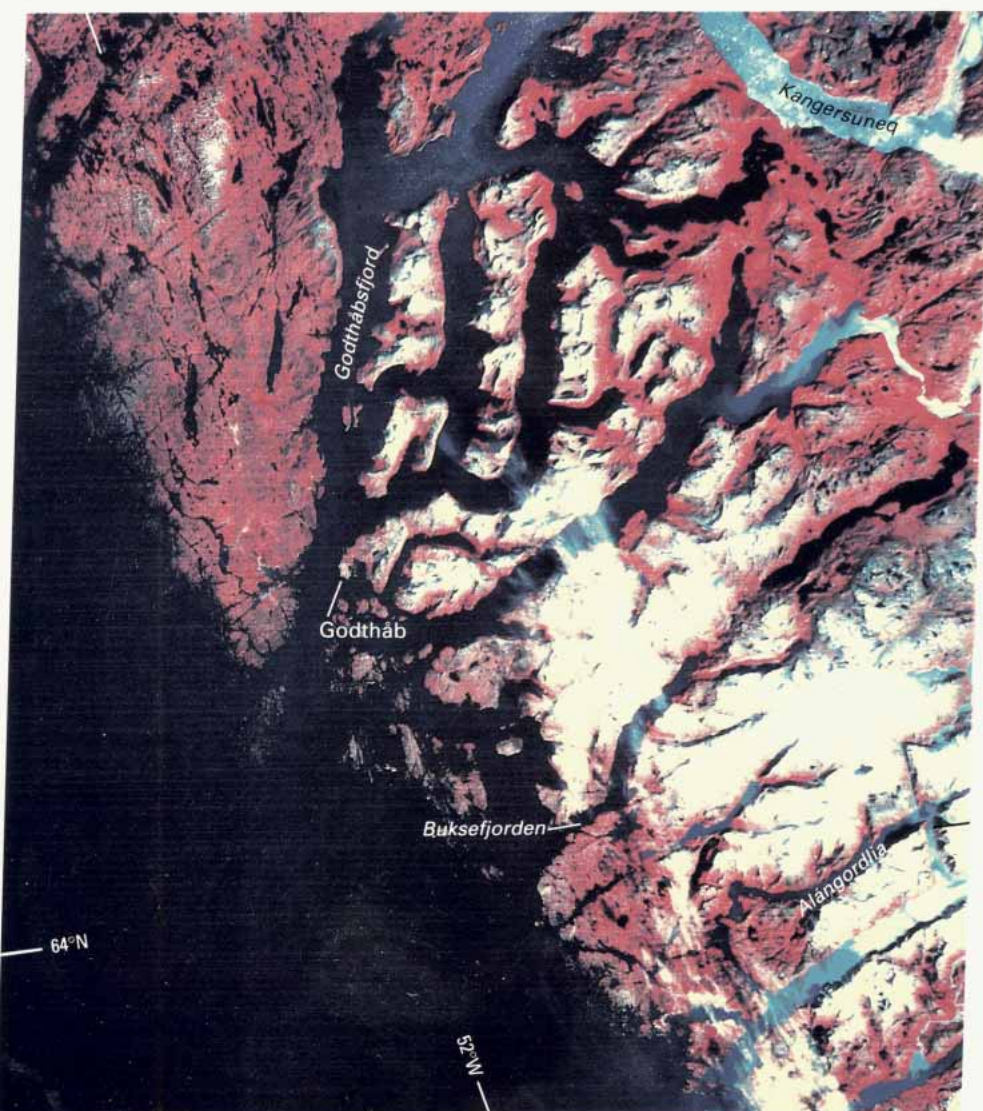
On the right-hand Landsat image (fig. 15B), the scene shows the interior parts of Godthåbsfjord and the ice-occupied tributary fjord of Kangarsuneq. The Inland Ice margin between Isortuarssûp sermia (outlet glacier) and the area around Isukasia also is visible.

The height of the transient snowline is estimated at 600 to 800 m. Three calf-ice-producing outlet glaciers of the Inland Ice, Kangiata nunâta sermia, Akugdlerssûp sermia, and Narssap sermia, can be identified. The total calf-ice production from these outlet glaciers is estimated to be

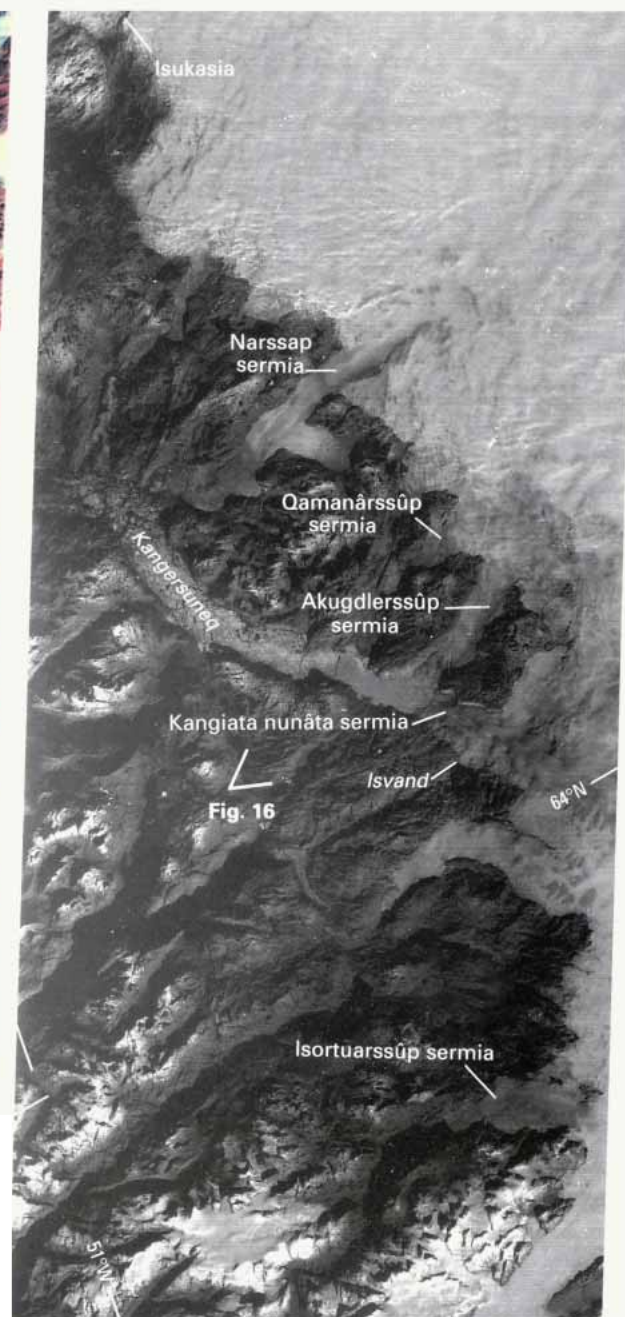
**Figure 14.**—Annotated parts of two versions (one black and white, one color) of the same Landsat MSS image of the Inland Ice margin of South-West Greenland including Frederikshåb Isblink, the largest piedmont glacier in West Greenland. A, Landsat 2 image (2209–13564, band 5). B, Landsat 2 false-color composite image (2209–13564, bands 4, 5, and 7; 19 August 1975; Path 5, Row 16) from the EROS Data Center, Sioux Falls, S. Dak. Each version allows interpretation of different types of features. Refer to text for a more detailed description of the image.



A



B



**Figure 15.**—Annotated parts of two Landsat 1 MSS images of the outer coast and Inland Ice margin in the vicinity of Godthåbsfjord, southern West Greenland. A, Landsat false-color composite image (1396–14252, bands 4, 5, and 7; 23 August 1973; Path 8, Row 15) from the EROS Data Center, Sioux Falls, S. Dak. B, Landsat image (1448–14124, band 7; 14 October 1973; Path 6, Row 15) from the EROS Data Center, Sioux Falls, S. Dak.

about  $10 \text{ km}^3 \text{ a}^{-1}$  of water equivalent (Weidick and Olesen, 1980) but has not been measured directly. The main calf-ice production is furnished by the Kangiata nunâta sermia (outlet glacier), which has receded approximately 20 km since the beginning of the 19th century (Weidick, 1968). The trimline zone left by the outlet glacier can be seen clearly on the image. Also, the ice-dammed lake Isvand is now materially larger than when described and mapped by Nansen, who passed here in 1888 after the first crossing of the Inland Ice (fig. 16).

Large ice-dammed lakes that have had jökulhlaups reported historically are present around Isortuarssûp sermia and Narssap sermia. The frequency of jökulhlaups is not known.

Iron ore deposits have been found in the Isukasia area, and their extent under the margin of the present Inland Ice margin has led to glaciological investigations and a detailed mapping of the subglacial topography in the

area (Colbeck, 1974). The ice margin around Isukasia has shown little change during this century and is advancing slowly at present. The sector farther south from Narssap sermia to Kangiata nunâta sermia, however, has experienced a pronounced recession during the same time interval, although most recent investigations around the glaciological station at Qamanârssûp sermia indicate an initial readvance during the last decade. Farther north at Isukasia, the ice margin has been under slow but steady readvance during the most recent decades.

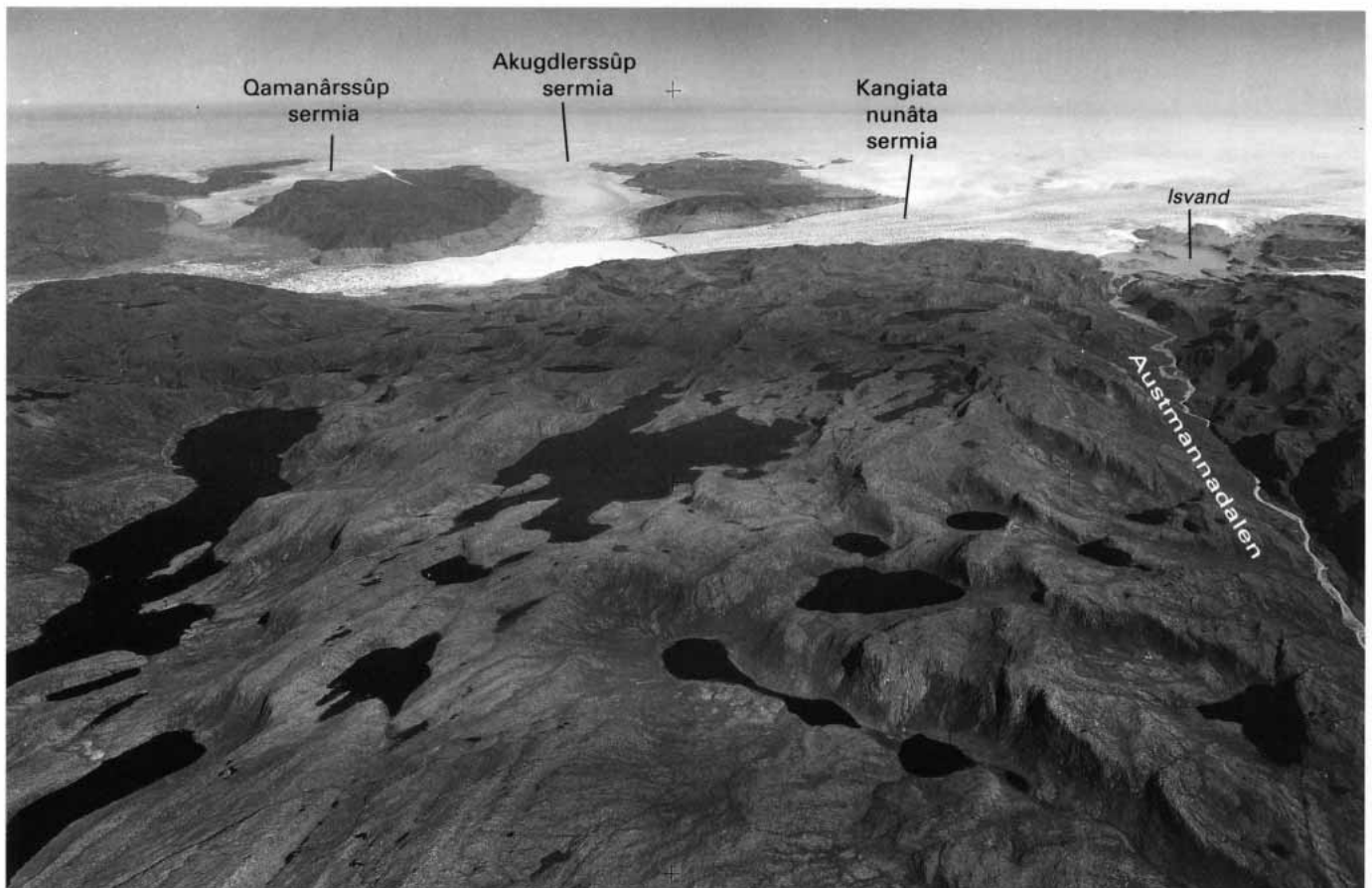
Figure 17 covers the area around Søndre Isortoq fjord and inland areas around the valley of Majorqaa. Four local ice caps in the highlands north of Søndre Isortoq and Majorqaa are indicated by the numbers 1-4. The existence of large subglacial valleys under ice caps 2 and 4 are clearly visible on the image.

Upglacier from the margin of the Inland Ice, the slush zone (from Muller, 1962) is characterized by dark-colored “swamps” and lakes that separate the 3- to 8-km-wide polygonal features. Closer to the ice margin, the flow patterns of ice streams extend from the large outlet glaciers to approximately 10 km into the Inland Ice. The transient snowline is situated at approximately 600 m around Søndre Isortoq and at 1,000 to 1,200 m over the Inland Ice margin.

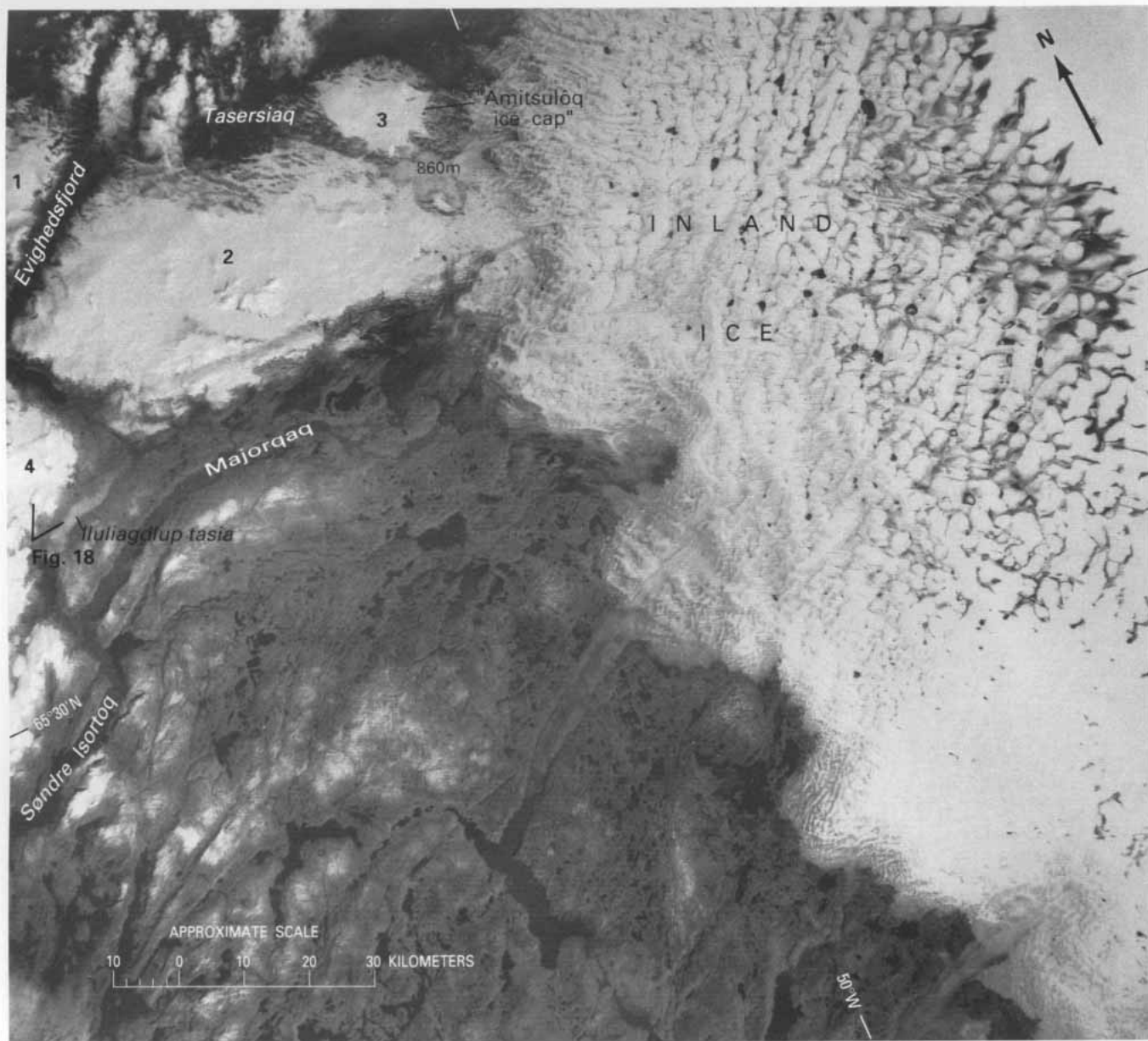
The image also shows two of the largest ice-dammed lakes in West Greenland, Iluliagdlop tasia and “lake 860 m.” The water level in both lakes varies, but details are known only from Iluliagdlop tasia.

Iluliagdlop tasia periodically drains under an outlet glacier of the ice cap (no. 4 on fig. 17) that dams its western end. Its eastern end is shown in figure 18. The catastrophic drainages (jökulhlaups) take place with intervals of 6 to 11 years (Helk, 1966), and with each draining, a volume

*Figure 16. —Oblique aerial photograph of the Inland Ice margin in the head of Kanger-suneq (see fig. 15 for location) taken 20 August 1948, looking east. On the left is the outlet of Qamanârssup sermia, where mass-balance measurements were made from 1978 to 1989. In the center are the outlets of Akugdlerssûp sermia and Kangiata nunâta sermia, which merged into one tidal outlet glacier earlier in this century. On the right are Isvand and Austmannadalen, where Nansen descended after the first crossing of the Inland Ice in 1888. Since then, Isvand has increased in area because the Inland Ice margin has receded. NSC aerial photograph, route 505 D-Ø, No. 4628. Reproduced with permission A 200187.*







**Figure 17.** —Annotated Landsat 3 MSS image of Sukkertoppen Iskappe (number 2), “Amitsulôq ice cap” (number 3) and two other local ice caps (numbers 1 and 4), and the Inland Ice margin, southern West Greenland. The elevation of an unnamed ice-dammed lake is given (860 m). Landsat image (30145–14142, band 7; 28 July 1978; Path 8, Row 14) from Canada Centre for Remote Sensing, Ottawa, Ontario.



**Figure 18.**—Oblique aerial photograph of local ice caps in the area south of Søndre Strømfjord taken 20 August 1948, looking east. The location is plotted in figure 17. In the foreground is the ice-dammed lake of Iluliagdilup tasia, and behind it is Sukkertoppen Iskappe (ice cap No. 2 of fig. 17). In the background this ice cap merges with the Inland Ice and "Amitsulôq ice cap" (ice cap No. 3 in fig. 17), where detailed mass-balance measurements were made between 1981 and 1990. NSC aerial photograph, route 505 D-Ø, No. 4719. Reproduced with permission A 200187.

of 5 to 6 km of water is released into Søndre Isortoq fjord. The last reported outburst took place in 1977. For large ice-dammed lakes that experience repeated jökulhlaups over a long period of time, satellite monitoring offers great possibilities for sequential (time-lapse) observations of lake level, especially for predicting when the lake level is anticipated to reach outburst height.

Figure 19A shows the Inland Ice margin near Søndre Strømfjord Air Base and the site of a former glaciological station, “Mint Julep,” on the Inland Ice. This station was situated at an altitude of 1,800 m, and glaciological studies of the slush zone were made here in 1953 (Schuster, 1954; LaChapelle, 1955). During the “Mint Julep” investigations, it was concluded that the firn line could be placed between this camp and a position approximately 3 mi farther to the west (fig. 19B). The results and descriptions from this locality stress the necessity of using the glacier facies classification of the Inland Ice developed by Benson (1959, 1961, 1962, 1967) and subsequent modifications by Muller (1962) and by Benson and Motyka (1979) (fig. 19C). The sharp boundary just west of the position of the former “Mint Julep” station indicated on figure 19A must be interpreted as the approximate height of the snowline on Benson’s profile (fig. 19C) (firn limit area of fig. 19B), because the wet-snow line is upglacier from the “Mint Julep” station. Figure 19A can also be compared with the original field observations of the ice facies and superimposed ice zone of the ablation area of the “Mint Julep” station shown in figure 19B.

That the numerous lakes and rivers in the “zone of large lakes” on the Landsat image seem rather unchanged from those given on the maps of the “Mint Julep” project indicates that the supraglacial drainage patterns at least partly reflect subglacial topography. The part of the ablation area consisting of bare glacier ice can be delineated on figure 19A as a lower zone that is more gray in tone than the slush zones (with lakes) that appear closer to the “Mint Julep” station. In the region covered by the image, the ice margin was thinning in most of the decades in this century, but a readvance has taken place in the 1970’s, which, in places, covers the trimline zone formed in the first half of this century.

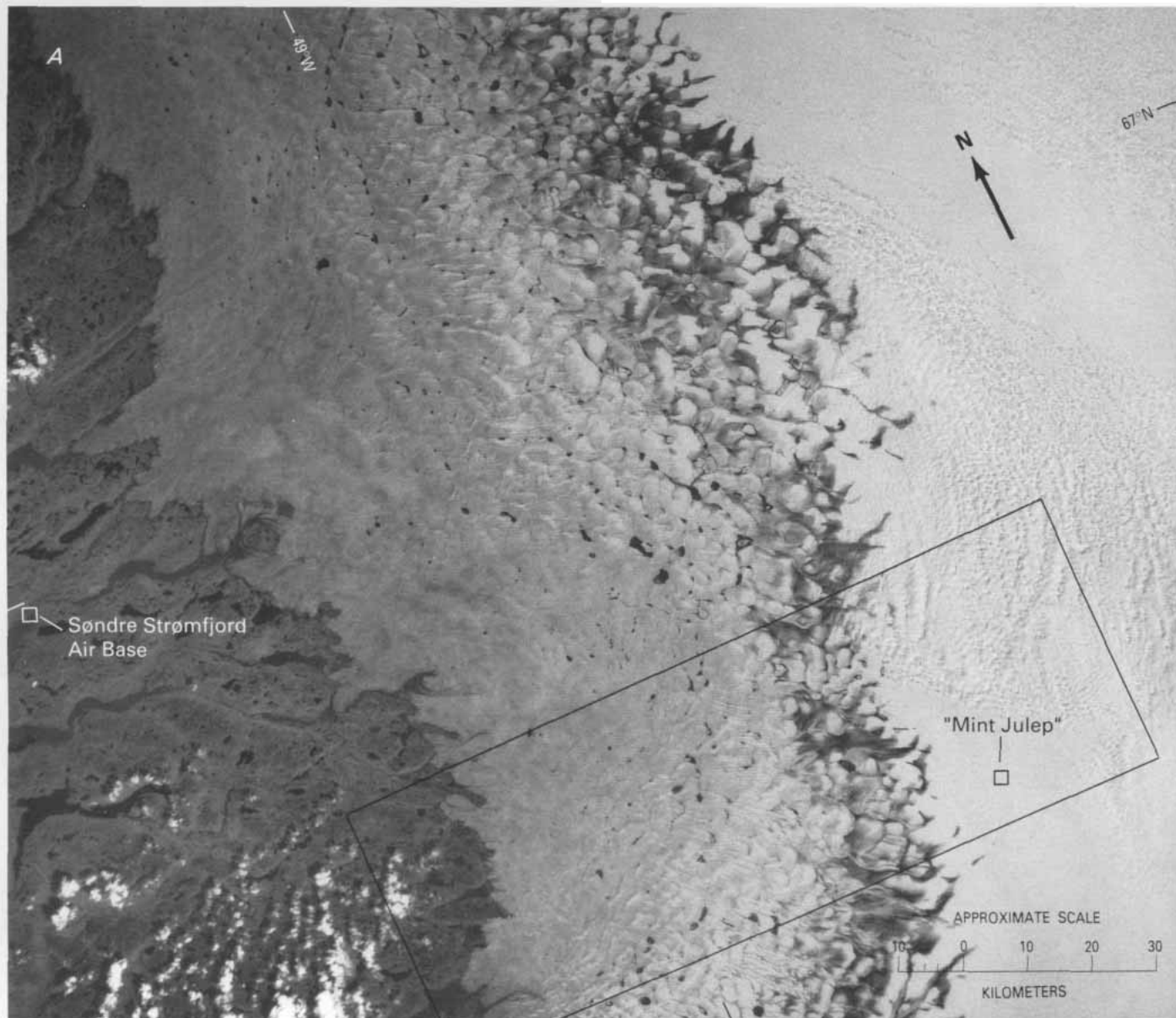
## Images of Central West Greenland

The region is dominated by the low gneiss terrain around the southern and inner parts of Disko Bugt, the high basalt plateaus of Disko and Nûgssuaq, and the high metasediment plateaus of the interior Umanak district. All these landscape forms are covered by Landsat images in figures 20, 21, and 22A.

Figure 20A covers the area of the Inland Ice margin from the outlet glaciers of Sarqardliup sermia and Alángordliup sermia in the south to the areas of Jakobshavn Isbrae and Sermeq avangnardleq to Eqip sermia in the north. Farther north, ice streams leading to the outlet glaciers of Kangilerngata sermia and Sermeq kujatdleq also are visible.

Jakobshavn Isfjord is apparent in its full extent (approximately 40 km) from the town of Jakobshavn (Ilulíssat) to the calving terminus of Jakobshavn Isbrae. A zone 6 km wide at the head of the fjord is covered by fast ice with large pieces of calf ice, whereas the rest of the fjord is closely filled with brash ice.

Jakobshavn Isbrae has a calf-ice production rate of 26 to 44 km<sup>3</sup> a<sup>-1</sup> (Bauer and others, 1968; Carbonnell and Bauer, 1968) and is therefore the dominant ice-producing outlet to Disko Bugt (table 3 and fig. 7). Jakobshavn Isbrae is formed by a major ice stream from the east and a



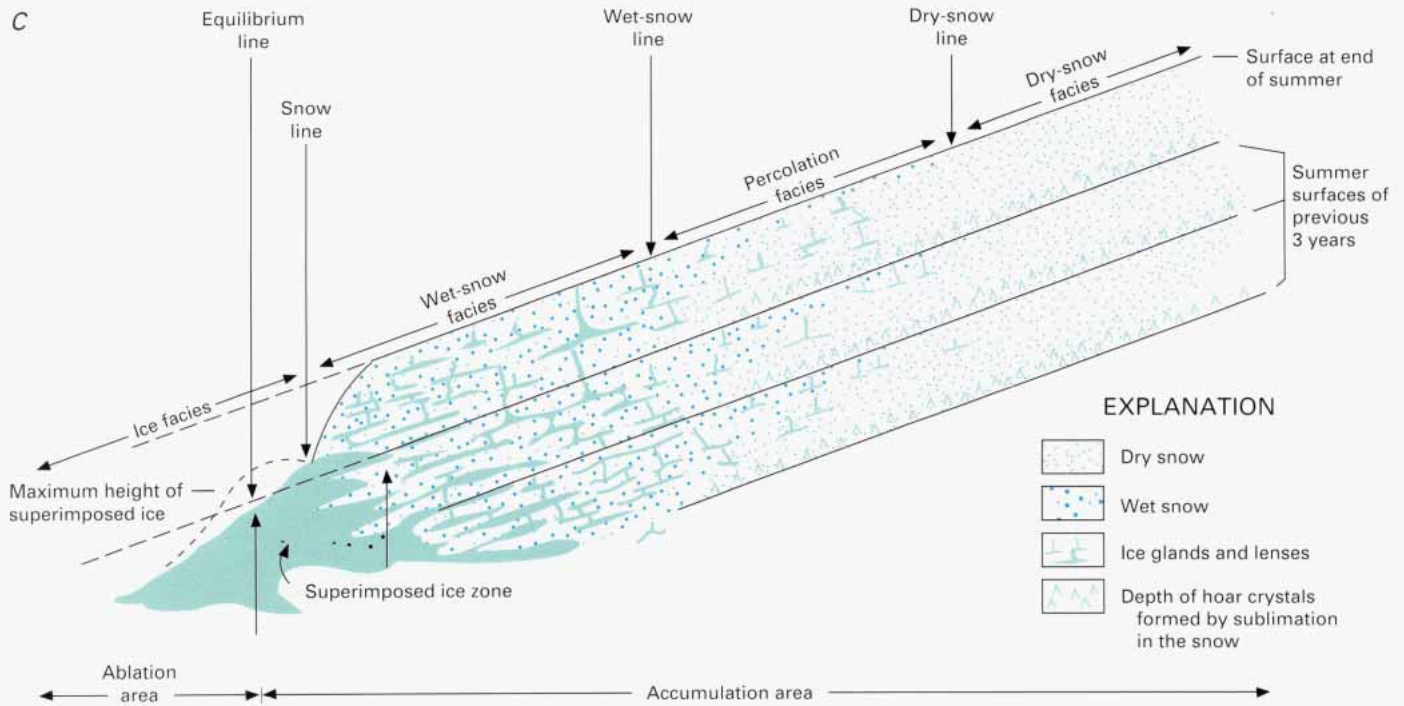
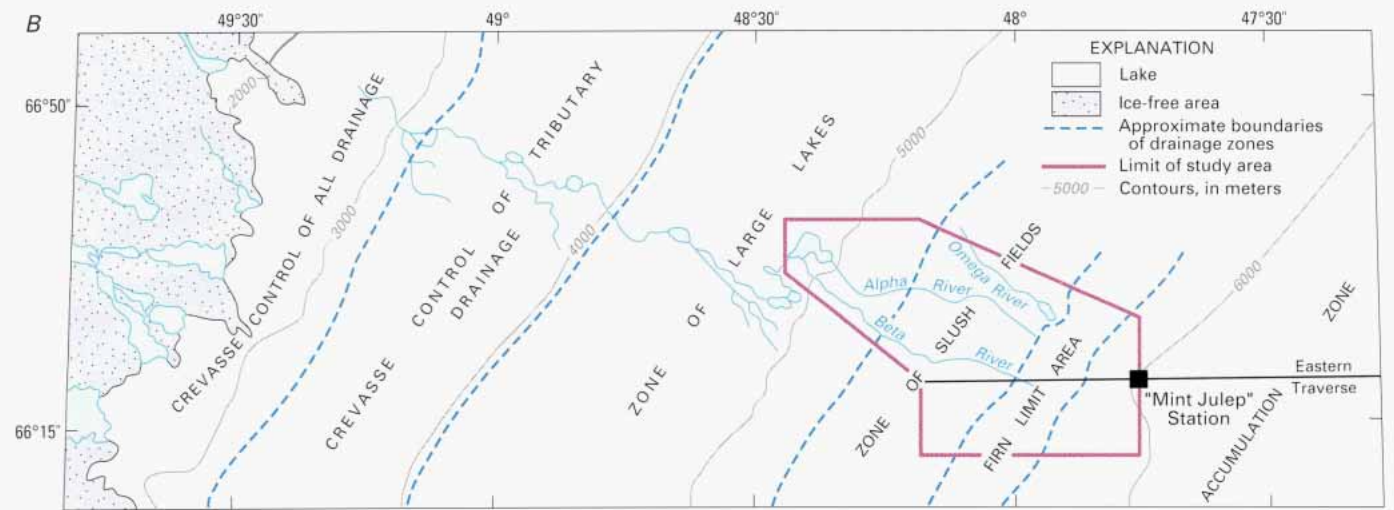
**Figure 79.**—Inland ice margin east of the Søndre Strømfjord Air Base. A, Annotated part of a Landsat 3 MSS image (3014514140, band 7; 28 July 1978; Path 8, Row 13) indicates the glacier facies division of Benson and Motyka (1979) shown on the profile in figure 19C. The dark zone on the Landsat image to the west of "Mint Julep" station might be interpreted as the approximate height of the snowline. The inset frame indicates the area described by the "Mint Julep" investigations (fig. 19B). B, Sketch of field classification of the Inland Ice margin at "Mint Julep" station based on investigations during 1953 (Holmes, 1955). The area is identified on figure 19A for comparison of the glacier facies, although the data were obtained from a different year. C, Generalized cross section of

glacier facies according to Benson and Motyka (1979). The annual layers are drawn schematically with constant thickness for simplicity and slope upward to indicate increasing altitude. From the top down (from Carl S. Benson, written commun., 1982):

**Dry-Snow Facies:** Above the dry-snow line, negligible melting occurs; this area is the dry-snow facies.

**Percolation Facies:** Between the dry-snow line and the wet-snow line, melting occurs at the surface, but the annual accumulation of snow is not completely wetted nor does its temperature reach the melting point. Even a slight amount of surface meltwater percolates downward along irregular paths that include lateral wetting on selected snow strata: the snow





between wetted pathways may remain several degrees below 0 °C. The percolating meltwater freezes in the snow and forms a complex network of ice lenses and vertical pipelike ice glands. Percolation decreases with altitude and becomes negligible at the dry-snow line.

**Wet-Snow Facies:** Below the wet-snow line, the entire annual accumulation of snow is wetted, and its temperature reaches the melting point. Large ice glands and lenses are common throughout the snow and firn of the wet-snow facies. [Editor's note: Muller (1962) defined a slush zone as the lower part of Benson's wet-snow facies, extending from the snowline upglacier into the wet-snow facies of Benson, or what Muller called the percolation zone (Williams and others, 1991)].

**Ice Facies:** Below the snowline, bare ice is exposed, and the annual accumulation of snow is melted and either converted to superimposed ice above the equilibrium line or is lost by runoff below the equilibrium line.

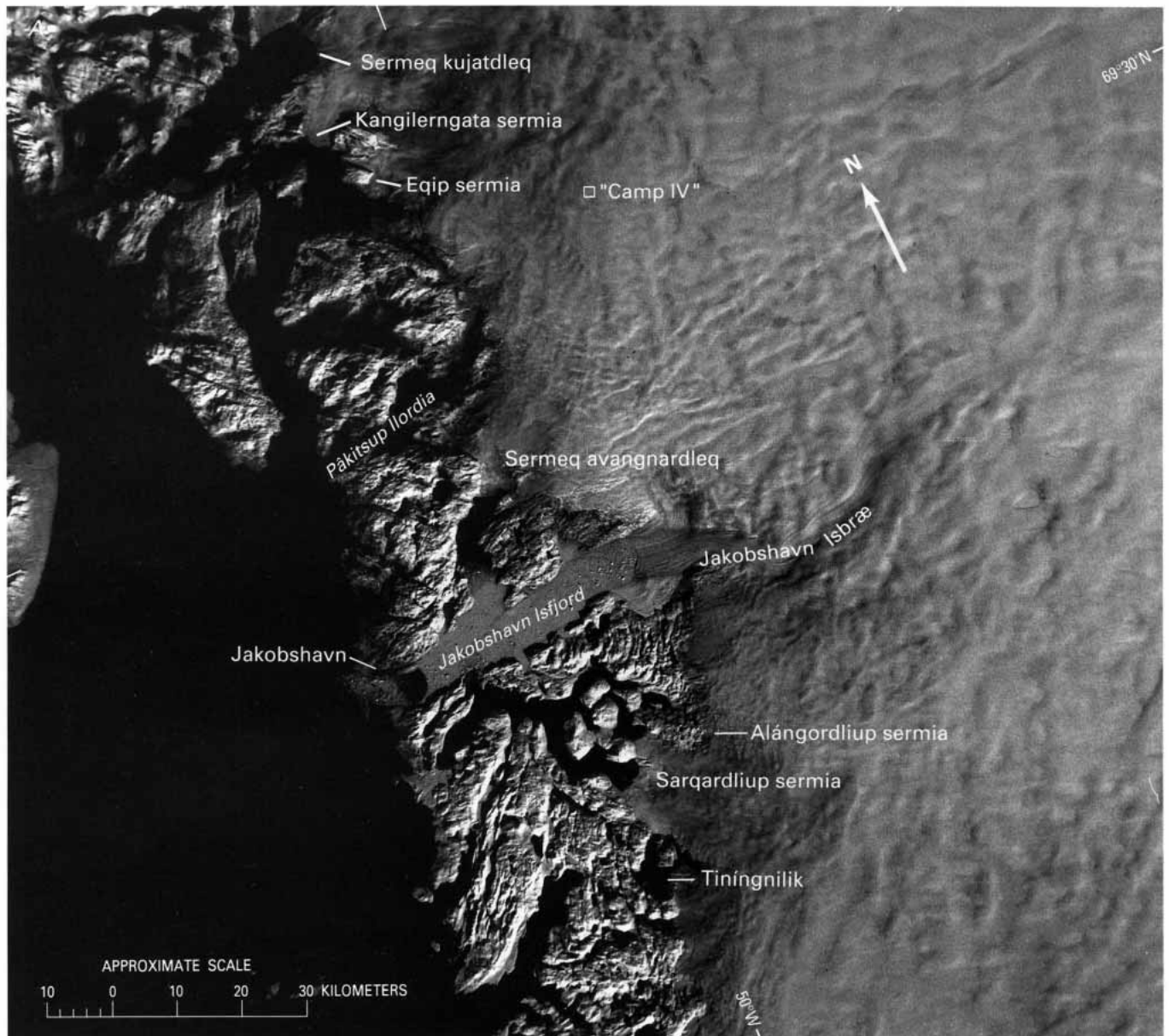
The equilibrium line separates the ablation area from the accumulation area. It also defines the lower limit of the superimposed ice zone. The upper limit of the superimposed ice zone extends above the snowline and blends with large ice masses formed within the snow and firn of the wet-snow facies.

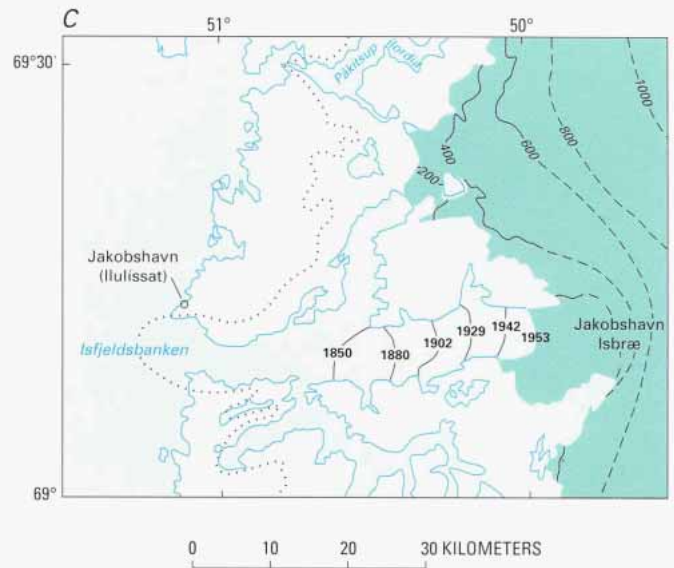
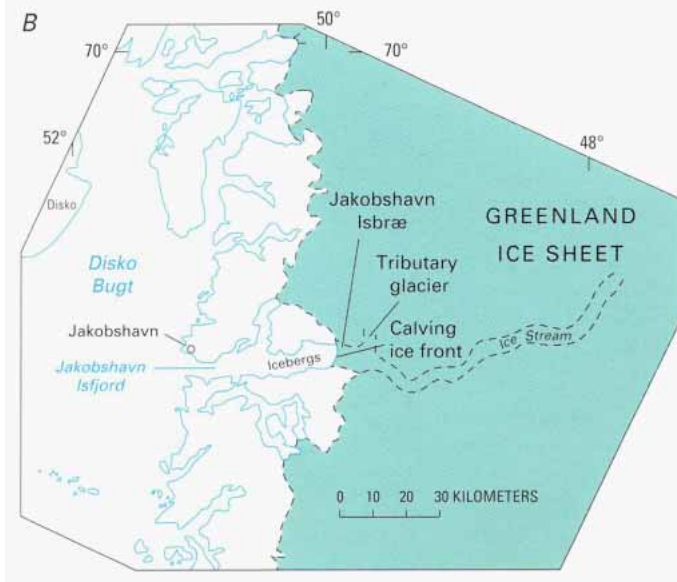
The image of figure 19A covers only the details of lower parts of the wet-snow facies and of the ice facies shown schematically here in figure 19C.

minor tributary from the north. On figure 20A the primary and secondary ice streams that feed the Jakobshavn Isbrae tidal outlet glacier can be delineated clearly. On the accompanying sketch map (fig. 20B) (Williams, 1986) the sinuous nature of the main ice stream can be traced approximately 100 km into the Inland Ice from the terminus of Jakobshavn Isbrae. As noted by Williams (1986), "this 150km long path of Jakobshavn Isbrae (measured from the mouth of Jakobshavn Isfjord to the end of the ice stream in the Inland Ice) is comparable to the length of the longest, nearly straight fjord in Greenland, Søndre Strømfjord [plate B]. It is concluded that Jakobshavn Isbrae flows in a subglacial valley that, if the ice cover were removed, would be almost identical to Søndre Strømfjord."

During the period 1851-1953 the front of Jakobshavn Isbrae receded 26 km. Since 1953 the position of its terminus has been approximately stationary (Kollmeyer, 1980) (fig. 20C). None of the neighboring outlets to Disko Bugt have shown comparable frontal changes; Sarqardliup sermia and Alángordliup sermia have been nearly stationary throughout the last 80 years; however, an advance seems to have started since the

**Figure 20.**—A, Annotated Landsat 2 MSS image of Jakobshavn Isbrae and Jakobshavn Isfjord, central West Greenland. Landsat image (22087-14293, band 7; 9 October 1980; Path 11, Row 11) from Canada Centre for Remote Sensing, Ottawa, Ontario. B, Sketch map of the ice streams in the Inland Ice that feed into the Jakobshavn Isbrae outlet glacier (from Williams, 1986). C, Sketch map of ice margin changes around Jakobshavn Isbrae. The dotted line indicates the position about 8,000 years ago. The light gray areas near the present ice margin are areas that have become ice free in the past 100 years. Dashed lines show the topography of the ice. Contour interval 200 m.





1960's. Sermeq avangnardleq, Eqip sermia, and Kangilerngata sermia generally receded only a little during the same period, but at Eqip sermia an initial readvance of the northern flank seems to have developed since the 1960's.

The pronounced thinning of the Inland Ice margin around Jakobshavn Isbrae induced a change in flow direction of parts of the ice margin; because of the transverse nature of the subglacial mountain ridges at the margin of the Inland Ice in this part of Greenland, the thinning resulted in a transfer of ice from the Jakobshavn drainage basin to the Sarqardliup sermia and Alángordliup sermia outlet glaciers. This hypothesis provides an explanation for the nearly stationary condition of their ice margins in spite of the increased ablation during this century (Weidick, 1968). The trend of subglacial ridges can be seen forming parts of the southern limit of the southernmost of the large ice streams leading to Jakobshavn Isbrae (fig.20A).

On the Inland Ice margin north of Jakobshavn Isbrae (at Pâkitsup ilordlia), the repeated mapping of the ice surface in 1959 and 1982 indicated an average thinning near the ice margin of 14 m up to an elevation of 500 m (Thomsen and others, 1988). In spite of the thinning of the surface, the retention of the drainage patterns on the surface of the ice indicates the influence of the subsurface relief even at ice thicknesses of 400 to 600 m.

The locations of the "Camp IV" and "Camp VI" stations occupied by the Expeditions Polaires Françaises (EPF, 1947–55) and Expedition Glaciologique Internationale au Groenland (EGIG, 1957–60) are in the area of figure 20A. The approximate position of "Camp IV" is shown on figure 20A. "Camp VI" was located just north of the image above the north arrow. They are situated at altitudes of 1,096 m ("Camp IV") and 1,598 m ("Camp VI"), and their geographical coordinates are given in table 13. According to the reports from the EPF, the firn line was estimated at 1,420 m in this area (Holtzscherer and Bauer, 1954). Braithwaite and Thomsen (1984a) estimated an ELA of 1,300 m for the region.

Figure 21 shows the morphology of Disko island and Nûgssuaq peninsula. Physiographically, the relatively low landscape of Archean gneisses around Boyes Sø (lake) at the base of Nûgssuaq is characterized by numerous lakes. Nûgssuaq and Disko are in marked contrast, as they have been built up by Mesozoic and Tertiary sediments and lavas to an elevation of 1,000 to 1,500 m.





**Figure 21.**—Annotated Landsat 2 MSS image mosaic of Disko and Nûgssuaq, central West Greenland. Landsat images (top, 20938–14230, band 5; 17 August 1977; Path 14, Row 10; bottom, 20937–14174, band 5; 16 August 1977; Path 13, Row 11) from Canada Centre for Remote Sensing, Ottawa, Canada.

The basaltic plateaus are covered by extensive local ice caps and incised by numerous cirques near the coast, which dissect the area into many alpine peaks. The transient snowline at the time of the year this image was acquired is close to the glaciation limit of the area, increasing from approximately 800 m at the outer coast to about 1,400 m at the Inland Ice margin.

The only large lake in the basaltic area is in the central part of the Nûgsuaq peninsula. The lake takes its name from tasíngortartoq, a Greenlandic word meaning “what turns to become a lake.” Tasíngortarsua relates to the lake’s variable areal extent, evidence of which can be seen from the lighter tonal band along its shores. At the west end of Tasíngortarsua, extensive trimlines surround the larger outlet glaciers of the local ice caps and document a recent recession of these lobate glaciers.

Similar widespread trimline zones can be seen generally around the outlet glaciers from the local ice caps on Disko and are related primarily to the recession during this century. It is documented that the Kuán-erssuit valley at the end of last century was still partly filled with glaciers over most of its length, whereas the same valley is free of glaciers today (Weidick, 1968).

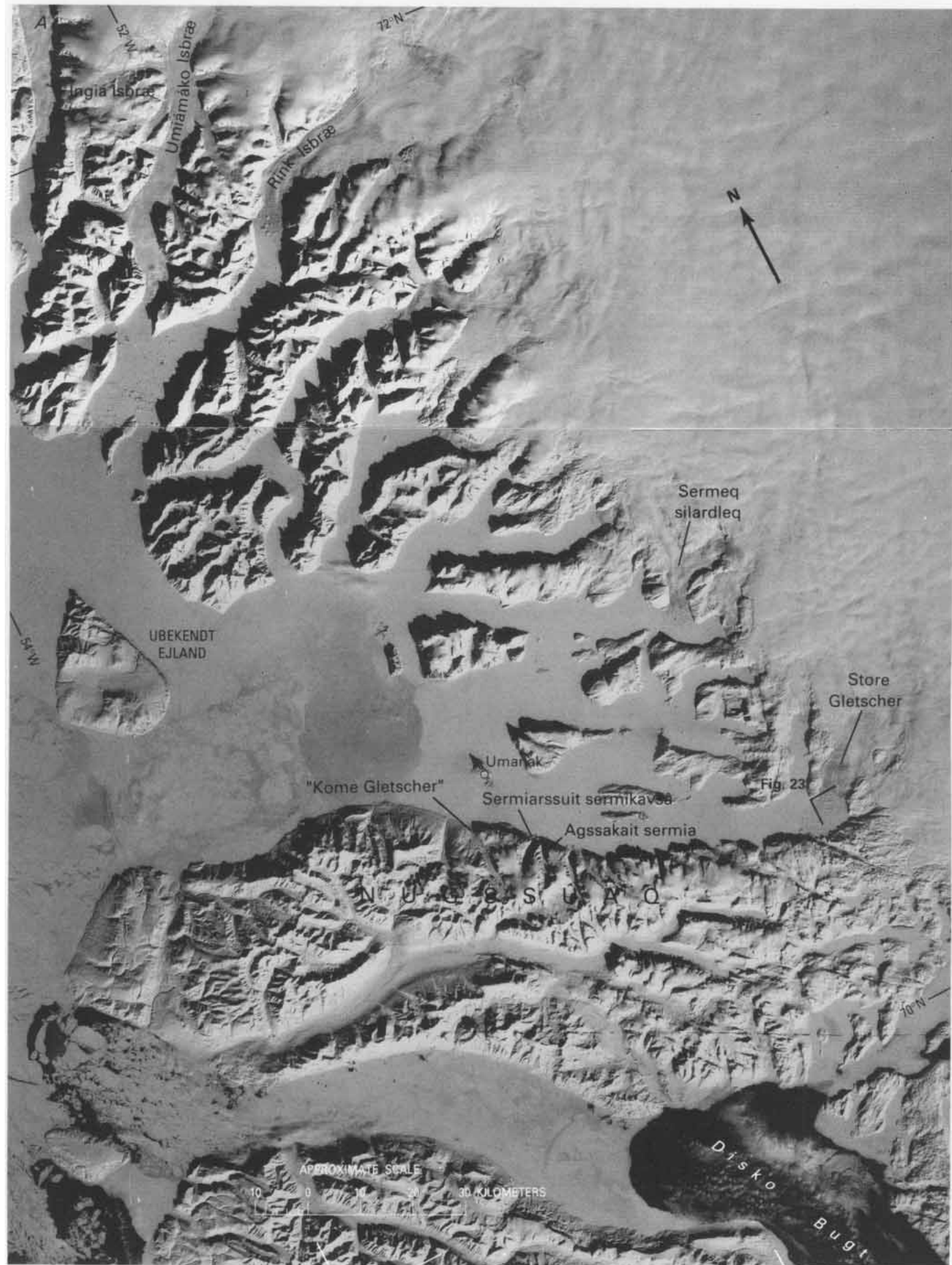
Figure 22A shows Ubekendt Ejland, the town of Umanak, and the Inland Ice margin from Store Gletscher to Íngia Isbrae; the names of the individual outlet glaciers are shown on the sketch maps in figure 22B. This sector of the Inland Ice has the largest concentration of calf-ice-producing outlet glaciers in Greenland (Reeh, 1985; fig. 7). The 11 outlet glaciers in the fjord complex (Store Gletscher to Íngia Isbrae with the exception of “Qaumarujuk Gletscher,” which does not discharge into the fjord) have an estimated total calf-ice production of about  $45 \text{ km}^3 \text{ a}^{-1}$  (table 3), approximately equal to that of Disko Bugt, where most calf-ice production is concentrated in the single outlet glacier of Jakobshavn Isbrae (Stove and others, 1984?).

In the fast ice that covers the Umanak Fjord complex, concentrations of calf ice are visible on figure 22A at the termini of Store Gletscher (see also fig. 23), Sermeq silardleq, and Rink Isbrae, each having high calf-ice production greater than  $5 \text{ km}^3 \text{ a}^{-1}$  (table 3 and fig. 22B). Ice streams in the marginal areas of the Inland Ice, which can be delineated because of characteristic flow patterns, are faintly visible and are most pronounced at the outlet glaciers mentioned above, especially those having visible calf ice at their termini. Within the Inland Ice, the approximate extent of flow patterns of ice streams that feed into the calf-ice-producing outlet glaciers of Umanak Fjord and the northern part of Disko Bugt is shown in figure 22B.

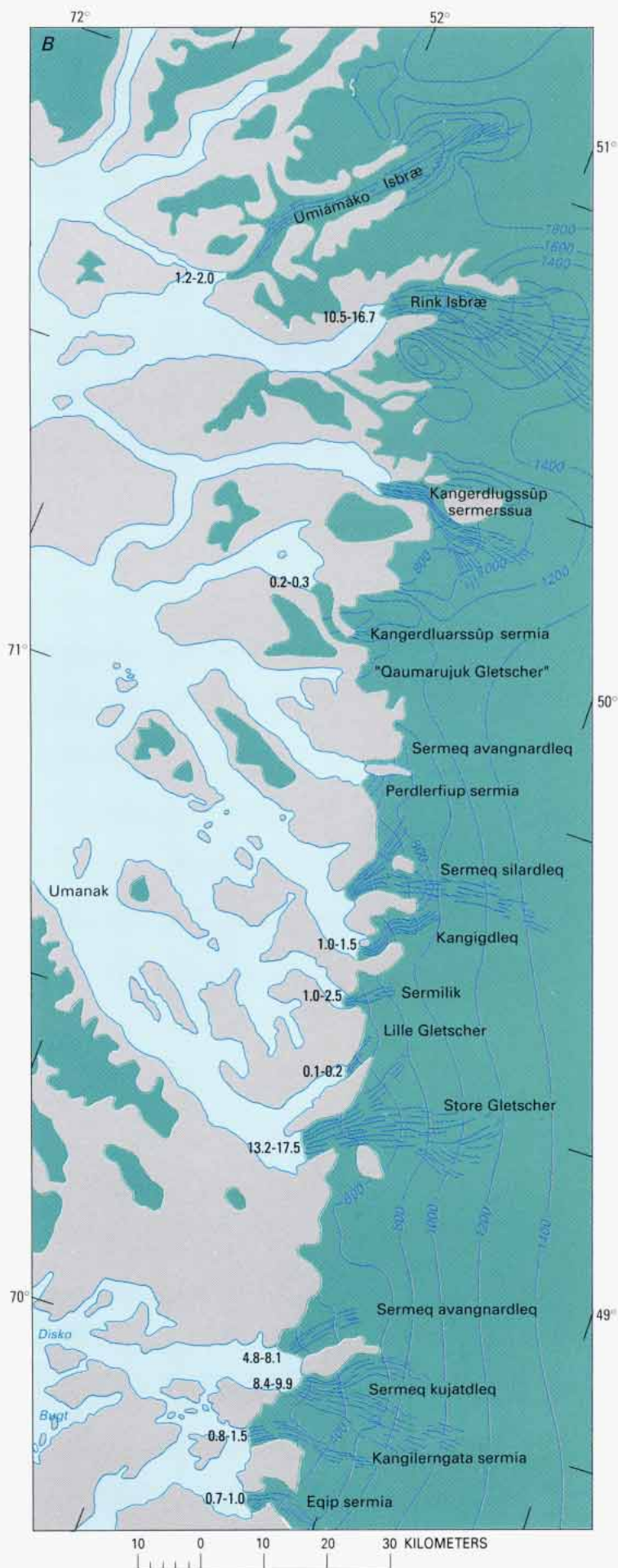
## Images of Northern West Greenland

The relatively low and uniform gneissic areas of the Upernavik district are, with the exception of a transitional area at Svartenhuk Halvø to the south, dominated by the presence of the Inland Ice margin at the outer coast, as shown on figures 24 and 26. Figure 24 covers the Inland Ice margin from Upernavik Isstrøm to Ussing Bræer. The Inland Ice margin is separated from the sea only by a narrow rim of relatively low islands and headlands; maximum elevations are in the vicinity of Qagssersuaq north of Upernavik Isstrøm (1,160 m).

Several calf-ice-producing outlet glaciers are connected to ice streams delineated on the satellite images. Calf-ice production of these outlet glaciers in Melville Bugt was investigated during the cruises of the U.S.







**Figure 22.—A,** Annotated Landsat 1 MSS image mosaic of Umanak Fjord complex, central West Greenland. Landsat images (top, 1240–14585; Path 14, Row 9; bottom, 1240–14591; Path 14, Row 10; band 5; 20 March 1973) from the EROS Data Center, Sioux Falls, S. Dak. **B,** Sketch map of the interior of northern Disko Bugt and Umanak Fjord complex. Illustrated are the names of individual outlet glaciers, their approximate calving ice production in cubic kilometers per year as numbers shown at the terminus of each tidal outlet glacier (see also table 3), and the extent of the ice streams into the Inland Ice according to flowlines and other morphologic indicators discernible on low-solar-illumination-angle Landsat images. Contour lines indicate ice-surface elevation at intervals of 200 m.



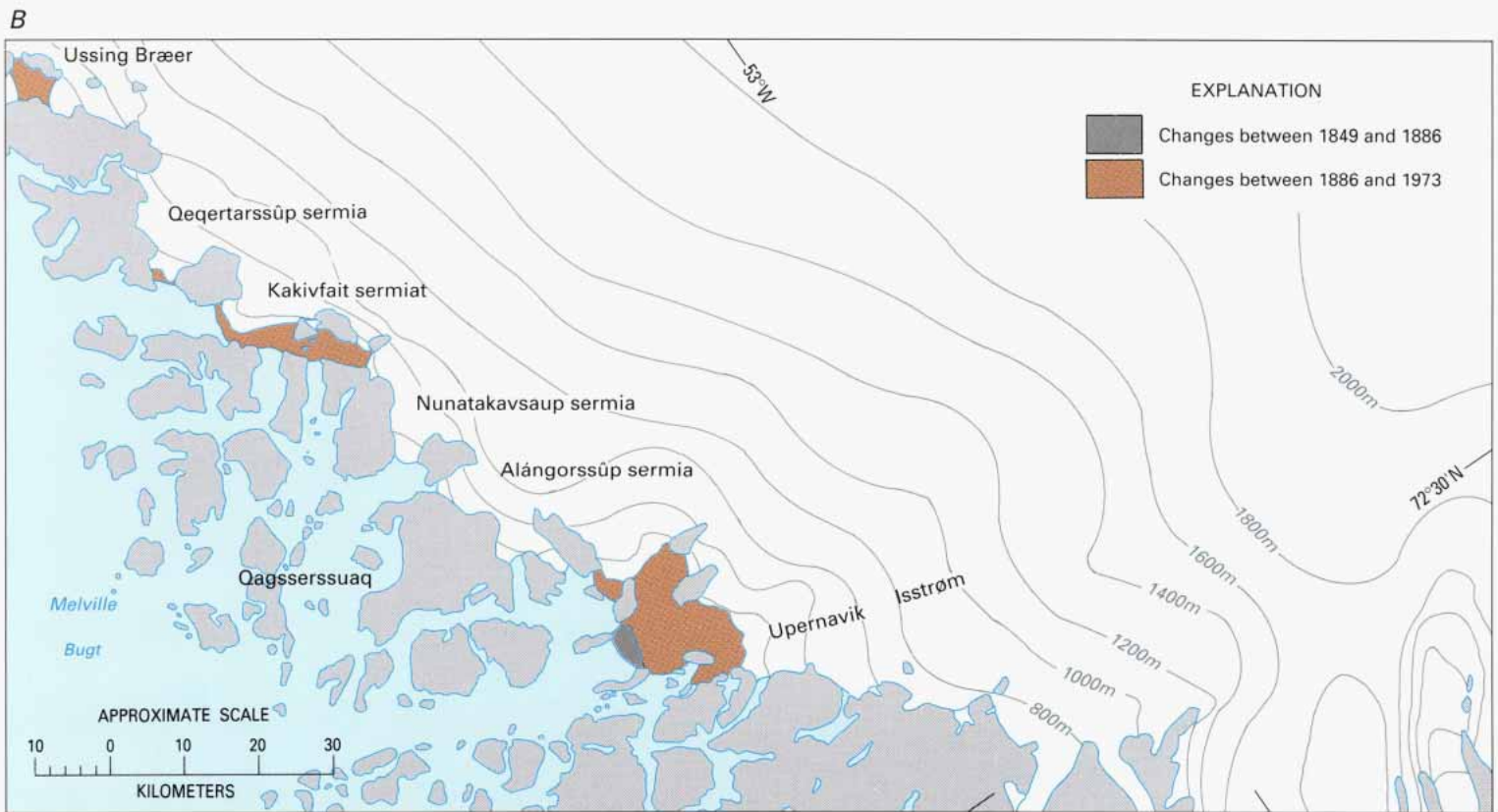
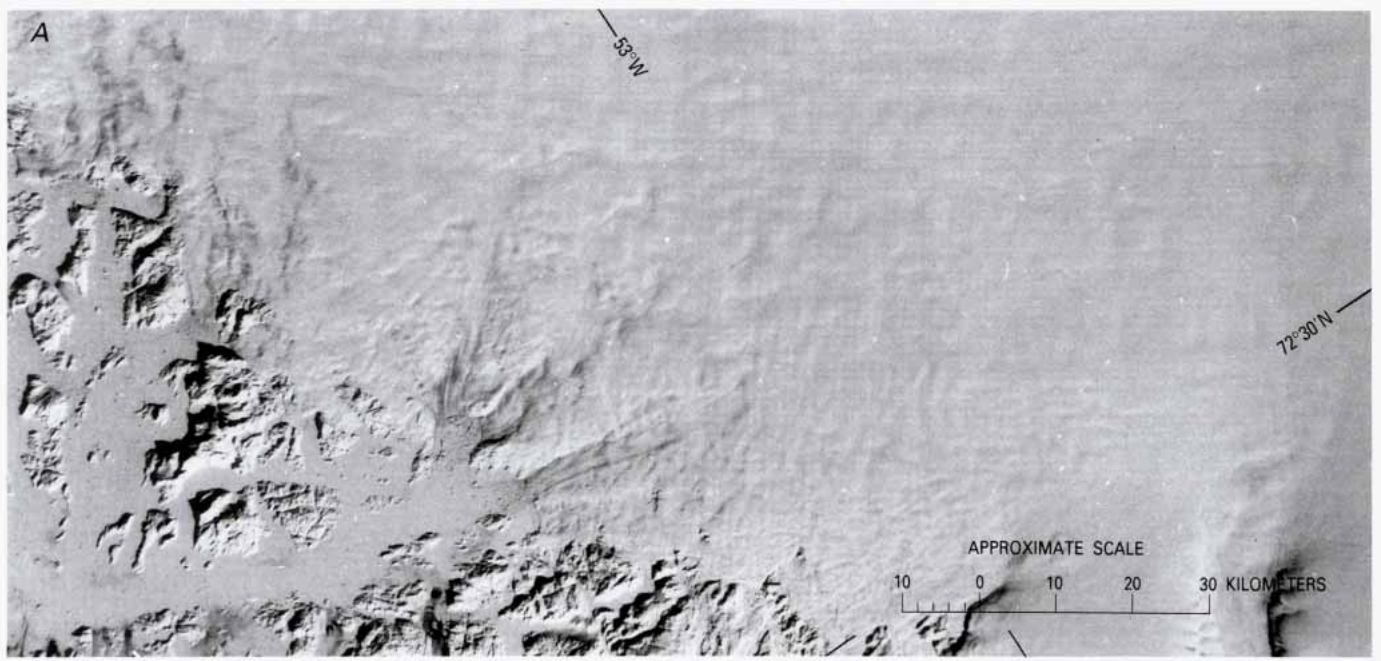
Coast Guard cutter “Westwind” in the 1970’s (Kollmeyer, 1980). The results, listed in table 3, indicate a total calf-ice production in the Melville Bugt region, which also includes glaciers of North-West Greenland, of at least 70 km<sup>3</sup>.

The sketch map (fig. 24B) indicates the names of outlet glaciers and recent termini positions taken from Landsat images compared to the frontal positions determined by Ryder (1889) at the end of the last century. The largest changes in the positions of the ice margin are those associated with the ice streams, especially the one leading to the terminus of Upernavik Isstrøm. Large parts of the ice margin, because they are floating, approach the characteristics of an ice shelf (fig. 25), and the position of the ice margin is extremely variable for large sectors (Kollmeyer, 1980).

In figure 26, details of the ice margin around Ussing Bræer show the jagged skerries and peninsulas of the southern part of Melville Bugt. Here the ice cover forms a veneer over the subglacial continuation of the landscape and protrudes into Melville Bugt from numerous calf-ice-producing outlet glaciers. The calf-ice production is indicated by scattered, large icebergs clustered at some distance from the termini of the

**Figure 23.** —Oblique aerial photograph of the front of Store Gletscher taken 15 July 1948, looking southeast (see fig. 22A for location). In the background a nunatak separates the tidal outlet glaciers of Sermeq avangnardleq and Sermeq kujatdleq, glaciers that drain into Disko Bugt (see fig. 22B). The lakes on the ice surface in the background are situated in the catchment area of Sermeq avangnardleq. NSC aerial photograph, route 520 G-SØ, No. 1370. Reproduced with permission A 200187.





**Figure 24.**—A, Landsat 2 MSS image of the Inland Ice margin in the southern part of Melville Bugt, northern West Greenland. Landsat image (2060–15090, band 5; 23 March 1975; Path 20, Row 8) from the EROS Data Center, Sioux Falls, S. Dak. B, Sketch map of the Inland Ice margin showing named outlet glaciers. The current frontal positions of the outlet glaciers, as taken from satellite images, are compared with positions determined by Ryder (1889) at the end of the last century. Contours show ice-surface elevation at intervals of 200 m.

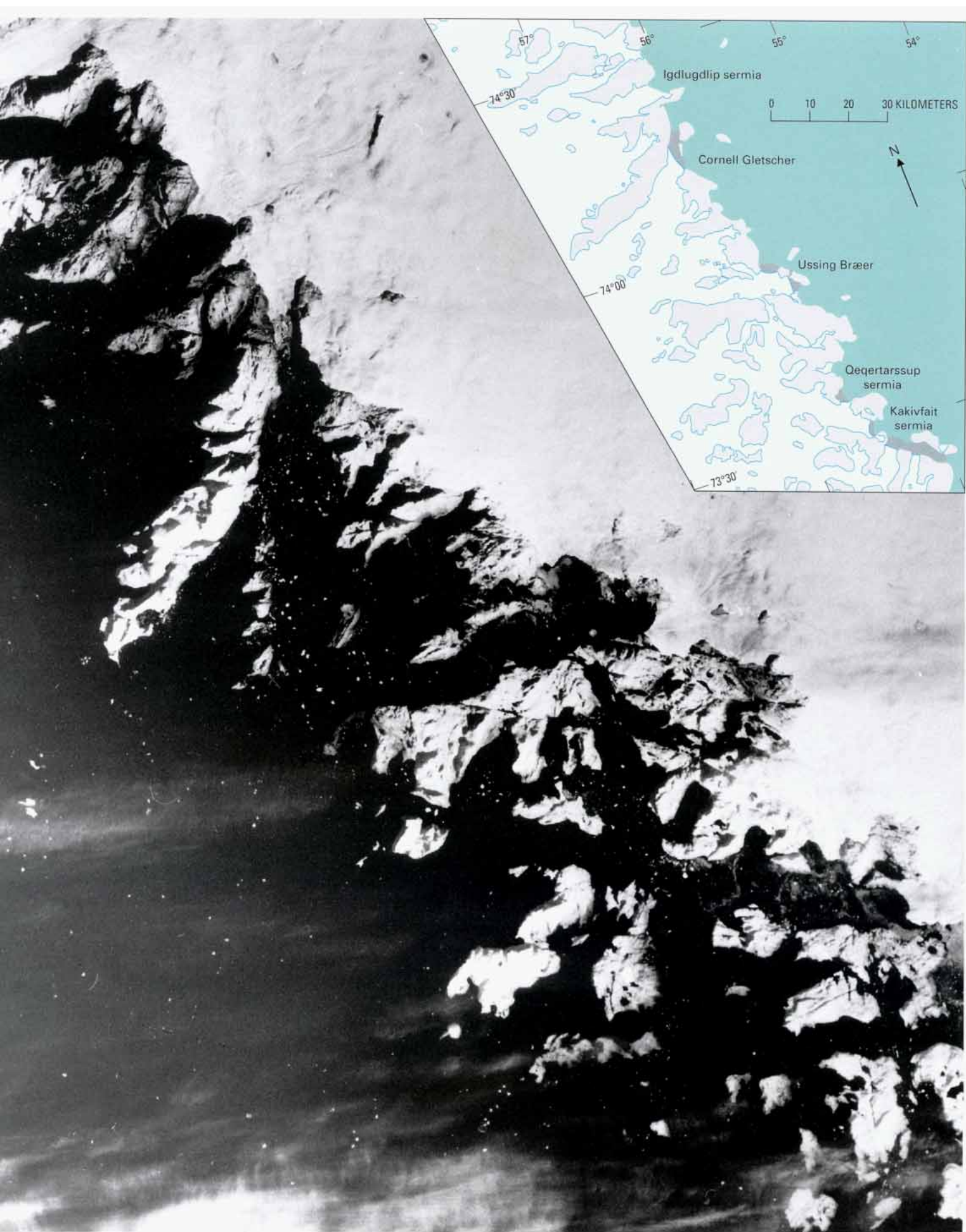
tidal outlet glaciers. A strong recession of the termini of the main ice streams (names and recession shown on the sketch map, fig. 26) has taken place during the 20th century. The recession seems, according to the investigations of the U.S. Coast Guard (Kollmeyer, 1980), to have continued up to the present time.



*Figure 25. —Oblique aerial photograph of the southernmost branch (Kakivfaiť sermiat) of Giesecke Bræer (see fig. 248, fig. 26) taken 23 July 1949, looking east. The major ice streams are winding through a hilly subglacial landscape like that now situated off the ice margin (a strandflat). NSC aerial photograph, route 535 B-Ø, No. 1606. Reproduced with permission A 200187.*

**Figure 26.**—Enlargement of part of a Landsat 2 MSS image of the Inland Ice margin in Melville Bugt between Cornel Gletscher and Giesecke Bræer, northern West Greenland. Giesecke Bræer is a collective name for the outlet glaciers of Qeqertarssûp sermia and Kakivfaiť sermiat. The inset is a sketch map of the area showing the approximate former extent of the ice margin (dark gray) taken from maps of 1886/437. Landsat image (21702–15263, band 6; 20 September 1979; Path 22, Row 7) courtesy of M. Kelly, Lancaster University, U.K.





# North Greenland

## Climatic Conditions

The North Greenland coastal region can be subdivided into two zones: (1) a coastal, subhumid fringe that has its greatest precipitation in the extreme western Thule region and in the extreme eastern region around Station Nord and (2) a drier interior area. Annual precipitation in the humid coastal areas is 100 to 300 mm, whereas in the inland areas dry or arid conditions prevail, so annual precipitation is as low as 70 mm (for example, at Jørgen Brønlund Fjord in Peary Land). Low annual accumulation is also the case for the northern slopes of the Inland Ice (Langway, 1961), whereas a local increase in accumulation (totaling 600 mm) can be found east of Thule (see fig. 5), presumably because cyclones (low pressure systems) move through the Davis Strait.

In spite of the generally frozen condition of the Arctic Ocean, the precipitation patterns described indicate that enough sea ice melts during the summer in these waters to act as a source of moisture to the northern coastal fringe. The general decrease of precipitation from the northern coast inland is reflected also in the increasing height of the glaciation limit in the same direction (see fig. 4).

The relatively continental conditions of the inland area also can be seen from the temperatures recorded at the meteorological stations given in table 7. The summer temperature of the inland station at Jørgen Brønlund Fjord is higher than at Station Nord at the outer coast.

The relatively short series of meteorological observations does not allow definitive statements concerning the magnitude of climatic fluctuations in North Greenland during the 20th century, although a known series (Benson, 1962) shows a parallel trend to fluctuations of West Greenland. Also, the stratigraphic record of firn at “Camp Century” indicates that a general warming trend took place during the middle part of this century (see fig. 47).

## Glaciological Conditions

Local ice caps and other local glaciers are widespread on the high plateaus, which are composed mainly of Cambrian and Ordovician sedimentary rocks. A confluence of local ice caps with the Inland Ice sheet occurs frequently, for example in the Thule region (around “Camp Tuto” (fig. 27A) and “Red Rock”) and around J.P. Koch Fjord and Independence Fjord (west of Marie Sophie Gletscher (see fig. 4I) in North Greenland).

TABLE 7.—Average temperatures for the months of January and July, annual average temperatures, and annual precipitation at selected stations in North Greenland  
[Data refer to 1961–70 averages from the Danish Meteorological Institute, Copenhagen]

Station	Location		Average temperatures (°C)			Average annual precipitation (millimeters per year)
	°N lat	°W long	January	July	Annual	
Dundas .....	77	69	−22.2	+3.9	−10.4	126
Jørgen Brønlund Fjord .....	82	30	−31	+6	−15	72–120(?) <sup>1</sup>
Station Nord.....	82	17	−30.6	+3.2	−17.0	170
Danmarkshavn.....	77	19	−24.4	+3.6	−12.5	109

<sup>1</sup> Measurements 1948–49 (Frstrup, 1961; Høy, 1970).





Figure 27.—**A**, Oblique aerial photograph of Harald Moltke Bræ and Store Landgletscher taken 27 August 1948, looking southeast. Store Landgletscher forms the western slope of a local ice cap that merges to the east with the Inland Ice proper. NSC aerial photograph, route 546A–SØ, No. 86. Reproduced with permission A 200187. **B**, Closeup of the ice cliffs of Store Landgletscher near "Camp Tuto." Photograph by A. Weidick, 8 July 1959. The locations of figures 27A and B are shown on figure 30A

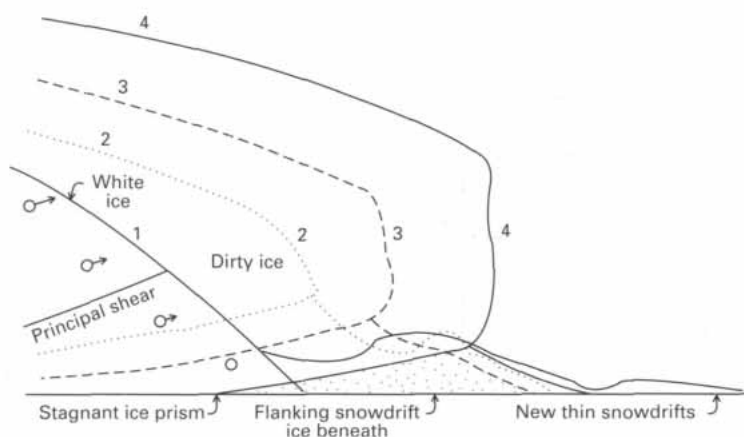


A widespread feature of the high arctic is termination of the margins of local glaciers and the Inland Ice in ice cliffs (fig. 27B). The Greenland ice sheet ends in a nearly vertical ice wall over long stretches where cliffs are as high as 50 m, but there are also steep ramps (Nobles, 1960) that, in some areas, are a transition to the normal, gentle termination of an ice cap or Inland Ice on a plain or highland.

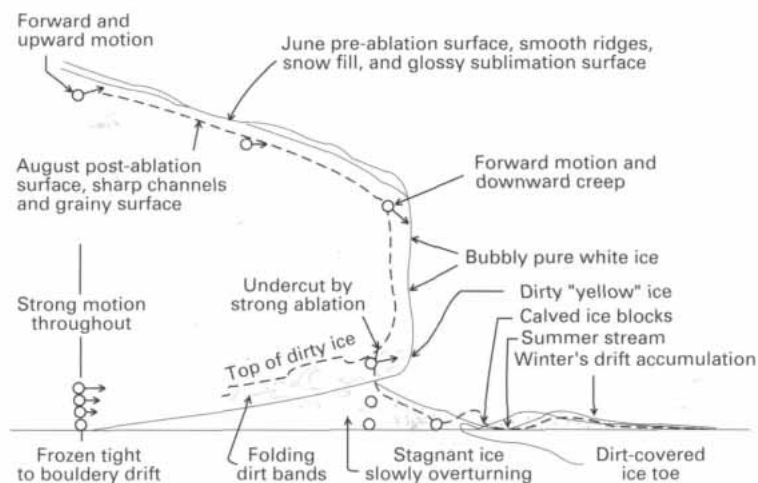
The nearly vertical ice cliffs contribute to the conventional ablation by dry calving, which is the spalling of ice fragments from the vertical front onto the glacial foreland. Because of the tendency for this material to build up at the glacier margin in the form of ice talus, transformation of the ice cliff to a more sloping feature also takes place.

The cause of the formation of the ice cliffs and steep ramps is still uncertain in general, but detailed studies at "Red Rock" (fig. 28) since 1953 (Goldthwait, 1971) point to a state of equilibrium between the flow distribution at the margin of a polar glacier and its ablation conditions as the probable cause. In addition, the ice cliffs are evidence of a slowly

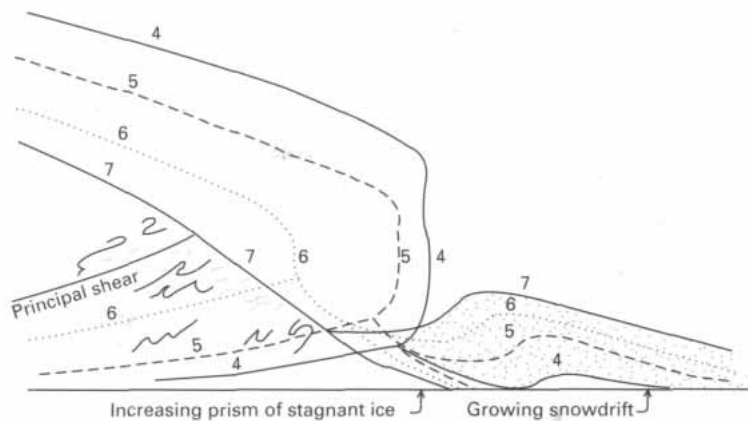
#### A. The advancing-waxing ice cliff — Decades of growth



#### B. The fully formed cliff (phase 4) — Static in mass balance



#### C. The retreating-waning ice cliff — Decades of disappearance



**Figure 28. —Sketch of the (A) formation, (B) balance, and (C) waning of an ice cliff based on the investigations at "Red Rock," Nuna-tarssuaq, Thule (from Goldthwait, 1971). A description of the process is given in the text. Numbers show advancing and retreating positions of ice front. Arrows show direction and relative amount of motion.**

advancing ice margin and seem to change character during a decade that corresponds with changes in mass balance and dynamics of the ice margin.

Figure 28 is taken from the investigations of Goldthwait (1971) and shows that the formation of the ice cliff (*A*) from a traditional sloping ice wedge may start with the arrival of a kinematic wave. The accelerated flow slowly forms a steep upper part that both buries and incorporates base material. It is essential that the glacier be frozen tight to the ground and that the upper part of the terminus plows into and incorporates material deposited at the base of the ice front. In its stable, fully grown stage (*B*), the cliff must have an upward-forward motion that equals the cliff ablation. Because the foot of the cliff is darkened by debris from the ice cliff, the albedo differs from the upper front. Ablation will cause a sharp and narrow overhang and facilitate the process of dry calving. At the retreating-waning phase shown in *C*, incorporation of dirty ice and debris makes the ice cliff thicker and thus increases the albedo and slows down movement at the same time.

The ice cliffs are distinctive features on the Landsat images and clearly delineate the margins of most of the North Greenland ice caps and the Inland Ice. An analysis of Landsat images therefore can add a temporal-geographical dimension in the investigation of these features and also some information on the patterns of glacier variations in the high arctic.

The calf-ice-producing outlet glaciers of North Greenland exhibit special features for the lobes that discharge to the Arctic Ocean, especially those situated at the northeast corner of Greenland between Independence Fjord and Nioghalvfjærdsfjorden. Calf ice is produced there mainly by a gradual advance of the glacier lobes into the fjords, which have been free of fast ice only recently. The glacier lobes are long and narrow with “sawtooth” edges (see figs. 38 and 40), similar to those in Antarctica (for example, Erebus Glacier Tongue, McMurdo Sound, West Antarctica; see fig. 31, p. B37, in U.S. Geological Survey Professional Paper 1386-B, Antarctica). Production of calf ice therefore takes place only occasionally by disintegration of entire parts of the termini of tidal outlet glaciers in North Greenland (Ahnert, 1963).

Surface rate of movement of all the tidal outlets in North Greenland has been determined on the basis of movement of surface structures of the glaciers in time-lapse aerial photographs taken between 1959 and 1979 (Higgins, 1988). The average rate of movement (see also table 3) varies from 895 m a<sup>-1</sup> (Petermann Gletscher) to 200 to 300 m a<sup>-1</sup> (Academy Gletscher and Nioghalvfjærdsbræ). Using the same method, Higgins also determined the rate of movement of a number of major outlets from local glaciers. The values ranged from 360 m a<sup>-1</sup> (outlet from Flade Isblink) to 40 to 60 m a<sup>-1</sup> (outlets from Hans Tavsens Iskappe (ice cap)).

The slow buildup of outlet glaciers from the northern slope of the Inland Ice margin, the relatively low elevation of the snowline (see fig. 4), and the occasional calving of the frontal parts of these outlet glaciers make their behavior similar to those of the ice shelves of Ellesmere Island, which form tabular icebergs or ice islands. Focal points for such ice island formation in Greenland are Petermann Gletscher (Dunbar, 1978; Higgins 1988, 1989), Ryder Gletscher, C.H. Ostenfeld Gletscher, Hunt Fjord on the north coast of Peary Land, and possibly Flade Isblink (Higgins, 1988, 1989).

## Mass-Balance Investigations

Mass-balance measurements of a few areas have been made in North Greenland, especially in connection with the American glaciological

investigations in the Thule area in the 1950's. Aside from the measurements of the accumulation of the Inland Ice proper, the work was concentrated in the localities of "Thule Ramp" ("Camp Tuto" on fig. 30), "Nunatarssuaq Ice Ramp" (east of "Red Rock," fig. 30) and on the western margin of "North Ice Cap" (west of "Red Rock," fig. 30).

The net balance (described as "net ablation") at "Nunatarssuaq Ice Ramp" covers the largest elevation difference, and the results (Nobles, 1960) are shown on figure 29 in a form comparable to the mass-balance results from South and West Greenland shown in figure 11. For the neighboring locality of "North Ice Cap," Goldthwait (1961) gives values of net ablation for 1955-56 of 0.9 to 1.4 m, 0.5 to 1.1 m, and 0 m at altitudes of 680, 800, and 900 m, respectively. For the "Thule Ramp," Schytt (1955, fig. 3-13) gives values of 0.9 to 1.1 m of water equivalent for the altitude interval of 500 to 600 m and between 0.9 and 0.4 m for the interval of 600 to 700 m.

At the ice cliff at "Red Rock" (margin of "North Ice Cap"), detailed measurements were made at the face of the ice cliff also. The surface ablation at the cliff averaged 2.0 m in the 1955 ablation season and 2.5 m in 1956 (Goldthwait, 1971).

For the eastern part of North Greenland, mass-balance measurements in the ablation area were undertaken at Christian Erichsen Iskappe in Peary Land (lat 77° N., long 25° W.) and on Admiralty and Britannia Gletschers in Dronning Louise Land (at lat 77° N., long 25° W. and lat 77° N., long 24° W., respectively) during the 1950's. More recently, studies of Storstrømmen were begun by the Alfred-Wegener-Institut, Germany.

The investigations on Christian Erichsen Iskappe (Høy, 1970) showed an ablation of 0.2 to 0.5 m of ice per year for the northern marginal areas at 900 m, whereas the southern marginal areas at the same elevation gave 0.1 to 0.2 m. The difference is believed to be caused by the occurrence of frequent foehn winds along the northern slope.

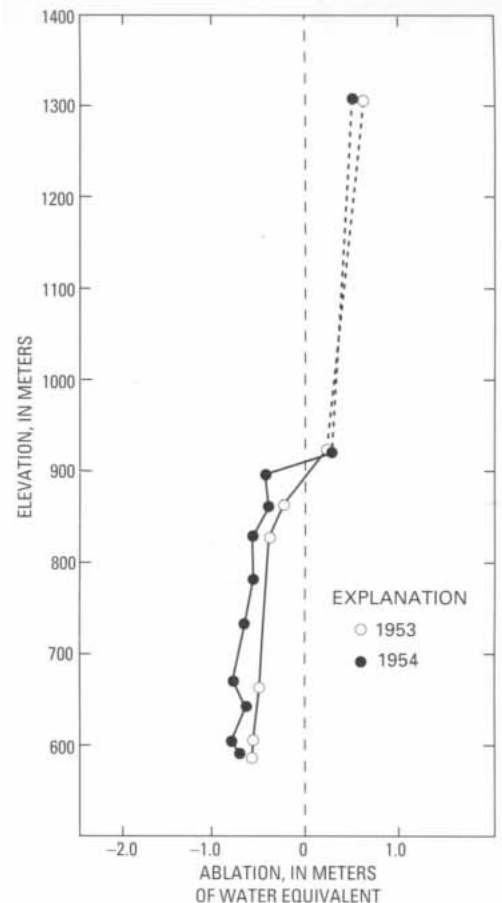
Admiralty and Britannia Gletschers are outlet glaciers from the Inland Ice. The decrease in elevation from the ice sheet to their termini is from 1,500 to 240 m and from 620 to 460 m, respectively. For both outlets, Lister (1958) gave a negative mass balance: for Admiralty Gletscher, 0.9 m of water equivalent (1952-53 balance year); for Britannia Gletscher, varying from 1.2 to 0.6 m of water equivalent (1952-53 and 1953-54 balance years, respectively).

## Glacier Variations and Glacier Hazards

First-order variations have been reported on all of the tidal outlet glaciers of the Inland Ice listed in table 8. With the possible exception of Petermann Gletscher, glacier recession has been documented in all reports. The sporadic observations of the frontal positions, as well as their sporadic disintegrations, do not allow for a statement of a general trend, although neoglacial moraines and trimline zones observed around these outlet glaciers are indicative of a general thinning, but the evidence is less well developed than in West Greenland.

Records of glacier fluctuations are confined to the individual expedition records, and these have been thoroughly interpreted by Koch (1928) and Davies and Krinsley (1962). An updating of this information for the western part of North Greenland has been made by Kollmeyer (1980).

The compilation of all information on glacier changes in North Greenland led Davies and Krinsley (1962) to the conclusion that although the high interior of the ice sheet is growing, a large majority of local ice caps and glaciers exhibit a condition of near equilibrium and that a significant number show evidence of recent recession. The greatest degree of



**Figure 29.**—The mass balance of the west slope of the Inland Ice at the "Nunatarssuaq Ice Ramp," Thule. Data after Nobles (1960).

TABLE 8.—*Calf-ice-producing outlet glaciers from the Inland Ice in North Greenland exhibiting first-order variations*

Glacier code	Name	Figure in text	Reference
2CE ....	Harald Moltke Bræ	27, 30	Mock (1966).
2DB ....	Heilprin Gletscher	30	Kollmeyer (1980).
2DB ....	Tracy Gletscher	30	Kollmeyer (1980).
2F .....	Petermann Gletscher(?)	34	Dunbar (1978).
2G .....	Ryder Gletscher	35, 37	Davies and Krinsley (1962).
2L .....	Academy Gletscher	41, 42	Davies and Krinsley (1962).
2N .....	Storstrømmen/ L. Bistrup Bræ	45	Reeh and others (1993).

retreat has taken place in tidal outlet glaciers (those glaciers whose fronts are afloat in the sea) or in small outlet glaciers that descend steeply from isolated ice caps. Davies and Krinsley (1962) correlate the general retreat, which started in the 1920's, with a decrease in precipitation at the same time. A subsequent general advance of tidal outlet glaciers was initiated in the 1950's (Higgins, 1988, 1989).

In several well-documented cases, glaciers have deviated from the trend described above. "North Ice Cap" has been expanding, whereas the neighboring margin of the Inland Ice ("Nunatarssuaq Ice Ramp") is retreating. Even better known is the Brother John Gletscher at Etah (see figs. 31 and 32), which advanced 2 km between 1861 and 1914 and since then has maintained this advanced frontal position, whereas the southern outlet glaciers from the same ice cap have retreated up to 1.5 km since the 1920's (for example, Morris Jesup Gletscher).

Surges or surgelike behavior has been observed at localities of the Inland Ice margin in this area. Surging was first noticed at Harald Moltke Bræ in North-West Greenland by Mock (1966), who reported a change in rate of surface movement from 1 km a<sup>-1</sup> in 1926–28 to 30 m a<sup>-1</sup> in 1937–38 to 300 m a<sup>-1</sup> in 1956. Later, a surging or pulsing event was described from a part of the Inland Ice margin in the inner western part of Victoria Fjord at "Brikkerne Gletscher" (Higgins and Weidick, 1988), where the average rate of movement of the major outlet increased from under 200 m a<sup>-1</sup> in 1953–63 to an average rate of movement of over 600 m a<sup>-1</sup> between 1963 and 1971. The glacier is shown in figure 38. Most recently, surge structures have been observed during the geologic mapping of Dronning Louise Land (H.F. Jepsen, oral commun., 1989).

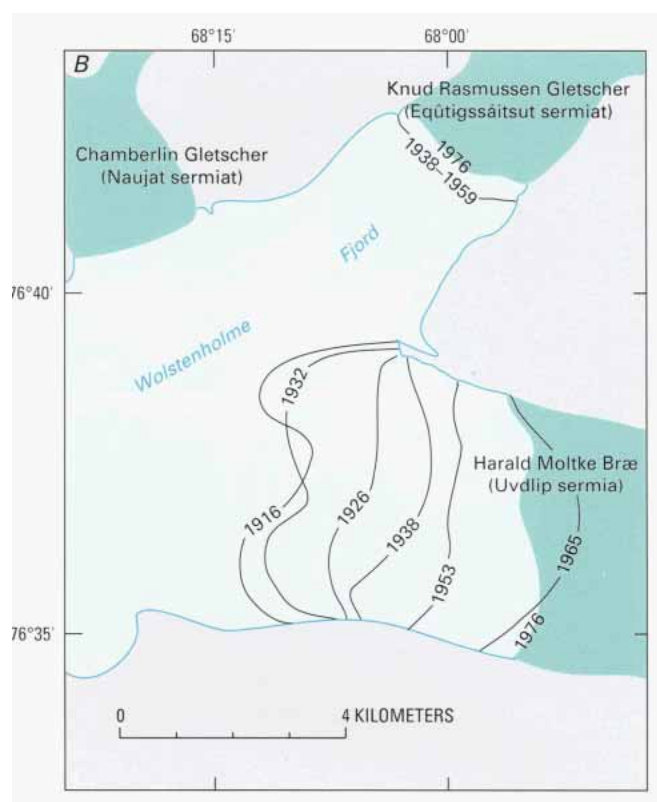
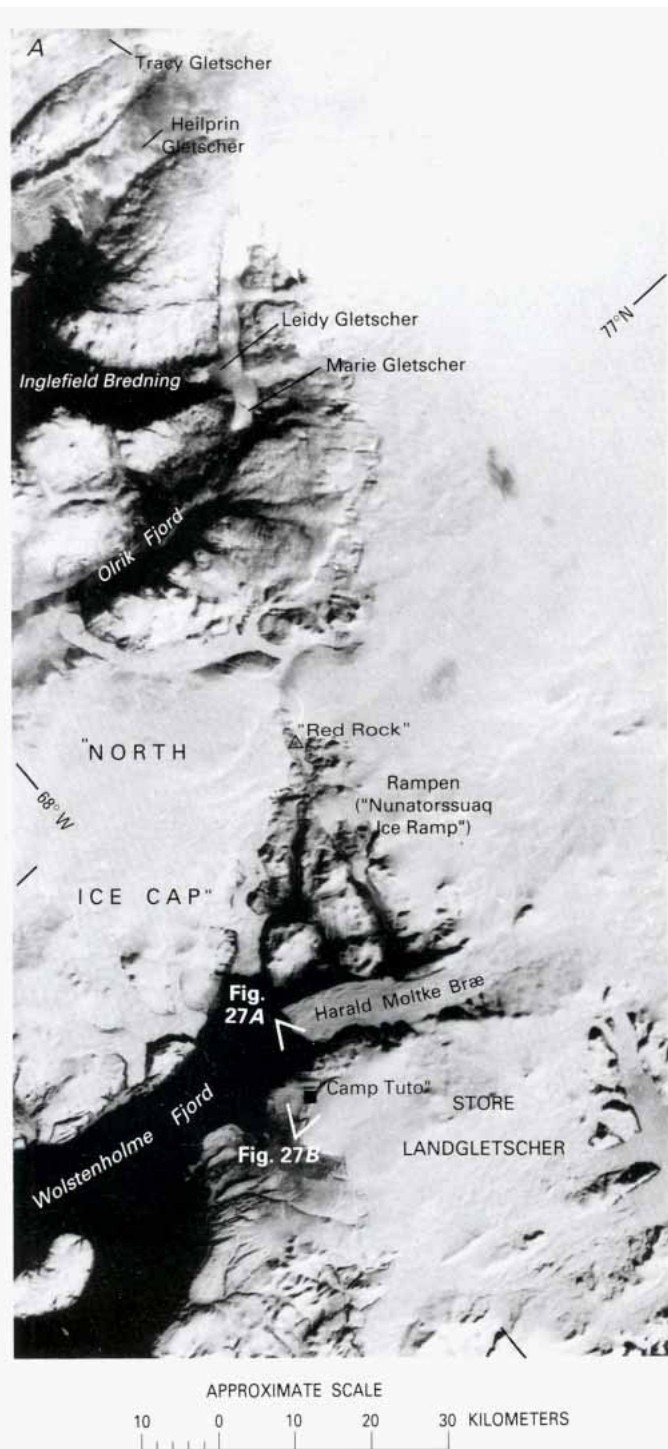
Draining of ice-dammed lakes occurs in North Greenland, but descriptions are rare. A lake at the Inland Ice margin in Warming Land (fig. 37) in the period 17 to 27 July 1984 released about 0.1 km<sup>3</sup> of water subglacially to Sherard Osborn Fjord (Henriksen, 1986). As a result, a cauldronlike depression appeared on the surface of the glacier.

## Images of North-West Greenland

The North-West Greenland area is shown on the Landsat images of figures 30A and 31. The main outlet glaciers from the Inland Ice in this part of Greenland are Harald Moltke Bræ into Wolstenholme Fjord, Marie Gletscher into Olrik Fjord, and Leidy Gletscher and Heilprin Gletscher into Inglefield Bredning.

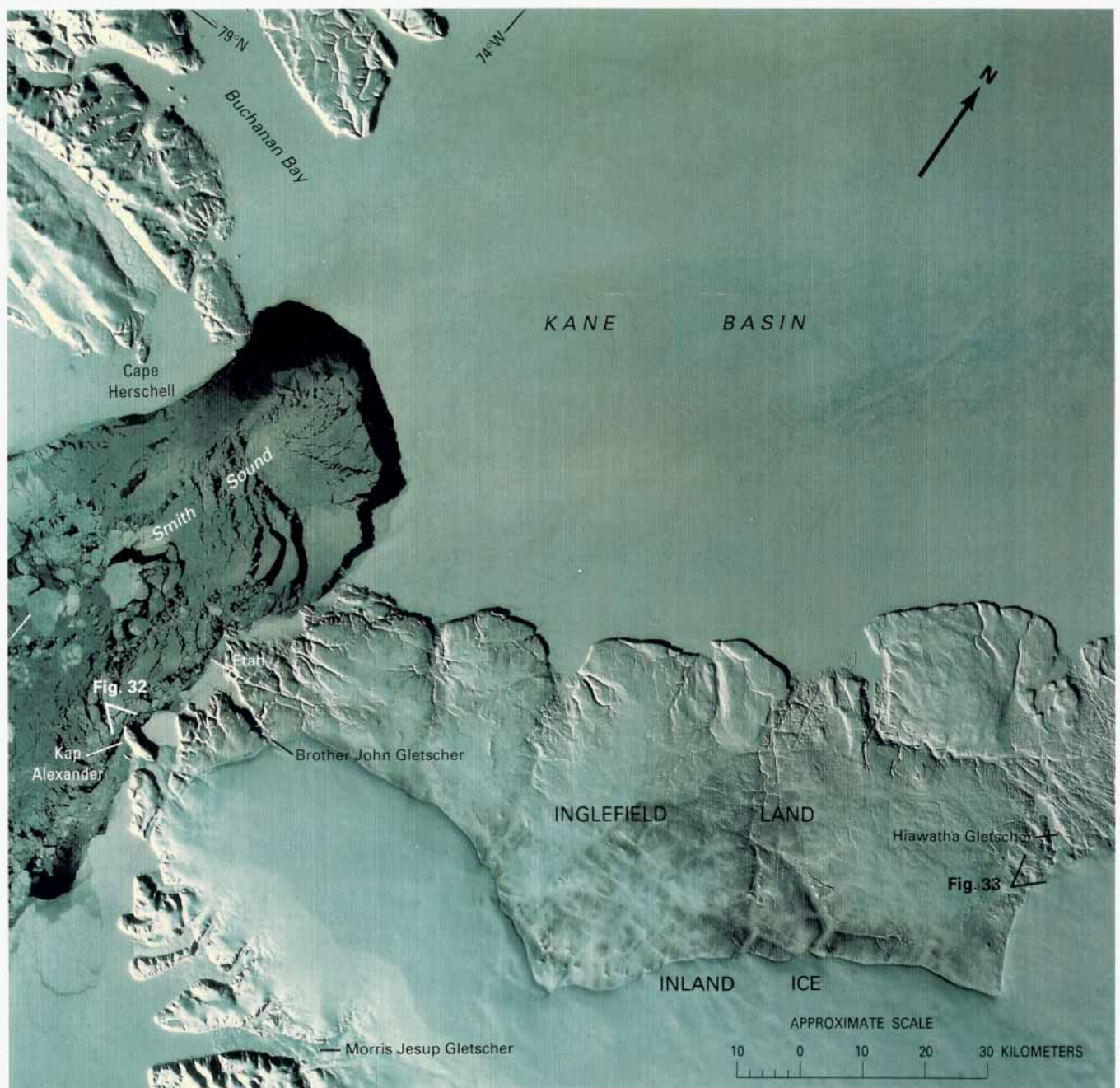
All the locations of the United States' glaciological investigations of the margins of the Inland Ice are covered by figure 30A, including "Red Rock," with the advancing "North Ice Cap" to the left and the receding

Inland Ice margin of “Nunatarssuaq Ice Ramp” to the right. The primary scientific effort, however, was concentrated at “Camp Tuto” (acronym for “Thule takeoff”), where a ramp was constructed for unloading and transporting supplies to support investigations in the interior parts of the Greenland ice sheet. The trail leads from “Camp Tuto” at Store Landgletscher and follows the southern side of Harald Moltke Bræ to avoid the crevassed areas around the northern nunataks of the mountainous area that continues north from the Melville Bugt coastland. The Landsat image (fig. 30A) reveals that the area east of “Camp Tuto” consists of a local ice cap that is interconnected with the Inland Ice sheet 20 to 30 km east of “Camp Tuto,” a fact that is not obvious on the older map sheets.



**Figure 30.** —A, A part of an annotated Landsat 1 MSS image of the Inland Ice margin and local ice caps around Wolstenholme Fjord and Inglefield Bredning, North-West Greenland. Landsat image (1062–16504, band 5; 23 September 1972; Path 34, Row 5) from the EROS Data Center, Sioux Falls, S. Dak. B, Recession and readvance of Harald Moltke Bræ between 1916 and 1976 (after Davies and Krinsley, 1962; Mock, 1966).





**Figure 31.** —Annotated Landsat 2 MSS false-color composite image of Inglefield Land, North-West Greenland. Landsat image (2070–17473, bands 4, 5, and 7; 2 April 1975; Path 45, Row 3, from the EROS Data Center, Sioux Falls, S. Dak.

Steep ramps and ice cliffs are widespread in the whole area from Olrik Fjord to Store Landgletscher, but the area is well known only around “Camp Tuto” and “Red Rock,” where the investigations were concentrated.

For Harald Moltke Bræ only, Mock (1966) provided data on its rate of movement, which infers a calf-ice production of  $0.1$  to  $2 \text{ km}^3 \text{ a}^{-1}$ . Off the northern parts of Heilprin Gletscher, the numerous icebergs also indicate a relatively high calf-ice production of this outlet. The recession of Harald Moltke Bræ is shown in figure 30B (after Davies and Krinsley, 1962; Mock, 1966). A similar, large, 20th century recession of the termini of Heilprin Gletscher and Tracy Gletscher (Kollmeyer, 1980) has been observed; these changes can be documented and monitored on Landsat images.

Figure 31 shows the local ice caps and the Inland Ice margin between the innermost parts of Wolstenholme Fjord and Inglefield Bredning and covers the area from Morris Jesup Gletscher at the north coast of

Inglefield Bredning to Hiawatha Gletscher, an outlet glacier from the Inland Ice margin to the central parts of Inglefield Land. Also, the Canadian side of Smith Sound around Cape Herschell on Ellesmere Island is included on this scene. Kane Basin is covered by fast ice, while open water prevails in Smith Sound.

In spite of the time of year (2 April 1975) and widespread snow cover, the local ice cap between Morris Jesup Gletscher and Inglefield Land (see also fig. 32) is well delineated and interconnects with the Inland Ice sheet for a distance of approximately 25 km. Because of the low solar elevation angle (15°), the ice divide of this local ice cap appears as a crestal ridge situated closer to the calf-ice-producing outlet glaciers around Morris Jesup Gletscher than to the land-based ice margins toward Inglefield Land. Ice cliffs and steep ramps are widespread features that sharply delineate the Inland Ice margin from ice-free Inglefield Land.

The history of Hiawatha Gletscher (fig. 33) has been recorded by Davies and Krinsley (1962). They state that when it was first mapped in 1922, the glacier extended into, but did not fill, a lake at its terminus. After 1922 it began to advance. By the 1950's its terminus was located at the same position as in 1922, although the glacier was wider and filled the valley. The same conditions existed in 1975 and can be seen on the Landsat image (fig. 31) and on the oblique aerial photograph (fig. 33).

**Figure 32.** —Oblique aerial photograph of the local ice cap over the southern part of Inglefield Land (see fig. 31 for location) taken 19 July 1950, looking northeast. Western margin of the ice cap shows transitions between steep slopes and ice cliffs. The two outlet glaciers in the foreground are Dodge Gletscher and storm Gletscher, situated north and south, respectively, of the headland of Kap Alexander. NSC aerial photograph, route 543 8, No. 2714. Reproduced with permission A 200/87.





**Figure 33.**—Oblique aerial photograph of the Inland Ice margin between Hiawatha Gletscher and Humboldt Gletscher in Inglefield Land taken 22 July 1953, looking north. The photograph's location is shown on figure 31. NSC aerial photograph, route 544 C–N, No. 11811. Reproduced with permission A 200187.

## Images of North Greenland

As was discussed earlier, because of orbital constraints the northernmost part of Greenland (north of about lat  $81\frac{1}{2}^{\circ}$  N.) is not covered by Landsat images, but figures 34, 35, and 41 show that all the interior parts of the fjords of North Greenland have been covered. Figure 34 coverage includes the Inland Ice margin in Washington Land from the northern part of the terminus of the Humboldt Gletscher to the upper part of Petermann Gletscher.

The transient snowline on Petermann Gletscher is situated at 800 to 900 m but at Humboldt Gletscher only at 600 to 800 m. Outlet glaciers from the numerous local ice caps of Washington Land are concealed by snow on figure 34, which was acquired on 2 August 1976. Exceptions are the lower parts of the outlet glacier lobes emanating from the ice caps at the west side of Petermann Gletscher.

With a width of approximately 100 km, the exact frontal position of Humboldt Gletscher has been difficult to establish on the basis of former historical records. The outlet glacier is considered to be the broadest glacier known in Greenland. The numerous lakes and drainage channels on the ablation zone of this outlet glacier as well as on Petermann Gletscher (visible on fig. 34) are indicative of a level surface essentially crevasse free. These glacier features are probably the result of the low rate of movement over a rather subdued subglacial topography.

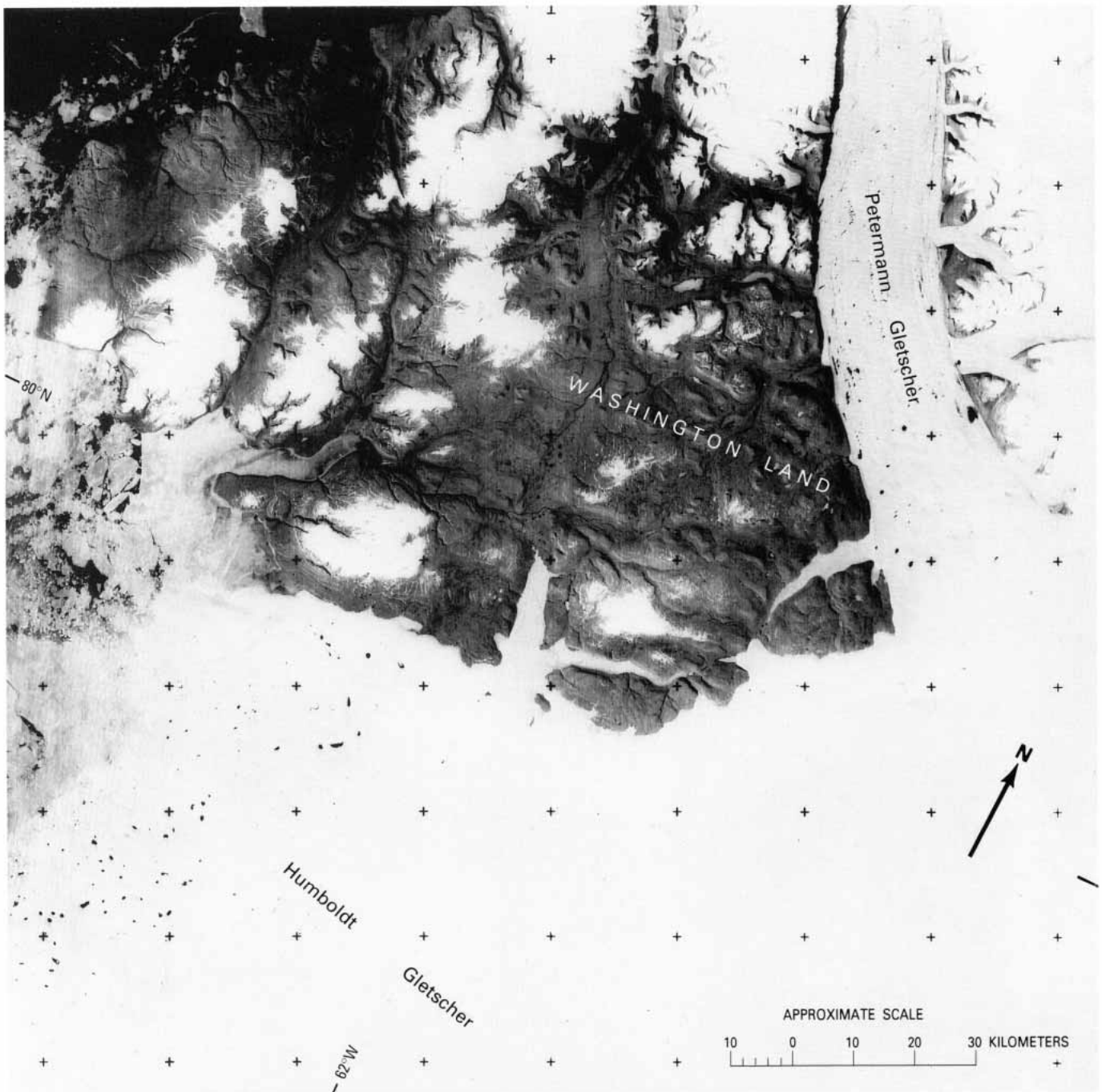
The rate of movement of the two outlet glaciers of figure 34, Humboldt Gletscher and Petermann Gletscher, is relatively slow (see table 3), and it is suspected that the front of Humboldt Gletscher is grounded. Icebergs, therefore, break off only during higher-than-normal tides. The estimated ice thickness of the detached parts of its terminus is approximately 400 m. Petermann Gletscher has an average slope of 6 percent. Large portions of its outer front are floating, and the terminus is only 3 to 4 m above the water level. Calf ice is produced by occasional disintegration of its terminus (Dunbar, 1978; Kollmeyer, 1980). The same conditions occur on other North Greenland outlet glaciers of the Inland Ice (for example, C.H. Ostenfeld Gletscher, see fig. 38) or on local glaciers (see fig. 40).

Figure 35, a Landsat image and sketch map of the Nyeboe Land, Warming Land, and Wulff Land areas, reveals that the typical patterns of the North Greenland landscape are plateaus underlain by Ordovician and Silurian sedimentary rocks and capped by numerous local ice caps. The transient snowline on the outlet glaciers of the local ice caps and on the margin of the Inland Ice can be seen clearly on figure 35A, especially on the outlet glaciers of Steensby Gletscher and Ryder Gletscher, where it reaches an altitude of approximately 800 m.

At the margin of the Inland Ice, steep ramps and ice cliffs frequently mark the border of the ice sheet. An example of a local glacier, a piedmont glacier that has a pronounced lobe, is shown in figure 36. In the pronounced ablation zones of Ryder Gletscher and Steensby Gletscher and on the intermediate margin of the Inland Ice, numerous lakes and drainage channels are indicative of a smooth glacier surface with few crevasses (fig. 37). These features are known from earlier descriptions (Davies and Krinsley, 1962; Ahnert, 1963). The outlet glaciers are floating and extend several kilometers into their respective fjords.

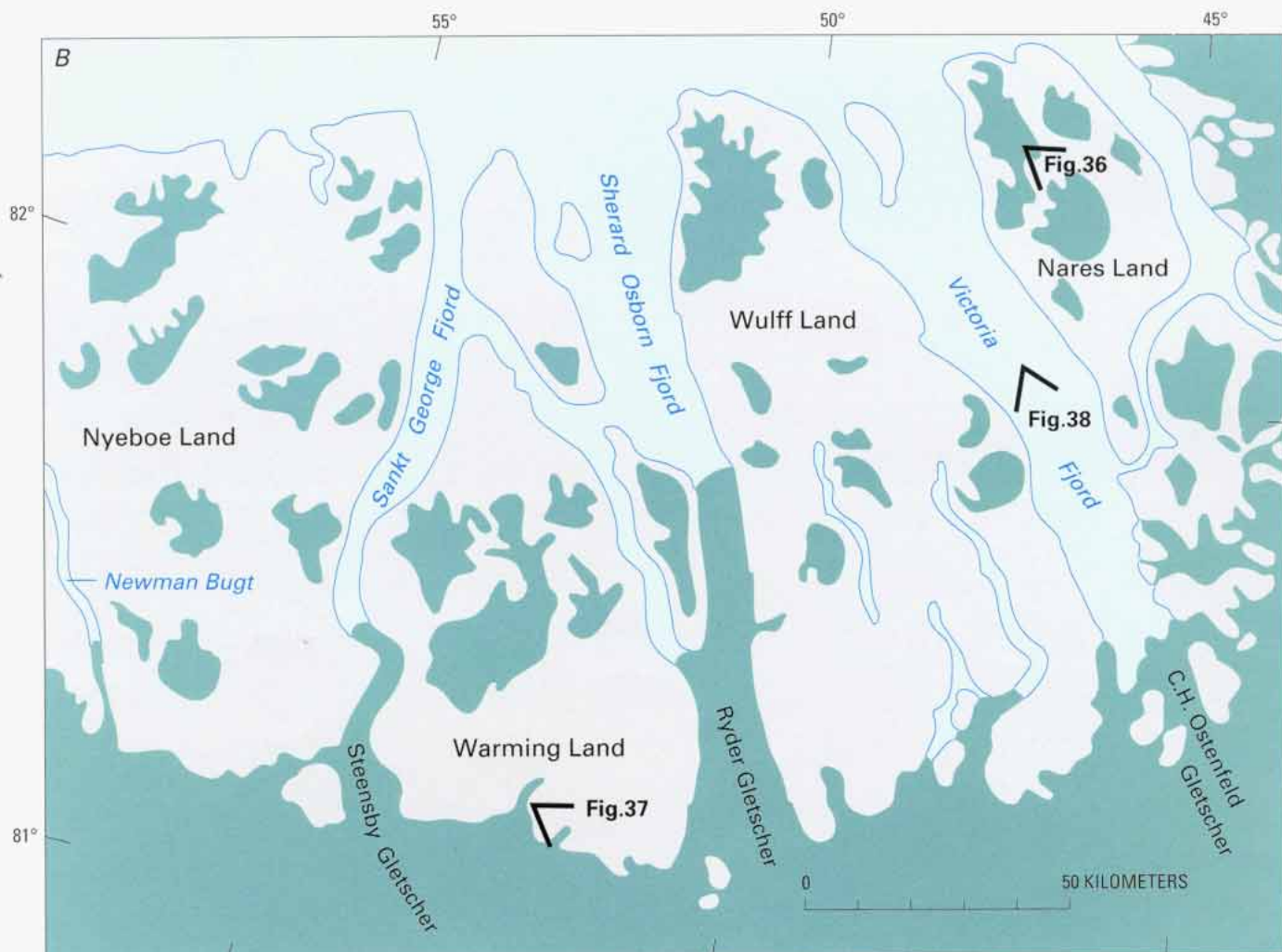
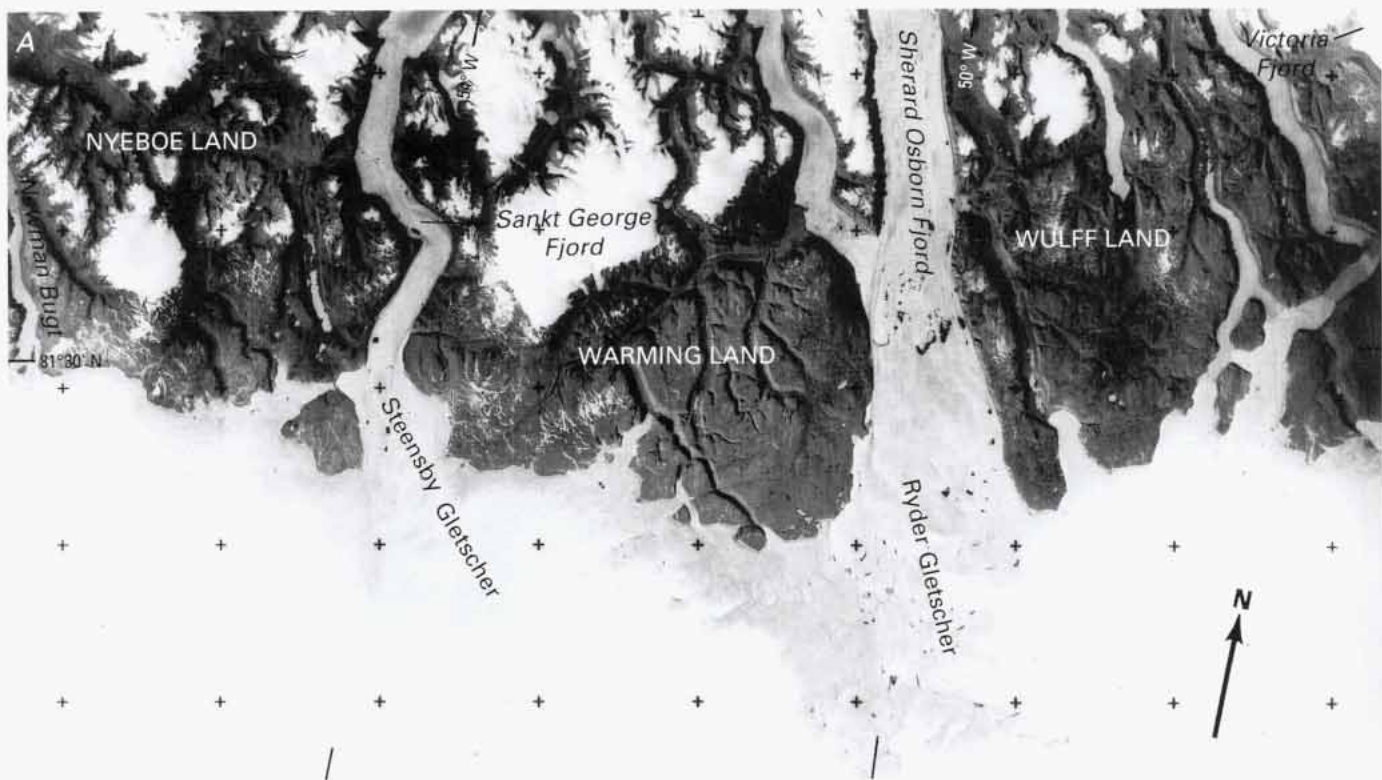
A gradual transition from the floating outlet glacier of the Inland Ice to pack ice, all intermingled with large, detached parts from the glacier terminus, can be seen at Steensby Gletscher, at the tributary leading to Sankt (Saint) George Fjord. Steensby Gletscher has an estimated thickness at its terminus of 75 to 108 m and has the characteristically low





**Figure 34.—Annotated Landsat 2 RBV image of Washington Land showing Humboldt Gletscher and Petermann Gletscher, North Greenland. Landsat image (2558–17503, band 3; 2 August 1976; Path 48, Row 1) from the EROS Data Center, Sioux Falls, S. Dak.**





◀ **Figure 35.**—A, A part of a Landsat 2 RBV image of the Inland Ice margin between Nyeboe Land and Wulff Land, North Greenland. The Landsat image (2544–18130, band 3; 19 July 1976; Path 40, Row 1) is from the EROS Data Center, Sioux Falls, S. Dak. B, Sketch of the area of A showing names of main geographic features and locations of figures 36, 37, and 38.



**Figure 36.**—Oblique aerial photograph of the expanded foot of an outlet piedmont glacier from a local ice cap in the central part of Nares Land, North Greenland. The glacier is viewed from the northwest. The well-defined margin and the smooth surface are characteristic of many of these outlet glaciers in North Greenland. Location of photograph shown on figure 35B. Photograph by J. Lautrup, 1984; copyright The Geological Survey of Greenland.

**Figure 37.**—Oblique aerial photograph of the Inland Ice margin at an unnamed outlet glacier between Steensby Gletscher and Ryder Gletscher, Warming Land, North Greenland (see fig. 35B for location). The area is viewed from the west. In the foreground, the calderalike depression in the outlet is caused by subglacial draining of an ice-dammed lake. In the background, the transition between gently sloping Inland Ice margin, steep ramps, and even ice cliffs can be seen faintly. Photograph by J. Lautrup, 1984; copyright The Geological Survey of Greenland.

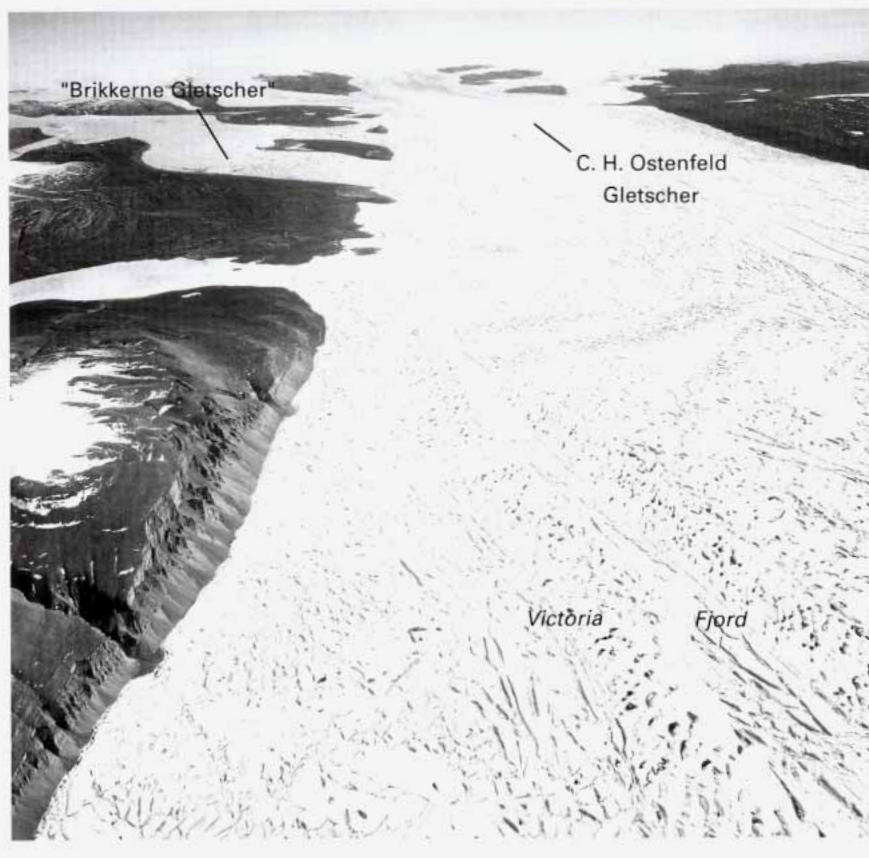


surface gradient of the floating outlet glaciers in North Greenland (1.4 percent or less; Ahnert, 1963). Glacier features of this part of North Greenland are illustrated in the aerial photographs of figures 36, 37, and 38.

As mentioned earlier, the northernmost part of Peary Land is beyond the reach of Landsat coverage (fig. 39). Just east of this region, in Hunt Fjord, one of the centers of formation of ice islands in North Greenland has been located (Higgins, 1989). The alpine landscape and typical glacier appearance are shown in figure 40

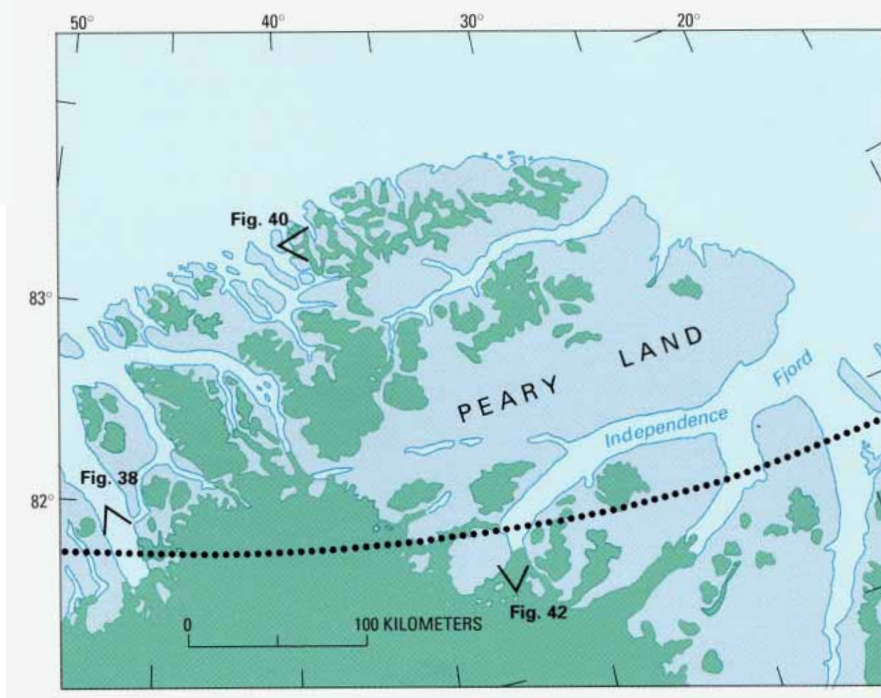
Reasonably frequent earlier records for the frontal positions of North Greenland floating outlet glaciers exist only for the glaciers at the head of Independence Fjord (Academy Gletscher and Marie Sophie Gletscher) (fig. 41A). Early frontal positions have been compiled by Fristrup (1952) and Davies and Krinsley (1962), and they are shown in figure 41B in an updated version based on newer aerial photographs taken on 27 July 1960 and 21 July 1978. On both of these dates the frontal positions were similar. Independence Fjord is white with fast ice; it contains great clusters of icebergs in an upright position, often of a tabular form, near the termini of both glaciers. Icebergs were not identical in form on the two sets of aerial photographs, so it is possible to conclude that calf ice produced in this fjord is not retained over many years but must be





**Figure 38.** —Oblique aerial photograph of C.H. Ostenfeld Gletscher and Victoria Fjord taken 5 July 1953, looking southeast. The floating segment of the tidal outlet glacier reaches from the lowermost nunatak in the background to the front of "Brikkerne Gletscher," a distance of 25 to 30 km. In front of the glacier are the tightly packed icebergs in Victoria Fjord. "Brikkerne Gletscher" is reported (Higgins and Weidick, 1988) to have surged around the end of the 1960's. The photograph's location is shown on figures 35B and 39. NSC aerial photograph route 547 D-SØ No. 11208. Reproduced with permission A 200187.

**Figure 39.** —The Peary Land area and the location of figures 38, 40, and 42. The approximate limit of Landsat 1, 2, and 3 coverage is shown by the dotted line.

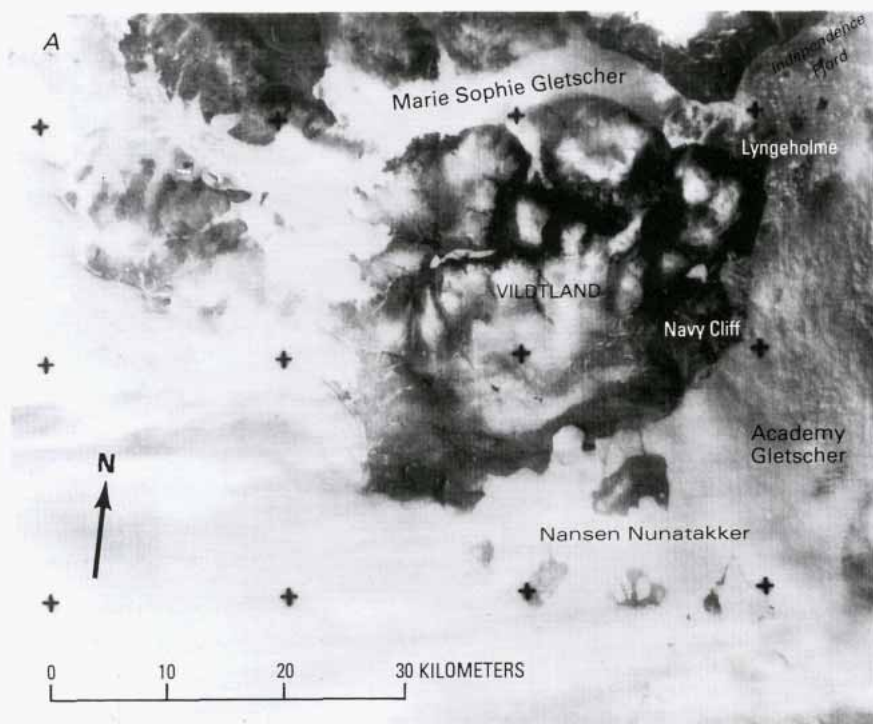




**Figure 40.**—Oblique aerial photograph of northernmost Peary Land (see fig. 39), approximately 83°19' N. lat, 40° W. long, seen from the west. This area, which cannot be covered by Landsat images (north of orbital coverage), consists essentially of alpine peaks. The floating glacier fronts here show the sawtooth appearance known from other North Greenland glacier fronts. NSC aerial photograph, route 547 M-Ø, No. 1804 (15 July 1950). Reproduced with permission no. A 200/87.

released during August each year. The descriptions from the earlier records also reveal that this dense packing of icebergs at the glacier termini implies that the determination of their precise positions from ground observations must be difficult. Figure 42, although taken in 1951, shows similar ice conditions in Independence Fjord.

Although the Landsat image shown in figure 41A (acquired on 15 August 1976) is not particularly detailed, the transient snowline is estimated to be at an elevation of 900 to 1,000 m. In Independence Fjord, open water is visible around the islands of Lyngeholme. The lakes at Navy Cliff can be delineated also, but the terminus of Academy Gletscher is veiled by low clouds. Although the area around Marie Sophie Gletscher appears to be clear, and the position of its terminus for this year (1976) is approximately 5 km west of the position shown on aerial photographs taken in 1960 and 1978, the sharply drawn edge might be the margin of a fog bank.



**Figure 41.** —A, Part of an annotated Landsat 2 RBV image of the head of Independence Fjord showing Marie Sophie Gletscher and Academy Gletscher, North Greenland. Landsat image (2571–17203, band 3; 15 August 1976; Path 30, Row 1) from the EROS Data Center, Sioux Falls, S. Dak. B, Updated sketch map of the changing positions of the termini of Marie Sophie Gletscher and Academy Gletscher (originally compiled by Davies and Krinsley (1962) and Fristrup (1952)).

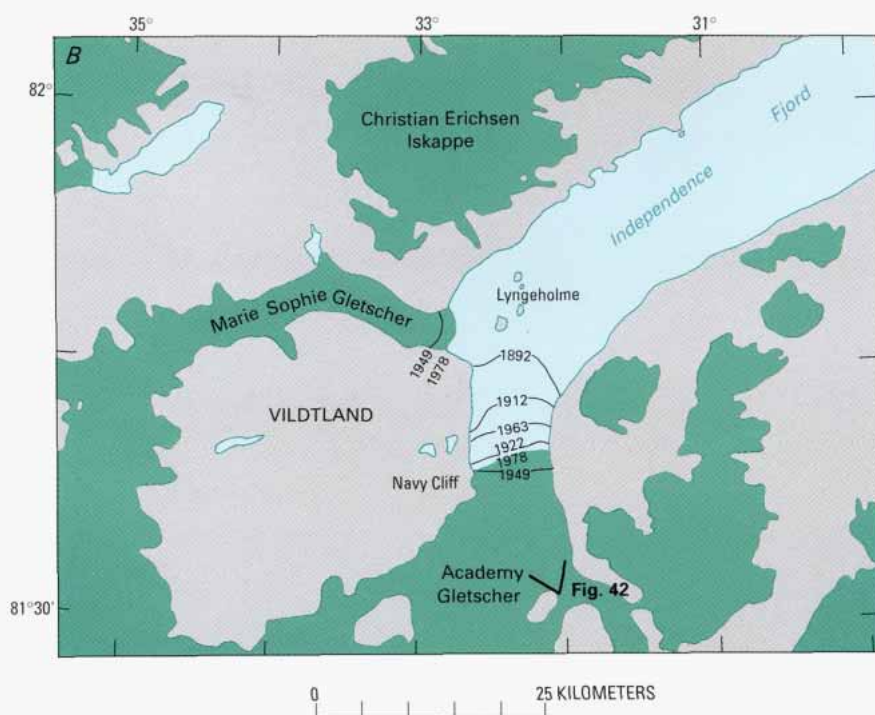






Figure 42. -Oblique aerial photograph of the head of Independence Fjord taken 10 August 1951, looking north (see fig. 418 for location). In the foreground Academy Gletscher can be seen with detached parts of the glacier front in upright position just off the front. The rest of Independence Fjord is covered by fjord ice. In the background to the left is Marie Sophie Gletscher, and in the center of the photograph are Lyngeholme and Christian Erichsen Iskappe. NSC aerial photograph, route 663 C-N, No. 14909. Reproduced with permission A 200187.

## Images of North-East Greenland

The area from Jøkelbugten to Hochstetter Forland (fig. 1) has been studied little, and the main glaciological investigations have been concentrated around Dronning Louise Land and the Storstrammen outlet glacier, localities that were the starting points for two crossings over the Inland Ice, namely those of I.P. Koch (1912–13) and the British North Greenland Expedition (1952–54). Investigations on mass balance and ice movement were later initiated in the Storstrømmen and Kronprins Christian Land areas by the Alfred-Wegener-Institut, Germany, and the Danish Polar Center (Reeh and others, 1993).

The region of North-East Greenland consists of a northern, relatively lowland part around Jøkelbugten and associated archipelago, where the coastal strip of 'ice-free land is narrow, and a southern part around Hochstetter Forland, which has moderate uplands and where the Inland Ice is separated from the outer coast by a 100- to 200-km-wide coastal strip. The Landsat images in figures 43 and 45 illustrate both types of landscape.

In figure 43 the islands of Hovgaard Ø, Lambert Land, and Schnauder Ø can be seen in the central parts of the Landsat image. Lambert Land separates the Inland Ice outlet glaciers of Nioghalvfjerdsbræ and Zachariae Isstrøm just as Hovgaard Ø splits Nioghalvfjerdsbræ into a main stream that flows into Nioghalvfjerdsfjorden and a northern outlet glacier, Spaltegletscher, that flows into Dijnphna Sund. Spaltegletscher is reported to have had a retreat of 18 km between 1907 and the 1950's (Davies and Krinsley, 1962), and, in spite of the errors in determining the old frontal positions, a major recession of the outlet glaciers must have taken place during the first half of the 20th century in this part of Greenland.

The character of the termini of Nioghalvfjerdsbræ and Zachariae Isstrøm makes determination of frontal changes difficult. An oblique aerial photograph (fig. 44) shows Zachariae Isstrøm from the east. In the foreground the disintegrating glacier terminus merges into fast ice of the semipermanently frozen fjord. The nunataks in the background are Hertugen af Orléans Land, which is on the southern side of the outlet glacier. In the right foreground a small part of the island of Schnauder Ø can be seen.

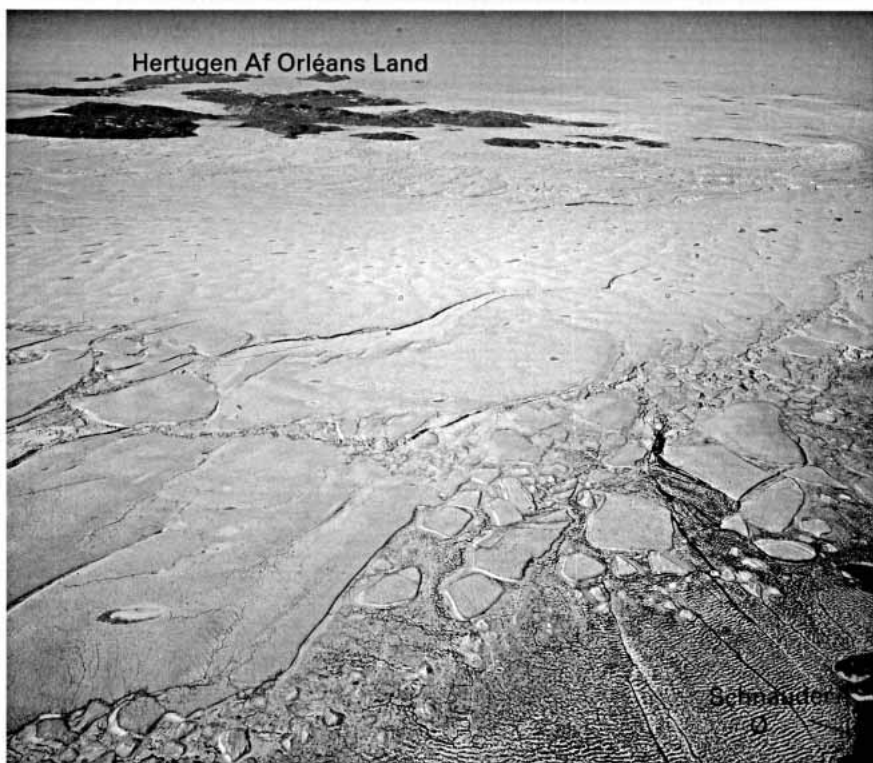
Jøkelbugten was described by Koch (1928) as the greatest example in Greenland of confluent ice, which is ice that has formed from the coalescence of ice tongues from several glaciers but has been given a definite form and trend by the presence of a continuous margin (ice front) along the seaward edge. According to the "Illustrated Glossary of Snow and Ice" (Armstrong and others, 1973), the area may be described also as a recently disintegrated ice shelf. On the Landsat image (fig. 43), acquired on 15 July 1976, fast ice, in spite of the season, still covers large parts of Nioghalvfjerdsfjorden and extends 60 km east of Norske Øer. The semipermanent condition of fast ice in this part of Greenland is illustrated.

Storstrammen and L. Bistrup Bræ at Borgfjorden are shown in figure 45. The lakes are still frozen on 25 June 1973, and fast ice rims the outer coast (for example, near Store Koldewey). Snowmelt has reached altitudes of 800 to 900 m, and melt patterns on the surface of the outlet glaciers are closely related to the receding snowline. The melt patterns can be located in the same positions on Landsat images from several consecutive years, although the movement of Storstrømmen is considered to be relatively great (up to 1.8 km a<sup>-1</sup> at the front, see table 3). The melt patterns might therefore be related to subglacial topography.

The abutment of the termini of Storstrømmen and L. Bistrup Bræ is clearly defined on the image despite the dense cover of calf ice in front of



**Figure 43.** —Annotated Landsat 2 MSS image of the terminus of the glacier lobes of Nioghalvfjærdsbræ and Zachariae Isstrøm, North-East Greenland. Landsat image (2540–14245, band 7; 15 July 1976; Path 72, Row 2) from the EROS Data Center, Sioux Falls, S. Dak.



*Figure 44. —Oblique aerial photograph of Zachariae Isstrøm taken 15 August 1950, looking west (see fig. 43 for location). NSC aerial photograph, route 659 A–V, No. 8156. Reproduced with permission no. A 200187.*

the glaciers. Since first mapped in 1906, the maximum recession of the common terminus is approximately 7 km; only a slight continuation of the recession would split up the two outlet glaciers into separate glacier lobes. A comparison of figure 45 with earlier maps of the area documents some recession of Soranerbræen and Borgjökelen in Dronning Louise Land. It is in the same region (Borgjökelen and Budolfi Isstrøm) that some of the surge structures mentioned previously are found.

A mosaic (fig. 46A), from three consecutive images along the same orbital path, gives an overview of the whole region of North-East Greenland. The entire coastal region from Germania Land and the island of Store Koldewey south to Kejser Franz Joseph Fjord is covered. A belt of pack ice carried from the Arctic Basin by the East Greenland Current is visible in a zone extending from Germania Land to Hochstetter Forland and Shannon. The length of the greatest ice floe (off Germania Land) is 30 km. The pack ice usually spreads during the course of the winter from its minimum in the Arctic Basin; it appears off Scoresbysund in October, off Angmagssalik in November, and off Julianehåb in South Greenland during February–March.

In the Landsat mosaic (fig. 46A), all of the coastal areas are covered by new snow. The only exceptions, the lowlands in the interior parts of Kejser Franz Joseph Fjord and around the outlet glaciers Waltershausen Gletscher and Adolf Hoel Gletscher, at the Inland Ice margin, serve to illustrate the low precipitation in these inland areas. The fjords are not yet frozen, and termini of all the Inland Ice outlet glaciers can be delineated clearly. Around Waltershausen Gletscher and Adolf Hoel Gletscher, flow patterns are visible in the Inland Ice, and subglacial topography is quite evident because of the low solar illumination angle (14°).

Recession of Soranerbræen seems to have been 3 to 5 km between 1906 and 1972, whereas for Heinkel Gletscher it was about 10 km between the 1930's and 1972. The front of Wordie Gletscher is in shadow, so it cannot be compared to earlier positions. Waltershausen and Adolf Hoel Gletschers show little change in their frontal positions since mapping in the area during the 1930's to 1950's.

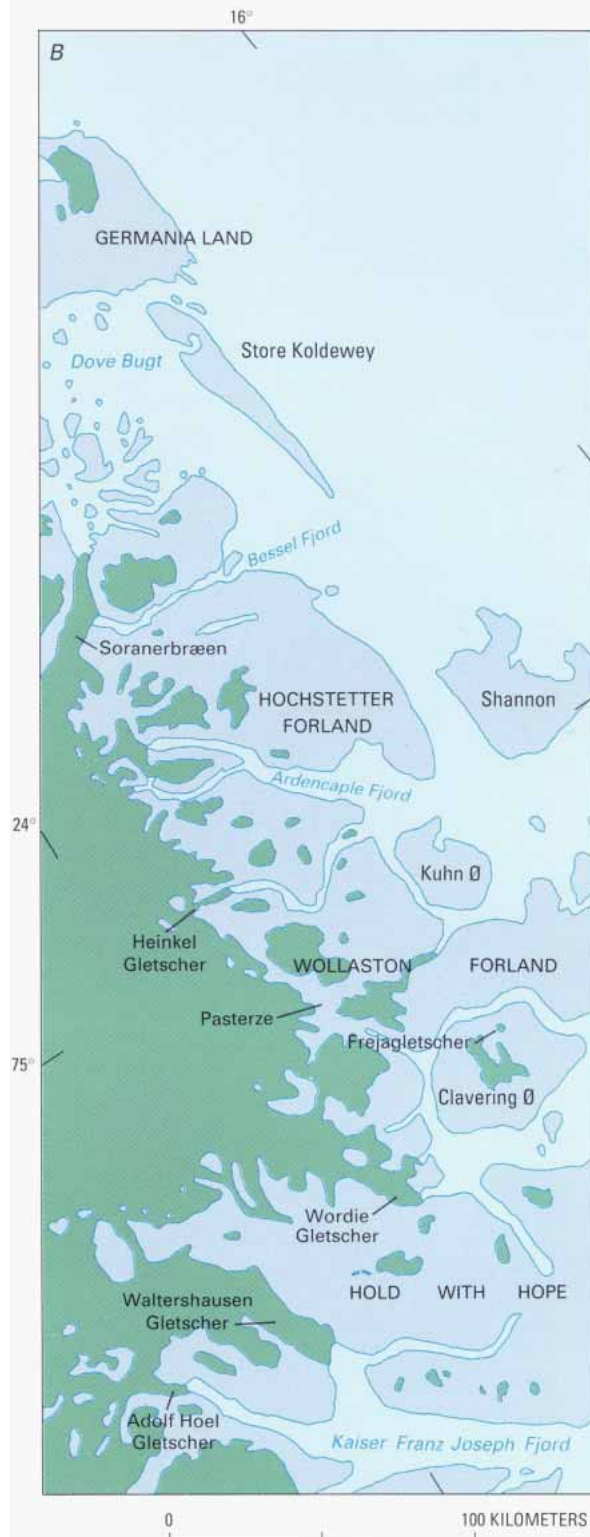


**Figure 45.—Annotated Landsat 1 MSS image of Storstrømmen and L. Bistrup Bræ at Borgfjorden, North-East Greenland. Landsat image (1337–13532, band 7; 25 June 1973; Path 4, Row 5) from the EROS Data Center, Sioux Falls, S. Dak.**





**Figure 46.**—A, Landsat 1 MSS false-color composite image mosaic of the coastal area between Germania Land and Keiser Franz Joseph Fjord, North-East Greenland. Landsat images (top, 1064–13354, Path 251, Row 5; middle, 1064–13360, Path 251,



Row 6; bottom, 1064–13363, Path 251, Row 7; bands 4, 5, and 7; 25 September 1972) from the EROS Data Center, Sioux Falls, S. Dak. B, The same area covered by the Landsat image mosaic, with the names of the main geographic features shown.

# East Greenland

## Climatic Conditions

Climatic conditions in East Greenland are dominated by the presence of the southward flowing, cold East Greenland Current along the entire coast. The current brings great masses of the "Storis" (East Greenland pack ice) southward, and the width and areal extent of this pack ice belt vary both according to season and, over a period of decades to centuries, according to general climatic fluctuations. The limits of this belt have therefore retreated considerably during the first half of this century. The fluctuations in extent of this pack-ice belt can be followed closely on Landsat and NOAA advanced very high resolution radiometer (AVHRR)-images and on satellite passive-microwave observations, such as the 1973–76 monthly record of sea ice in the Northern Hemisphere recorded by the electrically scanning microwave radiometer (ESMR) of the Nimbus 5 satellite (Parkinson and others, 1987). An example of a Landsat image showing pack-ice information is figure 46.

South of the Denmark Strait, the East Greenland Current mixes with a warm, westerly branch of the Gulf Stream, the Irminger Current, and the combined current flows around Kap Farvel and continues northward along the coast of West Greenland. As a result, the climatic conditions in East and West Greenland are quite different, with the most severe sea-ice conditions occurring along the east coast.

The meridional decrease in precipitation from south to north is quite marked, with 2,500 mm at lat 60° N. (Prins Christian Sund), about 900 mm at lat 65° N. (Angmagssalik), 450 mm at lat 70°30' N. (Kap Tobin at Scoresbysund), and about 200 mm at lat 74° N. (Daneborg). All of these meteorological stations are relatively close to the outer coast, so information on the decrease in precipitation toward inland areas is lacking. The distribution of vegetation, as given by Bøcher and others (1978), provides some indication, however. The plant provinces of East Greenland are a contrast to those of West Greenland, because the greatest width of the ice-free coastal strip in East Greenland occurs north of lat 70° N. In these wide, ice-free regions, dry conditions in the inland areas are very common. In East Greenland, in the regions south of lat 70° N. (for example, Scoresby Sund area), unlike in West Greenland, no zone of maximum precipitation (accumulation) is found in the interior (on the Inland Ice) (fig. 5).

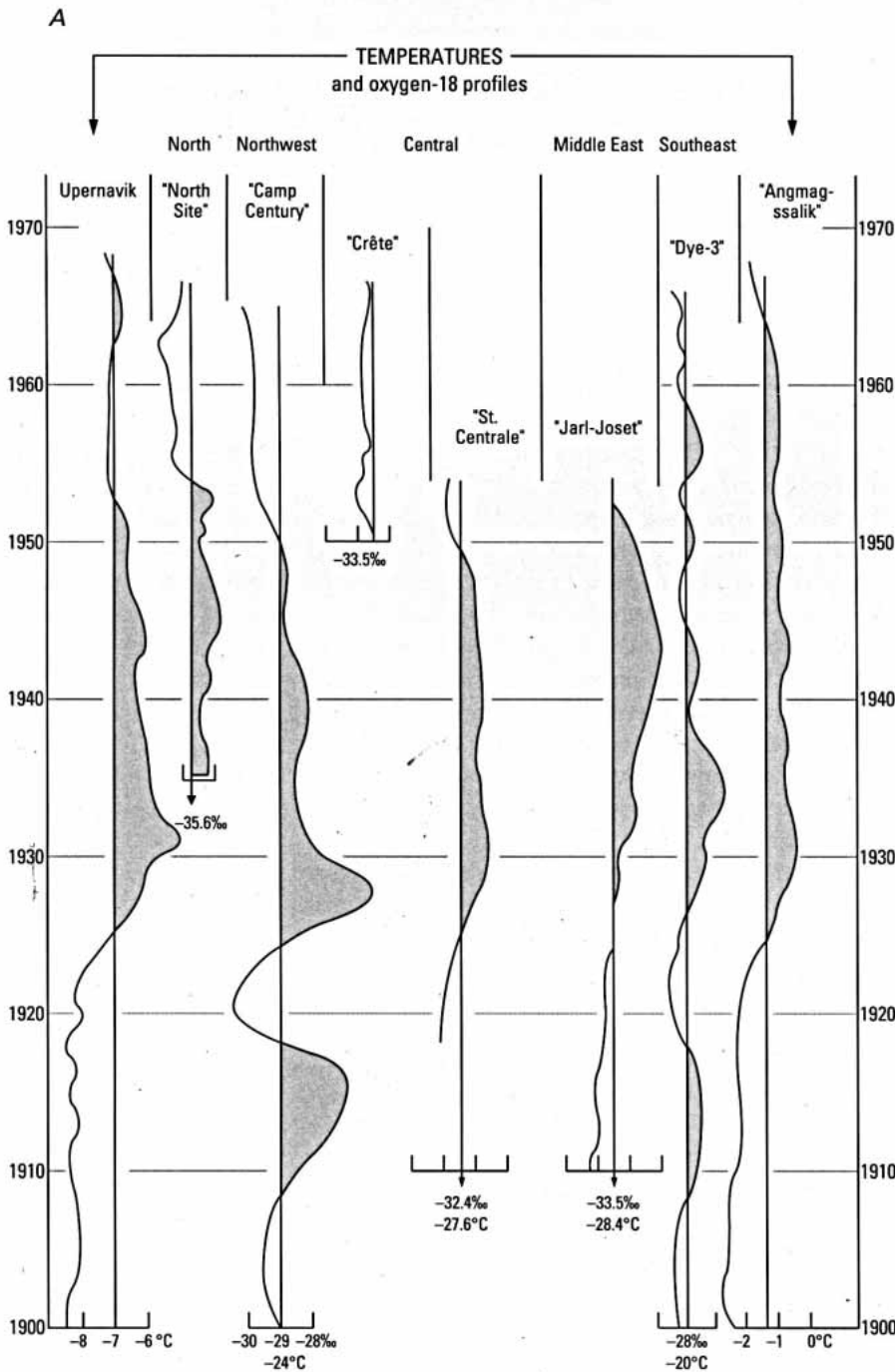
Measured temperature conditions in East Greenland are shown in table 9. Inland temperature measurements are scarce and apparently have been measured only during a 10-month period in 1891–92 at Hekla Havn on Danmark Ø (lat 70°27' N., long 26°16' W.) in the interior of Scoresby Sund. The January mean was –25°C, and that of July was +4.5 °C.

TABLE 9.—Average temperatures for the months of January and July, annual average temperatures, and annual precipitation at selected stations in East Greenland  
[Data refer to 1961–70 averages from the Danish Meteorological Institute, Copenhagen]

Station	Location		Average temperatures (°C)			Average annual precipitation (millimeters per year)
	°N lat	°W long	January	July	Annual	
Daneborg.....	74	20	–21.8	+3.7	–10.6	195
Kap Tobin.....	70	22	–17.4	+2.7	–8.2	448
Aputitêq.....	68	32	–10.7	+2.2	–4.8	606
Angmagssalik.....	66	38	–7.3	+6.6	–1.6	930
Tingmiarmiut.....	63	42	–6.2	+5.7	–1.2	1,521
Prins Christianssund.....	60	43	–3.3	+6.7	+0.9	2,480

The climatic conditions are reflected in the trend of the glaciation limit shown in figure 4. A special feature of East Greenland is the extremely low position of this limit at the outer coast; it is very close to sea level in South-East Greenland. In this region, the steepest gradient of this limit inland reaches altitudes of 1,500 m.

The climatic fluctuations can be demonstrated by the long observation record from Angmagssalik. Air temperatures from this meteorological station are compared to those of Upernavik in northern West Greenland in figure 47 and to the isotopic record of ice cores from the Inland Ice. The warm period of 1920-50 seems to have extended a decade longer at Angmagssalik, but otherwise the record from there follows the general trend observed at the other Greenland stations.



**Figure 47.**—A, Observed 10-year running-mean temperatures at Angmagssalik (right) and Upernavik (left) compared with 10-year running-mean  $O^{18}/O^{16}$  values at six Greenland ice sheet stations. ‰, per mil. B, Location of meteorological stations and ice-core drilling sites used for graphs in A (from Dansgaard and others, 1973).



## Glaciological Conditions

North of Scoresby Sund, the terrain is dominated by an eastern coastal foreland of sediments of varying geologic ages and an interior eastern belt of folded and metamorphic rocks (Caledonian mobile belt). Between Scoresby Sund and Kangerdlugssuaq, the highlands are formed by Tertiary basalts, whereas the narrow coastal stretch around Angmagssalik and farther south consists of Precambrian rocks.

The topography is generally highland, often forming alpine landscapes, and this, together with the varying climatic conditions, produces a wide variety of glacier types. In general, elevations in the interior of East Greenland exceed those of West Greenland. Examples of selected summit elevations along the eastern border of the Inland Ice are given in table 10 and range from 1,800 to 3,700 m. For comparison, it should be noted that mountain summits along the western margin of the Greenland ice sheet rarely exceed 1,500 m (with the exception of the Umanak district) and that they mainly occur at elevations of 700 to 1,000 m. As a consequence, the extensive ablation zone present on the western slope of the Inland Ice (figs. 17 and 19) is not found on the eastern slope of the Greenland ice sheet.

The plateaus in the region south of Scoresby Sund continue to the outer coast. The highest mountain in Greenland (Gunnbjørn Fjeld at lat 68°55'



TABLE 10.—*Maximum summit elevations of selected mountain peaks along the eastern border of the Inland Ice according to the International Civil Aviation Organization (ICAO) map sheets (1:1,000,000 scale)*

Name	Geographic coordinates		Summit elevation (m)
	°N. lat	°W. long	
Unnamed peak.....	76°18'	26°10'	~2,200
Holger Danske Tinde.....	74°27'	24°32'	2,148
Shackleton Bjerg.....	72°54'	28°50'	2,950
Arken.....	70°29'	29°43'	2,348
Gunnbjørn Fjeld.....	68°55'	29°53'	3,700
Mont Forel.....	66°57'	36°49'	3,360
Treforken.....	63°35'	42°06'	2,150
Husfjeldet.....	61°48'	43°10'	1,840

N., long 29°53' W.), with an elevation of 3,700 m, is located here. Large local ice caps in this area coalesce with the drainage systems emanating from the Inland Ice.

The high East Greenland mountains strongly affect the dynamics of the Inland Ice. They form the backbone of Greenland, forming in most places an effective barrier to the eastward drainage of the Inland Ice. The Greenlandic name for East Greenland, “Tunua” (its back side), also has meaning in a glaciological sense. Because of the damming-up against the eastern mountains, the main drainage from the Greenland ice sheet takes place toward the west, and consequently the ice divide has a position that is displaced well to the east on the ice sheet. Accumulation, ablation, and calf-ice production of the ice sheet therefore are concentrated mainly on the western slopes of the ice sheet. Little remains to flow out from the eastern margin. Although mass-balance measurements and observations of calf-ice production of East Greenland outlets are rare (table 3), the total rate of ablation and calf-ice production from this part of the ice sheet is considered to be relatively small. An example on the Inland Ice marginal areas is the upper reaches of Waltershausen Gletscher shown in figure 48.

In the extensive highland areas, at several localities ice caps merge with the Inland Ice. These ice caps are most common in the areas inside Kejser Franz Joseph Fjord and Scoresby Sund fjord complexes (especially the southern side) but also around Angmagssalik and in the southernmost part of East Greenland.

Mass-Balance Investigations

Mass-balance investigations in East Greenland were carried out on “Frøya Glacier” (present authorized name: Frejagletscher) on Clavering Ø at lat 74°24' N., long 20°50' W. It is a small valley glacier that has an area of 6.3 km<sup>2</sup>. Glaciological measurements covered the period between 3 August 1939 and 15 July 1940, an incomplete budget year. It was estimated that the mass-balance included a total accumulation of 1.4 x 10<sup>6</sup> m<sup>3</sup> of water and an ablation of at least 1.9 x 10<sup>6</sup> m<sup>3</sup> for a net deficit of 0.5 x 10<sup>6</sup> m<sup>3</sup> of water for the total budget year of 1939-40. The trend of the net balance curve for the measured period shows a resemblance to that of “Nunatarssuaq Ice Ramp” (fig. 29).

In spite of not covering a full budget year, the work on “Frøya Glacier” is still outstanding for the Greenland area because of its detailed description of the connection between mass-balance results and adherent energy exchange at the glacier surface (Ahlmann, 1942; Eriksson, 1942). No other mass-balance investigation on glaciers in East Greenland have been performed as thoroughly as those on “Frøya Glacier.”





*Figure 48. —Oblique aerial photograph of the upper parts of Waltershausen Gletscher taken 17 August 1950, looking northwest. The photograph shows the smooth surface of the upper part of the glacier. The lower parts are characterized by heavily pitted surfaces. Some pitting can be seen on the surface of a northern branch of Waltershausen Gletscher, indicated by "N" on the photograph. The structure seems identical with known surge patterns (see fig. 54) and might indicate a pulsing or surging behavior of these outlets. The location of the photograph is shown on figure 46A. NSC aerial photograph, route 632-NV, No. 1889. Reproduced with permission no. A 200187.*

Glacier hydrology investigations were initiated on Mitdluagkat Gletscher in East Greenland during the International Geophysical Year (IGY) program of 1956-58 by the Geographical Institute, Copenhagen University (Fristrup, 1961). The glacier is situated at the entrance to Sermilik west of Angmagssalik at lat 65°41'N, long 37°54' W. and covers an area of 36 km<sup>2</sup>. The continuous thinning and retreat of the lower reaches of this glacier can be traced back to 1933 and are still in progress, whereas a recent buildup of the firn area has become apparent (Hasholt, 1986).

## Glacier Variations and Glacier Hazards

In East Greenland, just as in West Greenland, the greatest sensitivity to climatic fluctuation is shown in single calving ice-producing outlet glaciers, some of which are related not to the Inland Ice but to local ice caps. Table 11 lists East Greenland glaciers that have exhibited first-order variation ( $\geq 5$  km). There has not been a systematic collection of information on glacier variations in East Greenland, although Sharp (1956) cited several references. The data provided in table 11 are based on a comparison of

map sheets published by the Geodetic Institute (National Survey and Cadastre) (mostly from information gathered during the 1930's) and, where possible, comparison to older information. A systematic mapping of the trimline zones and neoglacial moraines around the glaciers in some cases contributes to the list, especially in those instances in which a major retreat occurred before the date of the oldest published information. Landsat images can be especially valuable for mapping trimlines and monitoring glacier variation and calf-ice production. Dwyer (1993) used Landsat images to quantify terminus fluctuations and estimate surface velocities for the larger tidewater glaciers in the Kangerdlugssuaq region.

TABLE 11.—*Outlet glaciers that have exhibited first-order variations in East Greenland ( $\geq 5$  km)*

Glacier code	Name	Figure in text	Reference
3AB.....	Pasterze	46	Flint, 1948.
3GB.....	Kangerdlugssuaq Gletscher	59	This chapter.
3GC.....	Outlet glacier at Deception Ø (unnamed)	59	Ditto.
3GC.....	Outlet glacier at Ûartit (unnamed)	59	Ditto.
3HG.....	Kårale Gletscher	61	Ditto.
3IA .....	Midgårdgletscher	61	Ditto.
3IA .....	Fenrisgletscher	61	Ditto.
3IA .....	Helheimgletscher	61	Ditto.

Of the glaciers listed in table 11, only Pasteme is land based; it is reported to have receded more than 6 km between 1869 and 1922 (Sharp, 1956). The remaining glaciers are calf-ice-producing tidal outlet glaciers that cluster around Blosseville Kyst (coast) (code letter G) and Angmagssalik (code letters H and I). With the exception of Fenrisgletscher and possibly Ûartit, all reports document recession. Only Pasterze and Midgårdgletscher can be considered to be true outlet glaciers from the Inland Ice; the other outlet glaciers emanate from local ice caps in Kong Christian IX Land between Scoresby Sund and Angmagssalik. An evaluation of available data on the outlet glaciers from the Inland Ice generally shows either minor recessions or relatively static conditions.

On a small scale (frontal recessions of 1 to 2 km) variations are widespread; see, for example, the reports of the Louise Boyd expeditions (Bretz, 1935; Flint, 1948). Reports on the rate of recession are few, however. Measurement on Frejagletscher in 1952 showed a total recession of approximately 1 km from the neoglacial terminal moraines (Ahlmann, 1953). Around Angmagssalik, local glaciers have been investigated also. Tasissarssik glacier had a total recession of 900 m, which according to lichenometric dating, was initiated around 1830 $\pm$ 20 years (Gribbon, 1964). A recession of the terminus of Mitdluagkat Gletscher between 1933 and 1959 was found to be 400 m (Fristrup, 1961); recurring outburst floods from icedammed lakes were described also.

A conspicuous feature of East Greenland glaciers is the surging glaciers. Patterns associated with surging behavior can be seen on Waltershausen Gletscher in northern East Greenland (fig. 48). Several surging glaciers have been reported in Stauning Alper north of Scoresby Sund, in central East Greenland (Olesen and Reeh, 1969). Some of these glaciers can be seen on figure 52. Lobate moraines, which are characteristic of surge behavior, can be found on several glaciers, such as Dendritgletscher and Bartholin Bræ (see fig. 57B). The presence of these moraines implies that glacier surges might be widespread in East Greenland (Weidick, 1988b).

## Images of Northern East Greenland

The northernmost parts of northern East Greenland are shown on figure 46. As one continues to the south, figure 49 shows the interior and figure 52 the eastern parts of the area between Kong Oscar Fjord and Scoresby Sund. This area is the boundary between northern and central East Greenland.

On figure 49, the heads of the fjords are obscured by shadows from the surrounding mountains, some of which reach elevations of more than 2,000 m. In this area between two great fjord complexes (Kong Oscar Fjord and Scoresby Sund), the Inland Ice protrudes to the east as a 1,500- to 2,100-m-high plateau, which reaches to and includes Cecilia Nunatak.

The margin of the ice sheet around Cecilia Nunatak covers a high alpine landscape incised by a deep subglacial valley (see fig. 51). The low solar illumination angle of the image on 30 September 1978 (fig. 49) reveals the morphologic expression of the subglacial topography. As an overlay on the image, the routes of ground and airborne surveys that measured ice thickness are shown: the 1950 Expeditions Polaires Françaises, which used gravimetry, and the airborne radio-echosounding survey by the Electromagnetics Institut, Technical University of Denmark. The ice-thickness profiles determined by the surveys are shown in figure 50. A comparison of figure 50 (profiles) with the Landsat image (fig. 49) shows that the increasing thickness of the ice sheet toward the west gradually obscures the surface morphologic expression of the subglacial topography, especially when ice thickness exceeds 1,000 m.

In a geologic sense, the cross-hatched zone shown on figure 49 indicates the approximate border between an eastern Caledonian mobile belt ("fold belt") and a western foreland of these mountains; the foreland is mainly hidden under the ice sheet. There is no doubt that mapping of the subglacial geology will require nontraditional techniques. Broad details of the subglacial landscape can be determined from the low-solar-illumination-angle Landsat images (fig. 49) and ice-thickness profiles from radio-echosounding and gravimetric surveys (fig. 50). This information then can be linked to structural patterns (landscape) and known geology mapped in unglacierized areas. Airborne magnetometry and other ground-based or airborne geophysical methods will have to be employed also.

At the bottom of figure 49, the inner parts of Nordvestfjord can be seen, with its main outlet glaciers of F. Graae Gletscher and Daugaard-Jensen Gletscher (fig. 51). The latter glacier exhibits flow patterns that indicate that it drains a relatively large part of the Inland Ice. The rate of movement of this outlet glacier is the greatest measured in East Greenland; its terminus flows at a rate of 3 km a<sup>-1</sup> (Olesen and Reeh, 1969).

The middle parts of Kong Oscar Fjord and Nordvestfjord (the northern branch of Scoresby Sund) are shown in figure 52; the fjords are nearly free of sea ice. Clusters of brash ice can be seen only in the southern part of Kong Oscar Fjord along the coast of Mesters Vig. Isolated pieces of calf ice can be seen in Scoresby Sund. These presumably originate from the productive outlet glaciers (Daugaard-Jensen Gletscher and F. Graae Gletscher) at the head of Nordvestfjord.

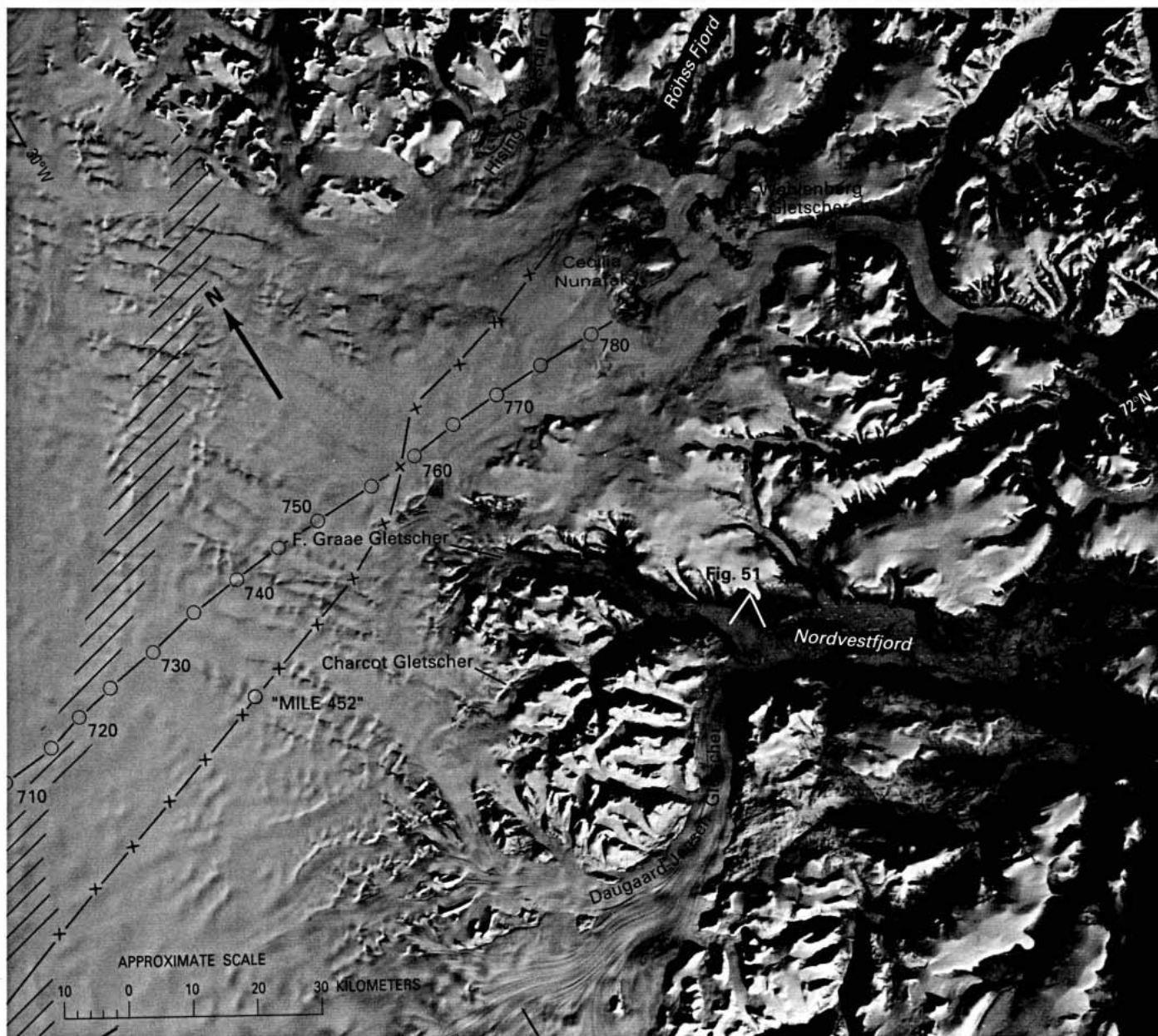


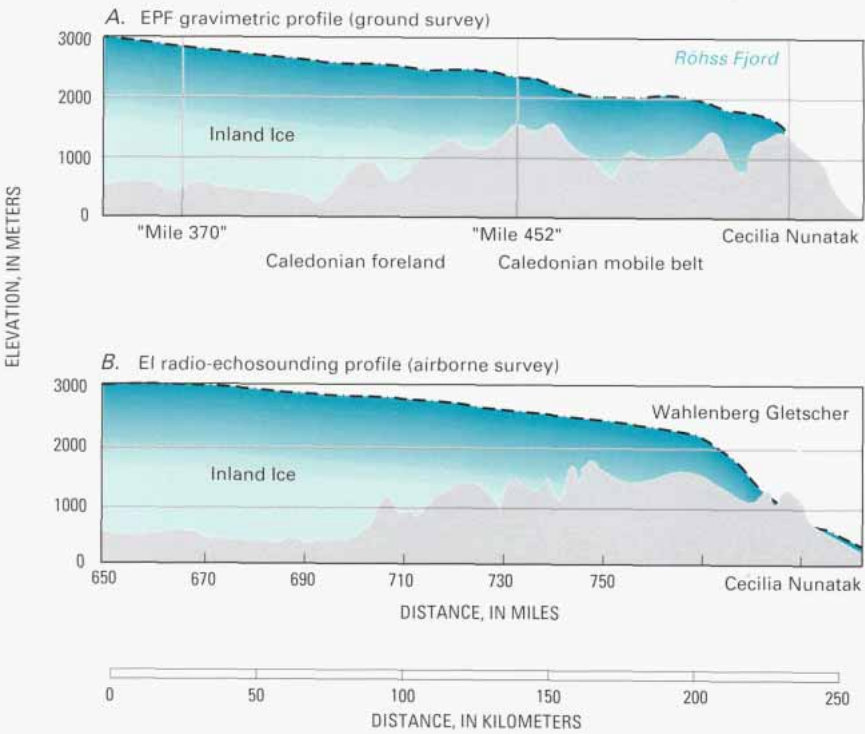
Figure 49. -Annotated Landsat 3 MSS image of the Inland Ice margin between Hisinger Gletscher at the head of Kejser Franz Joseph Fjord and Dagaard-Jensen Gletscher in Nordvestfjord, inner Scoresby Sund fjord complex, East Greenland. Landsat image (30209-13270, band 7; 30 September 1978; Path 251, Row 9) from Canada Centre for Remote Sensing, Ottawa, Ontario. Archived by the U.S. Geological Survey's Satellite Glaciology Project. The cross-ruled zone is the

approximate border between the Caledonian mobile belt to the east and its foreland to the west (mainly subglacial). The dashes and x's indicate the route of gravimetry surveys carried out by the 1950 Expéditions Polaires Françaises (EPF) through "Mile 452" to Cecilia Nunatak (Munck, 1950). The dashes and o's along route 710-780 show the ground track of airborne radio-echosounding surveys (Overgaard, 1981). Profiles along these two routes are shown in figure 50.



**Figure 50.**—Ground gravimetric and airborne radio-echosounding profiles in East Greenland. Figure 49 shows part of the routes. **A**, Profile based on the gravimetric work of the 1950 Expeditions Polaires Françaises (EPF) (Munck, 1950). **B**, Profile based on airborne radio-echosounding carried out in 1974 by the Electromagnetics Institute (EI), Technical University of Denmark (Overgaard, 1981).

**Figure 51.**—Oblique aerial photograph of Daugaard-Jensen Gletschertaken 17 August 1950, looking south (see fig. 49 for location). This outlet glacier from the Inland Ice has the greatest measured calf-ice production among all of the East Greenland tidal outlet glaciers, namely about 10 cubic kilometers per year (see table 3). NSC aerial photograph, route 651 B–V, No. 11947. Reproduced with permission A 200187.

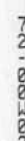




W022-001

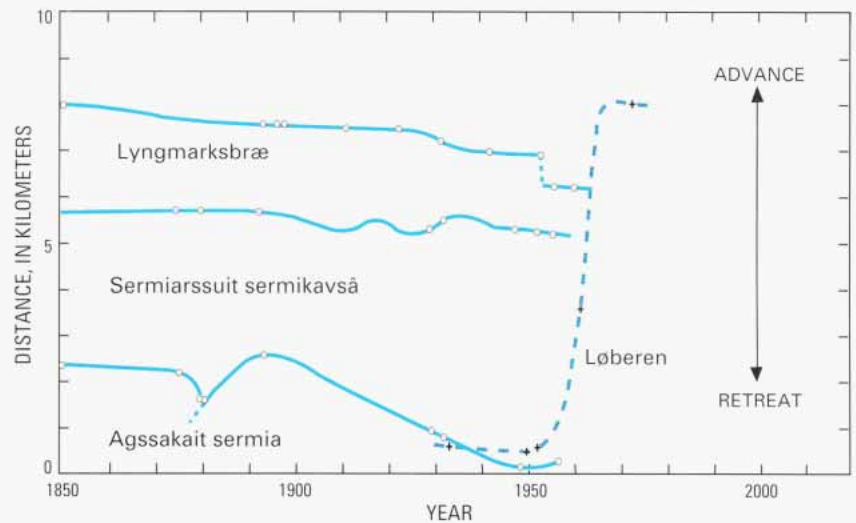
W022-001

128



Some of the glaciers in the area are known to surge (for example, Bjørnbo Gletscher and Løberen). Løberen has a well-documented record of its most recent changes. Løberen can be seen on the image to extend to Nordvestfjord (fig. 52). It reached this position during an advance of 7.5 km in the early 1960's at a minimum rate of advance of  $1 \text{ km a}^{-1}$  (Olesen and Reeh, 1969). The frontal change associated with this glacier surge is shown in figure 53, and the change is compared with those of a pulsing glacier (Agssakait sermia) and glaciers having more normal flow (Lyngmarksbræ and Sermiarssuit sermikavsâ) in West Greenland. The difference in behavior is evident in the maximum rate of advance (about  $1 \text{ km a}^{-1}$  for surging glaciers,  $100 \text{ m a}^{-1}$  for pulsing glaciers, and less for most other glaciers). The upper reaches of the surging Bjørnbo Gletscher are shown in figure 54.

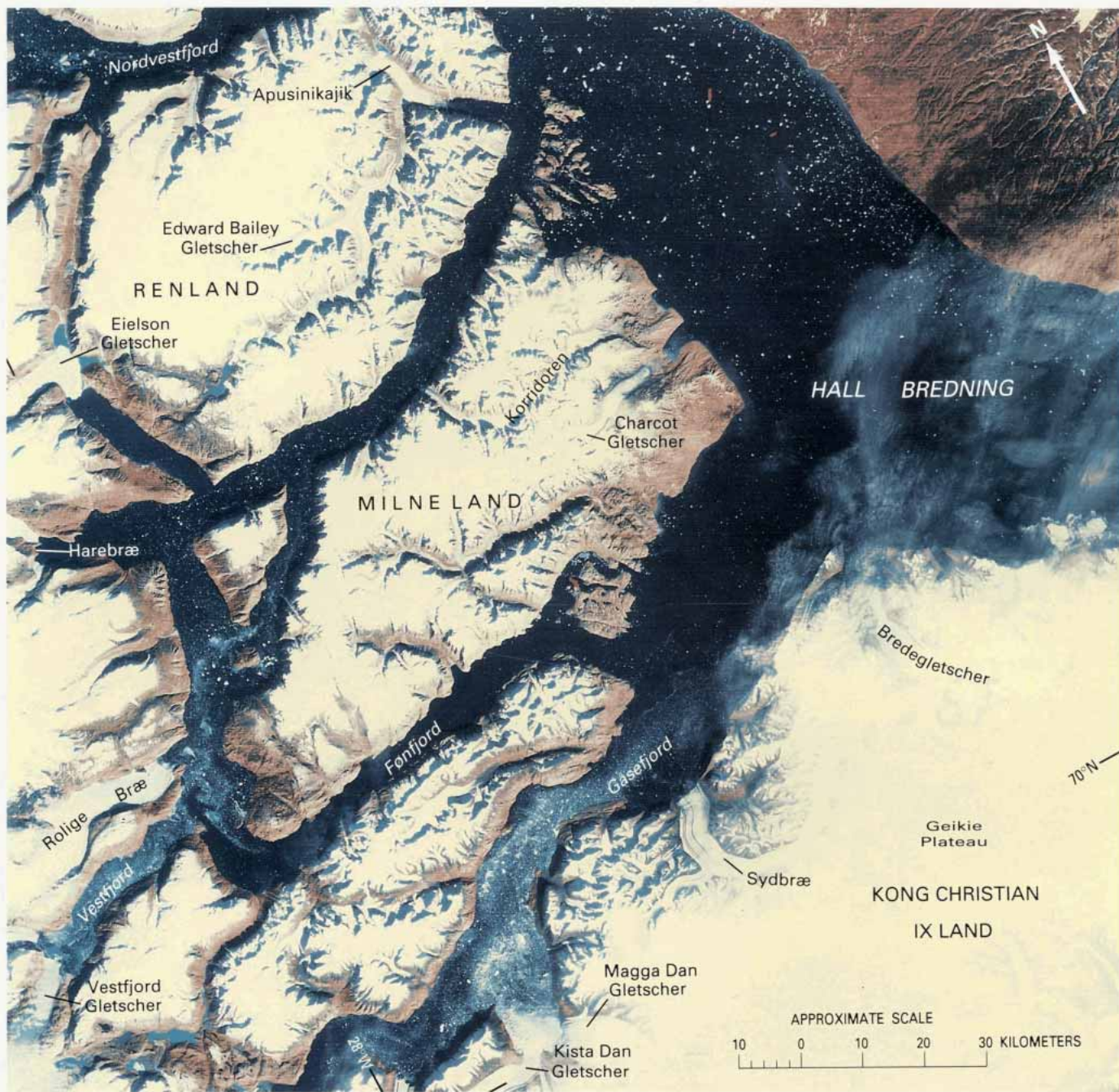
**Figure 53.-** Changes in the positions of the termini of four glaciers in Greenland. The variation of Løberen, a surging glacier in East Greenland, is compared with changes of Agssakait sermia, a pulsing glacier, and Sermiarssuit sermikavsâ and Lyngmarksbræ, both typical glaciers, of West Greenland. The West Greenland glaciers can be seen on figure 21; location of Løberen is shown on figure 52.



**Figure 54.** —Oblique aerial photograph of the Stauning Alper (fig. 52) taken 8 August 1951, looking northeast. The glacier in the foreground is a tributary to the surging Bjørnbo Gletscher, and the heavy pitting of the surface of the firn region is evidence of healing after a former surge. NSC aerial photograph, route 652 D-Ø, No. 4678. Reproduced with permission A 200187.







## Images of Central East Greenland

The central East Greenland region includes the Scoresby Sund fjord complex and the northernmost part of the Blosseville Kyst. Blosseville Kyst includes the area of Kong Christian IX Land from Scoresby Sund to Kangerdlugssuaq. Part of Scoresby Sund was previously discussed on two Landsat images (figs. 49 and 52); the latter image covers the area just north of figure 55 and was acquired on the same day. Figure 55 shows the central part of this fjord complex and the northernmost part of the Blosseville Kyst. The figure shows Hall Bredning and all the inner fjord branches of Scoresby Sund nearly ice free. The image was taken in early September, the optimum time to show the seasonal minimum ice

**Figure 55.** —Annotated Landsat 1 MSS false-color composite image of the central part of the Scoresby Sund fjord complex, East Greenland. The Landsat image (1042–13145, bands 4, 5, and 7; 3 September 1972; Path 247, Row 10) is from the EROS Data Center, Sioux Falls, S. Dak.

cover. Scattered calf ice from the northernmost branch, Nordvestfjord, and clusters of brash and calf ice in the southern fiord branches, Vestfjord and Gåsefjord, are indicative of the calf-ice-producing outlet glaciers. The magnitude of calf-ice production is given in table 3.

The vegetation-covered lowland areas appear pink on this false-color image, and the bare glacier ice (blue) can be distinguished from the snow-covered parts of the glaciers. On land, the snowline ascends from 800 m in the western parts of the image to more than 1,000 m in the eastern parts of the image.

In the central parts of figure 55, the neoglacial moraines appear gray, in contrast to the surrounding pink of the vegetation-clad lowland slopes. The extent of gray demonstrates that Charcot Gletscher and Korridoren have receded a few kilometers. The outlet glaciers from the Inland Ice in the western part of the image, as well as those from the local ice caps of Kong Christian IX Land on the south side of Scoresby Sund, show little apparent change in their termini. Comparison of the Landsat images to the relatively detailed historical map of Scoresby Sund contained in the report of the "East Greenland Expedition 1891-92" (Bay, 1895) also confirms that little has changed. The aerial photograph in figure 56 shows the area in more detail.

*Figure 56. —Oblique aerial photograph of Renland in the central part of Scoresby Sund taken 17 August 1950, looking southwest. In the foreground is Nordvestfjord and its coastal slopes rising from sea level up to about 2,000 m. In the background, Renland is covered by a large ice cap (right), and one of the outlet glaciers from this ice cover Apusinikajik, is visible on the left. The two ice floes in the foreground are detached parts of the tidal glaciers in the head of Nordvestfjord. Their size is estimated to be about 0.5 km. NSCAerial photograph, route 651 A-SW, No. 2906. Reproduced with permission A 200187.*





The glacier drainage system in the lower right corner of figure 55 (in Kong Christian IX Land) is somewhat veiled by thin clouds. It represents the upper part of tributaries that extend down to the head of Barclay Bugt on the Blosseville Kyst (fig. 57)

The most pronounced feature in the central part of figure 57 is the ice divide between Gåsefjord in the Scoresby Sund area and the northern parts of the Blosseville Kyst between Henry Land and Kap Ryder. The ice divide under the low solar illumination angle (9°) can be seen as a sharp crest on the Geikie Plateau. The continuation of this crest can be traced over quite a distance on the image. The crestal line delineates the major drainage areas of the ice cap in Kong Christian IX Land. The broken line on the image indicates the approximate location of the ice divide in the upland areas. The most obvious drainage basin is the one that extends from the Geikie Plateau to Bartholin Brae and Dendritgletscher. The margin of the western neighboring drainage basin extends north to the head of Gåsefjord in Scoresby Sund and is similar in size to that of Bartholin Brae and Dendritgletscher. Farther west, a third large sector of the local ice cap drains south to Kong Christian IV Gletscher in Nansen Fjord just east of Kangerdlugssuaq. Each of these major drainage basins has an area of 60 to 100 km<sup>2</sup>, and they dominate the entire area between Kangerdlugssuaq and Scoresby Sund (Kong Christian IX Land). The outline of the two major drainage basins at Blosseville Kyst is identical to the hydrological districts of 3E (Bartholin Brae and Dendritgletscher) and 3F (Kong Christian IV Gletscher) shown on figure 1. Watkins Bjerge (including Gunnbjørn Fjeld just off the image) is part of the divide of these drainage areas.

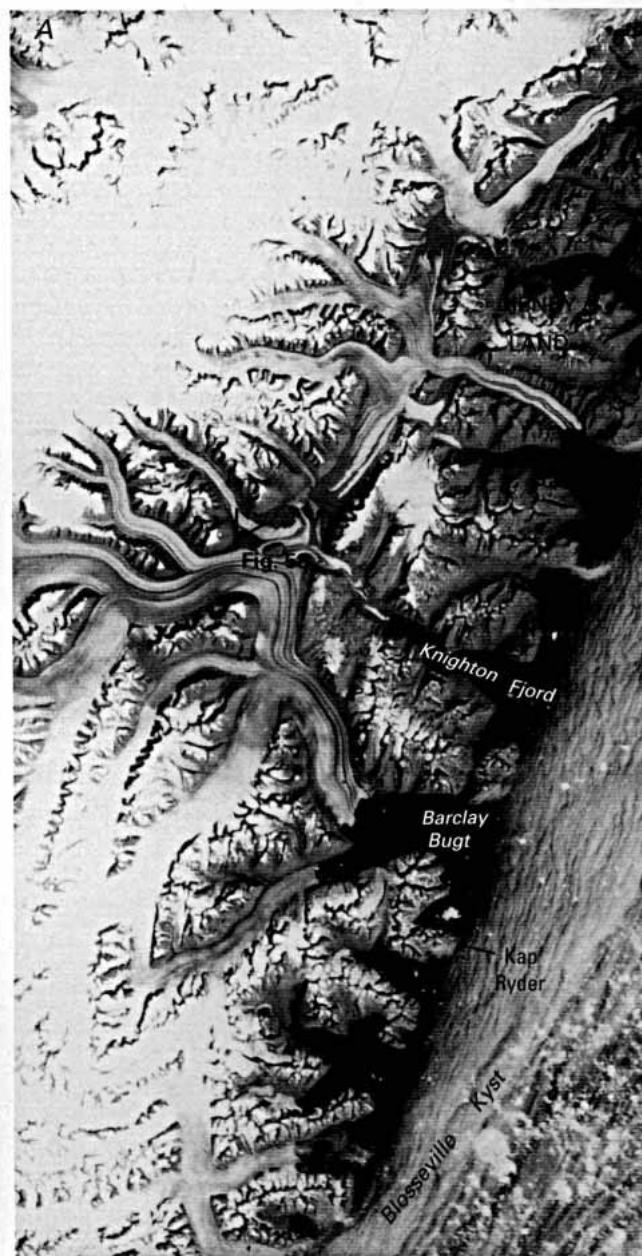
On figure 57A, the complex moraine patterns of the area between Dendritgletscher and Bartholin Brae can be seen in detail. The cloud cover over the ocean is extensive, but the coastline, with its numerous glacier lobes and topographic features, is shown clearly. The transient snowline on figure 57A rises from 700 m over the southern parts of the image to 1,000 to 1,300 m in its northern parts. Numerous cirques are visible in the basalt landscape, and a closer view of the moraines and landscape is shown in figure 58

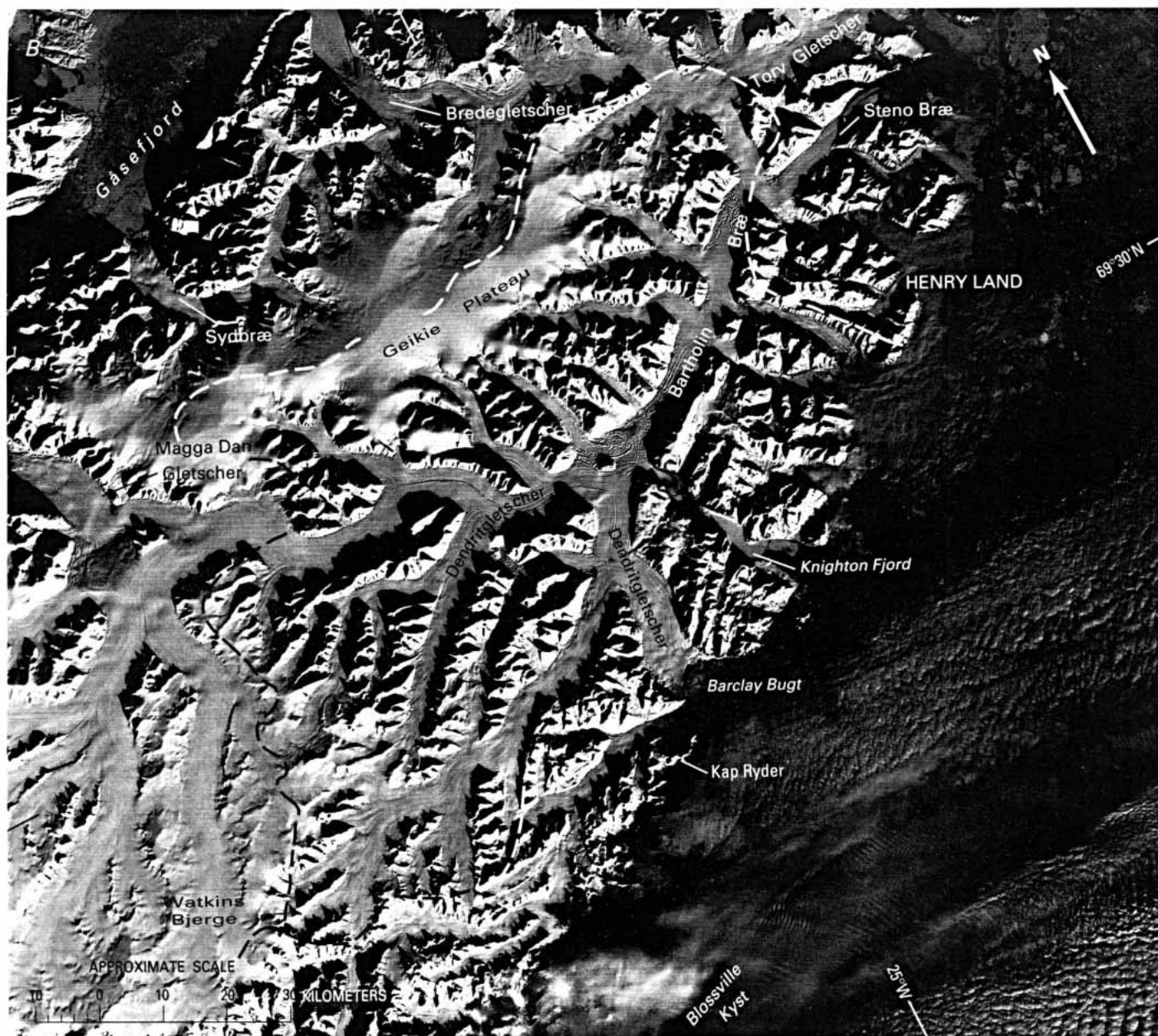
On figure 57B, well-defined flow patterns indicate that the main southwestern drainage of the ice cap leads to Dendritgletscher but with minor flow over the subglacial passes to other bays and inlets on the Blosseville Kyst between Henry Land and Kap Ryder. In the central part of Dendritgletscher, at between 400 and 600 m, a complex moraine system on a heavily crevassed surface of the glacier is visible; possibly this morphology indicates a surging glacier protruding into Knighton Fjord.

The image (fig. 57B) shows a totally snow-covered landscape on 20 October 1973, although the new snow cover is still thin. The inner parts of the fjords are covered with newly formed ice floes.

## Images of Southern East Greenland

The area between Kangerdlugssuaq and Kap Gustav Holm (the southern border of the East Greenland administrative division, according to figure 1), differs geologically from that north of Kangerdlugssuaq by being underlain by granodioritic gneisses instead of basalt. The area is so strongly related to the northern part of South-East Greenland by its landforms that these regions have been treated as one hydrologic unit (District 3H in fig. 1). The main ice divide of the Inland Ice abruptly ends





**Figure 57.**—**A**, Annotated Landsat 2 MSS image of the outer part of Kong Christian IX Land between Scoresby Sund and Blossville Kyst, East Greenland, showing complex moraine patterns. Landsat image (21655-12403, band; 4 August 1979; Path 244, Row 11) from the Canada Centre for Remote Sensing, Ottawa, Ontario. Archived by the U.S. Geological Survey's Satellite Glaciology project. **B**, Annotated Landsat 1 MSS image of the same area as **A**. Landsat image (1454-13020, band 7; 20 October 1973; Path 245, Row 11) from the EROS Data Center, Sioux Falls, S. Dak. The dashed line indicates approximate location of ice divide.

at the coast (see fig. 2), having descended from 3,000 m to sea level over a distance of only 100 km. In spite of the high mountains in the area, local glaciers are few and difficult to delineate from the Inland Ice proper.

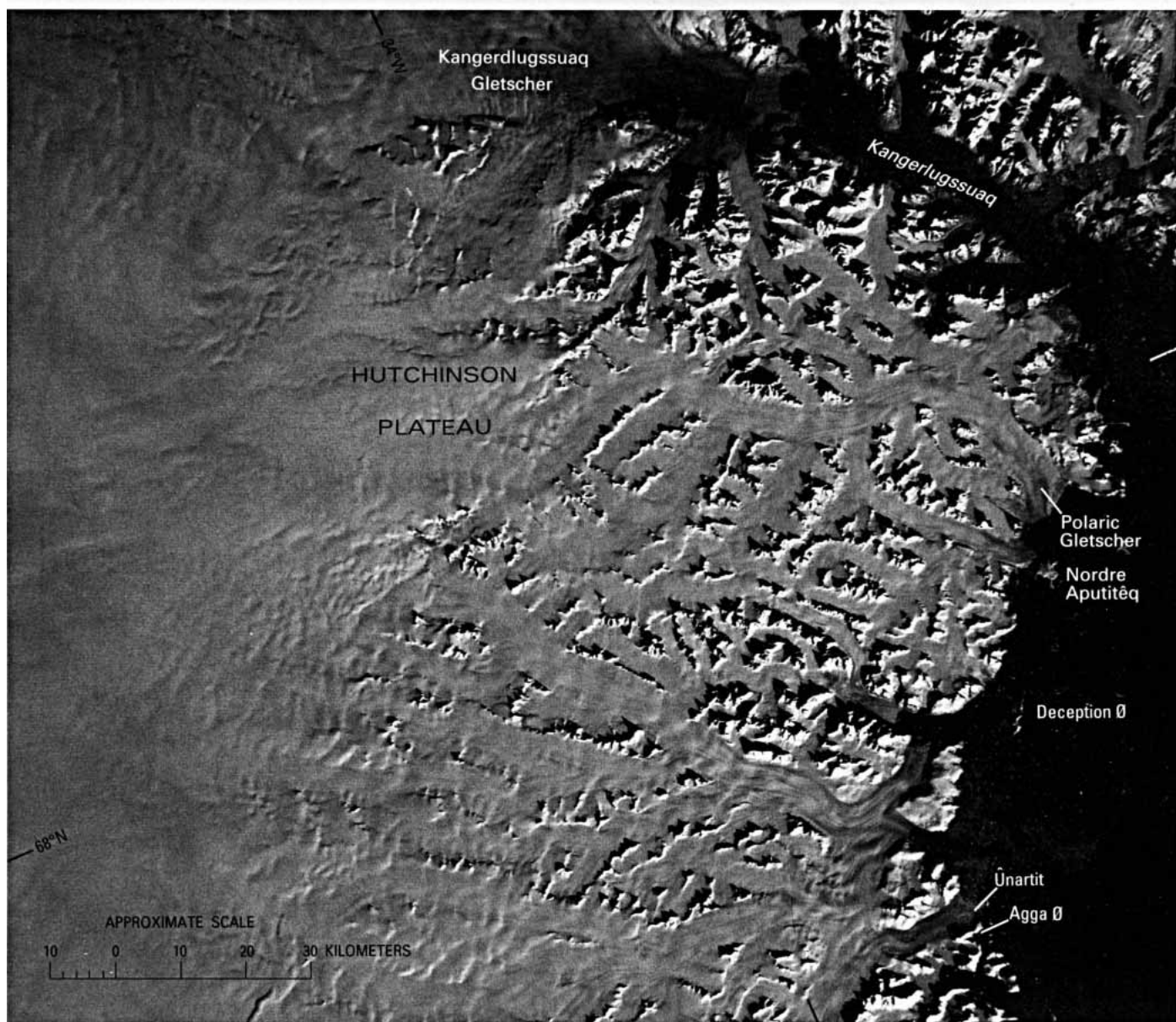
Figure 59 shows the northern half of the region from the fjord of Kangerdlugssuaq south to Ænartit. Both the coast and fjords are free of fast ice, but the landscape is totally covered by snow. The peaked ridges (2,500 to 3,000 m high) can be followed, to some extent, under the ice cover because the solar illumination angle is low. The main patterns on the uppermost part of the Inland Ice, however, seem to be steplike structures between 2,000 and 2,500 m and are situated where the Inland Ice is broken up into different ice streams by the high nunataks. The flow of these ice streams is controlled by subglacial valleys.

Besides the main drainage of the Inland Ice via Kangerdlugssuaq Gletscher to the head of Kangerdlugssuaq fjord, other major ice streams can be followed for long distances. Their flow patterns lead to the coast near Nordre Aputitêq (via the Polaric Gletscher), Deception O (via an unnamed glacier), and Ænartit (via an unnamed glacier).



**Figure 58.**—Oblique aerial photograph of the moraines between Bartholin Bræ and Dendritgletscher taken 8 August 1951, looking east. In the foreground is the moraine seen on figure 57A. In the background is the Blossville Kyst. NSC aerial photograph route 660 E-Ø, No. 12714. Reproduced with permission A 200187.

**Figure 59.**—Annotated Landsat 2 MSS image of the coastal area between Kangerdlugssuaq and Agga Ø, East Greenland. Landsat image (21355-13044, band 7; 8 October 1978; Path 250, Row 12) from Canada Centre for Remote Sensing, Ottawa, Ontario. Archived by the U.S. Geological Survey's Satellite Glaciology Project.



An analysis of figure 59 and comparison with old maps provides evidence of a recession up to 4 km west of Deception Ø, whereas the ice margin at Ûnartit during the same period seems to have advanced and reached the island of Ûnartit. However, although the glacier terminus at Ûnartit is characterized by ogivelike features, it is possible that some of the ice is actually fast ice. The remainder of the ice-margin is in nearly the same position as it was during the 1930's.

## Images of South-East Greenland

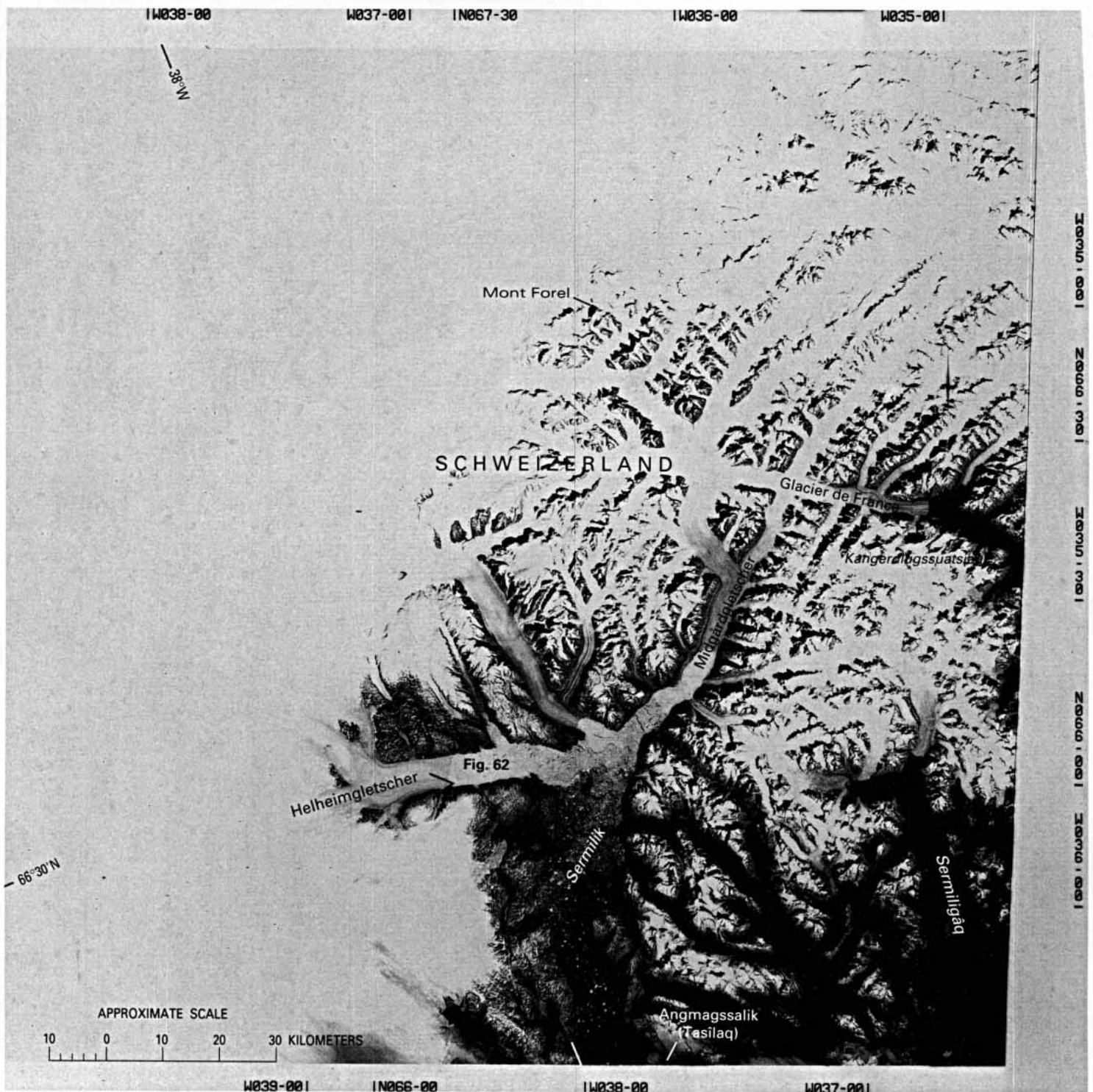
South-East Greenland is the only part of Greenland in which a relatively well-defined drainage from the Inland Ice can be determined easily. The entire area is situated between two ice divides; the northernmost divide ends at the coast north of Angmagssalik, and the southern one ends at the Kap Farvel area in South Greenland (see figs. 1 and 3). The coast where these two ice divides terminate is characterized by high alpine terrain; the region between the divides is characterized by a depression between the northern and the southern dome (fig. 3). Along the entire coast, the margin of the Inland Ice is separated from the coast only by a narrow coastal region. Local glaciers are few and are confined mainly to an area around Mont Forel. Outlet glaciers north of Glacier de France (about lat 66°33' N.) extending to the southernmost part of the Blosseville Kyst receive contributions from the Inland Ice as well as from local firn. Glacier de France and Midgårdgletscher (fig. 60) seem to be nourished only by local firn areas.

Figure 60 shows an area characterized by high alpine peaks, which in Schweizerland reaches altitudes of 3,360 m on Mont Forel. Also visible are the inner branches at Sermilik, Sermiligâq, and Kangerdlugssuaq. Only the innermost parts of the fjords are covered by fast ice in spite of the time of year (7 September 1972). The transient snowline lies at approximately 1,000 m.

The individual glaciers and medial moraines stand out clearly, and great changes in the frontal positions of the main outlet glaciers in the fjords can be documented by comparison of the Landsat images with published maps. Most of the outlet glaciers have retreated, as shown in figure 61. Fenrisgletscher has retreated 3 km, Midgårdgletscher 17 km, and the glacier in the western branch of Sermiligâq (Kârle Gletscher) 4 to 5 km since the early 1900's. The recession of Midgårdgletscher is particularly impressive: 5 km by 1968, 15 km by 1973, and 17 km by 1978, from the position of the termini in the 1930's as mapped by the Geodetic Institute (National Survey and Cadastre). For Helheimgletscher, however, its terminus on the 7 September 1972 Landsat image had advanced approximately 4 km. However, updating of the position of the terminus on the basis of 1978 and 1979 Landsat images indicates that this glacier had receded 1.5 km (between 1972 and 1979). Fenrisgletscher and Midgårdgletscher also continued to retreat. The termini of the outlet glaciers in the eastern branch of Sermiligâq fjord appeared to remain stationary during the same time interval. A closer view of the terminus of Helheimgletscher and surrounding landscape can be seen in figure 62. South of Helheimgletscher, recession of the Inland Ice margin can be observed in Johan Petersen Fjord also.

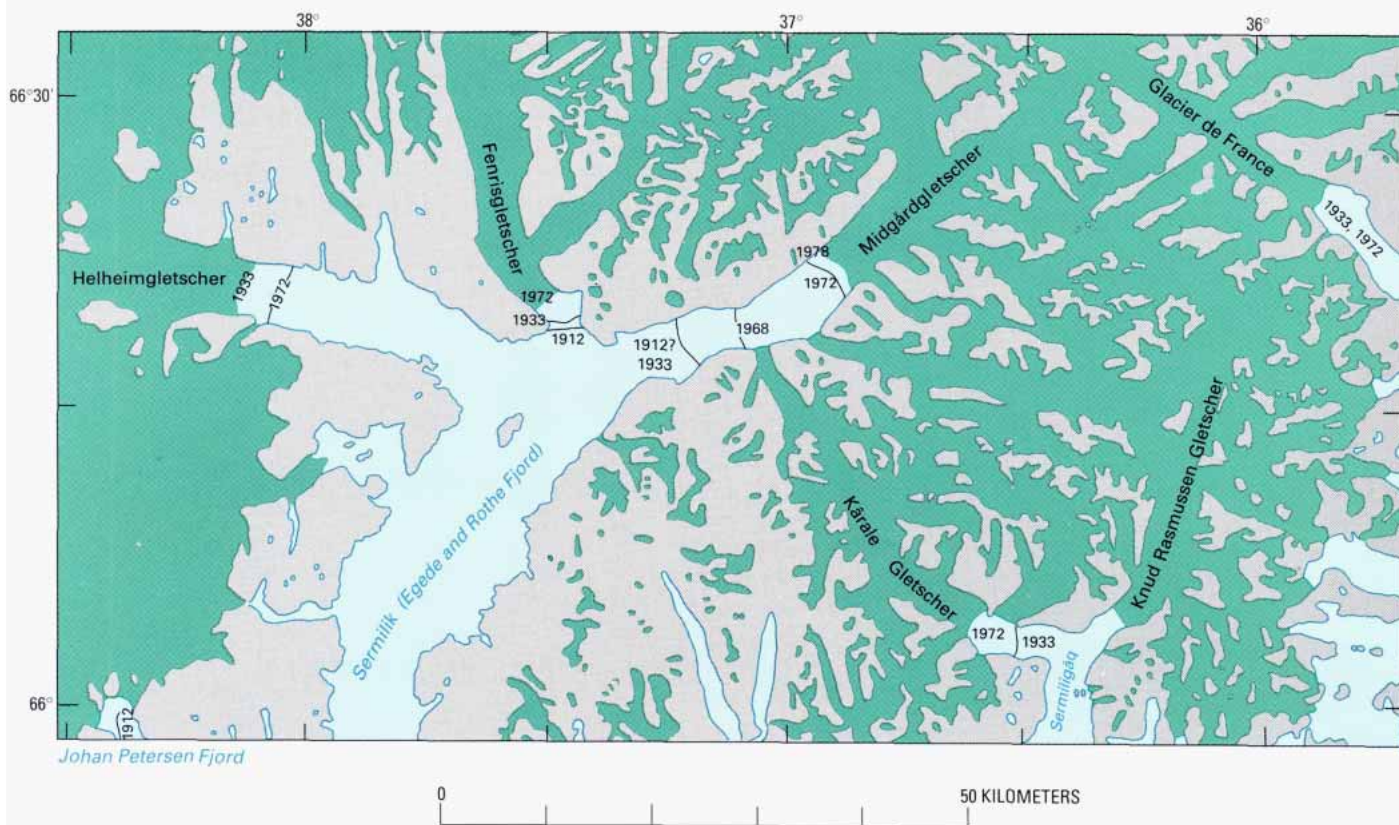
The coastal region farther south from Johan Petersen Fjord to Kap Cort Adelaer is covered by figure 63A, composed of most of three Landsat images. The image mosaic shows that the surface morphological expression of the subglacial landscape is visible through an ice thickness of 1,000 to 1,500 m at a solar illumination angle of 15° to 18°. On the index map (fig. 63B), the position of the "Dye-3" station is shown together with





contours of the subglacial landscape as measured by airborne radio-echosounding (from Overgaard and Gudmandsen, 1978). The station is situated 125 km from the coast and is close to the ice divide. The ice thickness here measures 2,000 m (surface elevation of 2,600 m). The ice sheet was drilled in 1981, and an ice core that included a total thickness of 2,000 m was recovered. The drilling was done in connection with the Greenland Ice Sheet Program (GISP) (Dansgaard and others, 1981). The measured subglacial topography at the "Dye-3" station can be compared to the patterns of the surface expression of subglacial morphology shown on the Landsat image. The subglacial valley mapped at the station seems to pass through the highlands to the inlet north of Jens Munk Ø.

**Figure 60.**—Annotated Landsat 1 MSS image of the area north of Angmagssalik, South-East Greenland. Landsat image (1046-13390, band 5; 7 September 1972; Path 251, Row 13) from the EROS Data Center, Sioux Falls, S. Dak.

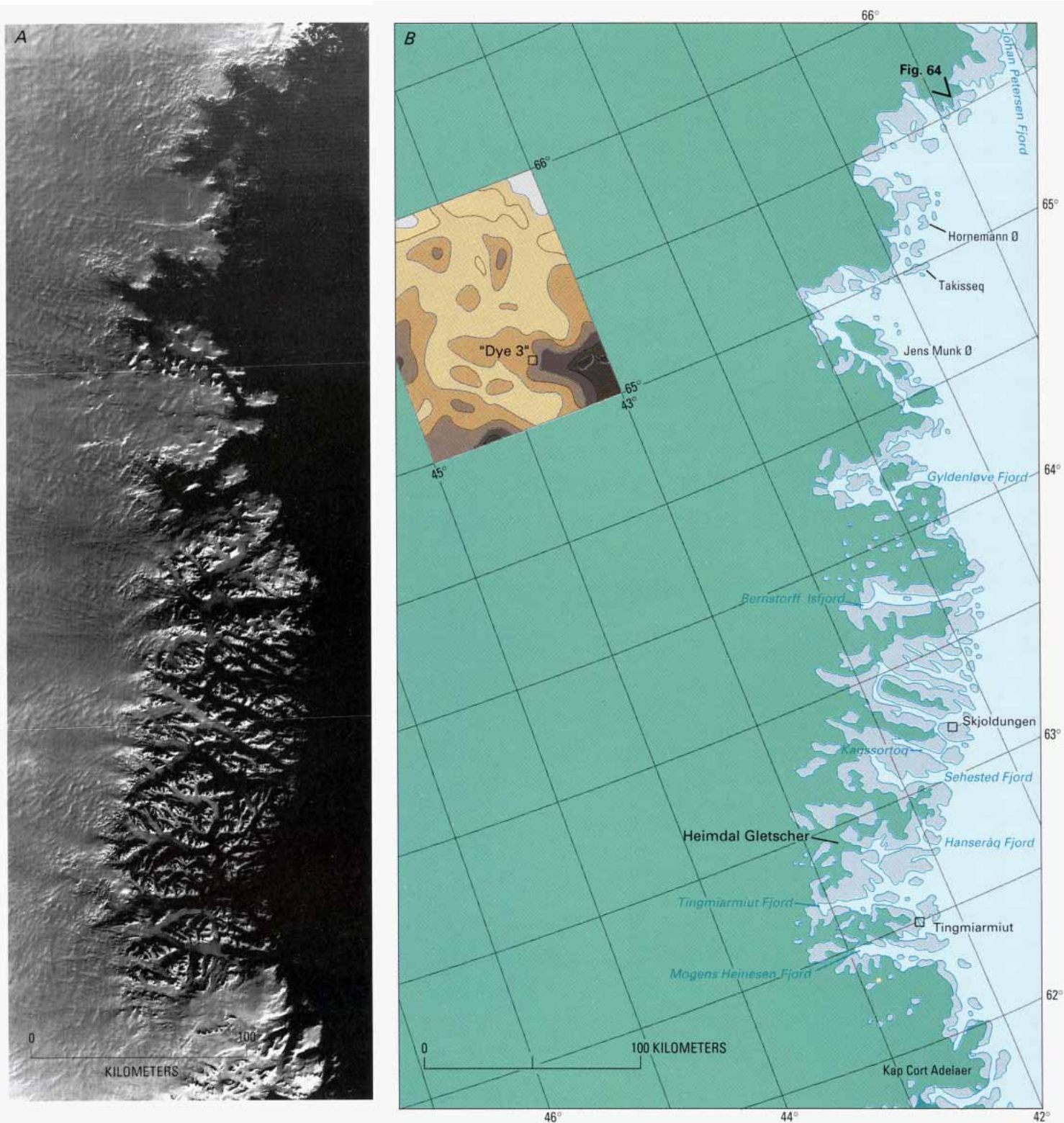


**Figure 61.** —Map of the head of Sermilik and Sermiligâq fjords at Angmagssalik, South-East Greenland, showing changes in the position of glacier termini by comparing Landsat images with previously published maps. Dates queried where uncertain.



**Figure 62.** —Oblique aerial photograph of the front of Helheimgletscher in the eastern head of Sermilik Fjord near Angmagssalik, 12 August 1984, looking west. The landscape is a transition between the high alpine land north of Angmagssalik and the upland hills west and southwest of this town. Location of the photograph shown on figure 60. Photograph by J.C. Escher, The Geological Survey of Greenland,





**Figure 63.** *A*, Landsat 1 MSS image mosaic of the coast from Johan Petersen Fjord to Kap Cort Adelaer, South-East Greenland. Landsat images (top, 1083–13450, Path 1, Row 14; middle, 1083–13455, Path 1, Row 15; bottom, 1083–13461, Path 1, Row 16; band 7; 14 October 1972) from the EROS Data Center, Sioux Falls, S. Dak. *B*, Sketch map of the area covered by *A* showing geographic place-names and location and determination of the subglacial topography at the "Dye-3" station and environs (in the inset). The contour map (in meters above mean sea level) of the bedrock (subglacial topography) is based on radio-echosounding surveys by Overgaard and Gudmandsen (1978). The darkest area is greater than 900 m, and the lightest area is less than 300 m.

The covering of Jens Munk Ø by a local ice cap, despite the low elevation of the island (maximum altitude in the northern part, 550 m; in the southern part, 680 m), demonstrates the low glaciation limit of the outer coast in this area. The area has a relatively high amount of precipitation for an arctic region (mostly as snowfall); 1,100 mm a<sup>-1</sup> were measured at Skjoldungen (fig. 63). The sound between Jens Munk Ø and the coast proper at the Inland Ice margin is covered by a semipermanent or permanent mixture of frozen calf ice and brash ice, often referred to as palaeocrystic ice (as, for example, in the standard legends of the Geodetic Institute (National Survey and Cadastre) 1:250,000-scale maps).

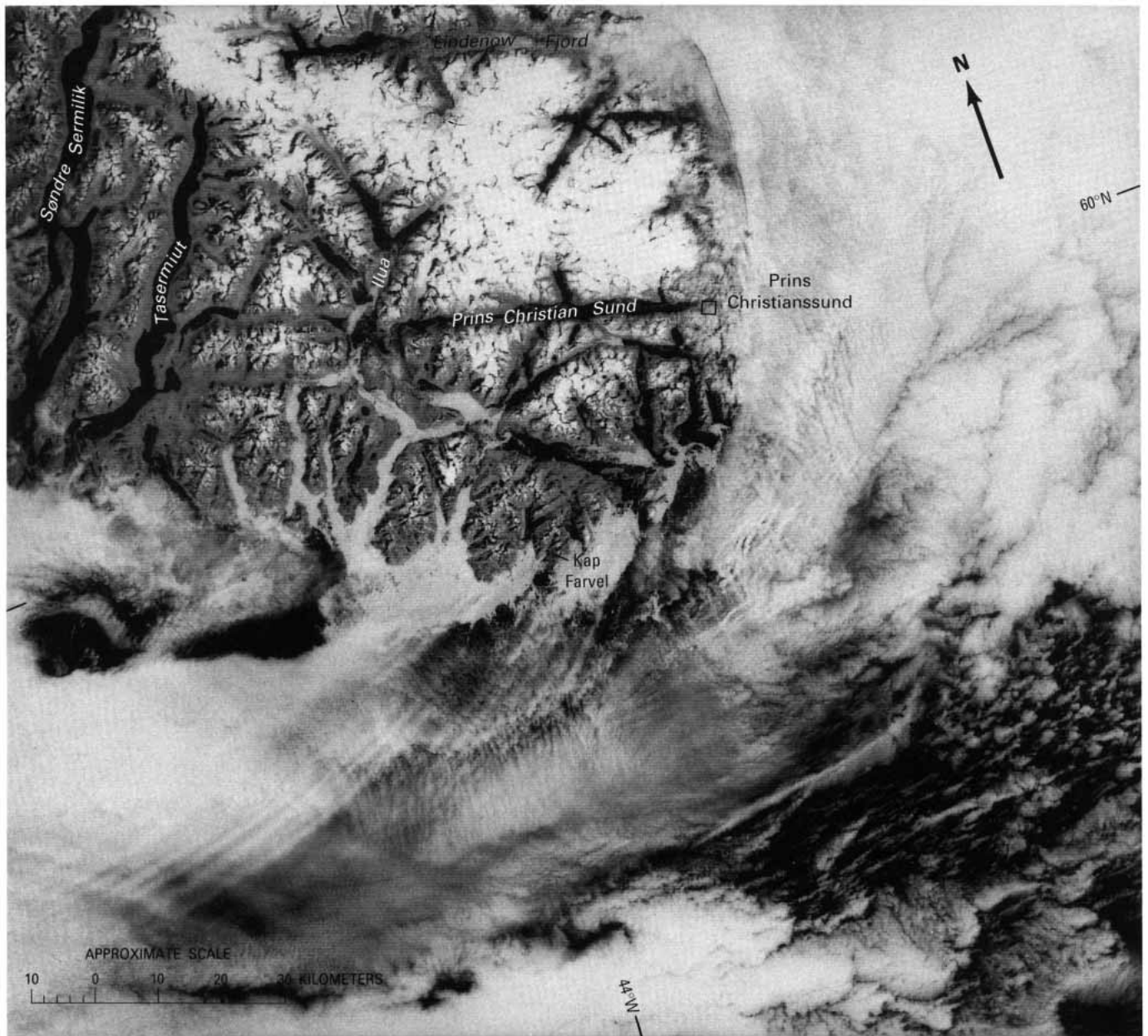
Changes in the position of the Inland Ice since the 1930's are small over the entire stretch of coast covered by figure 63, and a recession of as much as 1 to 2 km can be documented at only a few locations. The Inland Ice margin reaches the coast in a broad front, resting mainly on a gneissic plateau, which in some locations is only a few hundred meters high. Figure 64 gives a detailed view of the Inland Ice margin in the northern part of this region. In spite of the contact of the Inland Ice with the sea in many areas, relatively little calf ice is produced, the volume is small, and it is restricted to only a few places. Drainage from the ice sheet seems to be controlled by only a few small ice streams at the ice sheet margin. Such features can be seen at the heads of Bernstorff Isfjord, Kagssortoq, and Gyldenløve, Sehested, and Mogens Heinesen Fjords. Heimdal Gletscher, leading to Hanserâq Fjord, is another small ice stream similar in features to those just mentioned.

Coastal elevations gradually increase south of Jens Munk O and reach heights of 2,000 to 2,500 m in the alpine mountains of South Greenland. Figure 65, a Landsat image of the Kap Farvel area, is an example of this landscape. Most of the sea and the eastern coast is covered by cloud formations that penetrate the outermost parts of the fjords. The inland areas are clearly visible and show an alpine landscape that has elevations exceeding 2,300 m. The gradual transition from cirque and local valley glaciers to the local ice caps south of the Inland Ice can be seen on this image. In Ilua, a recession of approximately 3 km since the 1940's has been determined for the glacier lobe in the eastern branch of the fjord; for the western branch the recession has been approximately 2 km.

**Figure 64.** –Oblique aerial photograph of the Inland Ice margin seen from a point 65°31' N. lat, 38°45' W. long, 12 August 1984, looking north (see fig. 63). In the background are the landscapes around Johan Petersen Fjord and Helheimgletscher. The foreground is an example of the low, hilly landscape, the surfaces of which are mainly between 400 and 800 m and are partly covered by the Inland Ice margin. Photograph by T.F.D. Nielsen, The Geological Survey of Greenland.







**Figure 65.** —Annotated Landsat 2 MSS image of the area around Kap Farvel, the southern tip of Greenland. The image includes parts of South Greenland and southernmost South-East Greenland. Landsat image (21644–3232, band 6; 24 July 1979; Path 251, Row 18) from the Canada Centre for Remote Sensing, Ottawa, Ontario. Archived by the U.S. Geological Survey's Satellite Glaciology Project.

## Concluding Remarks

In the preceding pages, some of the applications of the Landsat images for studying and monitoring changes in the Greenland ice sheet, its outlet glaciers, and local ice caps are described. The obvious advantages include the large areal coverage on a single Landsat image (approximately 35,000 km<sup>2</sup> on a standard MSS scene), the repetitiveness of the orbit, which permits reimaging of each area on a regular schedule, and the orthographic nature of the image, which permits the easy transfer of information on the images to current topographic maps (for Greenland, this is usually at a scale of 1:250,000 with 50- to 100-m contour intervals or at a scale of 1:1,000,000 with 300-m contour intervals).

In addition, low solar-elevation-angle images can be used to delineate the Inland Ice from contiguous marginal ice caps and ice domes or refine generalized delineations that have been made from less detailed information (fig. 3). Local ice caps or ice domes are located in a few places in West Greenland but are especially common for certain regions of the ice sheet margin in East Greenland. The surface features on low solar-elevation-angle images also impart information about subsurface morphology, such as subglacial valleys and drainage patterns.

The wide geographical coverage of individual Landsat images is also valuable in determining the extent of the ablation area and the zonation of glacier facies on the outer parts of the Inland Ice. These glacier facies are especially well developed on the flat western slope of the Greenland ice sheet (fig. 19). If an exact determination of the position and movements of the transient snowline is made on the Landsat images, the measured mass-balance results of a few selected glaciers and outlets from the Inland Ice may be transferred to other glaciers, as suggested by Østrem (1975). However, this method requires that a sufficiently long glaciological mass-balance series be determined for selected glaciers. Current mass-balance measurements being taken in connection with the regional mapping of hydropower potential in Greenland may provide some of the necessary data.

An important factor in determining the total mass balance of the Inland Ice sheet is the measurement of the calf-ice Production (table 3). The present determinations are still uncertain. For the future, however, Landsat images can contribute essential knowledge in this field. However, direct determination of the rate of movement of the individual outlet glacier is also needed, as well as direct observation of the number of icebergs produced on both seasonal and annual bases. Figure 22B illustrates that large ice streams can be identified and delineated as widespread flowlines. The exact position and trend of the individual ice streams are then known well into the ice margin (fig. 20). There seems to be a connection between the area encompassed by these flowlines and the amount of calf ice produced, but only a closer investigation can verify the correct relationship. Another application of glacier dynamics involves a closer investigation of Landsat images to provide information about the extent and time variations of Greenland glacier surges and outburst floods (jökulhlaups), the latter resulting from failure of ice-dammed lakes. To document variations in termini position, especially those of first order, Landsat monitoring is ideal. However, not only the magnitude of large glacier changes but also the magnitude of short-term variations needs to be investigated on a broad basis in order to relate these variations to both glacier dynamics and long- and intermediate-term climatic fluctuations. A detailed mapping of first-order variations of glacier termini should be pursued.

NOAA satellite imagery is useful for some glaciological applications in Greenland. Figure 66 is a NOAA-H advanced very high resolution radiometer (AVHRR) image of most of Greenland. Although NOAA AVHRR images are acquired every 6 hours and can be used to show changes in large features, such as in sea ice, bare versus snow-covered glacier ice, and snow-covered versus snow-free terrain, the 1-km pixel resolution limits its usefulness for detailed studies of the Greenland ice sheet, its outlet glaciers, and local ice caps.

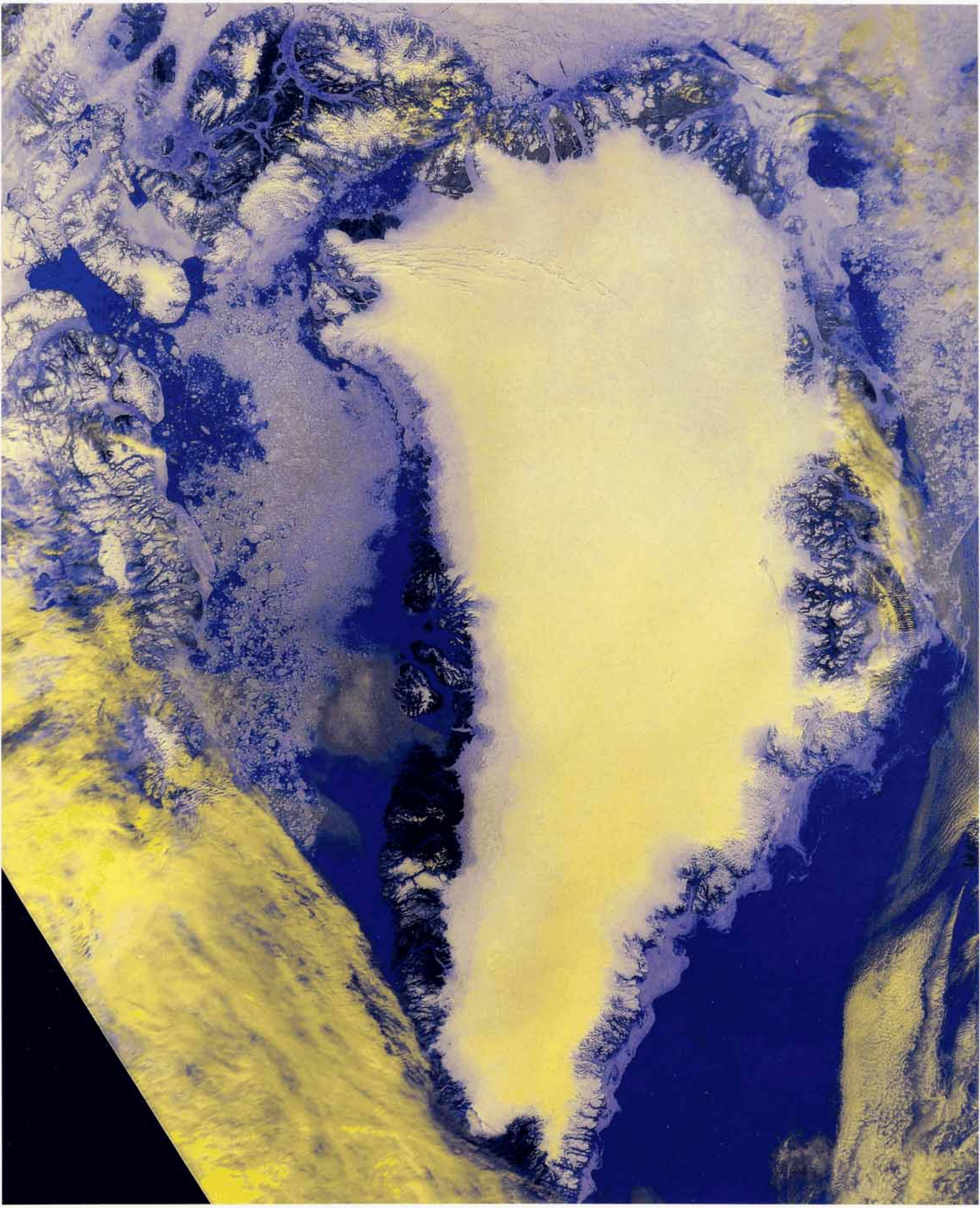
## Acknowledgments

The author is grateful for the large selection of Landsat scenes of Greenland collected by R.S. Williams, Jr., and J.G. Ferrigno of the U.S. Geological Survey, and by O.B. Olesen and H.H. Thomsen of The Geological Survey of Greenland and put at the author's disposal. Also, the author is grateful to the Danish National Survey and Cadastre for cooperation during the author's perusal and selection of oblique aerial photographs of Greenland from their superb collection and permission to publish selected photographs (A 200/87).

Help from other contributors is also very greatly appreciated: the review of the section on Greenlandic place-names by Professor Robert Petersen, Ilisimatusarfik/University of Greenland; the illustrations put at the author's disposal by W.F. Weeks, Cold Regions Research and Engineering Laboratory (CRREL) (fig. 19B); C.S. Benson, University of Alaska (fig. 19C); M. Kelly, University of Lancaster, U.K. (fig. 26); J. Lautrup, The Geological Survey of Greenland (figs. 36 and 37); W. Dansgaard, Geophysical Institute, Copenhagen (fig. 4); J.C. Escher (fig. 62) and T.F.D. Nielsen (fig. 64) The Geological Survey of Greenland; and the comments and advice furnished by W.S. Watt and the checking of the climatological data by R.J. Braithwaite, The Geological Survey of Greenland.

**Figure 66.**—NOAA-H advanced very high resolution radiometer (AVHRR) image of most of Greenland (0.8–1.1  $\mu\text{m}$ ) acquired on 25 June 1990 showing the Inland Ice, outlet glaciers, and separate ice caps. NOAA-H AVHRR images have a picture-element (pixel) resolution of about 1.1 km. Image processing by Mark Fahnestock, National Aeronautics and Space Administration, and Jo-Ann Bowell, USGS Flagstaff Image Processing Facility.







# LANDSAT IMAGES OF GREENLAND

By RICHARD S. WILLIAMS, Jr., and JANE G. FERRIGNO,  
U.S. GEOLOGICAL, SURVEY

## Introduction

There are 468 Landsat 1, 2, and 3 nominal scene centers within the part of Greenland that extends from about 81°30' N. lat (the approximate northern limit of the Landsat 1, 2, and 3 orbits) to its southernmost point (Kap Farvel) (fig. 67). This wedge-shaped area is covered by parts of 62 Landsat orbits (paths) (Path 243 to Path 53) and parts of 18 rows (Row 1, about 81°30' N. lat to Row 18, about 60° N. lat). Because Landsat orbits converge at high latitudes, sidelap of adjacent Landsat scenes increases toward the poles. Complete coverage of the part of Greenland covered by Landsat can therefore be accomplished with only about 120 Landsat images by using every Landsat scene at Row 18, with a gradual reduction to every ninth scene at Row 2. At Row 1, however, because of the almost east to west travel of the satellite (rather than the more northeast to southwest track in lower latitudes), every sixth scene is required.

For the majority of the 468 nominal Landsat scene centers in Greenland, one or more images is available (table 14). A problem for the casual user in the evaluation of Landsat images of Greenland is that the cloud-cover assessment appearing on either the computer or the microfiche/microfilm summaries of each image archived at the EROS Data Center and other Landsat archives can be unreliable; snow, for example, is often mistaken for clouds and vice versa. In addition, the 1972-80 16-mm microfilm cassettes from the EROS Data Center and the 76x127-mm microfiche (1978-82) from the Canada Centre for Remote Sensing contain only Landsat multispectral scanner (MSS) band 5 images, which are often overexposed and make it difficult to distinguish clouds from snow and vice versa. A special trip to the European Space Agency's satellite receiving station in Kiruna, Sweden, to examine higher quality "quick-look" archival Landsat prints was needed to make certain that all optimum Landsat 1, 2, and 3 images of Greenland were identified for analysis and listing in table 14.

More than 2,000 individual Landsat images were evaluated by direct inspection of MSS and return beam vidicon (RBV) images on paper prints, microfilm, microfiche, and quick-look archival paper prints in the search for the best available Landsat image of Greenland for each nominal scene center. Each optimum image was classified into one of the following four categories: excellent, good, fair to poor, and unusable. A fifth category was used to indicate no available image. The following table provides criteria for the classification and the number and percentage of nominal scenes that fall into each category.

Assessment category	Number of nominal scenes	Percentage of total
Excellent image (0 to ≤5 percent cloud cover)	328	70.1
Good image (>5 to ≤10 percent cloud cover)	30	6.4
Fair to poor image (>10 to ≤100 percent cloud cover)	68	14.5
Unusable image (100 percent cloud cover)	16	3.4
No image available (no image ever acquired)	26	5.6
Total	468	100

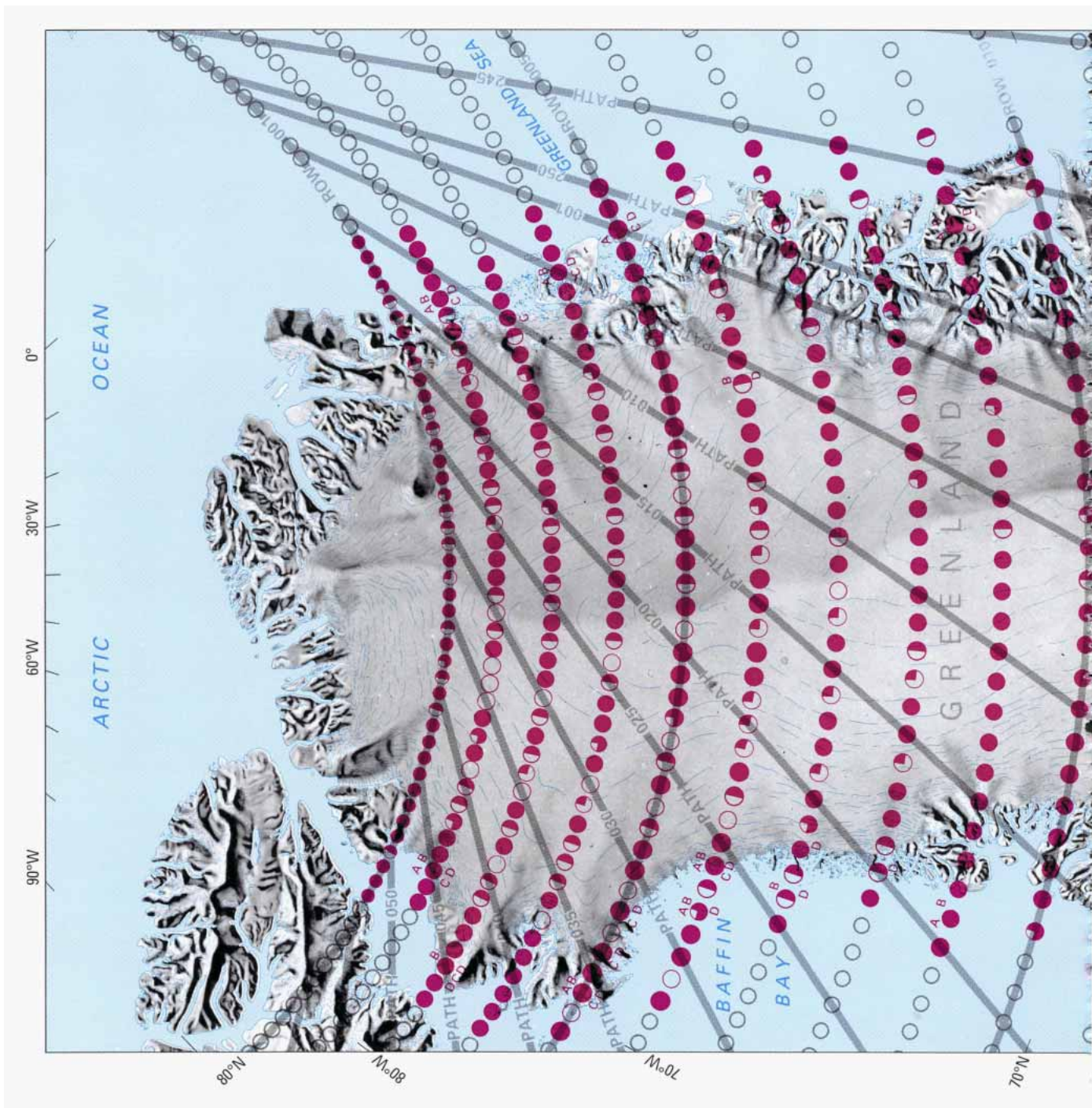
The first two categories, constituting 76.5 percent of the nominal scene centers, have little or no cloud cover, minimum snow cover in areas of exposed rock, or were acquired during times of low solar elevation angle (above the horizon), which maximizes morphologic details in the inland areas of the ice-sheet surface. Taking into account both image sidelap and suitability, virtually all of Greenland south of about 81°30' N. lat has high-quality Landsat 1, 2, and 3 MSS and RBV images available. About 5 percent of northern Greenland, the part that lies north of about 81°30' N. lat, could not be imaged, because it was beyond the Landsat 1, 2, and 3 orbits.

The RBV on Landsat 3 (launched on 5 March 1978) had a 30-m pixel resolution providing broad-band (0.505-0.750  $\mu\text{m}$ ) visible to near-infrared coverage. Unfortunately, many Landsat 3 RBV images of Greenland are overexposed and not generally useful. Of the usable Landsat 3 RBV images acquired, 50 subscenes (four overlapping subscenes encompass one standard MSS image) can be classified (by direct inspection) as good or fair to poor and have been listed in table 14.

Landsat 1, 2, and 3 MSS images of Greenland were also often overexposed. Research carried out in conjunction with the preparation of digital image mosaics of parts of the ice sheet in Antarctica with Landsat 1, 2, and 3 MSS images by Baerbel K. Lucchitta and her colleagues (written commun., 11 and 30 March 1983) at the U.S. Geological Survey's Branch of Astrogeology and Image Processing Facility (Flagstaff, Ariz.) reveals a serious problem for those planning digital processing of Landsat MSS images. Bands 4, 5, and 6, and to some extent MSS band 7, show detector saturation during times of high solar elevation angles from November through January (Southern Hemisphere; in the Northern Hemisphere, the problem would be most severe for images acquired during May through July). In the analysis of Landsat images of Antarctica, more than 50 percent of the area imaged by MSS bands 4, 5, and 6 is adversely affected by saturation of the MSS detectors; similar problems had also been discovered for snow-and-ice covered areas in Iceland (Ferrigno and Williams, 1983) and in Svalbard, Norway (Dowdeswell and McIntyre, 1986). Although the saturation of MSS sensors is widespread in areas of high reflectivity, the problem also occurs even more commonly with Landsat 3 RBV images (Ferrigno and others, 1983; Ferrigno and Williams, 1983).

The Landsat 4 and 5 spacecraft, launched on 16 July 1982, and 1 March 1984, respectively, have acquired additional images of Greenland (mostly Landsat thematic mapper (TM) images). These images, like all Landsat 4 and 5 images, are centered on a *different* path-row system than that used with previous Landsats, and it provides coverage a little farther north than is possible with Landsats 1, 2, and 3. This is the result of a slightly different orbital inclination and altitude, 99.09° and 919 km for Landsats 1, 2, and 3 and 98.2° and 705 km for Landsats 4 and 5. For Greenland, this means that Landsats 4 and 5 can image all but the northernmost 150 km of Peary Land, so complete coverage is available for the ice sheet and its northern outlet glaciers; only some small glaciers and outlying ice caps in Peary Land are excluded from coverage. The repeat cycle for Landsats 4 and 5 is also different, 16 days, as compared to 18 days for Landsats 1, 2, and 3.

Because neither satellite has on-board tape recorders, all Landsat 4 and 5 image data outside the range of satellite-receiving stations must be transmitted through a tracking and data relay satellite system (TDRSS). Not all of Greenland falls within the direct receiving radius of ground stations. The European Space Agency's satellite-receiving station at Kiruna, Sweden, covers all but the northwestern part of Greenland. When the Canada Centre for Remote Sensing operated two ground





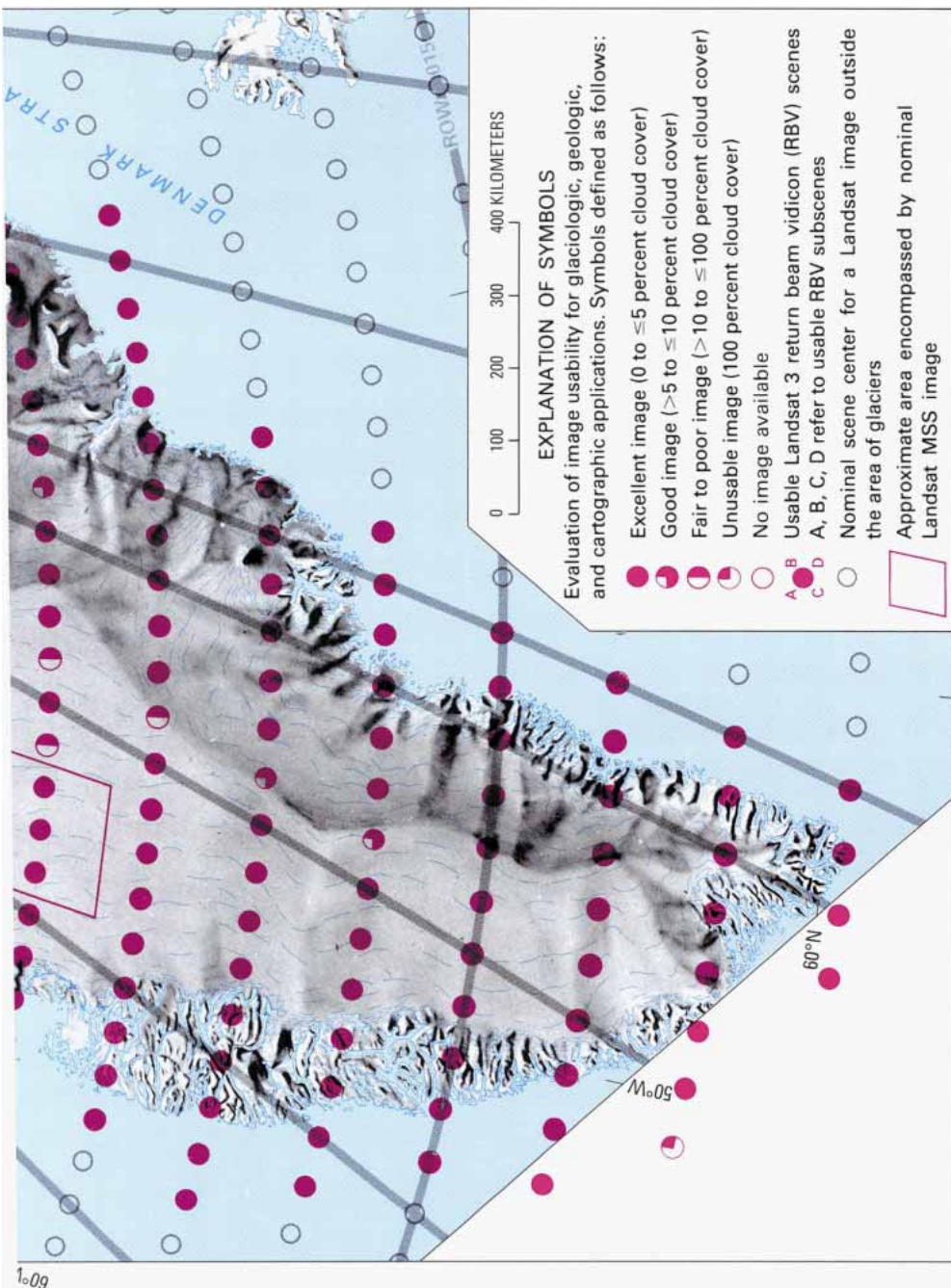


Figure 67.—Optimum Landsat 1, 2, and 3 multispectral scanner and return beam vidicon images of Greenland.



stations, the primary one at Prince Albert, Saskatchewan (continuously in operation since 1972), and the secondary ground station in Shoe Cove, Newfoundland (operational from 1978 to 1982), both stations could acquire data of Greenland, but the Shoe Cove station could acquire data over a greater part of Greenland. The Shoe Cove satellite-receiving station repetitively imaged the southern half of Greenland and acquired hundreds of microfiche images that were evaluated as part of the search for optimum Landsat images of the nominal scene centers.

## **Index Map to Optimum Landsat 1, 2, and 3 Images of Greenland**

Figure 67 is a 1:10,000,000-scale index map of Greenland. On this map are plotted the 468 nominal scene centers (path-row pairs) of all Landsat 1, 2, and 3 images that cover the Greenland ice sheet and other glaciers in Greenland. Each of the nominal scene centers is coded; the code is also used in the table of optimum Landsat 1, 2, and 3 MSS and RBV images of Greenland (table 14). The availability of the usable Landsat 3 RBV subscenes is indicated by the printing of one or more of the four subscenes (A, B, C, or D) around the periphery of the coded circles.

The path and row numbers for Landsat 1, 2, and 3 nominal scene centers follow the Extended Canadian or Worldwide Reference System (WRS) used by the U.S. Geological Survey's EROS Data Center, Sioux Falls, SD 57198. Complete imaging of the Earth's surface between about 81°30' N. and S. lat is achieved with Landsat 1, 2, and 3 MSS and RBV sensors in 251 orbits. These 251 orbits are divided into 119 rows of overlapping (15 percent), successive Landsat images acquired along the orbital path. The points of intersection of the orbital paths and rows are known as nominal scene centers. This index map includes all nominal scene centers that give coverage of Greenland including all or parts of 18 rows from Row 1 (about 81°30' N. lat) to Row 18 (southern tip of Greenland) and parts of 62 paths (Path 243 to Path 53).

More than 2,000 Landsat images were evaluated by direct inspection of 70-mm archival roll positive transparencies at NASA's Goddard Space Flight Center, microfilm and paper prints from the U.S. Geological Survey's EROS Data Center, microfilm from the Canada Centre for Remote Sensing, and quick-look archival paper prints from ESA's satellite-receiving station in Kiruna, Sweden. The optimum Landsat 1, 2, and 3 MSS and Landsat 2 and 3 RBV images of Greenland were then classified on the basis of cloud cover (table 14). In the inland-ice regions, the optimum image was selected both on the basis of minimum cloud cover and low solar elevation angle to enhance subtle morphologic details on the ice-sheet surface. Landsat 3 RBV images were evaluated (see table 14) on the basis of whether there were distinguishable ground features on the images. Only usable Landsat 3 subscenes (A, B, C, and D) are included in table 14. Landsat 3 RBV subscenes encompass slightly more than one overlapping quadrant (A, NW.; B, NE.; C, SW.; D, SE.) of an MSS nominal scene. At a scale of 1:10,000,000, a Landsat image encompasses a parallelogram-shaped area that has sides about 19 mm long.

Several Landsat images may have been acquired for many nominal scene centers in Greenland. Only the codes for the optimum images are given on this index map. More than one image in the optimum category may exist, although only one has been listed. For those involved in using

Landsat imagery to carry out time-lapse studies of glaciological phenomena in Greenland, it will be necessary to request that the U.S. Geological Survey's EROS Data Center, the Canada Centre for Remote Sensing, and the European Space Agency's satellite-receiving stations in Kiruna, Sweden, and Fucino, Italy, do a computer search for all Landsat images of a particular nominal scene center. Because of the possible inaccuracy of the cloud-cover rating on the computer printout, however, it will probably be necessary to inspect an MSS band 7 image to ascertain the overall usefulness of a particular scene.

All of the Landsat images discussed in the chapter are keyed to figure 10 on the basis of their geographic positions. The actual latitude and longitude of the nominal scene center is provided in table 14. It should be recognized, however, that the actual Landsat 1, 2, and 3 scene centers can vary up to 40 km from the latitude and longitude coordinates of the nominal scene center, depending upon the specific orbital path and framing; therefore, the precise location of any scene with the same path and row identifiers can also vary. For those figures in which the full Landsat image is printed, a data-annotation block is usually printed on the bottom of the image. Tick marks indicating the approximate latitude and longitude grid are plotted on the edges of the image. The actual, rather than the nominal, scene center of the image is noted in the left-hand part of the bottom annotation.








Figure 67 is the best available index map to optimum usable Landsat 1, 2, and 3 MSS and RBV images of Greenland and updates the Landsat index maps that include Greenland published jointly by the U.S. Geological Survey and the National Oceanic and Atmospheric Administration (NOAA) in 1982 (Index to Landsat Worldwide Reference Systems (WRS), Landsats 1, 2, 3, and 4, sheets 1 and 3, scale 1:10,000,000).

## Table of Optimum Landsat 1, 2, and 3 Images of Greenland

Table 14 provides information about the optimum Landsat 1, 2, and 3 MSS and Landsat 2 and 3 RBV images of Greenland.

The following explanation provides information about the optimum Landsat image for each of the path-row pairs that encompass Greenland. For the majority of path-row pairs, only one optimum image is given. In some cases, however, two scenes were needed to provide coverage of the nominal image area. Usually, when there is more than one image per nominal scene center, one image shows the area in the late summer (maximum melt of the prior season's snowcover to better delineate the ice-sheet, ice cap, or outlet glacier margins and supraglacial features; for example, see fig. 15), and the other image shows the area in late fall or early spring, when the low solar elevation angle reveals subtle morphologic details on the ice-sheet surface (for example, see fig. 20). During the winter it is too dark for Landsat images to be acquired for much of Greenland. The code column carries the same symbol that appears on figure 67.

A detailed explanation of the column headings for table 14 follows.

PATH-ROW AND NOMINAL SCENE CENTERS	Complete imaging of the Earth's surface between about 81°30' N. and S. lat with Landsat 1, 2, and 3 MSS and RBV sensors is achieved in 251 orbits. These orbits are divided into 119 rows of overlapping (15 percent), successive Landsat images acquired along the orbital path. The points of intersection of the orbital paths and the rows are known as nominal scene centers. This table includes all nominal scene centers that give coverage of the Greenland glaciers: parts of 18 rows from Row 1 (about 81°30' N. lat) to Row 18 (southernmost point of Greenland) and parts of 62 paths (orbits) (Path 243 on the east to Path 53 on the west).
LANDSAT IDENTIFICATION NUMBER	Each Landsat image acquired of the Earth's surface has a unique identification number. The first (left-hand) digit refers to the numbered Landsat series (for example, 1, 2, or 3). The other digits to the left of the hyphen record the number of days since launch of the spacecraft. The 5 numbers to the right of the hyphen record the time of acquisition of the image to the nearest 10 seconds in Greenwich Mean Time (G.m.t.). For example, Landsat image 1042-13142(Path 247, Row 9) of Scoresby Land, East Greenland, was acquired by Landsat 1, 42 days after the 23 July 1972 launch (3 September 1972) at 13 hr 14 min, 20 s G.m.t.
DATE	Date of acquisition of the Landsat image.
SOLAR ELEVATION ANGLE	Angle of the height of the Sun above the horizon. In Greenland, this can vary from 0° to about 55°, depending upon the latitude and time of year.
CODE	<p>Evaluation of image usability for glaciologic, geologic, and cartographic applications. Symbols defined as follows:</p> <ul style="list-style-type: none"><li> Excellent image (0 to 5 5 percent cloud cover)</li><li> Good image (&gt;5 to 5 10 percent cloud cover)</li><li> Fair to poor image (&gt;10 to ≤100 percent cloud cover)</li><li> Unusable image (100 percent cloud cover)</li><li> No image available</li><li> Nominal scene center for a Landsat image that lies beyond the coast of Greenland</li></ul> <p> Landsat 3 RBV subscenes are indicated as A, B, C, or D and encompass slightly more than one overlapping quadrant (A, NW.; B, NE.; C, SW.; D, SE.) of an MSS scene. Obscuration of surface features can be caused by clouds, overexposure of the image, electronic-processing artifacts, and so on. Direct evaluation of usable percentage of Landsat 3 RBV sub-scenes was made from either 1:500,000-scale paper prints or positive or negative film transparencies at the U.S. Geological Survey's EROS Data Center, Sioux Falls, SD 57198.</p>

## CLOUD COVER

Direct evaluation of cloud-cover percentage was made from either Landsat 1, 2, and 3 MSS band 7 or Landsat 2 RBV band 3 70-mm positive or negative film (1:3,369,000-scale) transparencies (archival rolls) located at NASA's Goddard Space Flight Center, Greenbelt, MD 20771; from MSS band 7 or RBV band 3 paper prints from the U.S. Geological Survey's EROS Data Center; from microfiche supplied by the Canada Centre for Remote Sensing; and by direct inspection of quick-look archival paper prints at the Kiruna, Sweden. Landsat MSS band 7 or RBV band 3 images were used for cloud-cover evaluation because of maximum discrimination between clouds and snow. If an MSS band 7 image was unavailable, then an MSS band 6 image was used, and so forth.

## REMARKS

The geographic place-name of prominent geographic features is given where applicable. Mention of noteworthy glaciological phenomena may also be given. The archive of the Landsat image is assumed to be the EROS Data Center unless otherwise specified. The U.S. Geological Survey's Satellite Glaciology Project (USGS-SGP) is given as the archive in some cases, because 1:1,000,000-scale paper prints of Landsat images of Greenland acquired by the Shoe Cove satellite receiving station in Newfoundland, Canada, were only available during the 4 years of operation of the facility (1978-82). Microfiche of the Landsat images of Greenland acquired during that period is held by the Satellite Glaciology Project and the Canada Centre for Remote Sensing. In addition, Landsat 1, 2, and 3 RBV imagery, formerly available from the EROS Data Center, is now only available for inspection at the USGS-SGP.



# References Cited

- Ahlmann, H.W., 1942, Studies in northeast Greenland. R. III. Accumulation and ablation on the Frøya Glacier; its regime in 1938–39 and 1939–40 *Geografiska Annaler*, v. 24, no. 1–2, p. 1–22.
- 1953, Glacier variations and climatic fluctuations: New York, American Geographical Society, Bowman Memorial Lectures, Series Three, 51 p.
- Ahnert, F., 1963, The terminal disintegration of Steensby Gletscher, north Greenland: *Journal of Glaciology*, v. 4, no. 35, p. 537–545.
- Ambach, W., 1972, Zur Schätzung der Eis-nettoablation im Randgebiet des Grönländischen Inlandeises [An assessment of net ice ablation in the marginal region of the Greenland Inland Ice]: *Polarforschung*, v. 42, no. 1, p. 18–23.
- Armstrong, T., Roberts, B., and Swithinbank, C., 1973, Illustrated glossary of snow and ice: Cambridge, Scott Polar Research Institute, Special Publication 4, 60 p.
- Bader, H., 1961, The Greenland ice sheet: U.S. Army Cold Regions Research and Engineering Laboratory, Report I-B2, 18 p.
- Bauer, A., 1954, Contribution à la connaissance de l'Inlandsis du Groenland. Deuxième partie: Synthèse glaciologique [Contribution to the knowledge of the Greenland Ice Sheet. Pt. 2 Glaciological synthesis] International Association of Scientific Hydrology, Publication No. 39, p. 270–296.
- Bauer, A., Baussart, M., Carbone, M., Kassser, P., Perroud, P., and Renaud, A., 1968, Missions aériennes de reconnaissance au Groenland 1957–58, observations aériennes et terrestres, exploitation des photographies aériennes, détermination des vitesses des glaciers velant dans Disko Bugt et Umanak Fjord [Aerial reconnaissance missions in Greenland 1957–58, aerial and land observations, use of the aerial photographs, determination of the velocity of glaciers calving into Disko Bugt and Umanak Fjord]: *Meddelelser om Grønland*, v. 173, no. 3, 116 p.
- Bay, E., 1895, Geologi, in *Den østgrønlandske Expedition 1891–92* [Geology, in *The East Greenland Expedition 1891–92*: *Meddelelser om Grønland*, v. 19, p. 147–187.
- Benson, C.S., 1959, Physical investigations on the snow and firn of northwest Greenland: 1952, 1953, and 1954: U.S. Army Snow, Ice, and Permafrost Research Establishment (SIPRE) [U.S. Army Cold Regions Research and Engineering Laboratory (CRREL)] Research Report No. 26, 62 p.
- 1960, Stratigraphic studies in the snow and firn of the Greenland Ice Sheet: Unpublished Ph.D. dissertation, Division of Geological Sciences, California Institute of Technology, 213 p.
- 1961, Stratigraphic studies in the snow and firn of the Greenland Ice Sheet: *Folia Geographica Danica*, v. 9, p. 13–37.
- 1962, Stratigraphic studies in the snow and firn of the Greenland Ice Sheet: Snow, Ice, and Permafrost Research Establishment (SIPRE) [U.S. Army Cold Regions Research and Engineering Laboratory (CRREL)] Research Report No. 70, 93 p. (Published version of C.S. Benson's Ph.D. dissertation of 1960.)
- 1967, Polar regions snow cover, in *Öura*, H., ed., *Physics of snow and ice*, International Conference on Low Temperature Science, I: Conference on Physics of Snow and Ice, Proceedings, v. 1, pt. 2, Hokkaido University, p. 1039–1063.
- Benson, C.S., and Motyka, R.J., 1979, Glacier-volcano interactions on Mt. Wrangell, Alaska, in *1977–78 Annual Report of the Geophysical Institute: Fairbanks, University of Alaska*, p. 1–25.
- Bindschadler, R.A., 1984, Jakobshavn Glacier drainage basin: A balance assessment: *Journal of Geophysical Research*, v. 89, no. C2, p. 2066–2072.
- Bindschadler, R.A., Zwally, H.J., Major, J.A., and Brenner, A.C., 1989, Surface topography of the Greenland ice sheet from satellite radar altimetry: National Aeronautics and Space Administration Special Publication SP-503, 105 p. (Includes 17 map plates.)
- Böcher, T., Fredskild, B., Holmen, E., and Jakobsen, E., 1978, Grønlands flora [The flora of Greenland], 3d ed.: Copenhagen, P. Haase, 327 p.
- Braithwaite, R.J., 1980a, Brief review of ablation studies in Greenland. Unpublished manuscript presented to the Working Group on Prediction of Glacier Runoff, Geilo, Norway, August 1980.
- 1980b, Regional modelling of ablation in West Greenland Grønlands Geologiske Undersøgelse, Report No. 98, 20 p.
- Braithwaite, R.J., and Olesen, O.B., 1984 [1985], Ice ablation in West Greenland in relation to air temperature and global radiation: *Zeitschrift für Gletscherkunde und Glazialgeologie*, v. 20, p. 155–168.
- Braithwaite, R.J., and Thomsen, H.H., 1984a, Runoff conditions at Paakitup Akuliarusersua, Jakobshavn, estimated by modelling Grønlands Geologiske Undersøgelse, Gletscher-hydrologiske Meddelelser No. 84/3, 22 p.
- 1984b, Runoff conditions at Kuussuup Tasia, Christianshåb, estimated by modelling: Grønlands Geologiske Undersøgelse, Gletscher-hydrologiske Meddelelser No. 84/2, 23 p.
- Bretz, J.H., 1935, Physiographic studies in East Greenland, in Boyd, L.A., *The fiord region of East Greenland*: American Geographical Society, Special Publication No. 18, p. 159–266.
- Brooks, R.L., 1979, Monitoring of thickness changes of the continental ice sheets by satellite altimetry: *Journal of Geophysical Research*, v. 84, no. B8, p. 3965–3968.
- Carbone, M., and Bauer, A., 1968, Exploitation des couvertures photographiques aériennes répétées du front des glaciers velant dans Disko Bugt et Umanak Fjord, Juin-Juillet 1964 [Use of repeated aerial photographic coverage of the front of glaciers calving into Disko Bugt and Umanak Fjord, June-July 1964]: *Meddelelser om Grønland*, v. 173, no. 5, 78 p.
- Clement, P., 1984a, Glaciological activities in the Johan Dahl Land area, South Greenland, as a basis for mapping hydropower potential. Grønlands Geologiske Undersøgelse, Report No. 120, p. 113–121.
- 1984b, Observationer omkring Hullet—Eisdæmmed Sø i Sydgrønland [Observations around Hullet—Anicedammed lake in South Greenland]: *Dansk Geologisk Forening, Årsskrift 1983*, p. 65–71.
- Colbeck, S.C., 1974, A study of glacier flow for an open-pit mine: An exercise in applied glaciology: *Journal of Glaciology*, v. 13, no. 69, p. 401–414.
- Dansgaard, W., Johnsen, S.J., Clausen, H.B., Dahl-Jensen, D., Gundestrup, N.S., Hammer, C.U., Hvidberg, C.S., Steffensen, J.P., Sveinbjörnsdottir, A.E., Jouzel, J., and Bond, G., 1993, Evidence for general instability of past climate from a 250-Kyr ice-core record: *Nature*, v. 364, no. 6434, p. 218–220.
- Dansgaard, W., Johnsen, S.J., Møller, J., and Langway, C.C., Jr., 1969, One thousand centuries of climatic record from Camp Century on the Greenland ice sheet: *Science*, v. 166, no. 3903, p. 377–381.
- Dansgaard, W., Johnsen, S.J., Clausen, H.B., and Gundestrup, N., 1973, Stable isotope glaciology: *Meddelelser om Grønland*, v. 197, no. 2, 53 p.
- Dansgaard, W., Gundestrup, N., and Johnsen, S.J., 1981, GISP deep drilling completed Ice, no. 66, p. 23.
- Davies, W.E., and Krinsley, D.B., 1962, The recent regimen of the ice cap margin in North Greenland, in *Symposium of Obergurgl, Austria (10–18 September 1962)*: International Association of Scientific Hydrology, Publication No. 58, p. 119–130.
- Dawson, A.G., 1983, Glacierdammed lake investigations in the Hullet area, South Greenland *Meddelelser om Grønland, Geoscience*, v. 11, 24 p.
- de Quervain, M., Brandenberger, F., Reinwarth, O., Renaud, A., Roch, A., and Schneider, R., 1969, Schneekundliche Arbeiten der Internationalen Glaziologischen Grönlandexpedition (Nivologie) [Snow hydrology research on the International Glaciological Expedition to Greenland (Snow study)]: *Meddelelser om Grønland*, v. 177, no. 4, 283 p.

- Douglas, B.C., Cheney, R.E., Miller, L., Agreen, R.W., Carter, W.E., and Robertson, D.S., 1990, Greenland ice sheet: Is it growing or shrinking?: *Science*, v. 248, no. 4953, p. 288.
- Dowdeswell, J.A., and McIntyre, N.F., 1986, The saturation of LANDSAT MSS detectors over large ice masses: *International Journal of Remote Sensing*, v. 7, no. 1, p. 151-164.
- Drygalski, E. von, 1897, Grönland-Expedition der Gesellschaft für Erdkunde zu Berlin 1891-1893, v. 1: Berlin, W.H. Kuhl, 555 p.
- Dunbar, M., 1978, Petermann Gletscher: Possible source of a tabular iceberg off the coast of Newfoundland *Journal of Glaciology*, v. 20, no. 84, p. 595-397.
- Dwyer, J.L., 1993, Monitoring characteristics of glaciation in the Kangerdlugssuaq Fjord region, East Greenland, using Landsat data: M.Sc. thesis, University of Colorado, Boulder, Colo., 238 p.
- Eriksson, B.E., 1942, Studies in North-East Greenland. Pt. IV. Meteorological records and the ablation on the Frøya Glacier in relation to radiation and meteorological conditions: *Geografiska h a l e r*, v. 24, no. 1-2, p. 23-50.
- Ferrigno, J.G., and Williams, R.S., Jr., 1983, Limitations in the use of Landsat images for mapping and other purposes in snow- and ice-covered regions: Antarctica, Iceland, and Cape Cod, Massachusetts, *in* Proceedings of the Seventeenth International Symposium on Remote Sensing of Environment: Ann Arbor, Mich., Environmental Research Institute of Michigan, v. 1, p. 335-355.
- Ferrigno, J.G., Williams, R.S., Jr., and Kent, T.M., 1983, Evaluation of Landsat 3 RBV images, *in* Oliver, R.L., James, P.R., and Jago, J.B., eds., *Antarctic Earth Science, Proceedings of the Fourth International Symposium on Antarctic Earth Sciences (16-20 August 1982)*, University of Adelaide, South Australia: Canberra, Australian Academy of Science, p. 446-449.
- Flint, R.F., 1948, Glacial geology and geomorphology, *in* Boyd, L.A., *The coast of Northeast Greenland: American Geographical Society, Special Publication No. 30*, p. 91-210.
- Forsberg, R., and Madsen, F., 1981, Geoid prediction in northern Greenland using collocation and digital terrain models: *Annales de Geophysique*, v. 37, no. 1, p. 31-36.
- Fristrup, B., 1952, Die Klimaänderungen in der Arktis und ihre Bedeutung besonders für Grönland [The climate change in the Arctic and its particular significance for Greenland]: *Erdkunde*, v. 6, no. 4, p. 201-212.
- 1961, Danish glaciological investigations in Greenland, *in* Raasch, G.O., ed., *Geology of the Arctic*, v. 2 First International Symposium on Arctic Geology, Proceedings, Calgary, Alberta, January 11-13, 1960, p. 735-746.
- 1966, *The Greenland Ice Cap*: Seattle: University of Washington Press, 312 p.
- Fushimi, H., Uemura, N., Higuchi, K., and Ikegami, K., 1979, Scientific studies made during the solo dogsled journeys to the North Pole and across Greenland: *Sangaku (Journal of the Japanese Alpine Club)*, 24 p.
- Goldthwait, R.P., 1961, Regimen of an ice cliff on land in Northwest Greenland *Folia Geographica Danica*, v. 9, p. 107-115.
- 1971, Restudy of Red Rock ice cliff, Nunatarssuaq, Greenland U.S. Army Cold Regions Research and Engineering Laboratory, Technical Report No. 224, 27 p.
- Greenland Ice Core Project (GRIP) Members, 1993, Climate instability during the last interglacial period recorded in the GRIP ice core: *Nature*, v. 364, no. 6434, p.203-207.
- Gribbon, P.W.F., 1964, Recession of glacier Tasissârssik A, East Greenland: *Journal of Glaciology*, v. 5, no. 39, p. 361-363.
- Grootes, P.M., Stuiver, M., White, J.W.C., Johnsen, S., and Jouzel, J., 1993, Comparison of oxygen isotope records from the GISP2 and GRIP Greenland ice cores: *Nature*, v. 366, no. 6455, p. 552-554.
- Gudmandsen, P.E., 1976, Studies of ice by means of radio echo sounding, *in* Peel, R.F., Curtis, L.F., and Barrett, E.C., eds., *Remote sensing of the terrestrial environment: Colston Papers No. 28*, p. 198-211.
- 1980, Electromagnetic studies of ice and snow, *in* Fraysse, Georges, ed., *Remote sensing application in agriculture and hydrology*, Proceedings of a seminar held at the Joint Research Centre of the Commission of the European Communities in the framework of the ISpra courses, Varese, Italy: Rotterdam, A.A. Balkema, p.389-416.
- Hasholt, B., 1986, Kortlægning af Mitdluagkat Gletscheren og nogle hydroglaciologiske observationer [Mapping of the Mitdluagkat Glacier and some hydroglaciological observations]: *Geografisk Tidsskrift*, v. 86, p. 9-16.
- Helk, J. V. , 1966, Glacier mapping in Greenland: *Canadian Journal of Earth Sciences*, v. 3, no. 6, p. 771-774.
- Henriksen, N., 1986, Tapping of en isdaemmet sø in Nordgrønland [Draining of an ice dammed lake in North Greenland]: *Geologi i Grønland*, v. 2, p. 42-47.
- Higgins, A., 1988, Glacier velocities from aerial photographs in North and North-East Greenland: Grønlands Geologiske Undersøgelse, Report No. 140, p. 102-105.
- 1989, North Greenland ice islands: *Polar Record*, v. 25, no. 154, p. 207-212.
- 1990, North Greenland glacier velocities and calice production: *Polarforschung*, v. 60, no. 1, p. 1-23.
- Higgins, A., and Weidick, A., 1988, The world's northernmost surging glacier?: *Zeitschrift für Gletscherkunde und Glazialgeologie*, v. 24, no. 2, p. 111-123.
- Hofmann, W., 1964, Die geodätische Lagemessung über das grön-ländischeInlandeisherInternationalenGlaziologischerGrønland-Expedition (EGIG), 1959 [The geodetic position measurement on the Greenland Ice Sheet of the International Glaciological Greenland Expedition (EGIG), 1959]: *Meddelelser om Grønland*, v. 173, no. 6, 145 p.
- 1974, Berichte die Internationale Glaziologische Grønland-Expedition (EGIG). 2, Die Geodätische Lagemessung—Eisbewegung 1959-1967in den EGIG-Profilen [Report of the International Glaciological Greenland Expedition (EGIG). 2, The geodetic determination of positions-ice movements 1959-1967 in the EGIG profile]: *Zeitschrift für Gletscherkunde und Glazialgeologie*, v. 10, p. 217-224.
- HolmesG.W.,1955Morphologyandhydrology of the Mint Julep area, southwest Greenland, *in* Project Mint Julep (Investigation of Smooth Ice Areas of the Greenland Ice Cap, 1953) Pt. 2: U.S. Arctic, Desert, Tropic Information Center, Special Scientific Reports, Publication A-104B, p. 1-50.
- Holtzscheler, J.J., and Bauer, A., 1954, Contribution à la connaissance de l'Inlandsis du Groenland [Contribution to the knowledge of the Greenland Ice Sheet]: International Association of Scientific Hydrology, Publication No. 39, p. 244-296.
- Hø y, T., 1970, Surveying and mapping in southern Peary Land, North Greenland *Meddelelser om Grønland*, v. 182, no. 3, 50 p.
- Knudsen, N.T., 1983, Photogrammetric investigations at glaciers in West Greenland: Grønlands Geologiske Undersøgelse, Report No. 115, p. 115-117.
- Koch, J.P., and Wegener, A., 1930, Wissenschaftliche Ergebnisse der dänischen Expedition nach Dronning Louises-Land und quer über das Inlandeish von Nordgrønland 1912-13 [Scientific results of the Danish expedition to Dronning Louise Land and the traverse of the Ice Sheet in North Greenland 1912-13]: *Meddelelser om Grønland*, v. 75, 676 p.
- Koch, L., 1928, Contributions to the glaciology of North Greenland: *Meddelelser om Grønland*, v. 65, pt. 2, p. 181-464.
- Kollmeyer, R.C., 1980, West Greenland outlet glaciers: An inventory of the major iceberg producers, *in* World Glacier Inventory, Proceedings of the Workshop at Riederalp, Switzerland, 17-22 September 1978: International Association of Hydrological Sciences, Publication No. 126, p. 57-45.
- Krabill, W.B., Thomas, R.H., Martin, C.F., and Swift, R.N., 1993, Analysis of the accuracy of airborne laser measurements of the elevation of the Greenland ice sheet [abs.], *in* Supplement to Eos (26 October 1993), 1993 Fall Meeting, American Geophysical Union: p. 234.

- LaChapelle, E., 1955, Ablation studies in the Mint Julep area, south-west Greenland, *in* Project Mint Julep (Investigation of Smooth Ice Areas of the Greenland Ice Cap, 1953) Pt. 2: U.S. Arctic, Desert, Tropic Information Center, Special Scientific Reports, Publication A-104A, p. 51-72.
- Langway, C.C., Jr., 1961, Accumulation and temperature on the Inland Ice of north Greenland, 1959 *Journal of Glaciology*, v. 3, no. 30, p. 1017-1044.
- Langway, C.C., Jr., Oeschger, H., and Dansgaard, W., 1985, The Greenland ice sheet program in perspective, *in* Greenland ice core: Geophysics, geochemistry, and the environment: American Geophysical Union Geophysical Monograph 33, p. 1-8.
- Lillestrand, R.L., and Johnson, G.W., 1971, Cartography of North Greenland Surveying and Mapping, v. 31, no. 2, p. 233-250.
- Lister, H., 1958, Glaciology, 1: The balance sheet or the mass balance, *in* Hamilton, R.A., ed., *Venture to the Arctic*: Pelican Books, A 432, p. 167-188.
- Loewe, F., 1936, Höhenverhältnisse und Massenhaushalt des Grönländischen Inlandeises [The elevation and mass-balance of the Greenland Ice Sheet]: *Beiträge zur Geophysik*, v. 46, p. 317-330.
- Loewe, F., and Wegener, K., 1933, Die Schneepegelbeobachtungen: Wissenschaftliche Ergebnisse der deutschen Grönland-Expedition Alfred Wegener 1929 und 1930/31 [Snow depth observations: Scientific results of the German Greenland expedition Alfred Wegener 1929 and 1930/31], v. 1, p. 153-171.
- Lysgaard, L., 1949, Recent climatic fluctuations: *Folia Geographica Danica*, v. 5, pt. 1 (text), 85 p.; pt. 2 (tables), 94 p.; pt. 3 (curves), 35 p.
- Madsen, F., 1979, Application of Doppler technique in Greenland for geodetic control: Second International Geodetic Symposium on Satellite Doppler Positioning, Austin, Tex: p. 989-999.
- Meier, M.F., 1974, Ice sheets and glaciers: *Encyclopedia Britannica*, 15th edition, v. 9, p. 175-186.
- Mock, S.J., 1966, Fluctuations of the terminus of the Harald Moltke Bræ Greenland: *Journal of Glaciology*, v. 6, no. 45, p. 369-373.
- Müller, F., 1962, Zonation in the accumulation area of the glaciers of Axel Heiberg Island, N.W.T., Canada: *Journal of Glaciology*, v. 4, no. 33, p. 302-311.
- 1978, Instructions for compilation and assemblage of data for a world glacier inventory. Supplement; identification/glacier number: Temporary Technical Secretariat for World Glacier Inventory, International Commission on Snow and Ice, Department of Geography, Swiss Federal Institute of Technology (ETH), Zürich, 7 p. plus appendix.
- Muller, F., Caflisch, T., and Müller, G., 1977, Instructions for compilation and assemblage of data for a world glacier inventory: Temporary Technical Secretariat for World Glacier Inventory, International Commission on Snow and Ice, Department of Geography, Swiss Federal Institute of Technology (ETH), Zürich, 28 p. plus appendix.
- Munck, F., 1950, Gravimetrie: Expéditions Polaires Françaises, Missions Paul-Émile Victor, Campagne au Groenland 1950 [Gravimetry: French Polar Expeditions, Missions Paul Émile Victor, 1950 campaign to Greenland]: *Rapports Préliminaires No. 15, Série Scientifique*, p. 57-64.
- Nobles, L.H., 1960, Glaciological investigations, Nunatarssuaq ice ramp, North-western Greenland U.S. Army Snow, Ice, and Permafrost Research Establishment, [U.S. Army Cold Regions Research and Engineering Laboratory (CRREL)] Technical Report 66, 57 p.
- Olesen, O.B., and Andreasen, J.-O., 1983, Glaciological, glacier-hydrological and climatological investigations around 66° N., West Greenland Grønlands Geologiske Undersøgelse, Report No. 115, p. 107-111.
- Olesen, O.B., and Reeh, N., 1969, Preliminary report on glacier observations in Nordvestfjord, East Greenland Grønlands Geologiske Undersøgelse, Report No. 21, p. 41-53.
- 1973, Glaciological observations in the south-western Scoresby Sund region: Grønlands Geologiske Undersøgelse, Report No. 58, p. 49-54.
- Østrem, G., 1975, ERTS data in glaciology—An effort to monitor glacier mass-balance from satellite imagery: *Journal of Glaciology*, v. 15, no. 73, p. 403-415.
- Overgaard, S., 1981, Radio-echosounding in Greenland, data catalogue 1974: Electromagnetic Institute, Technical University of Denmark, 104 p.
- Overgaard, S., and Gudmandsen, P.E., 1978, Radioglaciology, surface and bedrock contour maps at Dye-3 Electromagnetic Institute, Technical University of Denmark, Report No. 199, 4 p.
- Parkinson, C.L., Comiso, J.C., Zwally, H.J., Cavalieri, D.J., Gloersen, P., and Campbell, W.J., 1987, Arctic sea ice, 1973-1976 Satellite passive-microwave observations: National Aeronautics and Space Administration Special Publication SP-489, 296 p.
- Post, A., 1975, Preliminary hydrography and historic terminal changes of Columbia Glacier, Alaska: U.S. Geological Survey Hydrologic Investigations Atlas HA-559, 3 sheets.
- Radok, U., Barry, R.G., Janssen, D., Keen, R.A., Kiladis, G.N., and McInnes, B., 1982, Climatic and physical characteristics of the Greenland ice sheet; pt. I and II: Boulder, University of Colorado, Cooperative Institute for Research in Environmental Sciences, 193 p.
- Reeh, N., 1979, Surface contours and flow pattern of a perfectly plastic three-dimensional ice sheet with arbitrary bottom and edge topography [abs.]: *Journal of Glaciology*, v. 24, no. 90, p. 511-512.
- 1985, Greenland ice-sheet mass balance and sea-level change, *in* Glaciers, ice sheets, and sea level: Effects of a CO<sub>2</sub>-induced climatic change, report of a workshop held in Seattle, Washington, 13-15 September 1984: Washington, D.C., National Academy Press, p. 155-171.
- 1989, Dynamic and climatic history of the Greenland Ice Sheet; Chapter 14, *in* Fulton, R.J., ed., *Quaternary geology of Canada and Greenland Geological Survey of Canada, Geology of Canada*, no. 1, p. 793-822.
- Reeh, N., Oerter, H., and Bøggild, C.E., 1993, Mass balance and ice dynamics of the north-east Greenland ice-sheet margin, *in* Climate change, Sea level rise and associated impacts in Europe. Climate and sea level change on a century time scale: Participant No. 14, Alfred-Wegener-Institut für Polar- und Meeresforschung, Bremerhaven, Germany, Final Report (EPOC Programme PL890075), v. 3, 21 p.
- Rist, S., 1974, Jökulhlaupannáll 1971, 1972, og 1973 [Record of jökulhlaup events for 1971, 1972, and 1973]: *Jökull*, v. 23, p. 55-60.
- Ryder, C.H., 1889, Undersøgelse af Grønlands Vestkyst fra 72° til 74°35'N. Br., 1886 og 1887 [Investigations of the west coast of Greenland from 72° to 74°35'N. latitude, 1886 and 1887]: *Meddelelser om Grønland*, v. 8, no. 7, p. 203-270.
- Schuster, R.L., 1954, Snow studies, *in* Project Mint Julep (Investigations of a Smooth Ice Area of the Greenland Ice Cap) Pt. 3: U.S. Army Snow, Ice, and Permafrost Research Establishment, SIPRE Report 19, 11 p.
- Schytt, V., 1955, Glaciological investigations in the Thule ramp area: U.S. Army Snow, Ice, and Permafrost Research Establishment, SIPRE Report 28, 88 p.
- Seckel, H., 1977, Höhenänderungen im grönländischen Inlandeis zwischen 1959 und 1968 [Altitude changes of the Greenland Inland Ice between 1959 and 1968]: *Meddelelser om Grønland*, v. 187, no. 4, 58 p.
- Sharp, R.P., 1956, Glaciers in the Arctic: *Arctic*, v. 9, no. 1-2, p. 78-117.
- Stove, G.C., Green, K., Birnie, R.V., Davison, G., Bagot, K., Palmer, M., Kearn, G., Ritchie, P.F.S., and Sugden, D.E., [1984?], The use of Landsat data to monitor iceberg production; monitoring iceberg production from West Greenland tidewater glaciers using Landsat data: Results of the AGRISPINE experiment for the Jakobshavn Isbræ: Macaulay Institute for Soil Research, Craigiebuckler, Aberdeen, Scotland, and the National Remote Sensing Centre, Space and New Concepts Department, Royal Aircraft Establishment, Farnborough, Hampshire, England, 32 p.

- Thomas, R.H., Jozek, K., Kuivinen, K., and Krabill, W.B., 1993, Estimating changes in the elevation of the Greenland ice sheet [abs.], in *Supplement to Eos* (26 October 1993), 1993 Fall Meeting, American Geophysical Union: p. 23.
- Thomas, R.H., Krabill, W.B., Manizade, S.S., Swift, R.N., and Brenner, A.C., in press a, Comparison of radar altimeter data over Greenland with surface topography derived from airborne laser altimetry: Proceedings, 2d ERS-1 Symposium, Hamburg, Germany, October 1993.
- Thomas, R.H., Krabill, W.B., Manizade, S.S., and Jezek, K., in press b, Greenland ice sheet thickness changes measured by laser altimetry: Proceedings, 4th Workshop on Mass Balance of Greenland Ice Sheet and Related Topics, Amsterdam, Holland.
- Thomsen, H.H., 1986, Is og Vandkraft. Glaciologi i vandkraftprojektet bynære bassiner [Glaciology and hydropower. Glaciology for local hydropower projects]: Grønlands Geologiske Undersøgelse, Gletscher-hydrologiske Meddelelser No. 86B, 73 p.
- Thomsen, H.H., and Braithwaite, R.J., 1987, Use of remote-sensing data in modelling run-off from the Greenland ice sheet: *Annals of Glaciology*, v. 9, p. 215–217.
- Thomsen, H.H., Thorning, L., and Braithwaite, R.J., 1988, Glacier-hydrological conditions on the Inland Ice northeast of Jakobshavn/Ilulissat, West Greenland Grønlands Geologiske Undersøgelse, Report No. 138, map sheet with description.
- Thomsen, T., and Thomsen, H.H., 1986, Hydrological data collection, interpretation and analysis in Greenland, in *Hydrological applications of space technology*, Proceedings of the Cocoa Beach Workshop, Florida, August 1985: International Association of Hydrological Sciences, Publication No. 160, p. 273–282.
- Thorning, L., Thomsen, H.H., and Hansen, E., 1986, Geophysical investigations at the Inland Ice margin of the Pakitsoq basin, central West Greenland Grønlands Geologiske Undersøgelse, Report No. 130, p. 114–121.
- Vibe, C., 1967, Arctic animals in relation to climatic fluctuations: *Meddelelser om Grønland*, v. 170, no. 5, 227 p.
- Weidick, A., 1968, Observations on some Holocene glacier fluctuations in West Greenland *Meddelelser om Grønland*, v. 165, no. 6, 202 p.
- 1976, Glaciation and the Quaternary of Greenland, in Escher, A., and Watt, W.S., eds., *Geology of Greenland* Copenhagen, Geological Survey of Greenland, p. 430–459.
- 1985, The ice cover of Greenland Grønlands Geologiske Undersøgelse, Gletscher-hydrologiske Meddelelser No. 85/4, 10 p.
- 1988a, Gletschere i Sydgrønland [Glaciers in South Greenland]: Grønlands Geologiske Undersøgelse: Geologi i Grønland [Geology in Greenland], v. 2, 80 p.
- 1988b, Surging glaciers in Greenland—astatus: Grønlands Geologiske Undersøgelse, Report No. 140, p. 106–410.
- Weidick, A., Beggild, C.E., and Knudsen, N.T., 1992, Glacier inventory and atlas of West Greenland Grønlands Geologiske Undersøgelse, Report 158, 194 p.
- Weidick, A., and Olesen, O.B., 1980, Hydrological basins in West Greenland Grønlands Geologiske Undersøgelse, Report No. 94, 51 p.
- Williams, R.S., Jr., 1986, Jakobshavns Isbæ, western Greenland; Plate G-3 of Chap. 9, Glaciers and glacial landforms, in Short, N.M., and Blair, R.W., Jr., eds., *Geomorphology from space. A global overview of regional landforms*: National Aeronautics and Space Administration Special Publication SP-486, p. 542–543.
- 1987, Satellite remote sensing of Vatnajökull, Iceland *Annals of Glaciology*, v. 9, p. 127–185.
- Williams, R.S., Jr., Hall, D.K., and Benson, C.S., 1991, Analysis of glacier facies using satellite techniques: *Journal of Glaciology*, v. 37, no. 125, p. 120–128.
- Zwally, H.J., 1989, Growth of Greenland ice sheet: Interpretation: *Science*, v. 246, no. 4937, p. 1589–1591.
- Zwally, H.J., Brenner, A.C., Major, J.A., Bindshadler, R.A., and Marsh, J.G., 1989, Growth of Greenland ice sheet: Measurement: *Science*, v. 246, no. 4937, p. 1587–1589.
- 1990, Response to Douglas and others (1990) letter in *Science* (v. 248, no. 4953, p. 288): *Science*, v. 248, no. 4953, p. 288–289.
- Zwally, H.J., Thomas, R.H., and Bindshadler, R.A., 1981, Ice-sheet dynamics by satellite laser altimetry: Greenbelt, Md., National Aeronautics and Space Administration, Goddard Space Flight Center, Technical Memorandum No. 82128, 11 p.



---

---

## **TABLES 12-14**

---

---

TABLE 12.—*Geographic place-names of the cited natural features and towns in Greenland*

All place-names are indicated on the index map, plate 1. The following list includes the type and name of each feature and its location in figures, tables, and geographic areas. Quotation marks indicate unauthorized place-names. The areas (administrative units) referred to in this index are shown in figure 1, and the following abbreviations have been used:

N	NorthGreenland
NW	North-West Greenland
W	WestGreenland
nW	northern West Greenland
cW	central West Greenland
sW	southern West Greenland
SW	South-WestGreenland
S	SouthGreenland
NE	North-East Greenland
E	EastGreenland
nE	northern East Greenland
cE	central East Greenland
sE	southern East Greenland
SE	South-East Greenland

“Inl.Ice” in the “Area” column refers to former or existing stations on the Inland Ice.

Geographic place-name (alternative name)	Feature	Figure	Table	Area
A.B. Drachmann Gletscher	outlet glacier	45		NE
Academy Gletscher	tidal outlet glacier	41,42	398	N
Admiralty Gletscher	outlet glacier	8,45		NE
Adolf Hoel Gletscher	tidal outlet glacier	46		nE
Agga Ø (near Unartit)	island	Plate 1		sE
Agssakait sermia	valley glacier	8,21,22,53		c W
Akugdlerussûp sermia	tidal outlet glacier	15,16		sW
Alágordlia	fjord	15		sW
Alágordliup sermia	tidal outlet glacier	Plate 1	3	c W
Alágorsûp sermia	outlet glacier	24		nW
“Amitsulôq ice cap”	ice cap	8,17,18		sW
Angmagssalik (Tasîlaq)	town	47,60	199	SE
Apusiniakajik	valley glacier	55,56		cE
Aputaiuitsoq	mountain	13		S
Aputitêq (Nordre Aputitêq)	station	59	9	cE
Ardencaple Fjord	fjord	46		NE
Arken	mountain	Plate 1	10	cE
Arsuk Brae	tidal outlet glacier	Plate 1	3	SW
Austmannadalen	valley	16		sW
Barclay Bugt	bay	57		cE
Bartholin Brae	outlet glacier	57,58		cE
Bernstorff Isfjord	fjord	63		SE
Bessel Fjord	fjord	46		NE
Bjørnbo Gletscher	valley glacier	52,54		cE
Blosseville Kyst	coast	57,58		cE-sE
Borgfjorden	fjord	45		NE
Borgjökelen	outlet glacier	45		NE
Boyes Sø (Isortoq)	lake	21		c W
Brede gletscher	outlet glacier	55,57		cE
“Brikkerne Gletscher”	tidal outlet glacier	38		N
Britannia Gletscher	outlet glacier	8,45		NE
Brother John Gletscher	outlet glacier	31,32		N W
Buchanan Bay	bay	31		Canada
Budolfi Isstrøm	outlet glacier	45		NE
Buksefjorden (Kangerdluarssúnguaq)	fjord	15		sW
“Camp IV”	station	20		Inl.Ice
“Camp VI”	station	20		Inl.Ice
“Camp Century”	station	47		Inl.Ice
“Camp Tuto”	station	8,27,30		NW
Cape Herschel I	cape	31		Canada
Cecilia Nunatak	mountain	49,50		nW-cW
Chamberlin Gletscher (Naujat sermiat)	tidal outlet glacier	30		NW
Charcot Gletscher (in Nordvestfjord)	outlet glacier	49	3	cE
Charcot Gletscher (on Milne Land)	valley glacier	55		cE

TABLE 12.—*Geographic place-names of the cited natural features and towns in Greenland—Continued*

Geographic place-name (alternative name)	Feature	Figure	Table	Area
C.H. Ostenfeld Gletscher	tidal outlet glacier	35,38	3	N
Christian Erichsen Iskappe	local ice cap	8,41,42		N
Christianshåb (Qasigiáguít)	town	1		c W
Clavering Ø	island	46		nE
Cornell Gletscher (Ikigssûp sermerssua)	tidal outlet glacier	26		nW
“Crøte”	station	47		Inl.Ice
Daneborg	station	Plate 1	9	nE
Danmark Ø (in Scoresby Sund)	island	Plate 1		cE
Danmarkshavn	station	1	7	NE
Daugaard-Jensen Gletscher	tidal outlet glacier	49,51	3	cE
Deception Ø	island	59	11	sE
Dendrit Gletscher	tidal outlet glacier	57,58		cE
Denmark Strait	strait	Plate 1		sE
Dietrichson Gletscher (in Melville Bugt)	tidal outlet glacier	Plate 1	3	NW
Dijmphna Sund	sound	43		N
Disko (Qeqertarsuaq)	island	21		c W
Disko Bugt	bay	21,22		c W
Dodge Gletscher	outlet glacier	32		NW
Dove Bugt	bay	46		NE
Dronning Louise Land	area	45		NE
Dundas (in Wolstenholme Fjord)	station	Plate 1	7	NW
“Dye-2”	station	Plate 1		Inl.Ice
“Dye-3”	station	47,63		Inl.Ice
Døcker-Smith Gletscher	tidal outlet glacier	Plate 1	3	NW
Edward Bailey Gletscher	glacier	55		cE
Egedesminde (Ausiait)	town	Plate 1	1	c W
Eielson Gletscher	tidal outlet glacier	55		cE
Ejner Mikkelsen Gletscher	outlet glacier	45		NE
Eqalorutsit kangigdlît sermiat (Qajutapsermia)	tidal outlet glacier	13	3	S
Eqalorutsit kitdlît sermiat	tidal outlet glacier	13	3,5	S
Eqip sermia	tidal outlet glacier	8,20,22	3	c W
Etah	abandoned settlement	31		NW
Evighedsfjord (Kangerdlugssuatsiaq)	fjord	17	6	sW
F. Graae Gletscher	tidal outlet glacier	49	3	cE
Fenrisgletscher	tidal outlet glacier	61	11	SE
Flade Isblink	ice cap	Plate 1		N
Fleming Fjord	fjord	52		cE
Franske Øer	islands	43		NE
Frederikshåb (Pâmiut)	town	Plate 1		SW
Frederikshåb Isblink	piedmont glacier	14		SW-SW
Frejagletscher (“Frøya Glacier”)	valley glacier	8,46		nE
Fønfjord (Ujuâkajîpkangertiva)	fjord	55		cE
Gade Gletscher (in Melville Bugt)	tidal outlet glacier	Plate 1	3	NW
Geikie Plateau	area	55,57		cE
Germania Land	area	45,46		NE
Giesecke Bræer (collective name for Qeqertarsûp sermia and Kakivfait sermiat)	tidal outlet glacier	24,25,26	5	nW
Glacier de France	tidal outlet glacier	61		SE
“Gletscher33”	cirque glacier	8		s W
Godhavn (Qeqertarsuaq)	town	21	1	c W
Godthåb (Nûk)	town	15	1,4	SW
Godthåbsfjord (Nûk kangerdlua)	fjord	15		SW
Gunnbjørn Fjeld (at Blossville Kyst)	mountain	Plate 1		sE
Gyldenløve Fjord	fjord	63		SE
Gåsefjord (Orqungmut kangertiva)	fjord	55,57		cE
Hagen Bræ	tidal outlet glacier	Plate 1	3	N
Hall Bredning	bay	55		cE
Hans Tausen Iskappe (Hans Tausen Iskappe)	ice cap	Plate 1		N
Hanserâq Fjord	fjord	63		SE
Harald Moltke Bræ (Uvdlip sermia)	tidal outlet glacier	27,30	3, 8	NW
Harebræ	tidal outlet glacier	55		æ

TABLE 12. –*Geographic place-names of the cited natural features and towns in Greenland* –Continued

Geographic place-name (alternative name)	Feature	Figure	Table	Area
Harefjord (in Scoresby Sund)	fjord	Plate 1		cE
Hayes Gletscher (in Melville Bugt)	tidal outlet glacier	Plate 1	3,5	nW
Heilprin Gletscher (Qaqujâstûp sermia)	tidal outlet glacier	30	3,8	NW
Heimdal Gletscher	tidal outlet glacier	63		SE
Heinkel Gletscher	tidal outlet glacier	46		nE
Hekla Havn (in Scoresby Sund)	bay	Plate 1		cE
Helheimgletscher	tidal outlet glacier	61,62	11	SE
Henry Land	area	57		cE
Henson Gletscher (near Peary Land)	tidal outlet glacier	Plate 1	3	N
Hertugen af Orléans Land	area	43,44		NE
Hiawatha Gletscher	outlet glacier	33		NW
Hisinger Gletscher	tidal outlet glacier	49		nE
Hochstetter Forland	area	46		NE
Hold with Hope	area	46		nE
Holger Danske Tinde (near Wordie Gletscher)	mountain	Plate 1	10	nE
Holsteinsborg (Sisimiut)	town	Plate 1	1,4	c W
Hornemann Ø	island	63		SE
Hovgaard Ø	island	43		N
Hullet	lake	13		S
Humboldt Gletscher	tidal outlet glacier	33,34	3	NW-N
Hunt Fjord	fjord	Plate 1		N
Husfjeldet (near Kap Cort Adelaer)	mountain	Plate 1	10	SE
Hutchinson Plateau	area	59		sE
Igdlugdlip sermia	tidal outlet glacier	26		nW
Ikerasagssuaq (Prins Christian Sund)	sound	65		S
Ilua	fjord	65		S
Iluliagdlop tasia	lake	17,18		s W
Independence Fjord	fjord	41,42		N
Ingia Isbrae (Sagdlarutsip sermia)	tidal outlet glacier	22	3	c W
Inglefield Bredning (Kangerdlugssuaq)	fjord	30		NW
Inglefield Land	area	31		NW
Isfjeldsbanken	iceberg bank	20		c W
Isortuarssûp sermia	outlet glacier	8,15		sW
Isukasia	locality	15		sW
Isvand	lake	15,16		s W
Jakobshavn (Ilulíssat)	town	20,21	1	c w
Jakobshavn Isbrae (Sermeq kujatdleq)	tidal outlet glacier	20	3,5	c w
Jakobshavn Isfjord (Kangia)	fjord	20		c w
“Jarl-Joset”	station	47		Int.Ice
Jens Munk Ø	island	63		SE
Johan Petersen Fjord	fjord	61,63,64		SE
J.P. Koch Fjord (near Peary Land)	fjord	Plate 1		N
Julianehåb (Qaqortoq)	town	13	1,4	S
Jungersen Gletscher (near Peary Land)	tidal outlet glacier	Plate 1	3	N
Jøkelbugten (off Hertugen af Orleans Land)	bay	Plate 1		N-NE
Jørgen Brønlund Fjord	fjord	Plate 1	7	N
Kakivfait sermiat	tidal outlet glacier	24,25,26		nW
Kagssortoq	fjord	63		SE
Kane Basin	sound	31		NW-N
Kangerdluarssûp sermia	tidal outlet glacier	22	3	c W
Kangerdlugssuaq (Inglefield Bredning)	fjord	30		NW
Kangerdlugssuaq (Søndre Strømfjord)	fjord	Plate 1		sW-cW
Kangerdlugssuaq	fjord	59		sE
Kangerdlugssuaq Gletscher	tidal outlet glacier	59	11	sE
Kangerdlugssuatsiaq Kângertivatsiaq)	fjord	60		SE
Kangerdlugssuatsiaq (Evighedsfjord)	fjord	17		sW
Kangerdlugssuatsiaq (Lindenow Fjord)	fjord	65		SE-S
Kangerdlugssûp sermerssua	tidal outlet glacier	22	3	c W
Kangersuneq	fjord	15		sW
Kangiata nunâta sermia	tidal outlet glacier	15,16	5	sW
Kangigdleq	tidal outlet glacier	22	3	c W
Kangilerngata sermia	tidal outlet glacier	20,22	3	c W
Kap Alexander	cape	31,32		NW



TABLE 2.- *Geographic place-names of the cited natural features and towns in Greenland -Continued*

Geographic place-name (alternative name)	Feature	Figure	Table	Area
Kap Bellevue	cape	45		NE
Kap Cort Adelaer	cape	63		SE
Kap Farvel	cape	65		S
Kap Gustav Holm	cape	Plate 1		sE-SE
Kap Ryder	cape	57		cE
Kap Tobin (near Scoresby Sund)	cape	Plate 1	9	cE
Kârale Gletscher	tidal outlet glacier	61	11	SE
Kejser Franz Joseph Fjord	fjord	46		nE
Kista Dan Gletscher	tidal outlet glacier	55		cE
Knighton Fjord	fjord	57		sE
Knud Rasmussen Gletscher (Apusêq)	glacier	61		SE
Knud Rasmussen Gletscher (Eqûtigssáitsut sermiat)	tidal outlet glacier	30		N W
Knud Rasmussen Land	area	47		NW-N
Kofoed-Hansen Bræ	glacier	45		NE
“Kome Gletscher”	valley glacier	8,21,22		CW
Kong Christian IV Gletscher (at Blosseville Kyst)	tidal outlet glacier	Plate 1		sE
Kong Christian IX Land	area	55		cE
Kong Oscar Fjord	fjord	52		nE-cE
Kong Oscar Gletscher (in Melville Bugt)	tidal outlet glacier	Plate 1	3	NW
Korridoren	valley glacier	55		cE
Kronprins Christian Land	area	43		N
Kuánerssuit	valley	21	6	c W
Kuhn Ø	island	46		nE
Lambert Land	area	43		NE
L. Bistrup Bræ	tidal outlet glacier	45		NE
Leidy Gletscher	tidal outlet glacier	30		N W
Lille Gletscher (Sermeq avangnardleq)	tidal outlet glacier	22	3	c W
Lindenow Fjord (Kangerdlugssuatsiaq)	fjord	65		SE-S
Lyngeholme	islands	41,42		N
Lyngmarksbræ	glacier	21,53		c W
Løberen	valley glacier	52,53		cE
Magga Dan Gletscher	tidal outlet glacier	55,57		cE
Majorqaq	valley	17		sW
Marie Gletscher	tidal outlet glacier	30		N W
Marie Sophie Gletscher	tidal outlet glacier	41,42	3	N
Melville Bugt	coast	26		nW-NW
Mesters Vig	station, bay	52		cE
Midgårdgletscher	tidal outlet glacier	61	11	SE
“Milcent”	station	Plate 1		Inl.Ice
“Mile 370”	station	50		Inl.Ice
“Mile 452”	station	49,50		Inl.Ice
Milne Land	area	55		cE
“MintJulep”	station	19		Intl.Ice
Mitdluagkat Gletscher (near Angmagssalik)	valley glacier	Plate 1		SE
Mogens Heinesen Fjord (Sikuijivíteq)	fjord	63		SE
Mont Forel	mountain	60	10	SE
Morris Jesup Gletscher (Neqip sermia)	outlet glacier	31		NW
Nanortalik	town	Plate 1	1	S
Nansen Fjord (on Blosseville Kyst)	fjord	Plate 1		sE
Nansen Gletscher (in Melville Bugt)	tidal outlet glacier	Plate 1	3	N W
Nansen Nunatakker	mountains	41		N
Nares Land	area	35,36		N
Narssap sermia	tidal outlet glacier	15		sW
Narssaq	town	13		S
Narssaq Bræ	cirque glacier	8,11,13		S
Narssarssuaq	station	13	4	S
Navy Cliff	locality	41		N
Newman Bugt	fjord	35		N
Nioghalvfjærdsbræ	tidal outlet glacier	43	3	N-NE
Nioghalvfjærdsfjorden	fjord	43		N-NE
Nordbogletscher (Kûkulûp sermia)	outlet glacier	8,13		S
Nordenskiöld Gletscher (Akuliarutsip sermerssua) near Christianshåb	outlet glacier	Plate 1	3	c W

TABLE 12. —*Geographic place-names of the cited natural features and towns in Greenland—Continued*

Geographic place-name (alternative name)	Feature	Figure	Table	Area
Nordre Aputitêq	station	59	9	sE
Nordre Sermilik	fjord	13		S
Nordvestfjord	fjord	49,52,55,56		cE
Norske Øer	islands	43		NE
“North Central”	station	Plate 1		Inl.Ice
“North Ice Cap”	ice cap	8,30		N W
“North Site”	station	47		Inl.Ice
Nûgssuaq	peninsula	21,22		c W
Nunatakavsaup sermia	tidal outlet glacier	24		nW
“Nunatarssuaq Ice Ramp”	outlet glacier	8,29,30		N W
Nyeboe Land	area	35		N
Olrik Fjord	fjord	30		NW
Pâkitsoq/Pâkitsup ilordlia (outer and inner part of the same fjord) and Pâkitsup akuliaruserssua (locality in Pâkitsup ilordlia); all also designate a hydropower locality at the nearby Inland Ice margin	fjord	8,11,20		c W
Pasterze	outlet glacier	46	11	nE
Peary Gletscher (in Melville Bugt)	tidal outlet glacier	Plate 1	3	N W
Peary Land	area	39		N
Perdlerfiup sermia	tidal outlet glacier	22	3	c W
Petermann Gletscher	tidal outlet glacier	34	3,8	N
Pitugfik (Thule)	airfield	Plate 1		NW
Polaric Gletscher	tidal outlet glacier	59		SE
Polhem Dal	valley	52		nE
Prins Christian Sund (Ikerasagssuaq)	sound	65		S
Prins Christianssund (weather station)	station	65	9	S
Qagsserssuaq	peninsula	24		nW
Qajâ (in Jakobshavn Isfjord)	archeological site	Plate 1		c W
Qamanârssûp sermia	outlet glacier	8,15,16		c W
Qânâq (in Inglefield Bredning)	town	Plate 1		N W
Qapiarfiup sermia	ice cap	8		sW
“Qaumarujuk Gletscher”	outlet glacier	822		c W
Qeqertarssûp sermia	tidal outlet glacier	24,26		nW
Qôrqup sermia	tidal outlet glacier	13		S
Rampen (“Nunatarssuaq Ice Ramp”)	outlet glacier	8,29,30		N w
“Red Rock” (Rødefjeld)	mountain	28,30		NW
Renland (Tugtut nunât)	area	55,56		cE
Rink Gletscher (in Melville Bugt)	tidal outlet glacier	Plate 1	3	N W
Rink Isbrae (Kangigdliup sermia)	tidal outlet glacier	22	3	c W
Röhss Fjord	fjord	49,50		nE-cE
Rolige Bræ	tidal outlet glacier	55		cE
Ryder Gletscher	tidal outlet glacier	35,37	38	N
Sankt George Fjord	fjord	35		N
Sarqardliup sermia	tidal outlet glacier	20	3	c w
SchnauderØ	island	43,44		NE
Schuchert Dal	valley	52		cE
Schuchert Elv	river	52		cE
Schuchert Gletscher	valley glacier	52		cE
Schweizerland	area	60		SE
Scoresby Land	area	52		cE
Scoresby Sund	fjord complex	Plate 1; 49,51,52,55		cE
Scoresbysund (Igdlorqortôrmiut)	town	Plate 1	1	cE
Sehested Fjord	fjord	63		SE
Sermeq (in Søndre Sermilik)	tidal outlet glacier	12	5	S
Sermeq avangnardleq (Lille Gletscher)	tidal outlet glacier	22	3	c W
Sermeq avangnardleq (in Jakobshavn Isfjord)	tidal outlet glacier	Plate 1	3	c W
Sermeq avangnardleq (south coast of Nûgssuaq)	tidal outlet glacier	22,23	3	cW
Sermeq avangnardleq (Umanak district)	tidal outlet glacier	22	3	c W
Sermeq kujatdleq (Store Gletscher)	tidal outlet glacier			c W
Sermeq kujatdleq (south coast of Nûgssuaq)	tidal outlet glacier	20,22,23	3	c W

TABLE 12. --Geographic place-names of the cited natural feature and towns in Greenland- Continued

Geographiplace-name (alternative name)	Feature	Figure	Table	Area
Sermeq silardleq	tidal outlet glacier	22	3	c W
Sermiarssuit Sermikavsâ	valley glacier	21,22,53		c W
Sermiligâq	fjord	60,61		SE
Sermilik (south of Godthåb)	fjord and outlet glacier	14		SW
Sermilik (Egede and Rothe Fjord, near Angmagssalik)	fjord	60,61,62		SE
Sermilik (glacier in Umanak district)	tidal outlet glacier	22	3	c W
Sermilik Bræ (South Greenland)	tidal outlet glacier	Plate 1	3	S
Shackleton Bjerg (near Hisinger Gletscher)	mountain	Plate 1	10	nE
Shannon	island	46		NE
Sherard Osborn Fjord	fjord	35		N
Sikuijuitsoq	fjord	Plate 1		c W
Skeldal	valley	52		cE
Skjoldungen	station	63		SE
Smith Sound	sound	31		NW
Soranerbræen	tidal outlet glacier	45,46		NE
Spaltegletscher	tidal outlet glacier	43		N
“Station Centrale” (“Eismitte”)	station	47		Inl.Ice
Station Nord	station	Plate 1	7	N
Stauning Alper	area	52,54		cE
Steensby Gletscher	tidal outlet glacier	35	3	N
Steenstrup Gletscher	tidal outlet glacier	Plate 1	3	nW-NW
Steno Bræ	tidal outlet glacier	57		cE
Store Gletscher (Sermeq kujatdleq)	tidal outlet glacier	8, 22, 23	3	c w
Store Koldewey	island	45, 46		NE
Store Landgletscher	outlet glacier	27,30		NW
Storgletscher	valley glacier	52		cE
Storm Gletscher	outlet glacier	32		NW
Storstrømmen	tidal outlet glacier	45	3, 8	NE
Sukkertoppen (Manîtsaq)	town	Plate 1	1	sw
Sukkertoppen Iskappe	ice cap	Plate 1		sw
“Summit”	station	Plate 1		Inl.Ice
Suzanne Bræ	outlet glacier	45		NE
Svartenhuk Halve	peninsula	Plate 1		cW-nW
Sydbæ	outlet glacier	55,57		cE
Søndre Isortoq	fjord	17		sW
Søndre Sermilik	fjord	12,65		S
Søndre Strømfjord (Kangerdlugssuaq)	airfield	Plate 1	4	sW-cW
Takisseq	island	63		SE
Tasermiut	fjord	65		S
Tasersiaq	lake	17		sw
Tasersiaq Gletscher	outlet glacier	8		SW
Tasíngortarssua	lake	21		cW
Tasíssârssik (Tasílaq)	fjord	Plate 1		SE
Thule(Qânâq)	town	Plate 1	1	NW
Thule Air Base (Pitugfik)	airfield	Plate 1		NW
Tingmiarmiut	station	63	9	SE
Tingmiarmiut Fjord (Tingmiarmît kangertivat)	fjord	63		SE
Tiníngnilik	lake	20		c W
Torv Gletscher	tidal outlet glacier	57		cE
Tracy Gletscher(Qeqertârssûssarssûpsermia)	tidal outlet glacier	30	3, 8	NW
Trail Ø	island	52		nE
Treforken	mountain		10	SE
Tunugdliarfik	fjord	13		S
Ubekendt Ejland	island	22		c W
Umanak(Umánaq)	town, fjord	21,22	1	c W
Umiámáko Isbræ (Umiámáko sermia)	tidal outlet glacier	22	3, 5	c W
Únartit	islands	59	11	sE
Upernavik	town	47	1, 4	nW
Upernavik Isstrøm (Sermeq)	tidal outlet glacier	24	3, 5	nW
Ussing Bræer	tidal outlet glacier	24,26	5	nW

TABLE 12.—*Geographic place-names of the cited natural features and towns in Greenland—Continued*






















Geographic place-name (alternativename)	Feature	Figure	Table	Area
Valhaltindegletscher	cirque glacier	8,11,13		S
Vestfjord	fjord	55		cE
Vestfjord Gletscher	tidal outlet glacier	55	3	cE
Victoria Fjord	fjord	35,38		N
Vildtland	area	41		N
WahlenbergGletscher	outlet glacier	49,50		nE-cE
Waltershausen Gletscher	tidal outlet glacier	46,48		nE
Warming Land	area	35,37		N
Washington Land ,	area	34		N
Watkins Bjerger	mountain	57		sE
Wollaston Forland	area	46		nE
WolstenholmeFjord(Umánapkangerdlua)	fjord	30		N W
Wordie Gletscher	tidal outlet glacier	46		nE
Wulff Land	area	35		N
ZachariaeIsstrøm	tidaloutletglacier	4 3 , 44	3	NE



TABLE 13.- Stations on the Greenland Ice Sheet (Inland Ice) (see plate 1)
























Station	Geographic coordinates (lat, long)	Universal Transverse Mereator (UTM) coordinates	Reference
“Dye-3”	65°11' N., 43°49' W.	E555420 N7229410	Langway and others (1985).
“Mint Julep”	66°17' N., 47°46' W.	E375860 N7354240	Holmes (1955).
“Dye-2”	66°23' N., 46°11' W.	E447100 N7363140	Langway and others (1985).
“Camp IV”	69°40' N., 49°31' W.	E557520 N7729400	Holtzschere and Bauer (1954).
“Camp VI”	69°42' N., 48°16' W.	E605800 N7734790	Holtzschere and Bauer (1954).
“Milcent”	70°18' N., 45°35' W.	E478050 N7799430	Langway and others (1985).
“Station Centrale”	70°55' N., 40°38' W.	E440410 N7868910	Holtzschere and Bauer (1954).
“Crête”	71°07' N., 37°19' W.	E560800 N7891250	Langway and others (1985).
“Jarl-Joset”	71°21' N., 33°29' W.	E482750 N7916500	de Quervain and others (1969).
“Summit”	72°17' N., 37°56' W.	E536230 N8020860	Langway and others (1985).
GISP2 site	72°35' N., 38°29' W.	E517260 N8054080	Grootes and others (1993).
GRIP site	72°34' N., 37°37' W.	E545700 N8052660	Greenland Ice Core Project (GRIP) Members (1993).
“Worth Central”	74°37' N., 39°36' W.	E482230 N8280930	Langway and others (1985).
“Worth Site”	75°46' N., 42°27' W.	E569970 N8410660	Langway and others (1985).
“Camp Century”	77°10' N., 61°08' W.	E546280 N8566110	Langway and others (1985).
Hans Tavsens Iskappe	82°30' N., 38°20' W.	E509720 N9160700	Langway and others (1985).

TABLE 14.—*Optimum Landsat 1, 2, and 3 images of Greenland*

Path-Row	Nominal scene center (lat-long)	Landsat identification number	Date	Solar elevation angle (degrees)	Code (see fig. 67 for explanation)	Cloud cover (percent)	Remarks
243–10	70°35'N. 20°34'W.	No image available					
243–11	69°17'N. 22°36'W.	No image available					
244–9	71°50'N. 19°42'W.	22051–12452	9 Sep 80	23		50	Archived by ESA <sup>1</sup>
244–9	71°50'N. 19°42'W.	22069–12453	21 Sep 80	20		50	
244–10	70°35'N. 22°00'W.	30346–12472	14 Feb 79	6		0	Bartholin Brae, Magga Dan Gletscher; archived by ESA
244–10	70°35'N. 22°00'W.	21997–1245X <sup>2</sup>	11 Jul 80	–39		0	Bartholin Brae, Magga Dan Gletscher; partial image-archived by USGS-SGP <sup>3</sup>
244–11	69°17'N. 24°02'W.	30346–12474	14 Feb 79	7		0	Archived by ESA
244–11	69°17'N. 24°02'W.	21655–12403	4 Aug 79	37		5	Archived by USGS-SGP; image used for figure 57A
244–12	67°59'N. 25°51'W.	21997–12460	11 Jul 80	43		0	Archived by USGS-SGP
245–8	73°04'N. 18°32'W.	1076–13023	7 Oct 72	11		0	
245–9	71°50'N. 21°08'W.	1076–13030	7 Oct 72	12		0	
245–10	70°35'N. 23°26'W.	1382–13031	9 Aug 73	34		10	
245–11	69°17'N. 25°28'W.	1454–13020	20 Oct 73	9		10	Bartholin Brae, Geikie Plateau, Magga Dan Gletscher; snow surface detail; image used for figure 57B
245–11	69°17'N. 25°28'W.	21278–12320	23 Jul 78	39		0	Bartholin Brae, Geikie Plateau, Magga Dan Gletscher; archived by ESA
245–12	67°59'N. 27°17'W.	1454–13022	20 Oct 73	11		30	
245–12	67°59'N. 27°17'W.	21278–12323	23 Jul 78	40		0	Archived by ESA
246–7	74°16'N. 17°00'W.	22053–12560	5 Sep 80	22		0	Archived by ESA
246–8	73°04'N. 19°59'W.	22053–12563	5 Sep 80	23		0	Archived by ESA
246–9	71°50'N. 22°35'W.	1077–13084	8 Oct 72	12		0	
246–9	71°50'N. 22°35'W.	22053–12565	5 Sep 80	24		5	Archived by ESA
246–10	70°35'N. 24°52'W.	1077–13091	8 Oct 72	13		0	

<sup>1</sup> ESA is the European Space Agency, which archives Greenland data at Kiruna, Sweden, and Fucino, Italy.<sup>2</sup> X in the Landsat identification number refers to a missing or illegible number on the image in USGS-SGP archive.<sup>3</sup> USGS-SGP is the U.S. Geological Survey-Satellite Glaciology Project.

TABLE 14.—*Optimum Landsat 1, 2, and 3 images of Greenland—Continued*

Path-Row	Nominal scene center Oat-long)	Landsat identification number	Date	Solar elevation angle (degrees)	Code (see fig. 67 for explanation)	Cloud cover (percent)	Remarks
246-10	70°35'N. 24°52'W..	22053-12572	5 Sep 80	25		15	Archived by ESA
246-11	69°17'N. 26°54'W.	1077-13093	8 Oct 72	14		0	
246-11	69°17'N. 26°54'W.	22053-12574	5 Sep 80	26		30	Archived by ESA
246-12	67°59'N. 28°43'W.	22233-12570	4 Mar 81	14		0	Archived by ESA
247-6	75°25'N. 15°00'W.	1042-13131	3 Sep 72	21		0	
247-7	74°16'N. 18°26'W.	1042-13133	3 Sep 72	23		10	
247-8	73°04'N. 21°25'W.	1042-13140	3 Sep 72	24		50	
247-9	71°50'N. 24°01'W.	1042-13142	3 Sep 72	25		20	Schuchert Dal, Storgletscher, Bjørnbo Gletscher; image used for figure 52
247-9	71°50'N. 24°01'W.	30169-13035- ABCD	2 Aug 78	29		0-50	Landsat 3 RBV <sup>4</sup>
247-9	71°50'N. 24°01'W.	22000-1302X	14 Jul 80	39		0	Partial image; archived by USGS-SGP
247-10	70°35'N. 26°18'W.	1042-13145	3 Sep 72	26		20	Kong Christian IX Land, Milne Land, Renland; image used for figure 55
247-10	70°35'N. 26°18'W.	22000-13023	14 Jul 80	40		0	Archived by USGS-SGP
247-11	69°17'N. 28°20'W.	1078-13152	9 Oct 72	14		15	Kong Christian IX Land
247-11	69°17'N. 28°20'W.	22000-13025	14 Jul 80	41		5	Meltwater ponds on Kong Christian IV Gletscher; archived by USGS-SGP
247-12	67°59'N. 30°09'W.	1078-13154	9 Oct 72	15		15	
247-12	67°59'N. 30°09'W.	22396-13001	14 Aug 81	35		10	Archived by USGS-SGP
248-6	75°25'N. 16°26'W.	1079-13190	10 Oct 72	7		0	
248-7	74°16'N. 19°52'W.	1079-13193	10 Oct 72	8		0	Wollaston Forland, Clavering Ø
248-7	74°16'N. 19°52'W.	22055-13073	7 Sep 80	21		10	Archived by ESA
248-8	73°04'N. 22°51'W.	1079-13195	10 Oct 72	10		0	Traill Ø, Kejser Franz Joseph Fjord
248-8	73°04'N. 22°51'W..	22055-13080	7 Sep 80	22		20	Archived by ESA
248-9	71°50'N. 25°27'W.	1079-13202	10 Oct 72	11		0	Scoresby Sund
248-9	71°50'N. 25°27'W.	21623-13021	3 Jul 79	40		0	Archived by ESA

<sup>4</sup> Landsat 1,2, and 3 RBV data, formerly for sale from the U.S. Geological Survey's EROS Data Center, are now available only for inspection at the USGS-SGP.

TABLE 14.—*Optimum Landsat 1, 2, and 3 images of Greenland—Continued*

Path-Row	Nominal scene center (latlong)	Landsat identification number	Date	Solar elevation angle (degrees)	Code (see fig. 67 for explanation)	Cloud Cover (percent)	Remarks
248-10	70°35'N. 27°44'W.	22001-13081	15 Jul 80	40	●	0	Archived by USGS-SGP
248-11	69°17'N. 29°46'W.	30746-13043	20 Mar 80	20	●	0	Snow surface features, scanlines missing; archived by ESA
248-11	69°17'N. 29°46'W.	22397-13053	15 Aug 81	34	●	0	Archived by CCRS <sup>5</sup>
248-12	67°59'N. 31°35'W.	21695-13045	13 Sep 79	24	●	0	Archived by USGS-SGP
248-12	67°59'N. 31°35'W.	22235-13083	6 Mar 81	15	●	0	Snow surface features; archived by ESA
248-13	66°40'N. 33°13'W.	21695-13052	13 Sep 79	25	●	0	Archived by USGS-SGP
248-13	66°40'N. 33°13'W.	22235-13085	6 Mar 81	16	●	0	Snow surface features; archived by ESA
249-6	75°25'N. 17°52'W.	1368-13244	26 Jul 73	33	◐	15	Hochstetter Forland
249-7	74°16'N. 21°18'W.	1368-13250	26 Jul 73	35	◐	15	ClaveringØ, Wordie Gletscher
249-8	73°04'N. 24°17'W.	1368-13253	26 Jul 73	36	●	0	Kejser Franz Joseph Fjord
249-9	71°50'N. 26°53'W.	1368-13255	26 Jul 73	37	●	0	Upper Scoresby Sund, Wahlenberg and Daugaard-Jensen Gletschers; meltwater ponds
249-10	70°35'N. 29°10'W.	22056-13143	8 Sep 80	25	●	0	Archived by USGS-SGP
249-11	69°17'N. 31°12'W.	21354-12583	7 Oct 78	15	●	0	Kong Christian IV Gletscher; archived by USGS-SGP
249-12	67°59'N. 33°01'W.	21354-12590	7 Oct 78	16	●	0	Kangerdlugssuaq area; archived by USGS-SGP
249-13	66°40'N. 34°39'W.	21354-12592	7 Oct 78	17	●	5	Kap Gustav Holm; archived by USGS-SGP
249-14	65°20'N. 36°08'W.	21354-12595	7 Oct 78	18	●	0	Archived by USGS-SGP
250-5	76°31'N. 15°20'W.	22057-13181	9 Sep 80	18	●	0	Archived by ESA
250-6	75°25'N. 19°18'W.	22057-13184	9 Sep 80	19	●	0	Archived by ESA
250-7	74°16'N. 22°44'W.	22057-13190	9 Sep 80	20	●	0	Archived by ESA
250-7	74°16'N. 22°44'W.	22237-13175	8 Mar 81	11	●	0	Snow surface features; archived by ESA
250-8	73°04'N. 25°43'W.	21643-13133	23 Jul 79	36	●	0	Archived by ESA
250-8	73°04'N. 25°43'W.	22237-13182	8 Mar 81	12	●	0	Snow surface features; archived by ESA
250-9	71°50'N. 28°19'W.	21643-13140	23 Jul 79	37	●	0	Archived by ESA

<sup>5</sup> CCRS is the Canada Centre for Remote Sensing, Ottawa, Ontario.



TABLE 14.—*Optimum Landsat 1, 2, and 3 images of Greenland—Continued*

Path-Row	Nominal scene center (lat-long)	Landsat identification number	Date	solar elevation angle (degrees)	Code (see fig. 67 for explanation)	Cloud cover (percent)	Remarks
250-9	71°50'N. 28°19'W.	22237-13184	8 Mar 81	13	●	0	Snow surface features; archived by ESA
250-10	70°35'N. 30°36'W.	21643-13142	23 Jul 79	38	●	0	Archived by ESA
250-10	70°35'N. 30°36'W.	22237-13191	8 Mar 81	14	●	0	Archived by ESA
250-11	69°17'N. 32°38'W.	21643-13145	23 Jul 79	39	●	0	Archived by ESA
250-11	69°17'N. 32°38'W.	22237-13193	8 Mar 81	15	●	0	Snow surface features; archived by ESA
250-12	67°59'N. 34°27'W.	1045-13325	6 Sep 72	27	●	0	
250-12	67°59'N. 34°27'W.	21355-13044	8 Oct 78	16	●	0	Blosseville Kyst, Hutchinson Plateau; image used for figure 59; archived by USGS-SGP
250-12	67°59'N. 34°27'W.	21643-13151	23 Jul 79	40	●	0	Archived by ESA
250-12	67°59'N. 34°27'W.	22237-13200	8 Mar 81	16	●	0	Archived by ESA
250-13	66°40'N. 36°06'W.	1045-13331	6 Sep 72	28	●	0	
250-13	66°40'N. 36°06'W.	21643-13154	23 Jul 79	41	●	0	Archived by ESA
250-13	66°40'N. 36°06'W.	22237-19202	8 Mar 81	17	●	0	Schweizerland; archived by ESA
250-14	65°20'N. 37°34'W.	21643-13160	23 Jul 79	42	●	0	Archived by ESA
250-14	65°20'N. 37°34'W.	22237-13205	8 Mar 81	18	●	0	Snow surface features; archived by ESA
250-15	63°59'N. 38°55'W.	21355-13060	8 Oct 78	19	●	0	Archived by USGS-SGP
250-15	63°59'N. 38°55'W.	21643-13163	23 Jul 79	43	●	5	Archived by ESA
250-16	62°38'N. 40°09'W.	1045-13343	6 Sep 72	32	●	0	
250-16	62°38'N. 40°09'W.	21355-13062	8 Oct 78	20	●	0	Archived by USGS-SGP
250-17	61°16'N. 41°16'W.	22075-13231	27 Sep 80	24	●	0	Archived by ESA
250-17	61°16'N. 41°16'W.	22237-13220	8 Mar 81	21	●	0	Archived by ESA
250-18	59°54'N. 42°19'W.	21643-13174	23 Jul 79	47	●	0	Archived by ESA
251-5	76°31'N. 16°46'W.	1064-13354	25 Sep 72	12	●	0	Store Koldewey; image used for figure 46
251-5	76°31'N. 16°46'W.	21302-13051	16 Aug 78	27	●	0	Archived by ESA
251-6	75°25'N. 20°44'W.	1064-13360	25 Sep 72	13	●	0	Hochstetter Forland; image used for figure 46

TABLE 14.—*Optimum Landsat 1, 2, and 3 images of Greenland—Continued*

Path-Row	Nominal scene center (lat-long)	Landsat identification number	Date	Solar elevation angle (degrees)	Code (see fig. 67 for explanation)	Cloud cover (percent)	Remarks
251-4	75°25'N. 20°44'W.	21302–13053	16 Aug 78	28	●	0	Archived by ESA
251-7	74°16'N. 24°10'W.	1064-13363	25 Sep 72	14	●	0	Clavering Ø , Wordie Gletscher; image used for figure 46
251-7	74°16'N. 24°10'W.	21302–13060	16 Aug 78	29	●	0	Archived by ESA
251-8	73°04'N. 27°09'W.	1064–13365	25 Sep 72	15	◐	10	Shackleton Bjerg
251-9	71°50'N. 29°45'W.	30209–13270	30 Sep 78	18	●	0	Image used for figure 49; archived by USGS-SGP
251-10	70°35'N. 32°02'W.	30209–13272	30 Sep 78	19	●	0	Archived by USGS-SGP
251-11	69°17'N. 34°04'W.	21644–13203	24 Jul 79	40	◐	10	Archived by USGS-SGP
251-12	67°59'N. 35°53'W.	30227–13283	18 Oct 78	12	●	0	Snow surface features; archived by USGS-SGP
251-13	66°40'N. 37°32'W.	104613390	7 Sep 72	28	●	5	Schweizerland; image used for figure 60
251-13	66°40'N. 37°32'W.	22382–13233	31 Jul 81	39	●	0	Archived by ESA
251-14	65°20'N. 39°00'W.	22382–13240	31 Jul 81	40	●	5	Archived by ESA
251-15	63°59'N. 40°21'W.	22058–13280	10 Sep 80	29	●	0	Archived by USGS-SGP
251-15	63°59'N. 40°21'W.	22382–13242	31 Jul 81	41	●	0	Archived by ESA
251-16	62°38'N. 41°35'W.	22058–13283	10 Sep 80	30	●	5	Archived by USGS-SGP
251-17	61°16'N. 42°42'W.	22076–13285	28 Sep 80	27	●	0	Archived by USGS-SGP
251-18	59°54'N. 43°45'W.	1568–13370	11 Feb 74	14	◐	10	
251-18	59°54'N. 43°45'W.	31253–13270	9 Aug 81	43	●	0	Kap Farvel, South Greenland; archived by ESA
1-5	76°31'N. 18°12'W.	1245-13423	25 Mar 73	15	●	0	
1-5	76°31'N. 18°12'W.	30156–13304–ACD	8 Aug 78	29	A C ○ D	0-40	Gernania Land, Store Koldewey; Landsat 3 RBV
1-5	76°31'N. 18°12'W.	22041–13294	24 Aug 80	24	●	0	Archived by ESA
1-6	75°25'N. 22°10'W.	1245-13430	25 Mar 73	16	●	0	
1-7	74°16'N. 25°36'W.	1245-13432	25 Mar 73	17	●	0	Waltershausen Gletscher
1-7	74°16'N. 25°36'W.	21645–1324X	25 Jul 79	35	●	0	Partial scene; archived by ESA
1-8	73°04'N. 28°35'W.	1245-13435	25 Mar 73	18	●	0	Shackleton Bjerg

TABLE 14.—*Optimum Landsat 1, 2, and 3 images of Greenland—Continued*

























Path-Row	Nominal scene center (lat-long)	Landsat identification number	Date	Solar elevation angle (degrees)	Code (see fig. 67 for explanation)	Cloud cover (pct)	Remark
1-8	73°04'N. 28°35'W.	21645-13250	25 Jul 79	36		10	Archived by ESA
1-9	71°50'N. 31°11'W.	21645-13252	25 Jul 79	37		0	Archived by ESA
1-9	71°50'N. 31°11'W.	22095-13312	17 Oct 80	9		0	Archived by CCRS
1-10	70°35'N. 33°28'W.	22095-13314	17 Oct 80	10		0	Archived by CCRS
1-11	69°17'N. 35°30'W.	22095-13321	17 Oct 80	11		0	Archived by CCRS
1-12	67°59'N. 37°19'W.	22041-13323	24 Aug 80	31		0	Archived by ESA
1-12	67°59'N. 37°19'W.	22221-13312	20 Feb 81	10		5	Archived by USGS-SGP
1-13	66°40'N. 38°58'W.	21645-13270	25 Jul 80	41		0	Archived by ESA
1-14	65°20'N. 40°26'W.	1083-13450	14 Oct 72	15		0	Image used for figure 63
1-14	65°20'N. 40°26'W.	21645-13273	25 Jul 80	42		0	Archived by ESA
1-15	63°59'N. 41°47'W.	1083-13455	14 Oct 72	17		0	Image used for figure 63
1-15	63°59'N. 41°47'W.	21645-13275	25 Jul 80	43		0	Archived by ESA
1-16	62°38'N. 43°01'W.	1083-13461	14 Oct 72	18		0	Image used for figure 63
1-16	62°38'N. 43°01'W.	21645-13282	25 Jul 80	44		0	Archived by ESA
1-17	61°16'N. 44°08'W.	30750-13300	24 Mar 80	28		20	Søndre Sermilik fjord; image used for figure 12; archived by ESA; scanlines missing
1-17	61°16'N. 44°08'W.	21645-13284	25 Jul 80	44		5	Archived by ESA
1-18	59°54'N. 45°11'W.	22419-13311	6 Sep 81	16		0	Archived by CCRS
24	77°33'N. 15°01'W.	2530-13284	5 Jul 76	35		5	
25	76°31'N. 19°38'W.	1300-13480	19 May 73	32		5	
26	75°25'N. 23°36'W.	1300-13482	19 May 73	34		40	
27	74°16'N. 27°02'W.	1300-13485	19 May 73	35		80	
2-8	73°04'N. 30°01'W.	22096-13XXX	18 Oct 80	7		0	Archived by USGS-SGP
2-9	71°50'N. 32°37'W.	21718-13330	6 Oct 79	13		10	Archived by CCRS
2-10	70°35'N. 34°54'W.	22060-13373	12 Sep 80	23		0	Snow surface features; archived by CCRS

TABLE 14.—*Optimum Landsat 1, 2, and 3 images of Greenland—Continued*

Path-Row	Nominal scene center (lat-long)	Landsat identification number	Date	Solar elevation angle (degrees)	Code (see fig. 67 for explanation)	Cloud cover (percent)	Remarks
2-11	69°17'N. 36°56'W.	22060-13375	12 Sep 80	24	●	0	Snow surface features; archived by CCRS
2-12	67°59'N. 38°45'W.	22060-13382	12 Sep 80	25	●	0	Snow surface features; archived by CCRS
2-13	66°40'N. 40°24'W.	22096-13384	18 Oct 80	13	●	0	Snow surface features; archived by CCRS
2-44	65°20'N. 41°52'W.	22060-13391	12 Sep 80	27	●	0	Snow surface features; archived by CCRS
2-15	63°59'N. 43°13'W.	1228-13522	8 Mar 73	19	◐	10	Snow surface features
2-45	63°59'N. 43°13'W.	22060-13393	12 Sep 80	29	●	0	Snow surface features; archived by CCRS
2-46	62°38'N. 44°37'W.	1228-13525	8 Mar 73	20	●	0	Snow surface features
2-16	62°38'N. 44°37'W.	22060-13400	12 Sep 80	30	●	0	Snow surface features; archived by CCRS
2-17	61°16'N. 45°34'W.	1228-13531	8 Mar 73	22	●	5	Narssarssuaq area; snow surface features; image used for figure 13
2-17	61°16'N. 45°34'W.	22060-13402	12 Sep 80	31	●	0	Snow surface features; archived by CCRS
2-18	59°54'N. 46°37'W.	1228-13534	8 Mar 73	23	●	0	
2-18	59°54'N. 46°37'W.	21682-13354	31 Aug 79	27	●	0	Archived by CCRS
34	77°33'N. 16°27'W.	1391-13521	18 Aug 73	25	●	0	
34	77°33'N. 16°27'W.	30176-13420-C	28 Aug 78	21	<sup>C</sup> ●	0	Landsat 3 RBV
3-5	76°31'N. 21°04'W.	1391-13523	18 Aug 73	26	◐	20	
3-5	76°31'N. 21°04'W.	30176-13422-AB	28 Aug 78	22	<sup>A</sup> ● <sup>B</sup>	0	Landsat 3 RBV
36	75°25'N. 25°02'W.	30356-13430	24 Feb 79	5	◐	20	Snow surface features; archived by ESA
36	75°25'N. 25°02'W.	30842-13341	24 Jun 80	37	◐	10	Archived by ESA
3-7	74°16'N. 28°28'W.	22043-13415	26 Aug 80	25	●	0	Archived by ESA
38	73°04'N. 31°27'W.	22079-13422	1 Oct 80	15	◐	25	Snow surface features; archived by USGS-SGP
3-9	71°50'N. 34°03'W.	22385-13391	3 Aug 81	34	●	5	Archived by CCRS, ESA
3-10	70°35'N. 36°20'W.	1085-13551	16 Oct 72	10	◐	20	
3-10	70°35'N. 36°20'W.	22385-13393	3 Aug 81	35	●	5	Archived by CCRS, ESA
3-11	69°17'N. 38°22'W.	22223-13423	22 Feb 81	10	◐	10	Archived by CCRS



TABLE 14.—*Optimum Landsat 1, 2, and 3 images of Greenland—Continued*

Path-Row	Nominal scene center Oat-long)	Landsat identification number	Date	Solar elevation angle (degrees)	Code (see fig. 67 for explanation)	Cloud cover (percent)	Remarks
3-11	69°17'N. 38°22'W.	22385-13400	3 Aug 81	36	●	0	Archived by ESA
3-12	67°59'N. 40°11'W.	22223-13425	22 Feb 81	11	◐	10	Archived by CCRS
3-12	67°59'N. 40°11'W.	22385-13402	3 Aug 81	37	●	0	Archived by ESA
3-13	66°40'N. 41°50'W.	30356-13455	24 Feb 79	12	●	0	Snow surface features; archived by ESA
3-13	66°40'N. 41°50'W.	22043-13442	26 Aug 80	32	●	0? <sup>s</sup>	Archived by ESA
3-14	65°20'N. 43°19'W.	30356-13462	24 Feb 79	13	●	0	Snow surface features; archived by ESA
3-14	65°20'N. 43°19'W.	22043-13445	26 Aug 80	33	●	5?	Archived by ESA
3-15	63°59'N. 44°39'W.	30356-13464	24 Feb 79	14	●	0	Snow surface features; archived by ESA
3-15	63°59'N. 44°39'W.	22043-13451	26 Aug 80	34	●	5?	Archived by ESA
3-16	62°38'N. 45°53'W.	30356-13471	24 Feb 79	16	●	0	Archived by ESA
3-16	62°38'N. 45°53'W.	22043-13454	26 Aug 80	35	●	0	Archived by ESA
3-17	61°16'N. 47°01'W.	22061-13461	13 Sep 80	30	●	0	Archived by CCRS
44	77°33'N. 17°53'W.	1337-13530	25 Jun 73	35	●	0	
4-5	76°31'N. 22°30'W.	1337-13532	25 Jun 73	36	●	0	Storstrammen area; meltwater ponds; image used for figure 45
4-5	76°31'N. 22°30'W.	21342-13304,	25 Sep 78	12	●	0	Archived by ESA
4-6	75°25'N. 26°28'W.	21342-13302	25 Sep 78	13	●	5	Archived by ESA
4-7	74°16'N. 29°54'W.	21324-13300	7 Sep 78	21	●	0	Archived by ESA
4-8	73°04'N. 32°53'W.	21324-13302	7 Sep 78	22	●	0	Archived by ESA
4-9	71°50'N. 35°29'W.	21324-13305	7 Sep 78	23	●	0	Archived by ESA
4-10	70°35'N. 37°46'W.	30159-13500	11 Aug 78	33	◐	10?	Archived by ESA
4-11	69°17'N. 39°48'W.	22098-13492	20 Oct 80	10	◑	60	Archived by CCRS
4-12	67°59'N. 41°37'W.	22098-13494	20 Oct 80	11	◑	60	Archived by USGS-SGP
4-13	66°40'N. 43°16'W.	21342-13332	25 Sep 78	20	◐	10?	Archived by ESA

<sup>s</sup> ? indicates uncertainty by the editors in evaluating cloud-cover percentage on archival images.

TABLE 14.—*Optimum Landsat 1,2, and 3 images of Greenland- Continued*

Path-Row	Nominal scene center (lat-long)	Landsat identification number	Date	Solar elevation angle (degrees)	Code (see fig. 67 for explanation)	Cloud cover (percent)	Remarks
4-14	65°20' • • N. 44°45'W.	21342-13334	25 Sep 78	21		10?	Archived by ESA
4-14	65°20' • • N. 44°45'W.	22224-13493	23 Feb 81	13		50	Archived by CCRS
4-15	63°59'N. 46°05'W.	22224-13495	23 Feb 81	14		0	Snow surface features; archived by CCRS
4-16	62°38'N. 47°19'W.	22224-13502	23 Feb 81	15		0	Snow surface features; scanlines missing; archived by CCRS
4-17	61°16'N. 48°27'W.	21324-13340	7 Sep 78	32		0	Area southeast of Frederikshåb; archived by CCRS
54	77°33'N. 19°19'W.	22045-13521	28 Aug 80	21		0	Archived by ESA
54	77°33'N. 19°19'W.	30160-13531- ABCD	12 Aug 78	27		0-?	Germania Land; snow surface overexposed; Landsat 3 RBV
5-5	76°31'N. 23°56'W.	22045-13523	28 Aug 80	22		0	Storstrømmen area, numerous meltwater ponds; archived by ESA
5-6	75°25'N. 27°54'W.	22045-13530	28 Aug 80	23		0	Archived by ESA
5-7	74°16'N. 31°20'W.	22045-13532	28 Aug 80	24		0	Archived by ESA
5-8	73°04'N. 34°19'W.	22045-13535	28 Aug 80	26		0	Archived by ESA
5-9	71°50'N. 36°55'W.	22045-13541	28 Aug 80	27		0	Archived by ESA
5-10	70°35'N. 39°12'W.	22045-13544	28 Aug 80	28		0	Archived by ESA
5-11	69°17'N. 41°14'W.	1447-14052	13 Oct 73	12		5	
5-11	69°17'N. 41°14'W.	22045-13550	28 Aug 80	29		0	Archived by ESA
5-12	67°59'N. 43°03'W.	22045-13553	28 Aug 80	30		0	Archived by ESA
5-13	66°40'N. 44°42'W.	22045-13555	28 Aug 80	31		0	Archived by ESA
5-14	65°20'N. 46°11'W.	22045-13562	28 Aug 80	32		0	Archived by ESA
5-14	65°20'N. 46°11'W..	22225-13551	24 Feb 81	14		0	Snow surface features; archived by CCRS
5-15	63°59'N. 47°31'W.	22045-13564	28 Aug 80	33		0	Archieved by ESA
5-15	63°59'N. 47°31'W.	22225-13554	24 Feb 81	15		0	Snow surface features; archived by CCRS
5-16	62°38'N. 48°45'W.	1447-14072	13 Oct 73	18		0	Frederikshåb Isblink
5-16	62°38'N. 48°45'W.	2209-13564	19 Aug 75	38		0	Frederikshåb Isblink; melt ponds; image used for figure 14

TABLE 14.—*Optimum Landsat 2, 3, and 3 images of Greenland*- Continued

























Path-Row	Nominal scene center Lat-long	Landsat identification number	Date	Solar elevation angle (degrees)	Code (see fig. 67 for explanation)	Cloud cover (percent)	Remarks
5-17	61°16'N. 49°53'W.	1447-14075	13 Oct 73	19		0	
6-4	77°33'N. 20°45'W.	2498-13522	3 Jun 76	34		0	
6-5	76°31'N. 25°22'W.	2498-13525	3 Jun 76	35		10	
6-6	75°25'N. 29°20'W.	2516-13525	21 Jun 76	38		30	
6-6	75°25'N. 29°20'W.	30035-13583-BD	9 Apr 78	22		0	Some snow surface features; Landsat 3 RBV
6-7	74°16'N. 32°46'W.	2174-13594	15 Jul 75	37		5	
6-8	73°04'N. 35°45'W.	2462-13550	28 Apr 76	30		10	
6-9	71°50'N. 38°21'W.	1448-14101	14 Oct 73	9		80	
6-10	70°35'N. 40°38'W.	1448-14103	14 Oct 73	10		60	
6-11	69°17'N. 42°40'W.	21344-13440	27 Sep 78	17		40	Snow surface features; archived by ESA
6-12	67°59'N. 44°29'W.	1448-14112	14 Oct 73	13		0	Snow surface features
6-13	66°40'N. 46°08'W.	22226-14003	25 Feb 81	13		5	Snow surface features; archived by CCRS
6-14	65°20'N. 47°37'W.	21344-13451	27 Sep 78	21		0	Archived by ESA
6-15	63°59'N. 48°57'W.	1448-14124	14 Oct 73	16		0	Image used for figure 15
6-15	63°59'N. 48°57'W.	30143-14032	26 Jul 78	43		15	Ablation features; archived by ESA
6-16	62°38'N. 50°11'W.	1448-14130	14 Oct 73	18		10	Image used for figure 14
6-16	62°38'N. 50°11'W.	22226-14015	25 Feb 81	16		0	Frederikshåb Isblink; archived by CCRS
6-17	61°16'N. 51°19'W.	No usable data					
7-3	78°29'N. 16°48'W.	22029-14030	12 Aug 80	25		0	Archived by ESA
7-4	77°33'N. 22°11'W.	2194-14092	4 Aug 75	29		5	Hertugen af Orléans Land
7-5	76°31'N. 26°48'W.	22065-14041	17 Sep 80	15		0	Snow surface features; archived by ESA
7-6	75°25'N. 30°47'W.	2068-14104	31 Mar 75	18		0	
7-7	74°16'N. 34°12'W.	21723-140XX	11 Oct 79	9		5	Image archived by USGS-SGP
7-8	73°04'N. 37°11'W.	22047-14052	30 Aug 80	25		0	Archived by ESA

TABLE 14.—*Optimum Landsat 1, 2, and 3 images of Greenland—Continued*

Path-Row	Nominal scene center (lat-long)	Landsat identification number	Date	Solar elevation angle (degrees)	Code (see fig. 67 for explanation)	Cloud cover (percent)	Remarks
7-9	71°50'N. 39°47'W.	22047-14054	30 Aug 80	26	●	0	Archived by ESA
7-10	70°35'N. 42°05'W.	22047-14061	30 Aug 80	27	●	0	Archived by ESA
7-11	69°17'N. 44°06'W.	22047-14063	30 Aug 80	28	●	0	Archived by ESA
7-11	69°17'N. 44°06'W.	22227-14053	26 Feb 81	11	◐	15	Snow surface features; archived by CCRS
7-12	67°59'N. 45°56'W.	22047-14070	30 Aug 80	29	●	0	Archived by ESA
7-12	67°59'N. 45°56'W.	22227-14055	26 Feb 81	12	◐	20	Snow surface features; archived by CCRS
7-13	66°40'N. 47°34'W.	22047-14072	30 Aug 80	30	●	0	Ablation features; archived by ESA
7-13	66°40'N. 47°34'W.	22227-14062	26 Feb 81	13	●	0	Snow surface features; archived by CCRS
7-14	65°20'N. 49°03'W.	22227-14064	26 Feb 81	14	◑	10	Archived by CCRS
7-14	65°20'N. 49°03'W.	22353-14045	2 Jul 81	45	●	0	Archived by ESA
7-15	63°59'N. 50°23'W.	21705-14035	23 Sep 79	24	●	0	Archived by ESA
7-16	62°38'N. 51°37'W.	21705-14041	23 Sep 79	25	●	0	Archived by ESA
8-2	79°19'N. 11°59'W.	2536-14020	11 Jul 76	32	●	0	
83	78°29'N. 18°14'W.	2536-14023	11 Jul 76	33	●	0	
84	77°33'N. 23°37'W.	21274-13491	19 Jul 78	33	●	0	Archived by ESA
85	76°31'N. 28°14'W.	30145-14104	28 Jul 78	32	●	0	Archived by ESA
86	75°25'N. 32°13'W.	30145-14110	28 Jul 78	33	●	0	Archived by ESA
8-7	74°16'N. 35°38'W.	2446-14063	12 Apr 76	24	●	0	
88	73°04'N. 38°37'W.	21256-13500	1 Jul 78	39	●	0	Archived by ESA
8-9	71°50'N. 41°13'W.	22228-14102	27 Feb 81	9	●	0	Archived by CCRS
8-10	70°35'N. 43°31'W.	22228-14104	27 Feb 81	10	●	0	Snow surface features; archived by USGS-SGP
8-11	69°17'N. 45°32'W.	22228-14111	27 Feb 81	12	●	0	Archived by CCRS
8-12	67°59'N. 47°22'W.	30145-14133	28 Jul 78	39	●	0	Numerous meltwater ponds; archived by CCRS and ESA
8-12	67°59'N. 47°22'W.	22228-14113	27 Feb 81	13	●	5	Snow surface features; archived by USGS-SGP



TABLE 14.—*Optimum Landsat 1, 2, and 3 images of Greenland*—Continued

Path-Row	Nominal scene center (lat-long)	Landsat identification number	Date	Solar elevation angle (degrees)	Code (see fig. 67 for explanation)	Cloud cover (percent)	Remarks
8-13	66°40'N. 49°00'W.	21256-13521	1 Jul 78	44	●	0	
8-13	66°40'N. 49°00'W.	30145-14140	28 Jul 78	40	◐	20	Numerous meltwater ponds; image used for figure 19; archived by CCRS and ESA
8-14	65°20'N. 50°29'W.	1216-14262	24 Feb 73	14	◐	30	
8-14	65°20'N. 50°29'W.	30145-14142	28 Jul 78	41	●	5	Numerous meltwater ponds; image used for figure 17; archived by CCRS and ESA
8-15	63°59'N. 51°49'W.	1396-14252	23 Aug 73	36	◐	15	Image used for figure 15
8-15	63°59'N. 51°49'W.	30145-14145	28 Jul 78	42	●	0	Archived by CCRS and ESA
8-16	62°38'N. 53°03'W.	21328-13564	11 Sep 78	30	●	0	Archived by USGS-SGP
9-2	79°19'N. 13°25'W.	2537-14074	12 Jul 76	32	●	0	
9-3	78°29'N. 19°40'W.	2537-14081	12 Jul 76	33	●	0	Lambert Land, Zachariae Isstrøm; meltwater ponds
94	77°33'N. 25°03'W.	30380-14160	20 Mar 79	12	●	0	Snow surface features; archived by ESA
94	77°33'N. 25°03'W.	22049-14151	1 Sep 80	20	●	0	Archived by ESA
9-5	76°31'N. 29°40'W.	30380-14163	20 Mar 79	13	●	0	Snow surface features; archived by ESA
9-5	76°31'N. 29°40'W.	22049-14153	1 Sep 80	21	●	0	Archived by ESA
96	75°25'N. 33°39'W.	22049-14160	1 Sep 80	22	●	0	Archived by ESA
9-7	74°16'N. 37°04'W.	22049-14162	1 Sep 80	23	●	0	Archived by ESA
98	73°04'N. 40°03'W.	1073-14283	4 Oct 72	12	◐	10	
98	73°04'N. 40°03'W.	22049-14165	1 Sep 80	24	●	0	Archived by ESA
9-9	71°50'N. 42°39'W.	1073-14290	4 Oct 72	13	●	0	
9-10	70°35'N. 44°57'W.	1073-14292	4 Oct 72	14	●	5	Snow surface features
9-11	69°17'N. 46°58'W.	1073-14295	4 Oct 72	15	◐	10	
9-11	69°17'N. 46°58'W.	22049-14180	1 Sep 80	27	●	5	Ablation features; archived by ESA
9-12	67°59'N. 48°48'W.	1073-14301	4 Oct 72	17	●	0	Snow surface features
9-12	67°59'N. 48°48'W.	21635-14123	15 Jul 79	42	●	5	Ablation features; archived by ESA

TABLE 14. —*Optimum Landsat 1, 2, and 3 images of Greenland—Continued*

Path-Row	Nominal scene center Oat-long)	Landsat identification number	Date	Solar elevation angle (degrees)	Code (see fig. 67 for explanation)	Cloud cover (percent)	Remarks
9-13	66°40'N. 50°26'W.	1073-14304	4 Oct 72	18	●	0	Søndre Strømfjord area; snow surface features
9-13	66°40'N. 50°26'W.	21635-14125	15 Jul 79	43	◐	10	Ablation features; archived by ESA
9-14	65°20'N. 51°55'W.	1073-14310	4 Oct 72	19	●	0	Sukkertoppen area
9-15	63°59'N. 53°15'W.	21671-14141	20 Aug 79	37	●	0	Archived by CCRS
10-2	79°19'N. 14°52'W.	2197-14254	7 Aug 75	26	●	0	
10-3	78°29'N. 21°07'W.	2197-14261	7 Aug 75	27	●	0	Lambert Land, Zachariae Isstrøm; meltwater ponds
10-3	78°29'N. 21°07'W.	3013-14215-C	4 Sep 78	18	c ◐	30	Landsat 3 RBV
10-4	77°33'N. 26°29'W.	2142-14213	13 Jun 75	35	◐	10	
10-5	76°31'N. 31°07'W.	1308-14335	27 May 73	34	●	5	
10-6	75°25'N. 35°05'W.	1308-14341	27 May 73	35	◐	30	
10-7	74°16'N. 38°31'W.	1308-14344	27 May 73	36	◐	20	
10-8	73°04'N. 41°29'W.	1074-14342	5 Oct 72	11	●	0	
10-9	71°50'N. 44°05'W.	1074-14344	5 Oct 72	13	●	0	
10-10	70°35'N. 46°23'W.	1074-14351	5 Oct 72	14	●	0	
10-11	69°17'N. 48°25'W.	1074-14353	5 Oct 72	15	●	0	
10-11	69°17'N. 48°25'W.	21276-14034	21 Jul 78	39	◐	30	Ablation features; archived by ESA
10-12	67°59'N. 50°14'W.	2484-14190	20 May 76	41	●	0	
10-12	67°59'N. 50°14'W.	21276-14041	21 Jul 78	40	●	0	Ablation features; archived by ESA
10-13	66°40'N. 51°52'W.	21276-14043	21 Jul 78	41	●	5	Søndre Strømfjord, Sukkertoppen Iskappe; archived by FSA
10-14	65°20'N. 53°21'W.	21276-14050	21 Jul 78	43	●	5	Archived by ESA
11-2	79°19'N. 16°18'W.	2216-14305	26 Aug 75	20	●	0	Hovgaard Ø, Nioghalvfjerdsfjorden
11-3	78°29'N. 22°33'W.	2216-14312	26 Aug 75	21	◐	15	Zachariae Isstrøm; meltwater ponds
11-4	77°33'N. 27°55'W.	22051-14263	3 Sep 80	19	◐	20	Archived by ESA
11-5	76°31'N. 32°33'W.	22051-14270	3 Sep 80	20	◐	70	Archived by ESA

TABLE 14. *Optimum Landsat 1, 2, and 3 images of Greenland- Continued*

Path-Row	Nominal scene center (lat-long)	Landsat identification number	Date	Solar elevation angle (degrees)	Code (see fig. 67 for explanation)	Cloud cover (percent)	Remarks
11-6	75°25'N. 36°31'W.	22051-14272	3 Sep 80	21		10	Archived by ESA
11-7	74°16'N. 39°57'W.	22051-14275	3 Sep 80	22		0	Archived by ESA
11-8	73°04'N. 42°55'W.	22051-14281	3 Sep 80	23		0	Archived by ESA
11-9	71°50'N. 45°31'W.	22087-14284	9 Oct 80	12		0	Snow surface features; archived by CCRS
11-10	70°35'N. 47°49'W.	22051-14290	3 Sep 80	26		5	Snow surface features; archived by ESA
11-11	69°17'N. 49°51'W.	21655-14234	4 Aug 79	37		5	Jakobshavn Isfjord; meltwater ponds; archived by CCRS
11-11	69°17'N. 49°51'W.	22087-14293	9 Oct 80	14		0	Jakobshavn Isfjord; snow surface features; archived by CCRS; image used for figure 20
11-12	67°59'N. 51°40'W.	31480-14322	24 Mar 82	22		5	Partial image (75%); archived by ESA
11-12	67°59'N. 51°40'W.	31642-14341	2 Sep 82	29		0	Partial image (75%); archived by ESA
11-13	66°40'N. 53°18'W.	31480-14325	24 Mar 82	24		0	Partial image (75%); archived by ESA
11-13	66°40'N. 53°18'W.	31642-14344	2 Sep 82	30		0	Partial image (75%); archived by ESA
11-14	65°20'N. 54°47'W.	21709-14262	27 Sep 79	21		0	Archived by ESA
12-1	80°01'N. 10°33'W.	2540-14243	15 Jul 76	30		0	
12-2	79°19'N. 17°44'W.	2540-14245	15 Jul 76	31		0	Hovgaard Ø, Lambert Land; image used for figure 43
12-2	79°19'N. 17°44'W.	30167-14324- ABCD	19 Aug 78	22		30-50	Landsat 3 RBV
12-3	78°29'N. 23°59'W.	22052-14315	4 Sep 80	17		5	Archived by ESA
12-4	77°33'N. 29°21'W.	22052-14322	4 Sep 80	19		5	Archived by ESA
12-5	76°31'N. 33°59'W.	2073-14390	5 Apr 75	19		50	
12-6	75°25'N. 37°57'W.	21584-14254	25 May 79	35		70	Archived by ESA
12-7	74°16'N. 41°23'W.	No image available					
12-8	73°04'N. 44°21'W.	22088-1434X	10 Oct 80	10		25	Archived by USGS-SGP
12-9	71°50'N. 46°57'W.	22088-14343	10 Oct 80	11		0	Archived by CCRS
12-10	70°35'N. 49°15'W.	2468-14300	4 May 76	34		5	
12-10	70°35'N. 49°15'W.	22088-14345	10 Oct 80	12		5	Archived by CCRS

TABLE 14.—*Optimum Landsat 1, 2, and 3 images of Greenland—Continued*













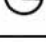











Path-Row	Nominal scene center (lat-long)	Landsat identification number	Date	Solar elevation angle (degrees)	Code (see fig. 67 for explanation)	Cloud cover (percent) <sup>f</sup>	Remarks
12-10	70°35'N. 49°15'W.	31589-14383	11 Jul 82	40		10	Ablation features; partial image (75%); archived by ESA
12-11	69°17'N. 51°17'W.	22088-14352	10 Oct 80	14		0	Jakobshavn Isfjord; archived by CCRS
12-11	69°17'N. 51°17'W.	31589-14390	11 Jul 82	41		0	Ablation features; partial image (75%); archived by ESA
12-12	67°59'N. 53°06'W.	31589-14392	11 Jul 82	42		0	Partial scene (75%); archived by ESA
12-13	66°40'N. 54°44'W.	31481-14383	25 Mar 82	24		0	Partial image (75%); archived by ESA
13-1	80°01'N. 12°00'W.	2127-14371	29 May 75	30		0	
13-2	79°19'N. 19°10'W.	2182-14432	23 Jul 75	29		60	
13-3	78°29'N. 25°25'W.	2452-14390	18 Apr 76	21		10	
13-4	77°33'N. 30°48'W.	2127-14383	29 May 75	33		85	
13-5	76°31'N. 35°25'W.	No image available					
13-6	75°25'N. 39°23'W.	No usable data					
13-7	74°16'N. 42°49'W.	No usable data					
13-8	73°04'N. 45°48'W.	No usable data					
13-9	71°50'N. 48°24'W.	2469-14352	5 May 76	34		0	
13-10	70°35'N. 50°41'W.	21729-14364	17 Oct 79	10		0	Archived by CCRS
13-11	69°17'N. 52°43'W.	20937-14174	16 Aug 77	33		5	Archived by CCRS; image used for figure 21
13-11	69°17'N. 52°43'W.	21729-14370	17 Oct 79	11		0	Archived by CCRS
13-12	67°59'N. 54°32'W.	21729-14373	17 Oct 79	12		0	Archived by CCRS
13-13	66°40'N. 56°10'W.	2469-14370	5 May 76	38		0	
14-1	80°01'N. 13°26'W.	21640-1436X	20 Jul 79	29		0	Archived by ESA
14-2	79°19'N. 20°36'W.	2075-14492	7 Apr 75	16		0	Lambert Land, Kronprins Christian Land; band 4
14-2	79°19'N. 20°36'W.	21640-14370	20 Jul 79	30		0	Archived by ESA
14-3	78°29'N. 26°51'W.	2075-14494	7 Apr 75	17		0	Snow surface features
14-4	77°33'N. 32°14'W.	22072-14435	24 Sep 80	11		0	Snow surface features; archived by ESA



TABLE 14.—*Optimum Landsat 1, 2, and 3 images of Greenland—Continued*

























Path-Row	Nominal scene center (lat-long)	Landsat identification number	Date	Solar elevation angle (degrees)	Code (see fig. 67 for explanation)	Cloud cover (percent)	Remarks
14-5	76°31'N. 36°51'W.	22072-14442	24 Sep 80	12		20	Archived by ESA
14-6	75°25'N. 40°49'W.	1240-14573	20 Mar 73	14		0	
14-7	74°16'N. 44°15'W.	1240-14580	20 Mar 73	15		0	
14-8	73°04'N. 47°14'W.	22072-14453	24 Sep 80	15		0	Snow surface features; archived by CCRS and ESA
14-9	71°50'N. 49°50'W.	1078-14575	9 Oct 72	11		20	Archived by ESA
14-9	71°50'N. 49°50'W.	1240-14585	20 Mar 73	17		0	Íngia Isbraë, Rink Isbrae; image used for figure 22
14-10	70°35'N. 52°07'W.	1240-14591	20 Mar 73	19		0	Nûgssuaq; image used for figure 22
14-10	70°35'N. 52°07'W.	20938-14230	17 Aug 77	32		10	Nûgssuaq; archived by CCRS; image used for figure 21
14-10	70°35'N. 52°07'W.	22072-14462	24 Sep 80	18		0	Archived by CCRS and ESA
14-11	69°17'N. 54°09'W.	1240-14594	20 Mar 73	20		5	Disko
14-11	69°17'N. 54°09'W.	22072-14464	24 Sep 80	19		0	Archived by CCRS and ESA
15-1	80°01'N. 14°52'W.	21335-143XX	18 Sep 78	10		10	Partial image (80%); archived by ESA
15-2	79°19'N. 22°02'W.	21335-14313	18 Sep 78	11		10	Archived by ESA
15-3	78°29'N. 28°17'W.	21533-14400	4 Apr 79	17		0	Archived by ESA
15-4	77°33'N. 33°40'W.	21533-14402	4 Apr 79	18		0	Archived by ESA
15-5	76°31'N. 38°17'W.	21533-14405	4 Apr 79	19		0	Archived by ESA
15-6	75°25'N. 42°15'W.	21533-14411	4 Apr 79	20		0	Archived by ESA
15-7	74°16'N. 45°41'W.	21533-14414	4 Apr 79	21		0	Archived by ESA
15-8	73°04'N. 48°40'W.	21533-14420	4 Apr 79	22		0	Archived by ESA
15-9	71°50'N. 51°16'W.	21533-14423	4 Apr 79	23		0	Archived by ESA
15-10	70°35'N. 53°33'W.	21533-14425	4 Apr 79	24		0	Archived by ESA
15-10	70°35'N. 53°33'W.	21677-14464	26 Aug 79	29		0	Archived by CCRS
15-11	69°17'N. 55°35'W.	21533-14432	4 Apr 79	25		0	Archived by ESA
15-11	69°17'N. 55°35'W.	21677-14471	26 Aug 79	31		0	Archived by USGS-SGP

TABLE 14.—*Optimum Landsat 1, 2, and 3 images of Greenland—Continued*
























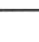
Path-Row	Nominal scene center (lat-long)	Landsat identification number	Date	Solar elevation angle (degrees)	Code (see fig. 67 for explanation)	Cloud cover (percent)	Remarks
16-1	80°01'N. 16°18'W.	2077-15002	9 Apr 75	16		70	
16-2	79°19'N. 23°28'W.	2077-15005	9 Apr 75	17		10	
16-3	78°29'N. 29°43'W.	2508-14491	13 Jun 76	34		0	
16-4	77°33'N. 35°06'W.	2508-14493	13 Jun 76	35		0	
16-5	76°31'N. 39°43'W.	2490-14502	26 May 76	34		0	
16-6	75°25'N. 43°41'W.	No usable data					
16-7	74°16'N. 47°07'W.	No usable data					
16-8	73°04'N. 50°06'W.	No usable data					
16-9	71°50'N. 52°42'W.	21678-14520	27 Aug 79	28		5	Archived by CCRS
16-10	70°35'N. 54°59'W.	1350-15095	8 Jul 73	41		5	
16-10	70°35'N. 54°59'W.	21678-14523	27 Aug 79	29		0	Archived by CCRS
16-11	69°17'N. 57°01'W.	21678-14525	27 Aug 79	30		0	Archived by CCRS
17-1	80°01'N. 17°44'W.	247415003	10 May 76	26		30	
17-2	79°19'N. 24°54'W.	No usable data					
17-3	78°29'N. 31°09'W.	2077-15011	9 Apr 75	18		25	
17-4	77°33'N. 36°32'W.	2077-15014	9 Apr 75	19		60	
17-5	76°31'N. 41°09'W.	2077-15020	9 Apr 75	20		25	
17-6	75°25'N. 45°07'W.	2077-15023	9 Apr 75	21		0	
17-7	74°16'N. 48°33'W.	2077-15025	9 Apr 75	23		0	
17-8	73°04'N. 57°32'W.	2077-15032	9 Apr 75	24		0	
17-8	73°04'N. 51°32'W.	21679-14573	28 Aug 79	27		0	Archived by CCRS
17-9	71°50'N. 54°08'W.	21679-14575	28 Aug 79	28		0	Archived by CCRS
17-10	70°35'N. 56°25'W.	21661-14575	10 Aug 79	34		10	Archived by CCRS
18-1	80°01'N. 19°10'W.	21644-14594	24 Jul 79	28		0	Archived by ESA

TABLE 14.—*Optimum Landsat 1, 2, and 3 images of Greenland—Continued*

Path-Row	Nominal scene center (lat-long)	Landsat identification number	Date	Solar elevation angle (degrees)	Code (see fig. 67 for explanation)	Cloud cover (percent)	Remarks
18-2	79°19'N. 26°20'W.	22400-15021	18 Aug 81	22	●	5	Archived by ESA
18-3	78°29'N. 32°35'W.	21698-15014	16 Sep 79	13	●	5	Archived by ESA
18-4	77°33'N. 37°58'W.	22022-15062	5 Aug 80	28	●	0	Archived by ESA
18-4	77°33'N.. 37°58'W.	22274-15050	14 Apr 81	22	●	0	Archived by ESA
18-5	76°31'N. 42°35'W.	22022-15065	5 Aug 80	30	●	5	Archived by ESA
18-5	76°31'N. 42°35'W.	22274-15052	14 Apr 81	23	●	0	Archived by ESA
18-6	75°25'N. 46°33'W.	22022-15071	5 Aug 80	31	●	0	Archived by ESA
18-6	75°25'N. 46°33'W.	22274-15055	14 Apr 81	24	●	0	Archived by ESA
18-7	74°16'N. 49°59'W.	21698-15032	16 Sep 79	18	●	0	Snow surface features; archived by ESA
18-8	73°04'N. 52°58'W.	2060-15090	23 Mar 75	17	●	0	Upernavik Isstrøm; image used for figure 24
18-8	73°04'N. 52°58'W.	22022-15081	5 Aug 80	33	●	5	Archived by USGS-SGP and ESA
18-9	71°50'N. 55°34'W.	2060-15093	23 Mar 75	18	●	0	Upernavik, Íngia Isbræ
18-9	71°50'N. 55°34'W.	22040-15084	23 Aug 80	28	●	0	Archived by CCRS and ESA
19-1	80°01'N. 20°36'W.	2493-15055	29 May 76	30	◐	10	
19-2	79°19'N. 27°46'W.	2170-15175	11 Jul 75	32	●	0	
19-3	78°29'N. 34°01'W.	2062-15182	25 Mar 75	12	●	0	
19-4	77°33'N. 39°24'W.	2169-15130	10 Jul 75	34	◐	60	
19-5	76°31'N. 44°01'W.	No image available			○		
19-6	75°25'N. 47°59'W.	No usable data			◑		
19-7	74°16'N. 51°25'W.	No usable data			◑		
19-8	73°04'N. 54°24'W.	2153-71505	8 Apr 79	23	◐	80	
19-9	71°50'N. 57°00'W.	2457-15100	23 Apr 76	30	●	5	
19-9	71°50'N. 57°00'W.	30174-15155-AB	26 Aug 78	28	A ○ B	10-80	Landsat 3 RBV
20-1	80°01'N. 22°02'W.	2529-15045	4 Jul 76	31	◐	30	

TABLE 14.—Optimum Landsat 1, 2, and 3 images of Greenland—Continued

























Path-Row	Nominal scene center (lat-long)	Landsat identification number	Date	Solar elevation angle (degrees)	Code (see fig. 67 for explanation)	Cloud cover (percent)	Remarks
20-2	79°19'N. 29°12'W.	2152–15180	23 Jun 75	33		20	
20-3	78°29'N. 35°27'W.	2152–15183	23 Jun 75	34		10	
20-4	77°33'N. 40°50'W.	2062–15185	25 Mar 75	15		0	
20-5	76°31'N. 45°27'W.	2062–15191	25 Mar 75	17		0	
20-6	75°25'N. 49°25'W.	No usable data					
20-7	74°16'N. 52°51'W.	2242–15185	21 Sep 75	16		0	
20-8	73°04'N. 55°50'W.	2062–15203	25 Mar 75	18		20	
20-8	73°04'N. 55°50'W.	30157–15210-D	9 Aug 78	32	 D	85	Landsat 3 RBV
20-8	73°04'N. 55°50'W.	21682–15145	31 Aug 79	24		20	Upernavik Isstrøm; archived by USGS-SGP
20-9	71°50'N. 58°26'W.	2494–15145	30 May 76	39		0	
21-1	80°01'N. 23°28'W.	21305–15040	19 Aug 78	21		5	Archived by ESA
21-2	79°19'N. 30°38'W.	21323–15052	6 Sep 78	16		10	Archived by ESA
21-3	78°29'N. 36°53'W.	2081–15241	13 Apr 75	20		20	
21-4	77°33'N. 42°16'W.	21323–15061	6 Sep 78	18		0	Archived by ESA
21-5	76°31'N. 46°53'W.	21323–15063	6 Sep 78	19		0	Archived by ESA
21-6	75°25'N. 50°51'W.	No usable data					
21-7	74°16'N. 54°17'W.	21251–15040	26 Jun 78	38		10	Archived by ESA
21-8	73°04'N. 57°16'W.	21251–15042	26 Jun 78	39		0	Archived by ESA
22-1	80°01'N. 24°54'W.	22296–15264	6 May 81	25		0	Kronprins Christian Land; archived by ESA
22-2	79°19'N. 32°04'W.	2461–15300	27 Apr 76	23		5	
22-3	78°29'N. 38°19'W.	2461–15302	27 Apr 76	24		0	
22-4	77°33'N. 43°42'W.	2461–15305	27 Apr 76	26		0	
22-5	76°31'N. 48°19'W.	22422–15261	9 Sep 81	18		0	Archived by ESA
22-6	75°25'N. 52°17'W.	21702–15260	20 Sep 79	15		0	Archived by ESA

TABLE 14.— *Optimum Landsat 1, 2, and 3 images of Greenland—Continued*
















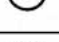








Path-Row	Nominal scene center (lat-long)	Landsat identification number	Date	Solar elevation angle (degrees)	Code (see fig. 67 for explanation)	Cloud cover (percent)	Remarks
22-7	74°16'N. 55°43'W.	30159-15320-D	11 Aug 78	30		70	Landsat 3 RBV
22-7	74°16'N. 55°43'W.	21702-15263	20 Sep 79	16		10	Image archived by University of Lancaster, U.K.; image used for figure 26
22-7	74°16'N. 55°43'W.	22404-15271	22 Aug 81	26		0	Archived by ESA
23-1	80°01'N. 26°20'W.	2155-15345	26 Jun 75	32		50	
23-2	79°19'N. 33°30'W.	2155-15351	26 Jun 75	33		85	
23-3	78°29'N. 39°45'W.	2497-15293	2 Jun 76	33		5	
23-4	77°33'N. 45°08'W.	2443-15312	9 Apr 76	19		80	
23-5	76°31'N. 49°45'W.	2443-15315	9 Apr 76	20		10	
23-6	75°25'N. 53°43'W.	2443-15321	9 Apr 76	22		30	
23-7	74°16'N. 57°09'W.	2443-15324	9 Apr 76	23		50	
24-1	80°01'N. 27°46'W.	2175-15460	16 Jul 75	30		25	
24-2	79°19'N. 34°56'W.	2156-15410	27 Jun 75	33		20	
24-3	78°29'N. 41°11'W.	2156-15412	27 Jun 75	34		20	
24-4	77°33'N. 46°34'W.	No image available					
24-5	76°31'N. 51°11'W.	No image available					
24-6	75°25'N. 55°10'W.	No image available					
24-7	74°16'N. 58°35'W.	30143-15432	26 Jul 78	35		15	
24-7	74°16'N. 58°35'W.	30143-15432-BD	26 Jul 78	35		0-50	Landsat 3 RBV
25-1	80°01'N. 29°12'W.	2069-15574	1 Apr 75	13		10	Snow surface features
25-2	79°19'N. 36°22'W.	No usable data					
25-3	78°29'N. 42°37'W.	21309-15280	23 Aug 78	22		70	Archived by ESA
25-4	77°33'N. 48°00'W.	21345-15301	28 Sep 78	9		40	Archived by ESA
25-5	76°31'N. 52°37'W.	21345-15304	28 Sep 78	11		15	Archived by ESA
25-6	75°25'N. 56°36'W.	30144-15484	27 Jul 78	33		0	Ablation features; archived by ESA



TABLE 14.—*Optimum Landsat 1, 2, and 3 images of Greenland—Continued*



Path-Row	Nominal scene center (lat-long)	Landsat identification number	Date	Solar elevation angle (degrees)	Code (see fig. 67 for explanation)	Cloud cover (percent)	Remarks
25-6	75°25'N. 56°36'W.	21345-15310	28 Sep 78	12	●	0	Archived by ESA
25-7	74°16'N. 60°01'W.	30144-15490	27 Jul 78	34	●	0	Archived by ESA
25-7	74°16'N. 60°01'W.	21345-15313	28 Sep 78	13	●	0	Archived by ESA
26-1	80°01'N. 30°38'W.	22408-15474	26 Aug 81	18	●	0	Snow surface features; archived by ESA
26-2	79°19'N. 37°48'W.	22048-15515	31 Aug 80	18	●	0	Archived by ESA
26-3	78°29'N. 44°03'W.	22048-15521	31 Aug 80	19	●	0	
26-4	77°33'N. 49°26'W.	22048-15524	31 Aug 80	20	●	0	
26-5	76°31'N. 54°03'W.	22048-15530	31 Aug 80	26	●	0	
26-6	75°25'N. 58°02'W.	3014515542- ABCD	28 Jul 78	33		5-20	Landsat 3 RBV
26-6	75°25'N. 58°02'W.	22048-15533	31 Aug 80	22	●	0	Archived by ESA
27-1	80°01'N. 32°04'W.	2140-15520	11 Jun 75	31	●	5	
27-2	79°19'N. 39°14'W.	2070-16035	2 Apr 75	14	●	5	
27-3	78°29'N. 45°30'W.	2178-16040	19 Jul 75	31	◐	90	
27-4	77°33'N. 50°52'W.	2501-15525	6 Jun 76	34	●	0	
27-5	76°31'N. 55°30'W.	No image available			○		
27-6	75°25'N. 59°28'W.	21527-15495	29 Mar 79	17	◐	20	
28-1	80°01'N. 33°30'W.	2179-16090	20 Jul 75	29	◑	10	
28-2	79°19'N. 40°41'W.	2179-16092	20 Jul 75	30	●	0	
28-3	78°29'N. 46°56'W.	2179-16095	20 Jul 75	31	●	5	
28-4	77°33'N. 52°18'W.	22356-16010	5 Jul 81	35	◑	10	Partial image (75%); archived by ESA
28-5	76°31'N. 56°56'W.	22356-16013	5 Jul 81	36	◐	15	Archived by ESA
28-6	75°25'N. 60°54'W.	30183-16062- ABD	4 Sep 78	21		0	Landsat 3 RBV
28-6	75°25'N. 60°54'W.	22356-16015	5 Jul 81	37	◑	10	Archived by ESA
29-1	80°01'N. 34°56'W.	2143-16091	14 Jun 75	32	◐	60	

TABLE 14. —Optimum Landsat 1, 2, and 3 image Greenland- Continued

























Path-Row	Nominal scene center (lat-long)	Landsat identification number	Date	Solar elevation angle (degrees)	Code (see fig. 67 for explanation)	Cloud cover (percent)	Remarks
29-2	79°19'N. 42°07'W.	2143-16094	14 Jun 75	33		90	
29-3	78°29'N. 48°22'W.	21259-15483	4 Jul 78	34		0	Archived by ESA
29-4	77°33'N. 53°44'W.	21259-15490	4 Jul 78	35		0	Archived by ESA
29-5	76°31'N. 58°22'W.	21259-15492	4 Jul 78	36		0	Archived by ESA
29-6	75°25'N. 62°20'W.	20575-16031	19 Aug 76	27		0	Archived by CCRS
30-1	80°01'N. 36°22'W.	2571-17203	15 Aug 76	20		80	Landsat 2 RBV, image used for figure 41
30-2	79°19'N. 43°33'W.	No image available					
30-3	78°29'N. 49°48'W.	No image available					
30-4	77°33'N. 55°10'W.	No image available					
30-5	76°31'N. 59°48'W.	2521-16041	26 Jun 76	36		0	Melville Bugt
30-6	75°25'N. 63°46'W.	1760-16190	22 Aug 74	26		0	Archived by CCRS
31-1	80°01'N. 37°49'W.	2572-17261	16 Aug 76	20		90	Landsat 2 RBV
31-2	79°19'N. 44°59'W.	2504-16091	9 Jun 76	33		25	
31-3	78°29'N. 51°14'W.	2504-16094	9 Jun 76	34		50	
31-4	77°33'N. 56°37'W.	No usable data					
31-5	76°31'N. 61°14'W.	No image available					
31-4	75°25'N. 65°12'W.	No image available					
32-1	80°01'N. 39°15'W.	2075-16321	7 Apr 75	15		0	
32-2	79°19'N. 46°25'W.	1240-16391	20 Mar 73	9		0	
32-3	78°29'N. 52°40'W.	1240-16393	20 Mar 73	11		0	
32-4	77°33'N. 58°03'W.	1240-16400	20 Mar 73	12		0	
32-5	76°31'N. 62°40'W.	22432-16233	19 Sep 81	14		0	Archived by ESA
32-5	76°31'N. 62°40'W.	30169-16284- CD	21 Aug 78	25		50-60	Landsat 3 RBV
32-6	76°25'N. 66°38'W.	22432-16235	19 Sep 81	15		0	Archived by ESA

TABLE 14.—*Optimum Landsat 1, 2, and 3 images of Greenland—Continued*















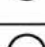









Path-Row	Nominal scene center (lat-long)	Landsat identification number	Date	Solar elevation angle (degrees)	Code (see fig. 67 for explanation)	Cloud cover <sub>r</sub> (percent)	Remarks
33-1	80°01'N. 40°41'W.	No usable data					
33-2	79°19'N. 47°51'W.	No image available					
33-3	78°29'N. 54°06'W.	1062-16495	23 Sep 72	10		90	
33-4	77°33'N. 59°29'W.	1295-16453	14 May 73	30		30	
33-5	76°31'N. 64°06'W.	No image available					
33-6	75°25'N. 68°04'W.	No image available					
34-1	80°01'N. 42°07'W.	2473-16381	9 May 76	26		0	
34-2	79°19'N. 49°17'W.	No image available					
34-3	78°29'N. 55°32'W.	No usable data					
34-4	77°33'N. 60°55'W.	1350-16503	8 Jul 73	34		30	
34-5	76°31'N. 65°32'W.	1062-16504	23 Sep 72	12		5	Hayes Gletscher; image used for figure 30
34-5	76°31'N. 65°32'W.	11484-16010	15 Aug 76	27		5	Archived by CCRS
34-5	76°31'N. 65°32'W.	30207-16403- CD	28 Sep 78	11		0 - 30	Superb snow surface features; Landsat 3 RBV
34-6	75°25'N. 69°30'W.	No image available					
35-1	80°01'N. 43°33'W.	2509-16371	14 Jun 76	32		0	
35-2	79°19'N. 50°43'W.	No image available					
35-3	78°29'N. 56°58'W.	No image available					
35-4	77°33'N. 62°21'W.	2456-16453	22 Apr 76	24		50	
35-5	76°31'N. 66°58'W.	10747-16474	9 Aug 74	29		0	Archived by CCRS
36-1	80°01'N. 44°59'W.	2521-17450	26 Jun 76	31		85	Landsat 2 RBV
36-2	79°19'N. 52°09'W.	1244-17020	24 Mar 73	11		0	
36-3	78°29'N. 58°24'W.	1244-17023	24 Mar 73	12		0	
36-4	77°33'N. 63°47'W.	1244-17025	24 Mar 73	13		0	
36-4	77°33'N. 63°47'W.	10406-17012	2 Sep 73	20		5	Archived by CCRS

TABLE 14.—*Optimum Landsat 1,2, and 3 images of Greenland—Continued*

























Path-Row	Nominal scene center (lat-long)	Landsat identification number	Date	Solar elevation angle (degrees)	Code (see fig. 67 for explanation)	Cloud cover (percent)	Remarks
36-5	76°31'N. 68°24'W.	1244-17032	24 Mar 73	14		5	
36-5	76°31'N. 68°24'W.	30173-16514- ABCD	25 Aug 78	23		50-90	Landsat 3 RBV
36-5	76°31'N. 68°24'W.	22364-16471	13 Jul 81	35		5	Archived by ESA
37-1	80°01'N. 46°25'W.	2589-17203	2 Sep 76	15		0	Snow surface features; Landsat 2 RBV
37-2	79°19'N. 53°35'W.	2169-16553	10 Jul 75	32		10	
37-3	78°29'N. 59°50'W.	2061-16560	24 Mar 75	12		30	
37-4	77°33'N. 65°13'W.	No image available					
37-5	76°31'N. 69°50'W.	No image available					
38-1	80°01'N. 47°51'W.	2553-17213	28 Jul 76	26		10	Landsat 2 RBV
38-2	79°19'N. 55°01'W.	21700-16561	18 Sep 79	11		50	Snow surface features; archived by ESA
38-2	79°19'N. 55°01'W.	22294-16585	4 May 81	26		0	Snow surface features; archived by ESA
38-3	78°29'N. 61°16'W.	21700-16563	18 Sep 79	12		5	Snow surface features; archived by ESA
38-3	78°29'N. 61°16'W.	22384-16572	2 Aug 81	28		12	Ablation features; archived by ESA
38-4	77°33'N. 66°39'W.	22420-16573	7 Sep 81	17		5	Archived by ESA
38-5	76°91'N. 71°16'W.	22420-16580	7 Sep 81	18		0	Archived by ESA
39-1	80°01'N. 49°17'W.	2591-17315	4 Sep 76	14		20	Landsat 2 RBV
39-2	79°29'N. 56°27'W.	No image available					
39-3	78°29'N. 62°42'W.	No image available					
39-4	77°33'N. 68°05'W.	2081-17075	13 Apr 75	21		0	
39-4	77°33'N. 68°05'W.	20567-16595	11 Aug 76	28		30	Archived by CCRS
39-5	76°31'N. 72°42'W.	No image available					
40-1	80°01'N. 50°43'W.	2544-18130	19 Jul 76	27		0	Image used for figure 35; Landsat 2 RBV
40-2	79°19'N. 57°53'W.	22386-17083	4 Aug 81	26		20	Archived by ESA
40-3	78°29'N. 64°08'W.	22386-17085	4 Aug 81	28		40	

TABLE 14.— *Optimum Landsat 1, 2, and 3 images of Greenland—Continued*



Path-Row	Nominal scene center (lat-long)	Landsat identification number	Date	Solar elevation angle (degrees)	Code (see fig. 67 for explanation)	Cloud cover (percent)	Remarks
40-4	77°33'N. 69°31'W.	20568-17054	12 Aug 76	27	●	5	Archived by CCRS
41-1	80°01'N. 52°09'W.	2556-17384	31 Jul 76	26	◐	20	Landsat 2 RBV
41-2	79°19'N. 69°19'W.	2480-17183	16 May 76	29	◐	30	
41-3	78°29'N. 65°34'W.	2551-17112	26 Jul 76	30	◐	25	Northern Inglefield Land; Landsat 2 RBV
41-4	77°33'N. 70°57'W.	2551-17115	26 Jul 76	31	●	0	Southern Inglefield Land, Inglefield Bredning; Landsat 2 RBV
42-1	80°01'N. 53°35'W.	2589-17205	2 Sep 76	16	●	5	Landsat 2 RBV
42-1	80°01'N. 53°35'W.	22388-17193	6 Aug 81	25	●	5	Ablation features; archived by ESA
42-2	79°19'N. 60°45'W.	2588-17154	1 Sep 76	17	◐	10	Landsat 2 RBV
42-2	79°19'N. 60°45'W.	22388-17195	6 Aug 81	26	◐	10	Ablation features; archived by ESA
42-3	78°29'N. 67°00'W.	2588-17160	1 Sep 76	19	●	5	Inglefield Land; Landsat 2 RBV
42-4	77°33'N. 72°23'W.	2588-17163	1 Sep 76	20	●	0	Kap Alexander; Landsat 2 RBV
43-1	80°01'N. 55°01'W.	2553-17220	28 Jul 76	27	●	0	Landsat 2 RBV
43-2	79°19'N. 62°11'W.	2553-17222	28 Jul 76	28	●	0	Landsat 2 RBV
43-3	78°29'N. 68°26'W.	2553-17225	28 Jul 76	30	●	0	Inglefield Land; Landsat 2 RBV
43-4	77°33'N. 73°49'W.	2553-17233	28 Jul 76	31	●	0	Kap Alexander; Landsat 2 RBV
44-1	80°01'N. 56°27'W.	2554-17274	29 Jul 76	27	●	5	Landsat 2 RBV
44-2	79°19'N. 63°38'W.	2608-17263	21 Sep 76	10	●	0	Landsat 2 RBV
44-3	78°29'N. 69°52'W.	2554-17283	29 Jul 76	29	●	5	Inglefield Land; Landsat 2 RBV
45-1	80°01'N. 57°53'W.	2542-18020	17 Jul 76	29	●	5	Petermann Gletscher; Landsat 2 RBV
45-2	79°19'N. 65°04'W.	2070-17471	2 Apr 75	14	●	5	Humboldt Gletscher
45-2	79°19'N. 65°04'W.	30182-17421- ABCD	3 Sep 78	17	A  B C D	0-80	Landsat 3 RBV
45-3	78°29'N. 71°19'W.	2070-17473	2 Apr 75	15	●	0	Inglefield Land; image used for figure 31
45-3	78°29'N. 71°19'W.	20555-17341	30 Jul 76	30	◐	20	Archived by CCRS
45-3	78°29'N. 71°19'W.	30182-17423- BCD	3 Sep 78	18	C  B C D	30-80	Landsat 3 RBV



TABLE 14.—*Optimum Landsat 1, 2, and 3 images of Greenland—Continued*

Path-Row	Nominal scene center (lat-long)	Landsat identification number	Date	Solar elevation angle (degrees)	Code (see fig. 67 for explanation)	Cloud cover (percent)	Remarks
46-1	80°01'N. 59°19'W.	2556-17390	31 Jul 76	27	●	5	Petermann Gletscher; Landsat 2 RBV
46-2	79°19'N. 66°30'W.	2556-17393	31 Jul 76	28	●	5	Landsat 2 RBV
46-3	78°29'N. 72°45'W.	11496-17080	27 Aug 76	21	●	0	Archived by CCRS
46-3	78°29'N. 72°45'W.	30201-17483-D	22 Sep 78	13	● <sub>D</sub>	5	Landsat 3 RBV; archived by CCRS
47-1	80°01'N. 60°45'W..	2544-18132	19 Jul 76	28	●	0	Petermann Gletscher; Landsat 2 RBV
47-2	79°19'N. 67°56'W.	2827-17344	28 Apr 77	24	●	5	
47-3	78°29'N. 74°11'W.	2520-17405	25 Jun 76	34	●	5	Landsat 2 RBV
48-1	80°01'N. 62°12'W..	2558-17503	2 Aug 76	26	●	5	Petermann Gletscher, Washington Land; Landsat 2 RBV; image used for figure 34
49-1	80°01'N. 63°38'W.	2559-17561	3 Aug 76	26	●	0	Petermann Gletscher, Washington Land; Landsat 2 RBV
50-1	80°01'N. 65°04'W.	2614-18002	27 Sep 76	6	◐	20	Landsat 2 RBV
51-1	80°01'N. 66°30'W.	2542-18023	17 Jul 76	30	●	0	Landsat 2 RBV
52-1	80°01'N. 67°56'W.	2549-18420	24 Jul 76	27	●	5	Landsat 2 RBV
53-1	80°01'N. 69°22'W.	2545-18193	20 Jul 76	29	●	0	Landsat 2 RBV